



UNIVERSITÀ  
DEGLI STUDI  
FIRENZE



UNIVERSITAT  
POLITÈCNICA  
DE VALÈNCIA

**STUDY AND CHARACTERIZATION OF THERMO-MECHANICAL PROPERTIES OF  
FIBER-REINFORCED AND NANO-STRUCTURED COMPOSITES  
BASED ON ENGINEERING AND HIGH PERFORMANCE POLYMERIC MATRICES  
FOR HIGH TEMPERATURE APPLICATIONS**

**Dissertation**

submitted to and approved by the

Department of Civil and Environmental Engineering  
University of Florence

and the

Institute of Technology of Materials  
Polytechnic University of Valencia

in candidacy for the degree of

Doctor of Philosophy  
in  
Civil and Environmental Engineering

by

Franco Dominici  
born 05/11/1970  
in Terni (TR), Italy

Submitted on 15/12/2017

Oral examination on 06/06/2018

Professorial advisors Prof. Luigi Torre

Prof. Juan López Martínez

**2017**

Author's email: [francodominici1@gmail.com](mailto:francodominici1@gmail.com)

Author's address: Strada di Perticara 83, 05100 Terni

Department of Civil and Environmental Engineering  
University of Florence  
Via S. Marta, 3  
50139 - Firenze  
Italy

## ACKNOWLEDGMENTS

*A sincere appreciation for my tutor, Prof. Luigi Torre, who guided me throughout the doctorate and beyond. With his excellence and academic authority, I was fortunate to learn a lot as a researcher and as a person. The incredible structure and performance of nanostructured polymeric composite materials, I begin to understand the mysterious micro/nano- world: an irreplaceable pillar to lay a solid foundation for my future career.*

*A sincere thank you to my tutor Prof. Juan López who welcomed me in his research group, provided me with all the tools and advice to carry out my studies in the best possible way. Thanks to him, I had the opportunity to get to know the wonderful Spanish culture and to meet fantastic scientists and friends.*

*Thanks to all the companions of the UPV, in particular of the Alcoy Campus, with whom I shared a scientific and a life unforgettable experience.*

*A heartfelt thanks to Prof. Debora Puglia who always gave me expert advice and guidance and a lot of effective help far beyond imagination. With her teachings I grew a lot and I expanded my scientific and personal horizons.*

*A deep appreciation is for my colleagues in the STM group, Marco Rallini, Francesca Luzi, Maurizio Natali, Roberto Petrucci, Ivan Puri, Silvia Bittolo Bon, Xiaoyan He, Weijun Yang; with them I shared the happy and difficult moments of this course and I always found in them effective help and useful advice.*

*I want to express my gratitude to Prof. Josè Kenny, who started me in the world of materials science, making me passionate about research and tracing the path that led me to this result.*

*A passionate thank you I dedicate it to my wife Helen, who supported and endured me, always and unconditionally, during my academic career.*

*Lastly, I would prefer to appreciate myself, for the strong heart and courage in front of different frustrations and hardship of life. I think in some years, I will also appreciate myself, the guy who is now working hard to pursue a better life. I always believe that: follow excellence, success will chase us silently. Time gave me a few wrinkles and extra pounds, but I earn growth-up and knowledge!*

*Keep a heart of thankfulness, I am going forward!*



UNIVERSITÀ  
DEGLI STUDI  
FIRENZE

Dissertation by  
Franco Dominici



UNIVERSITAT  
POLITÈCNICA  
DE VALÈNCIA

Prof. Luigi Torre

Prof. Juan López

## ABSTRACT

Nowadays, many sectors require stated materials able to operate at temperatures higher than 150-200 °C for times of hundreds of hours, also in corrosive environmental conditions.

Recently, requirements for materials used by the richest industries like aircraft, oil refinery and land transportation have become more and more severe. The necessities of these industrial applications are a unique combination of thermal stability, chemical and solvent resistance, good mechanical properties over a wide range of temperatures, good fire resistance and electrical performance. The polymeric materials with these excellent properties are commonly defined engineering plastics or, in case of extremely particular properties, high performance polymers (HPPs). For the time being HPPs are expensive (50-150 \$/Kg) and therefore they can be used only in high quality and high added value applications.

The purpose of this doctoral work is the study, the development and the characterization of innovative composite materials based on High Performance Polymers (HPPs).

The combined effect of blending HPP matrices, reinforcing and nano structuring the materials allows producing composites with enhanced performances and/or distinctive properties for specific applications. Moreover, the addition of fibers and fillers, at a considerably lower price respect to the matrices, will decrease the cost of the materials.

Some of the major HPP matrices have been selected and characterized as polyetheretherketone (PEEK), polyetherimide (PEI), thermoplastic polyimide (TPI), polybenzimidazole (PBI) and polyimide (PI); in view of the productivity and with the objective of improving the processing step, blends of matrices that are not singularly extrudable, such as PI and PBI, have been considered. Due to the high processing temperature that causes strong effects of thermal degradation, the choice of reinforcing fibers has necessarily been limited to the only glass fibers (GF) and carbon fibers (CF), meanwhile different micro and nanofillers were utilized on single matrices, blends and fiber reinforced systems to study their effect on HPP performance. A novel use of a terephthalic-based filler, synthesized in our laboratories, has been considered for an efficient method of production of nanostructured hybrid composites.

A general improvement in terms on various thermomechanical properties was observed, definitively confirming the possibility of using such new HPPs composites as a less costly and better performing alternative to current high performances engineering plastics.

# Contents

## CHAPTER 1: COMPOSITE MATERIALS

1.1	<i>Thermoplastic polymers and High-Performance Polymers (HPPs)</i>	p.	1
1.2	<i>Fiber reinforced (FR) composites</i>	p.	6
1.3	<i>Nanostructured (NS) materials</i>	p.	8
1.3.1	<i>Selected families of nanocarriers</i>	p.	10
1.4	<i>Fiber reinforced nanostructured (FRNS) materials</i>	p.	21
1.5	<i>Aim of the study</i>	p.	23
1.6	<i>References</i>	p.	27

## CHAPTER 2: HIGH PERFORMANCE POLYMERIC MATRICES (HPPs)

2.1	<i>Selected neat matrices</i>	p.	28
2.1.1	<i>Polyetheretherketone (PEEK)</i>	p.	31
2.1.2	<i>Polyimide (PI) and Thermoplastic Polyimide (TPI)</i>	p.	42
2.1.3	<i>Polyetherimide (PEI)</i>	p.	47
2.1.4	<i>Polyamide-imide (PAI)</i>	p.	47
2.1.5	<i>Polybenzimidazole (PBI)</i>	p.	50
2.1.6	<i>Polyarylamide (PARA)</i>	p.	51
2.2	<i>Compounded matrices</i>	p.	52
2.2.1	<i>PEEK/PBI</i>	p.	53
2.2.2	<i>PEEK/PI</i>	p.	54
2.2.3	<i>PEK/PBI</i>	p.	56
2.3	<i>References</i>	p.	57

## CHAPTER 3: PROCESSING AND CHARACTERIZATION OF HPPS MATRICES

3.1	<i>Processing</i>	p.	58
3.1.1	<i>Extrusion, melt compounding and injection moulding</i>	p.	60
3.2	<i>Thermal characterization</i>	p.	61
3.2.1	<i>Differential scanning calorimetry (DSC)</i>	p.	61
3.2.2	<i>Thermo Gravimetric Analysis (TGA)</i>	p.	63
3.2.3	<i>Heat Deflection Temperature (HDT)</i>	p.	64
3.3	<i>Mechanical characterization</i>	p.	65
3.3.1	<i>Tensile tests at T room and high Temperature</i>	p.	65
3.3.2	<i>Impact test</i>	p.	66

3.3.3	<i>Dynamical Mechanical Thermal Analysis (DMTA)</i>	p.	66
3.4	<i>Morphological characterization</i>	p.	67
3.5	<i>Rheological characterization</i>	p.	68
3.6	<i>References</i>	p.	70

## **CHAPTER 4: NEAT MATRICES AND FIBER REINFORCED COMPOSITES**

4.1	<i>Neat matrices and fiber reinforced composites</i>	p.	71
4.2	<i>Thermal characterization of neat matrices and fiber reinforced composites</i>	p.	73
4.3	<i>Thermomechanical characterization of neat matrices and fiber reinforced composites</i>	p.	77
4.4	<i>Morphological characterization of neat matrices and fiber reinforced composites</i>	p.	80
4.5	<i>References</i>	p.	82

## **CHAPTER 5: NANOSTRUCTURED AND FIBER REINFORCED PEEK COMPOSITES**

5.1	<i>PEEK based nanocomposites</i>	p.	83
5.1.1	<i>Definition of the working parameters</i>	p.	83
5.2	<i>Nanostructured and Fiber Reinforced PEEK based composites</i>	p.	88
5.3	<i>Tensile tests at high temperature</i>	p.	93
5.4	<i>Morphological analysis</i>	p.	96
5.5	<i>Optimized formulations</i>	p.	100
5.6	<i>References</i>	p.	107

## **CHAPTER 6: NANOSTRUCTURED AND FIBER REINFORCED COMPOSITES**

6.1	<i>PEEK - PI based NS and FR composites</i>	p.	108
6.1.1	<i>Mechanical characterization by tensile test</i>	p.	108
6.1.2	<i>DSC thermal characterization</i>	p.	115
6.1.3	<i>Thermogravimetric characterization</i>	p.	117
6.1.4	<i>Morphological characterization</i>	p.	121
6.1.5	<i>Dynamic Thermo Mechanical Analysis</i>	p.	122
6.2	<i>References</i>	p.	126

## **CHAPTER 7: CALCIUM TEREPHTHALATE TRIHYDRATE SALTS (CATS)**

7.1	<i>Synthesis and characterization of CATS and anhydrous CATS</i>	p.	127
7.2	<i>References</i>	p.	134

## **CHAPTER 8: NANOSTRUCTURED AND FIBER REINFORCED COMPOSITES WITH TEREPHTHALATE SALTS**

<i>8.1 Composites based on PEEK</i>	<i>p. 135</i>
<i>8.2 Effect of CATAS on hybrid FR and NS composites</i>	<i>p. 140</i>
<i>8.3 Composites based on PBI / PEK</i>	<i>p. 145</i>
<i>8.4 References</i>	<i>p. 148</i>

## **CHAPTER 9: CONCLUSIONS**

<i>9.1 Results achieved</i>	<i>p. 149</i>
-----------------------------	---------------

# Figures Index

## CHAPTER 1:

### COMPOSITE MATERIALS

**Figure 1.1:** A comparison of standard plastics, engineering plastics, and high-performance plastics

**Figure 1.2:** Trend of the dispersion index  $D_i$  as a function of the total atoms

**Figure 1.3:** Crystalline structure of  $\text{TiO}_2$  (Rutilium and Anatase)

**Figure 1.4:** Crystalline structure of  $\text{SiO}_2$  and TEM image of crystalline nanosilica  $\alpha$  and a TEM image of nanosilicate dispersed in resin.

**Figure 1.5:** Alumina structure and TEM image of  $\text{Al}_2\text{O}_3$  nanometric particles

**Figure 1.6:** Crystalline structure characteristic of phyllosilicates

**Figure 1.7:** SEM images of the mineral and the crystalline structure of montmorillonite

**Figure 1.8:** Crystalline structure characteristic of phlogopite mica

**Figure 1.9:** Rocks, pyroxenes (single chain) and amphiboles (double chain), belong to the inosilicates family

**Figure 1.10:** Crystalline structure characteristic of wollastonite and TEM image which highlights the fibrous appearance

**Figure 1.11:** Images of the mineral and crystalline structure of sepiolite

## CHAPTER 2:

### HIGH PERFORMANCE POLYMERIC MATRICES (HPPs)

**Figure 2.1:** Elements produced with technical polymers and HPPs

**Figure 2.2:** Tubing for special uses, gears and impeller in fiber-reinforced HPPs, gaskets, bearings, membranes and valves made with HPPs

**Figure 2.3:** Molecular structure of the repeating unit of polyetheretherketone (PEEK) (a), polyetherimide (PEI) (b) and polyethersulfone (PES) (c)

**Figure 2.4:** Molecular structure of the repeating unit of some TPs of the polyaryletherketone family (PAEKs)

**Figure 2.5:** Nucleophilic aromatic substitution reaction scheme for the synthesis of PEAKs

**Figure 2.6:** Friedel-Crafts reaction scheme

**Figure 2.7:** Reaction scheme for the synthesis of high molecular weight PEEK with Rose process (a) and Victrex process (b)

**Figure 2.8:** Scheme of reactions for the synthesis of PEEK with soluble low temperature precursors

**Figure 2.9:** Viscosity of some Victrex PEEK grades according to the amount and type of additives amount



**Figure 2.10:** Two-step method of polyimide synthesis

**Figure 2.11:** Kapton-type polyimide.

**Figure 2.12:** Biphenyl-type polyimides and polyimides with a connecting group (-X) between the phthalimides

**Figure 2.13:** Synthesis route for PI-2080 soluble polyimide

**Figure 2.14:** PI chemical structure and appearance

**Figure 2.15:** PAI chemical structure (synthesis route by TMAC)

**Figure 2.16:** DMTA results for PAI in comparison with TPI, PEEK and PI

**Figure 2.17:** structure of PBI polymer

**Figure 2.18:** structure of PARA polymer

**Figure 2.19:** Storage modulus in a three-point bending experiment at 1 Hz

**Figure 2.20:** Scanning electron micrograph (SEM) at 4000x magnification. Spherical particles of Polyimide P84@NT with smooth surface.

**Figure 2.21:** Tensile strength versus temperature for GAZOLE™ 6200G polymer

## CHAPTER 3:

### PROCESSING AND CHARACTERIZATION OF HPPS MATRICES

**Figure 3.1:** DSM microextruder used detail of the extrusion chamber with mixing switch

**Figure 3.2:** Micropress and complete compounding, extrusion and injection system

**Figure 3.3.** DSC cell diagram (a) and Q200 TA Instrument (b)

**Figure 3.4.** TGA equipment with horizontal balance

**Figure 3.5:** Thermogravimetric analyzer model Seiko Exstar 6300

**Figure 3.6:** LR30K dynamometer used for tensile tests

**Figure 3.7:** Charpy e Izod Plásticos PIT-25

**Figure 3.8:** DMA, Rheometric Scientific, ARES N2 (a), a typical DMA tester with grips to hold sample and environmental chamber to provide different temperature (DMTA) conditions (b).

**Figure 3.9:** FESEM, Supra 25-Zeiss, Germany.

**Figure 3.10:** Parallel flat plate rheometer Ares model produced by Rheometric Scientific with a detail of parallel plates tool

## CHAPTER 4:

### NEAT MATRICES AND FIBER REINFORCED COMPOSITES

**Figure 4.1:** Trend for thermoplastic in aerospace composites

**Figure 4.2:** Required adjustments of the processing equipments for the preparation of HPPs and fiber reinforced HPPS

**Figure 4.3:** DSC profiles for neat HPPS matrices (neat grade), with indication of their colour, glass transition, HDT and CUT temperatures

**Figure 4.4:** Detected HDT temperatures for neat HPPs matrices (neat grade) and fiber reinforced compounds

**Figure 4.5:** Results of impact tests for neat HPPs matrices (neat grades) and fiber reinforced compounds

**Figure 4.6:** TG and DTG of some representative samples

**Figure 4.7:**  $G'$ ,  $G''$  and  $\tan \delta$  profiles for neat HPPs matrices (neat grades) and fiber reinforced compounds: PEEK based (a), TPI based (b) and PBI/PEEK based (c) composites

**Figure 4.8:** DMTA equipped with a camera (a), DSC profile for TPI heated between 25 and 400°C at 10°C/min (b) and Evolution of TPI transparency to opacity during the specific heating scan (c).

**Figure 4.9:**  $G'$  profiles for neat HPPs matrices (neat grades) (a) and fiber reinforced compounds: comparison of glass reinforced (b) and carbon reinforced (c) systems

**Figure 4.10:** FESEM images of neat HPPs at two different magnifications (a) and micrographs of compounds with glass and carbon fibers at 30% wt. (b)

## CHAPTER 5:

### NANOSTRUCTURED AND FIBER REINFORCED PEEK COMPOSITES

**Figure 5.1:** Results of tensile tests on specimens of nano composite materials based on PEEK

**Figure 5.2:** Results of the tensile tests on the specimens of pre-loaded matrices with glass fiber and carbon fiber with increasing contents

**Figure 5.3:** Results of tensile tests on specimens of nano composite materials with pre-loaded matrices with glass fiber

**Figure 5.4:** Results of tensile tests on specimens of nanocomposite materials with pre-loaded carbon fiber matrices

**Figure 5.5:** Tensile test results at room temperature on specimens of matrices preloaded with glass fiber and carbon fiber with increasing content

**Figure 5.6.** Results of tensile tests on specimens of nanocomposite materials with pre-loaded fiberglass matrices at  $T = 200^\circ\text{C}$

**Figure 5.7.** Results of tensile tests on specimens of nanocomposite materials with pre-loaded carbon fiber matrices at  $T = 200^\circ\text{C}$

**Figure 5.8:** Micrographs of the fragile fracture surface on a sample of matrices preloaded with glass fibers (a), carbon fibers (b), nanocomposite with Aerosil300 (c) and nanocomposite with COK84 (d), nanocomposite with Pangel S9 (e)

**Figure 5.9:** Micrographs of the fragile fracture surface for nanocomposites material with Hombitech RM 230 P (a), Nyglos 8 (b) and PDM-5B (c)

**Figure 5.10:** Tensile properties of optimized GF samples at  $T = 200^\circ\text{C}$

**Figure 5.11:** Tensile properties of optimized GF samples at  $T = 200^\circ\text{C}$

**Figure 5.12:** Best nanostructured and fiber reinforced PEEK based formulation

## CHAPTER 6:

### NANOSTRUCTURED AND FIBER REINFORCED COMPOSITES

**Figure 6.1:** Stress-Strain curves of PEEK-PI blends

**Figure 6.2:** Nyglos8 structure (a) and TEM micrograph (b)

**Figure 6.3:** Result of tensile test on nanostructured composites Elastic moduli (a), Strain at break (b) and Stress resistance (c)

**Figure 6.4:** Stress-strain diagram of the tests at  $T=200\text{ }^{\circ}\text{C}$

**Figure 6.5:** DSC curves at the second heating of the composites

**Figure 6.6:** Details of the DSC curves at the second heating: glass transition zone (a) and melting zone (b)

**Figure 6.7:** Results of dynamic TGA test on nano fillers

**Figure 6.8:** Results of dynamic TGA test on fiber reinforced and nanostructured blends

**Figure 6.9:** TG comparison of composite materials based on PEEK-PI blend

**Figure 6.10:** SEM micrographs of the produced composites

**Figure 6.11:** Graph of the DTMA curves of the nano-structured composites based on PEEK-PI:  $G'$  and  $G''$  (a) and  $\tan \delta$  (b)

**Figure 6.12:** DTMA curves of fiber reinforced and nanostructured composites based on PEEK-PI:  $G'$  and  $G''$  (a) and  $\tan \delta$  (b)

**Figure 6.13:**  $G'$  values at  $200\text{ }^{\circ}\text{C}$  obtained from the DTMA curves

## CHAPTER 7:

### CATS (CALCIUM TEREPHTHALATE TRIHYDRATE SALTS)

**Figure 7.1:** SEM micrographs for terephthalate salts of K (a), Na (b), Li (c), Ca (d-e) and Al (f-i)

**Figure 7.2:** Thermal analysis of  $\text{NaOOC}C_6H_4\text{COOH}$  (a),  $\text{KOOCC}_6H_4\text{COOH}$  (b),  $\text{NaOOC}C_6H_4\text{COONa}$  (c),  $\text{Mg}(\text{OOC}C_6H_4\text{COO}) \cdot \text{H}_2\text{O}$  (d),  $\text{Ca}(\text{OOC}C_6H_4\text{COO}) \cdot 3\text{H}_2\text{O}$  (e), and  $\text{Al}_2(\text{OOC}C_6H_4\text{COO})_3 \cdot 8\text{H}_2\text{O}$  (f)

**Figure 7.3:** Recycled and cheap raw materials used for the production of terephthalate salts

**Figure 7.4:** Projection of the crystal structure along the a axis. Roman numbers denote the symmetry operations I: x, y, z; II: 1-x, -y, 1-z; III: x,  $\frac{1}{2}$ -y,  $-\frac{1}{2}$ +z; IV: 1-x,  $\frac{1}{2}$ +y,  $\frac{1}{2}$ -z. Broken lines indicate hydrogen bonds and solid thin lines indicate coordinations around calcium ions (a). Projection of the crystal structure along the c axis (b). Stereoscopic drawing of the crystal structure showing the coordination of the oxygen atoms around the calcium ion (c).

**Figure 7.5:** SEM micrograph of calcium terephthalate trihydrate salts (CATS) produced in our laboratories

**Figure 7.6:** Results of TGA and DTG analysis on CATS samples

**Figure 7.7:** Infrared spectra of  $\text{CATS} \cdot 3\text{H}_2\text{O}$  and  $\text{CATAS}$  (a) and  $\text{CaTPA} \cdot 3\text{H}_2\text{O}$  and  $\text{CaTPA}$  (b)

**Figure 7.8:** FESEM morphologies of  $\text{CATS} \cdot 3\text{H}_2\text{O}$  ( $T = 105$ ) and  $\text{CATAS}$  (from  $T = 190$  up to  $T > 700$ )

## CHAPTER 8:

### NANOSTRUCTURED AND FIBER REINFORCED COMPOSITES WITH TEREPHTHALATE SALTS

**Figure 8.1:** Arrangement of polymer chains in a semi-crystalline polymer as PEEK

**Figure 8.2:** Results of DMTA test on CATAS reinforced composites:  $G'$  and  $G''$  (a) and  $\tan \delta$  (b)

**Figure 8.3:** Values of the  $G'$  modules of CATAS composites at 100 °C and at 200 °C

**Figure 8.4:** DSC scan for evaluation of rigid amorphous phase of PEEK (a) and PEEK- 30CATAS (b) composites

**Figure 8.5** Micrographs of the fragile fracture surface on sample of composites with CATAS

**Figure 8.6:** Graph of the DTMA curves of the carbon fiber reinforced and nano-structured composites based on PEEK:  $G'$  and  $G''$  (a) and  $\tan \delta$  (b)

**Figure 8.7:** Graph of the DTMA curves with values of  $G'$  at 100 °C and 200 °C

**Figure 8.8:** Micrographs of the fragile fracture surface on sample of composites with P5B and CATAS

**Figure 8.9:** Results of DMTA tests for PEK/PBI materials:  $G'$  and  $G''$  (a) and  $\tan \delta$  (b)

**Figure 8.10:** Graph of the DTMA curves with values of  $G'$  at 100°C and 200°C for PEK/PBI composites

# Tables Index

## CHAPTER 1:

### COMPOSITE MATERIALS

*Table 1.1: High-performance engineering thermoplastics*

*Table 1.2: Continuous service temperatures in air of high-performance engineering thermoplastics*

*Table 1.3: Selected Oxide-based fillers*

*Table 1.4: Selected fillers of mineral origin*

*Table 1.5: Classification of mineralogical species of phyllosilicates*

## CHAPTER 2:

### HIGH PERFORMANCE POLYMERIC MATRICES (HPPs)

*Table 2.1: Some features of Evonik PEEK line 2000 in pure grades, with 30% glass fiber and 30% carbon fiber*

*Table 2.2: Some characteristics of Evonik PEEK line 4000 in pure grades, with 30% of glass fiber and 30% of carbon fiber*

*Table 2.3: Some features of neat Victrex PEEK in the 150 line*

*Table 2.4: Some features of Victrex PEEK pure and with 30% glass fiber from the 450 line*

*Table 2.5: Chemical structure and T<sub>g</sub> and T<sub>m</sub> of various semycrystalline polyimides. The structures and values for ULTEM, an amorphous polyetherimide, and PEEK are also shown*

## CHAPTER 4:

### NEAT MATRICES AND FIBER REINFORCED COMPOSITES

*Table 4.1: Commercial HPPs and their fiber reinforced products containing glass and carbon fibers*

## CHAPTER 5:

### NANOSTRUCTURED AND FIBER REINFORCED PEEK COMPOSITES

*Table 5.1: List of produced PEEK-based formulations, to be tested for characterization of mechanical properties (commercial denomination, weight percent and abbreviated code)*

*Table 5.2: List of PEEK-based mixtures reformulated after the mechanical properties characterization tests*

*Table 5.3: Results of tensile tests on specimens of PEEK nanocomposites reformulated for the optimization of the mechanical properties*

*Table 5.4: Specimens of pre-loaded matrices with glass fiber and carbon fiber with increasing content produced for the characterization of mechanical properties*

**Table 5.5:** Formulations of the nanocomposites made with the matrices preloaded with 15% of glass fiber

**Table 5.6:** Formulations of the nano composites made with the matrices preloaded with 15% of carbon fiber

**Table 5.7:** Tensile properties of optimized GF samples at room temperature

**Table 5.8:** Tensile properties of optimized CF samples at room temperature

**Table 5.9:** Tensile properties of optimized CF samples at  $T = 200^{\circ}\text{C}$  – second optimization

## **CHAPTER 6:**

### **NANOSTRUCTURED AND FIBER REINFORCED COMPOSITES**

**Table 6.1:** Results of tensile tests on PEEK-PI blends

**Table 6.2:** Formulation of composites based on PEEK-PI blend matrix

**Table 6.3:** Result of tensile test on fiber reinforced and nanostructured composites at room temperature

**Table 6.4:** Result of tensile test on fiber reinforced and nanostructured composites at  $200^{\circ}\text{C}$

## **CHAPTER 8:**

### **NANOSTRUCTURED AND FIBER REINFORCED COMPOSITES WITH TEREPHTHALATE SALTS**

**Table 8.1:** Values of  $G'$  at  $100^{\circ}\text{C}$  and  $200^{\circ}\text{C}$  of PEEK-CATAS nanostructured composites

**Table 8.2:** Evaluation of the phase fractions obtained from the DSC analysis of the PEEK matrix and of the composite with 30% of CATAS

**Table 8.3:** New hybrid composite formulations with carbon fiber and CATAS

**Table 8.4:**  $G'$  values of DMTA at  $100^{\circ}\text{C}$  and at  $200^{\circ}\text{C}$  for CF and nanostructured (NS) composite materials compared to the matrix

**Table 8.5:** summary of the reinforcing weight content in the produced composites

**Table 8.6:** Formulations of samples produced based on PEK / PBI

**Table 8.7:**  $G'$  values of DMTA at  $100^{\circ}\text{C}$  and at  $200^{\circ}\text{C}$  for CF and NS composite materials compared to the matrix

## PREFACE

Nowadays, the polymeric materials are being used in an increasing number of industrial applications. They are progressively substituting traditional materials like metals, ceramics or naturals like wood. Because of needs for materials with so many different properties, both the academic and industrial world have expressed an interest in developing these materials in different ways: synthesis of new polymers was the first approach, followed by formulations of polymeric blends that permits to tailor the properties of different polymers and then production of composites based on polymeric matrix and reinforced with fibers, micro and nano fillers. Recently, requirements for materials in certain areas have become more and more severe. Sectors ranging from the automotive to the aircraft and to the petrochemical industry require stated materials able to operate with a Continuous Use Temperature (CUT) of 150-200 °C for many hours, often in corrosive environmental conditions. These polymeric materials are commonly defined engineering plastics or, in case of extremely particular properties, high performance polymers (HPP). Historically, one of the major driving forces for high performance polymers has involved military and aerospace applications, because the research and development requested to invest substantial resources. The next further development of these innovative materials is to extend the use to the richest industries like aircraft, oil refinery and land transportation. HPP are so expensive (50-150 \$/Kg) that is not affordable their use in mass production but only for high quality applications. The requirements of these industrial applications are a unique combination of thermal stability, chemical and solvent resistance, good mechanical properties on a wide range of temperatures, good fire resistance and electrical performances. Currently, the main development is advancing in order to formulate new polymeric matrices suitable to be offered to industrial markets. There is an available large area of development in order to formulate blending of these high performances polymers to obtain tailored properties for specific applications. Moreover, the studies about composites based on high performances polymers allow ample scope of research and development. Recently, the academic world is working on studies of fiber reinforced composites based on HPP matrices, to encounter the needs of demanding industries. The literature regarding the realization of nano composites based on HPP is very poor, so it seems to be the next development area for this class of materials. Trying to go two steps forward, probably the following improvement could be the production of a deal of composites/nanocomposite with fiber reinforced HPP matrices to satisfy all the various requirements for industrial applications.

The doctorate project activities are framed in this context, with the purpose to study and characterize the High-Performance Polymers and to produce and characterize blends, fiber-reinforced composites, microcomposites, nanocomposites or hybrid formulations of the previous

systems. The aims of the study can be identified in the production and characterization of innovative materials obtained with the use of HPP opportunely blended, reinforced and filled, in order to improve some properties for specific applications. Main properties to improve could be considered the thermal stability and the mechanical properties at high temperature in order to increase stiffness, tensile strength or toughness, especially in severe conditions like high temperature and corrosive environment. Another main aim of the study will concern the cost problems: the reduction of price of these materials could allow to access to composites based on High Performance Polymer matrices to a large range of industrial sectors that currently consider HPP not affordable.

The activities to carry out to achieve the aims involve the research of bibliographic literature about HPP matrices, reinforcement fibers, fillers, composites and nanocomposites. Then it will follow a phase of selection and finding of polymeric matrices belonging to different families like Polyaryletherketones (PAEK), Polyetherimides (PEI), Polyamide-imide (PAI), Polyimides (PI), thermoplastic polyimides (TPI), Polysulfones (PS), Polybenzimidazole (PBI), Polyamides (PA), Aromatic polyamides (PARA), Fluoropolymers (FP) and others. The selection will be done based on criteria like properties, costs, processability, versatility in applications, compatibility, etc. Afterwards it will be done a thermal characterization and other test necessary to the definition of process parameters needed for the realization of samples of HPP matrices. The samples produced will be used to perform the thermo-mechanical characterization of the matrices. The results of the tests will be used to understand the behaviour of the materials at different temperatures with particular attention to high range. The later activities will involve the study and the realization of HP polymeric blends and their thermo-mechanical characterization.

The next activity will be focused on investigation on the reinforcement fibers for HPP with particular attention to the compatibility fiber/matrix. It will be necessary to make thermal characterization of the fibers or master-batches with high ratio of fibers before the production of samples of composites fiber-reinforced (FR) based on HPP matrices. These materials will be characterized in order to their thermo-mechanical properties. The same investigation procedure will be used to study the FR materials produced with HP polymeric blends.

The most relevant phase of activities will concern the introduction of nanotechnology to further improve the properties of the developed polymers. After an accurate research of bibliographic literature about micro/nanofillers and nanocomposites, an adequate number of nanofillers will be selected, and a series of new polymer-based nanocomposites will be developed. Thermal characterization will be used to understand the processability of nanocomposites based on HPP matrices. After the production of nanostructured materials, the thermo-mechanical characterization will show the effect of the nanoreinforcements on the matrices. The knowledge acquired will permit



to design hybrid materials; the combined effect of blending HPP matrices, fiber reinforcing and nanostructuring the materials will allow to produce materials with various distinctive properties tailored for specific applications. Moreover, the addition of fibers and filler, at a considerably lower price respect to the matrices, could decrease the cost of the materials. The expected results at the end of the three years research will be: the development and the complete characterization of new nanocomposite thermoplastic matrices and their composites. Such materials will be able to retain their properties at higher temperatures and will be a valid and less costly alternative to current high-performance engineering plastics. Another aim of this thesis will be to put the basis for the development and optimization of the processing technologies for the production of such materials.

Author's email: [francodominici1@gmail.com](mailto:francodominici1@gmail.com)

Author's address: Strada di Peticara 83, 05100 Terni

Department of Civil and Environmental Engineering  
University of Florence  
Via S. Marta, 3  
50139 - Firenze  
Italy

## ACKNOWLEDGMENTS

*A sincere appreciation for my tutor, Prof. Luigi Torre, who guided me throughout the doctorate and beyond. With his excellence and academic authority, I was fortunate to learn a lot as a researcher and as a person. The incredible structure and performance of nanostructured polymeric composite materials, I begin to understand the mysterious micro/nano- world: an irreplaceable pillar to lay a solid foundation for my future career.*

*A sincere thank you to my tutor Prof. Juan López who welcomed me in his research group, provided me with all the tools and advice to carry out my studies in the best possible way. Thanks to him, I had the opportunity to get to know the wonderful Spanish culture and to meet fantastic scientists and friends.*

*Thanks to all the companions of the UPV, in particular of the Alcoy Campus, with whom I shared a scientific and a life unforgettable experience.*

*A heartfelt thanks to Prof. Debora Puglia who always gave me expert advice and guidance and a lot of effective help far beyond imagination. With her teachings I grew a lot and I expanded my scientific and personal horizons.*

*A deep appreciation is for my colleagues in the STM group, Marco Rallini, Francesca Luzi, Maurizio Natali, Roberto Petrucci, Ivan Puri, Silvia Bittolo Bon, Xiaoyan He, Weijun Yang; with them I shared the happy and difficult moments of this course and I always found in them effective help and useful advice.*

*I want to express my gratitude to Prof. Josè Kenny, who started me in the world of materials science, making me passionate about research and tracing the path that led me to this result.*

*A passionate thank you I dedicate it to my wife Helen, who supported and endured me, always and unconditionally, during my academic career.*

*Lastly, I would prefer to appreciate myself, for the strong heart and courage in front of different frustrations and hardship of life. I think in some years, I will also appreciate myself, the guy who is now working hard to pursue a better life. I always believe that: follow excellence, success will chase us silently. Time gave me a few wrinkles and extra pounds, but I earn growth-up and knowledge!*

*Keep a heart of thankfulness, I am going forward!*



UNIVERSITÀ  
DEGLI STUDI  
FIRENZE

Dissertation by  
Franco Dominici



UNIVERSITAT  
POLITÈCNICA  
DE VALÈNCIA

Prof. Luigi Torre

Prof. Juan López

## ABSTRACT

Nowadays, many sectors require stated materials able to operate at temperatures higher than 150-200 °C for times of hundreds of hours, also in corrosive environmental conditions.

Recently, requirements for materials used by the richest industries like aircraft, oil refinery and land transportation have become more and more severe. The necessities of these industrial applications are a unique combination of thermal stability, chemical and solvent resistance, good mechanical properties over a wide range of temperatures, good fire resistance and electrical performance. The polymeric materials with these excellent properties are commonly defined engineering plastics or, in case of extremely particular properties, high performance polymers (HPPs). For the time being HPPs are expensive (50-150 \$/Kg) and therefore they can be used only in high quality and high added value applications.

The purpose of this doctoral work is the study, the development and the characterization of innovative composite materials based on High Performance Polymers (HPPs).

The combined effect of blending HPP matrices, reinforcing and nano structuring the materials allows producing composites with enhanced performances and/or distinctive properties for specific applications. Moreover, the addition of fibers and fillers, at a considerably lower price respect to the matrices, will decrease the cost of the materials.

Some of the major HPP matrices have been selected and characterized as polyetheretherketone (PEEK), polyetherimide (PEI), thermoplastic polyimide (TPI), polybenzimidazole (PBI) and polyimide (PI); in view of the productivity and with the objective of improving the processing step, blends of matrices that are not singularly extrudable, such as PI and PBI, have been considered. Due to the high processing temperature that causes strong effects of thermal degradation, the choice of reinforcing fibers has necessarily been limited to the only glass fibers (GF) and carbon fibers (CF), meanwhile different micro and nanofillers were utilized on single matrices, blends and fiber reinforced systems to study their effect on HPP performance. A novel use of a terephthalic-based filler, synthesized in our laboratories, has been considered for an efficient method of production of nanostructured hybrid composites.

A general improvement in terms on various thermomechanical properties was observed, definitively confirming the possibility of using such new HPPs composites as a less costly and better performing alternative to current high performances engineering plastics.

# Contents

## CHAPTER 1: COMPOSITE MATERIALS

1.1	<i>Thermoplastic polymers and High-Performance Polymers (HPPs)</i>	p.	1
1.2	<i>Fiber reinforced (FR) composites</i>	p.	6
1.3	<i>Nanostructured (NS) materials</i>	p.	8
1.3.1	<i>Selected families of nanocarriers</i>	p.	10
1.4	<i>Fiber reinforced nanostructured (FRNS) materials</i>	p.	21
1.5	<i>Aim of the study</i>	p.	23
1.6	<i>References</i>	p.	27

## CHAPTER 2: HIGH PERFORMANCE POLYMERIC MATRICES (HPPs)

2.1	<i>Selected neat matrices</i>	p.	28
2.1.1	<i>Polyetheretherketone (PEEK)</i>	p.	31
2.1.2	<i>Polyimide (PI) and Thermoplastic Polyimide (TPI)</i>	p.	42
2.1.3	<i>Polyetherimide (PEI)</i>	p.	47
2.1.4	<i>Polyamide-imide (PAI)</i>	p.	47
2.1.5	<i>Polybenzimidazole (PBI)</i>	p.	50
2.1.6	<i>Polyarylamide (PARA)</i>	p.	51
2.2	<i>Compounded matrices</i>	p.	52
2.2.1	<i>PEEK/PBI</i>	p.	53
2.2.2	<i>PEEK/PI</i>	p.	54
2.2.3	<i>PEK/PBI</i>	p.	56
2.3	<i>References</i>	p.	57

## CHAPTER 3: PROCESSING AND CHARACTERIZATION OF HPPS MATRICES

3.1	<i>Processing</i>	p.	58
3.1.1	<i>Extrusion, melt compounding and injection moulding</i>	p.	60
3.2	<i>Thermal characterization</i>	p.	61
3.2.1	<i>Differential scanning calorimetry (DSC)</i>	p.	61
3.2.2	<i>Thermo Gravimetric Analysis (TGA)</i>	p.	63
3.2.3	<i>Heat Deflection Temperature (HDT)</i>	p.	64
3.3	<i>Mechanical characterization</i>	p.	65
3.3.1	<i>Tensile tests at T room and high Temperature</i>	p.	65
3.3.2	<i>Impact test</i>	p.	66

3.3.3	<i>Dynamical Mechanical Thermal Analysis (DMTA)</i>	p.	66
3.4	<i>Morphological characterization</i>	p.	67
3.5	<i>Rheological characterization</i>	p.	68
3.6	<i>References</i>	p.	70

## **CHAPTER 4: NEAT MATRICES AND FIBER REINFORCED COMPOSITES**

4.1	<i>Neat matrices and fiber reinforced composites</i>	p.	71
4.2	<i>Thermal characterization of neat matrices and fiber reinforced composites</i>	p.	73
4.3	<i>Thermomechanical characterization of neat matrices and fiber reinforced composites</i>	p.	77
4.4	<i>Morphological characterization of neat matrices and fiber reinforced composites</i>	p.	80
4.5	<i>References</i>	p.	82

## **CHAPTER 5: NANOSTRUCTURED AND FIBER REINFORCED PEEK COMPOSITES**

5.1	<i>PEEK based nanocomposites</i>	p.	83
5.1.1	<i>Definition of the working parameters</i>	p.	83
5.2	<i>Nanostructured and Fiber Reinforced PEEK based composites</i>	p.	88
5.3	<i>Tensile tests at high temperature</i>	p.	93
5.4	<i>Morphological analysis</i>	p.	96
5.5	<i>Optimized formulations</i>	p.	100
5.6	<i>References</i>	p.	107

## **CHAPTER 6: NANOSTRUCTURED AND FIBER REINFORCED COMPOSITES**

6.1	<i>PEEK - PI based NS and FR composites</i>	p.	108
6.1.1	<i>Mechanical characterization by tensile test</i>	p.	108
6.1.2	<i>DSC thermal characterization</i>	p.	115
6.1.3	<i>Thermogravimetric characterization</i>	p.	117
6.1.4	<i>Morphological characterization</i>	p.	121
6.1.5	<i>Dynamic Thermo Mechanical Analysis</i>	p.	122
6.2	<i>References</i>	p.	126

## **CHAPTER 7: CALCIUM TEREPHTHALATE TRIHYDRATE SALTS (CATS)**

7.1	<i>Synthesis and characterization of CATS and anhydrous CATS</i>	p.	127
7.2	<i>References</i>	p.	134

## **CHAPTER 8: NANOSTRUCTURED AND FIBER REINFORCED COMPOSITES WITH TEREPHTHALATE SALTS**

<i>8.1 Composites based on PEEK</i>	<i>p. 135</i>
<i>8.2 Effect of CATAS on hybrid FR and NS composites</i>	<i>p. 140</i>
<i>8.3 Composites based on PBI / PEK</i>	<i>p. 145</i>
<i>8.4 References</i>	<i>p. 148</i>

## **CHAPTER 9: CONCLUSIONS**

<i>9.1 Results achieved</i>	<i>p. 149</i>
-----------------------------	---------------

# Figures Index

## CHAPTER 1:

### COMPOSITE MATERIALS

**Figure 1.1:** A comparison of standard plastics, engineering plastics, and high-performance plastics

**Figure 1.2:** Trend of the dispersion index  $D_i$  as a function of the total atoms

**Figure 1.3:** Crystalline structure of  $TiO_2$  (Rutilium and Anatase)

**Figure 1.4:** Crystalline structure of  $SiO_2$  and TEM image of crystalline nanosilica  $\alpha$  and a TEM image of nanosilicate dispersed in resin.

**Figure 1.5:** Alumina structure and TEM image of  $Al_2O_3$  nanometric particles

**Figure 1.6:** Crystalline structure characteristic of phyllosilicates

**Figure 1.7:** SEM images of the mineral and the crystalline structure of montmorillonite

**Figure 1.8:** Crystalline structure characteristic of phlogopite mica

**Figure 1.9:** Rocks, pyroxenes (single chain) and amphiboles (double chain), belong to the inosilicates family

**Figure 1.10:** Crystalline structure characteristic of wollastonite and TEM image which highlights the fibrous appearance

**Figure 1.11:** Images of the mineral and crystalline structure of sepiolite

## CHAPTER 2:

### HIGH PERFORMANCE POLYMERIC MATRICES (HPPs)

**Figure 2.1:** Elements produced with technical polymers and HPPs

**Figure 2.2:** Tubing for special uses, gears and impeller in fiber-reinforced HPPs, gaskets, bearings, membranes and valves made with HPPs

**Figure 2.3:** Molecular structure of the repeating unit of polyetheretherketone (PEEK) (a), polyetherimide (PEI) (b) and polyethersulfone (PES) (c)

**Figure 2.4:** Molecular structure of the repeating unit of some TPs of the polyaryletherketone family (PAEKs)

**Figure 2.5:** Nucleophilic aromatic substitution reaction scheme for the synthesis of PEAKs

**Figure 2.6:** Friedel-Crafts reaction scheme

**Figure 2.7:** Reaction scheme for the synthesis of high molecular weight PEEK with Rose process (a) and Victrex process (b)

**Figure 2.8:** Scheme of reactions for the synthesis of PEEK with soluble low temperature precursors

**Figure 2.9:** Viscosity of some Victrex PEEK grades according to the amount and type of additives amount



**Figure 2.10:** Two-step method of polyimide synthesis

**Figure 2.11:** Kapton-type polyimide.

**Figure 2.12:** Biphenyl-type polyimides and polyimides with a connecting group (-X) between the phthalimides

**Figure 2.13:** Synthesis route for PI-2080 soluble polyimide

**Figure 2.14:** PI chemical structure and appearance

**Figure 2.15:** PAI chemical structure (synthesis route by TMAC)

**Figure 2.16:** DMTA results for PAI in comparison with TPI, PEEK and PI

**Figure 2.17:** structure of PBI polymer

**Figure 2.18:** structure of PARA polymer

**Figure 2.19:** Storage modulus in a three-point bending experiment at 1 Hz

**Figure 2.20:** Scanning electron micrograph (SEM) at 4000x magnification. Spherical particles of Polyimide P84@NT with smooth surface.

**Figure 2.21:** Tensile strength versus temperature for GAZOLE™ 6200G polymer

## **CHAPTER 3:**

### **PROCESSING AND CHARACTERIZATION OF HPPS MATRICES**

**Figure 3.1:** DSM microextruder used detail of the extrusion chamber with mixing switch

**Figure 3.2:** Micropress and complete compounding, extrusion and injection system

**Figure 3.3.** DSC cell diagram (a) and Q200 TA Instrument (b)

**Figure 3.4.** TGA equipment with horizontal balance

**Figure 3.5:** Thermogravimetric analyzer model Seiko Exstar 6300

**Figure 3.6:** LR30K dynamometer used for tensile tests

**Figure 3.7:** Charpy e Izod Plásticos PIT-25

**Figure 3.8:** DMA, Rheometric Scientific, ARES N2 (a), a typical DMA tester with grips to hold sample and environmental chamber to provide different temperature (DMTA) conditions (b).

**Figure 3.9:** FESEM, Supra 25-Zeiss, Germany.

**Figure 3.10:** Parallel flat plate rheometer Ares model produced by Rheometric Scientific with a detail of parallel plates tool

## **CHAPTER 4:**

### **NEAT MATRICES AND FIBER REINFORCED COMPOSITES**

**Figure 4.1:** Trend for thermoplastic in aerospace composites

**Figure 4.2:** Required adjustments of the processing equipments for the preparation of HPPs and fiber reinforced HPPS

**Figure 4.3:** DSC profiles for neat HPPS matrices (neat grade), with indication of their colour, glass transition, HDT and CUT temperatures

**Figure 4.4:** Detected HDT temperatures for neat HPPs matrices (neat grade) and fiber reinforced compounds

**Figure 4.5:** Results of impact tests for neat HPPs matrices (neat grades) and fiber reinforced compounds

**Figure 4.6:** TG and DTG of some representative samples

**Figure 4.7:**  $G'$ ,  $G''$  and  $\tan \delta$  profiles for neat HPPs matrices (neat grades) and fiber reinforced compounds: PEEK based (a), TPI based (b) and PBI/PEEK based (c) composites

**Figure 4.8:** DMTA equipped with a camera (a), DSC profile for TPI heated between 25 and 400°C at 10°C/min (b) and Evolution of TPI transparency to opacity during the specific heating scan (c).

**Figure 4.9:**  $G'$  profiles for neat HPPs matrices (neat grades) (a) and fiber reinforced compounds: comparison of glass reinforced (b) and carbon reinforced (c) systems

**Figure 4.10:** FESEM images of neat HPPs at two different magnifications (a) and micrographs of compounds with glass and carbon fibers at 30% wt. (b)

## CHAPTER 5:

### NANOSTRUCTURED AND FIBER REINFORCED PEEK COMPOSITES

**Figure 5.1:** Results of tensile tests on specimens of nano composite materials based on PEEK

**Figure 5.2:** Results of the tensile tests on the specimens of pre-loaded matrices with glass fiber and carbon fiber with increasing contents

**Figure 5.3:** Results of tensile tests on specimens of nano composite materials with pre-loaded matrices with glass fiber

**Figure 5.4:** Results of tensile tests on specimens of nanocomposite materials with pre-loaded carbon fiber matrices

**Figure 5.5:** Tensile test results at room temperature on specimens of matrices preloaded with glass fiber and carbon fiber with increasing content

**Figure 5.6.** Results of tensile tests on specimens of nanocomposite materials with pre-loaded fiberglass matrices at  $T = 200^\circ\text{C}$

**Figure 5.7.** Results of tensile tests on specimens of nanocomposite materials with pre-loaded carbon fiber matrices at  $T = 200^\circ\text{C}$

**Figure 5.8:** Micrographs of the fragile fracture surface on a sample of matrices preloaded with glass fibers (a), carbon fibers (b), nanocomposite with Aerosil300 (c) and nanocomposite with COK84 (d), nanocomposite with Pangel S9 (e)

**Figure 5.9:** Micrographs of the fragile fracture surface for nanocomposites material with Hombitech RM 230 P (a), Nyglos 8 (b) and PDM-5B (c)

**Figure 5.10:** Tensile properties of optimized GF samples at  $T = 200^\circ\text{C}$

**Figure 5.11:** Tensile properties of optimized GF samples at  $T = 200^\circ\text{C}$

**Figure 5.12:** Best nanostructured and fiber reinforced PEEK based formulation

## CHAPTER 6:

### NANOSTRUCTURED AND FIBER REINFORCED COMPOSITES

**Figure 6.1:** Stress-Strain curves of PEEK-PI blends

**Figure 6.2:** Nyglos8 structure (a) and TEM micrography (b)

**Figure 6.3:** Result of tensile test on nanostructured composites Elastic moduli (a), Strain at break (b) and Stress resistance (c)

**Figure 6.4:** Stress-strain diagram of the tests at  $T=200\text{ }^{\circ}\text{C}$

**Figure 6.5:** DSC curves at the second heating of the composites

**Figure 6.6:** Details of the DSC curves at the second heating: glass transition zone (a) and melting zone (b)

**Figure 6.7:** Results of dynamic TGA test on nano fillers

**Figure 6.8:** Results of dynamic TGA test on fiber reinforced and nanostructured blends

**Figure 6.9:** TG comparison of composite materials based on PEEK-PI blend

**Figure 6.10:** SEM micrographs of the produced composites

**Figure 6.11:** Graph of the DTMA curves of the nano-structured composites based on PEEK-PI:  $G'$  and  $G''$  (a) and  $\tan \delta$  (b)

**Figure 6.12:** DTMA curves of fiber reinforced and nanostructured composites based on PEEK-PI:  $G'$  and  $G''$  (a) and  $\tan \delta$  (b)

**Figure 6.13:**  $G'$  values at  $200\text{ }^{\circ}\text{C}$  obtained from the DTMA curves

## CHAPTER 7:

### CATS (CALCIUM TEREPHTHALATE TRIHYDRATE SALTS)

**Figure 7.1:** SEM micrographs for terephthalate salts of K (a), Na (b), Li (c), Ca (d-e) and Al (f-i)

**Figure 7.2:** Thermal analysis of  $\text{NaO}(\text{O}(\text{C}(\text{C}_6\text{H}_4)\text{C}(\text{O})\text{O})\text{H}$  (a),  $\text{KO}(\text{O}(\text{C}(\text{C}_6\text{H}_4)\text{C}(\text{O})\text{O})\text{H}$  (b),  $\text{NaO}(\text{O}(\text{C}(\text{C}_6\text{H}_4)\text{C}(\text{O})\text{O})\text{Na}$  (c),  $\text{Mg}(\text{O}(\text{O}(\text{C}(\text{C}_6\text{H}_4)\text{C}(\text{O})\text{O})\text{H}_2\text{O}$  (d),  $\text{Ca}(\text{O}(\text{O}(\text{C}(\text{C}_6\text{H}_4)\text{C}(\text{O})\text{O})\text{H}_2\text{O}) \cdot 3\text{H}_2\text{O}$  (e), and  $\text{Al}_2(\text{O}(\text{O}(\text{C}(\text{C}_6\text{H}_4)\text{C}(\text{O})\text{O})\text{H}_2\text{O})_3 \cdot 8\text{H}_2\text{O}$  (f)

**Figure 7.3:** Recycled and cheap raw materials used for the production of terephthalate salts

**Figure 7.4:** Projection of the crystal structure along the a axis. Roman numbers denote the symmetry operations I: x, y, z; II: 1-x, -y, 1-z; III: x,  $\frac{1}{2}$ -y,  $-\frac{1}{2}$ +z; IV: 1-x,  $\frac{1}{2}$ +y,  $\frac{1}{2}$ -z. Broken lines indicate hydrogen bonds and solid thin lines indicate coordinations around calcium ions (a). Projection of the crystal structure along the c axis (b). Stereoscopic drawing of the crystal structure showing the coordination of the oxygen atoms around the calcium ion (c).

**Figure 7.5:** SEM micrography of calcium terephthalate trihydrate salts (CATS) produced in our laboratories

**Figure 7.6:** Results of TGA and DTG analysis on CATS samples

**Figure 7.7:** Infrared spectra of  $\text{CATS} \cdot 3\text{H}_2\text{O}$  and  $\text{CATAS}$  (a) and  $\text{CaTPA} \cdot 3\text{H}_2\text{O}$  and  $\text{CaTPA}$  (b)

**Figure 7.8:** FESEM morphologies of  $\text{CATS} \cdot 3\text{H}_2\text{O}$  ( $T\ 105$ ) and  $\text{CATAS}$  (from  $T190$  up to  $T > 700$ )

## CHAPTER 8:

### NANOSTRUCTURED AND FIBER REINFORCED COMPOSITES WITH TEREPHTHALATE SALTS

**Figure 8.1:** Arrangement of polymer chains in a semi-crystalline polymer as PEEK

**Figure 8.2:** Results of DMTA test on CATAS reinforced composites:  $G'$  and  $G''$  (a) and  $\tan \delta$  (b)

**Figure 8.3:** Values of the  $G'$  modules of CATAS composites at 100 °C and at 200 °C

**Figure 8.4:** DSC scan for evaluation of rigid amorphous phase of PEEK (a) and PEEK- 30CATAS (b) composites

**Figure 8.5** Micrographs of the fragile fracture surface on sample of composites with CATAS

**Figure 8.6:** Graph of the DTMA curves of the carbon fiber reinforced and nano-structured composites based on PEEK:  $G'$  and  $G''$  (a) and  $\tan \delta$  (b)

**Figure 8.7:** Graph of the DTMA curves with values of  $G'$  at 100 °C and 200 °C

**Figure 8.8:** Micrographs of the fragile fracture surface on sample of composites with P5B and CATAS

**Figure 8.9:** Results of DMTA tests for PEK/PBI materials:  $G'$  and  $G''$  (a) and  $\tan \delta$  (b)

**Figure 8.10:** Graph of the DTMA curves with values of  $G'$  at 100°C and 200°C for PEK/PBI composites

# Tables Index

## CHAPTER 1:

### COMPOSITE MATERIALS

*Table 1.1: High-performance engineering thermoplastics*

*Table 1.2: Continuous service temperatures in air of high-performance engineering thermoplastics*

*Table 1.3: Selected Oxide-based fillers*

*Table 1.4: Selected fillers of mineral origin*

*Table 1.5: Classification of mineralogical species of phyllosilicates*

## CHAPTER 2:

### HIGH PERFORMANCE POLYMERIC MATRICES (HPPs)

*Table 2.1: Some features of Evonik PEEK line 2000 in pure grades, with 30% glass fiber and 30% carbon fiber*

*Table 2.2: Some characteristics of Evonik PEEK line 4000 in pure grades, with 30% of glass fiber and 30% of carbon fiber*

*Table 2.3: Some features of neat Victrex PEEK in the 150 line*

*Table 2.4: Some features of Victrex PEEK pure and with 30% glass fiber from the 450 line*

*Table 2.5: Chemical structure and T<sub>g</sub> and T<sub>m</sub> of various semycrystalline polyimides. The structures and values for ULTEM, an amorphous polyetherimide, and PEEK are also shown*

## CHAPTER 4:

### NEAT MATRICES AND FIBER REINFORCED COMPOSITES

*Table 4.1: Commercial HPPs and their fiber reinforced products containing glass and carbon fibers*

## CHAPTER 5:

### NANOSTRUCTURED AND FIBER REINFORCED PEEK COMPOSITES

*Table 5.1: List of produced PEEK-based formulations, to be tested for characterization of mechanical properties (commercial denomination, weight percent and abbreviated code)*

*Table 5.2: List of PEEK-based mixtures reformulated after the mechanical properties characterization tests*

*Table 5.3: Results of tensile tests on specimens of PEEK nanocomposites reformulated for the optimization of the mechanical properties*

*Table 5.4: Specimens of pre-loaded matrices with glass fiber and carbon fiber with increasing content produced for the characterization of mechanical properties*

**Table 5.5:** Formulations of the nanocomposites made with the matrices preloaded with 15% of glass fiber

**Table 5.6:** Formulations of the nano composites made with the matrices preloaded with 15% of carbon fiber

**Table 5.7:** Tensile properties of optimized GF samples at room temperature

**Table 5.8:** Tensile properties of optimized CF samples at room temperature

**Table 5.9:** Tensile properties of optimized CF samples at  $T = 200^{\circ}\text{C}$  – second optimization

## **CHAPTER 6:**

### **NANOSTRUCTURED AND FIBER REINFORCED COMPOSITES**

**Table 6.1:** Results of tensile tests on PEEK-PI blends

**Table 6.2:** Formulation of composites based on PEEK-PI blend matrix

**Table 6.3:** Result of tensile test on fiber reinforced and nanostructured composites at room temperature

**Table 6.4:** Result of tensile test on fiber reinforced and nanostructured composites at  $200^{\circ}\text{C}$

## **CHAPTER 8:**

### **NANOSTRUCTURED AND FIBER REINFORCED COMPOSITES WITH TEREPHTHALATE SALTS**

**Table 8.1:** Values of  $G'$  at  $100^{\circ}\text{C}$  and  $200^{\circ}\text{C}$  of PEEK-CATAS nanostructured composites

**Table 8.2:** Evaluation of the phase fractions obtained from the DSC analysis of the PEEK matrix and of the composite with 30% of CATAS

**Table 8.3:** New hybrid composite formulations with carbon fiber and CATAS

**Table 8.4:**  $G'$  values of DMTA at  $100^{\circ}\text{C}$  and at  $200^{\circ}\text{C}$  for CF and nanostructured (NS) composite materials compared to the matrix

**Table 8.5:** summary of the reinforcing weight content in the produced composites

**Table 8.6:** Formulations of samples produced based on PEK / PBI

**Table 8.7:**  $G'$  values of DMTA at  $100^{\circ}\text{C}$  and at  $200^{\circ}\text{C}$  for CF and NS composite materials compared to the matrix

## PREFACE

Nowadays, the polymeric materials are being used in an increasing number of industrial applications. They are progressively substituting traditional materials like metals, ceramics or naturals like wood. Because of needs for materials with so many different properties, both the academic and industrial world have expressed an interest in developing these materials in different ways: synthesis of new polymers was the first approach, followed by formulations of polymeric blends that permits to tailor the properties of different polymers and then production of composites based on polymeric matrix and reinforced with fibers, micro and nano fillers. Recently, requirements for materials in certain areas have become more and more severe. Sectors ranging from the automotive to the aircraft and to the petrochemical industry require stated materials able to operate with a Continuous Use Temperature (CUT) of 150-200 °C for many hours, often in corrosive environmental conditions. These polymeric materials are commonly defined engineering plastics or, in case of extremely particular properties, high performance polymers (HPP). Historically, one of the major driving forces for high performance polymers has involved military and aerospace applications, because the research and development requested to invest substantial resources. The next further development of these innovative materials is to extend the use to the richest industries like aircraft, oil refinery and land transportation. HPP are so expensive (50-150 \$/Kg) that is not affordable their use in mass production but only for high quality applications. The requirements of these industrial applications are a unique combination of thermal stability, chemical and solvent resistance, good mechanical properties on a wide range of temperatures, good fire resistance and electrical performances. Currently, the main development is advancing in order to formulate new polymeric matrices suitable to be offered to industrial markets. There is an available large area of development in order to formulate blending of these high performances polymers to obtain tailored properties for specific applications. Moreover, the studies about composites based on high performances polymers allow ample scope of research and development. Recently, the academic world is working on studies of fiber reinforced composites based on HPP matrices, to encounter the needs of demanding industries. The literature regarding the realization of nano composites based on HPP is very poor, so it seems to be the next development area for this class of materials. Trying to go two steps forward, probably the following improvement could be the production of a deal of composites/nanocomposite with fiber reinforced HPP matrices to satisfy all the various requirements for industrial applications.

The doctorate project activities are framed in this context, with the purpose to study and characterize the High-Performance Polymers and to produce and characterize blends, fiber-reinforced composites, microcomposites, nanocomposites or hybrid formulations of the previous

systems. The aims of the study can be identified in the production and characterization of innovative materials obtained with the use of HPP opportunely blended, reinforced and filled, in order to improve some properties for specific applications. Main properties to improve could be considered the thermal stability and the mechanical properties at high temperature in order to increase stiffness, tensile strength or toughness, especially in severe conditions like high temperature and corrosive environment. Another main aim of the study will concern the cost problems: the reduction of price of these materials could allow to access to composites based on High Performance Polymer matrices to a large range of industrial sectors that currently consider HPP not affordable.

The activities to carry out to achieve the aims involve the research of bibliographic literature about HPP matrices, reinforcement fibers, fillers, composites and nanocomposites. Then it will follow a phase of selection and finding of polymeric matrices belonging to different families like Polyaryletherketones (PAEK), Polyetherimides (PEI), Polyamide-imide (PAI), Polyimides (PI), thermoplastic polyimides (TPI), Polysulfones (PS), Polybenzimidazole (PBI), Polyamides (PA), Aromatic polyamides (PARA), Fluoropolymers (FP) and others. The selection will be done based on criteria like properties, costs, processability, versatility in applications, compatibility, etc. Afterwards it will be done a thermal characterization and other test necessary to the definition of process parameters needed for the realization of samples of HPP matrices. The samples produced will be used to perform the thermo-mechanical characterization of the matrices. The results of the tests will be used to understand the behaviour of the materials at different temperatures with particular attention to high range. The later activities will involve the study and the realization of HP polymeric blends and their thermo-mechanical characterization.

The next activity will be focused on investigation on the reinforcement fibers for HPP with particular attention to the compatibility fiber/matrix. It will be necessary to make thermal characterization of the fibers or master-batches with high ratio of fibers before the production of samples of composites fiber-reinforced (FR) based on HPP matrices. These materials will be characterized in order to their thermo-mechanical properties. The same investigation procedure will be used to study the FR materials produced with HP polymeric blends.

The most relevant phase of activities will concern the introduction of nanotechnology to further improve the properties of the developed polymers. After an accurate research of bibliographic literature about micro/nanofillers and nanocomposites, an adequate number of nanofillers will be selected, and a series of new polymer-based nanocomposites will be developed. Thermal characterization will be used to understand the processability of nanocomposites based on HPP matrices. After the production of nanostructured materials, the thermo-mechanical characterization will show the effect of the nanoreinforcements on the matrices. The knowledge acquired will permit



to design hybrid materials; the combined effect of blending HPP matrices, fiber reinforcing and nanostructuring the materials will allow to produce materials with various distinctive properties tailored for specific applications. Moreover, the addition of fibers and filler, at a considerably lower price respect to the matrices, could decrease the cost of the materials. The expected results at the end of the three years research will be: the development and the complete characterization of new nanocomposite thermoplastic matrices and their composites. Such materials will be able to retain their properties at higher temperatures and will be a valid and less costly alternative to current high-performance engineering plastics. Another aim of this thesis will be to put the basis for the development and optimization of the processing technologies for the production of such materials.

## CHAPTER 1: COMPOSITE MATERIALS

### 1.1 Thermoplastic polymers and High-Performance Polymers (HPPs)

A thermoplastic, or thermo softening plastic, is a polymer that becomes pliable or mouldable above a specific temperature and solidifies upon cooling. Most thermoplastics have a high molecular weight. The polymer chains associate through intermolecular forces, which weaken rapidly with increased temperature, yielding a viscous liquid. Thus, thermoplastics may be reshaped by heating and are typically used to produce parts by various polymer processing techniques such as injection moulding, compression moulding, calendaring, and extrusion. Thermoplastics differ from thermosetting polymers, which form irreversible chemical bonds during the curing process. Thermosets do not melt when heated: they decompose and do not reform upon cooling. Above its glass transition temperature and below its melting point, the physical properties of a thermoplastic change drastically without an associated phase change. Some thermoplastics do not fully crystallize below the glass transition temperature, retaining some or all their amorphous characteristics. Amorphous and semi-amorphous plastics are used when high optical clarity is necessary, as light is scattered strongly by crystallites larger than its wavelength. Amorphous and semi-amorphous plastics are less resistant to chemical attack and environmental stress cracking because they lack a crystalline structure. Brittleness can be decreased with the addition of plasticizers, which increases the mobility of amorphous chain segments to effectively lower the glass transition temperature. Modification of the polymer through copolymerization or through the addition of non-reactive side chains to monomers before polymerization can also lower it.

High performance plastics (**Figure 1.1**) differ from standard plastics and engineering plastics primarily by their temperature stability, but also by their chemical resistance and mechanical properties, production quantity, and price. There are many synonyms for the term high-performance plastics, such as: high temperature plastics, high-performance polymers, high performance thermoplastics or high-tech plastics. The name “high temperature plastics” is in use due to their continuous service temperature (CST), which is always higher than 150 °C by definition (although this is not their only feature). It is often spoken of polymers instead of plastics since both terms are synonyms in the engineering-use. If the term high-performance thermoplastics is used, it is because both the standard and technical as well as high-performance plastics are always thermoplastics. Thermosets and elastomers are outside of this classification and form their own classes. However, the differentiation from less powerful plastics has varied over time; while nylon and poly (ethylene terephthalate) were initially considered powerful plastics, they are now ordinary.

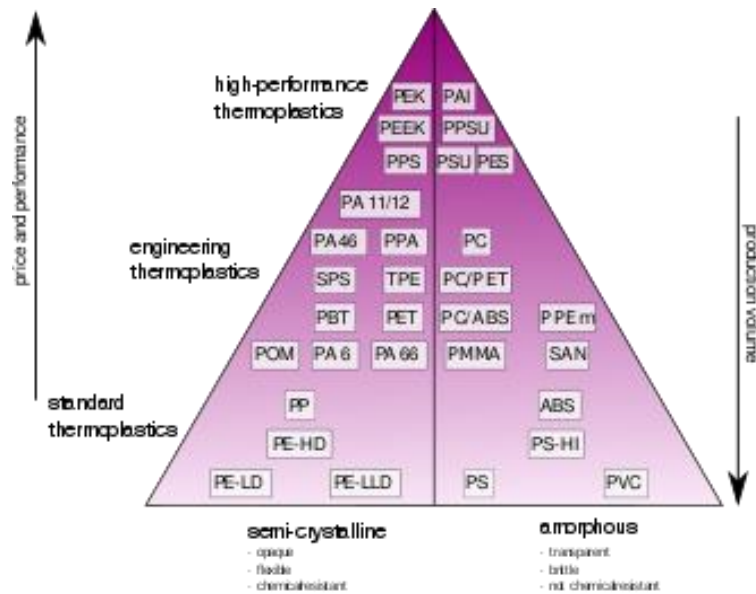


**Figure 1.1:** A comparison of standard plastics, engineering plastics, and high-performance plastics

The improvement of mechanical properties and thermal stability is and has always been an important goal in the research of new plastics. Since the early 1960s, the development of high-performance plastics has been driven by corresponding needs in the aerospace and nuclear technology. Synthetic routes for example for PPS, PES and PSU were developed in the 1960s by Philips, ICI and Union Carbide. The market entry took place in the early 70s. A production of PEEK (ICI), PEK (ICI) and PEI (General Electric and GE) via polycondensation was developed in the 1970s. PEK was offered since 1972 by Raychem, however, made by an electrophilic synthesis. Since electrophilic synthesis has in general the disadvantage of a low selectivity to linear polymers and it is using aggressive reactants, the product could hold only a short time on the market. For this reason, the majority of high-performance plastics are nowadays produced by polycondensation processes. In manufacturing processes by polycondensation, a high purity of the starting materials is important. In addition, the stereochemistry plays a role in achieving the desired properties in general. The development of new high-performance plastics is therefore closely linked to the development and economic production of the constituent monomers.

High performance plastics meet higher requirements than standard and engineering plastics because of their better mechanical properties, higher chemical and/or higher heat stability [Fink, 2008]. Especially the latter makes processing difficult, often special machines are required. Most high-performance plastics are, for example, specializes in a single property (e.g. the heat stability). They thus stand in contrast to engineering plastics, covering a wide range of functions. Some of their diverse applications include: fluid flow tubing, electrical wire insulators, architecture, and fiber optics. High performance plastics are relatively expensive: the price per kilogram may be between 5 (PA 46) and \$ 100 (PEEK) per kilo. The average value is slightly less than 15 US-Dollar/kg. High-

performance plastics are thus about 3 to 20 times as expensive as engineering plastics. In future also, there cannot be expected a significant price decline, since the investment costs for production equipment, the time-consuming development and the high distribution costs are going to remain constant. Since production volumes are very limited with 20.000 t/year, the high-performance plastics are holding a market share of just about 1%. Among the high-performance polymers, fluoropolymers have 45% market share (main representatives: PTFE), sulphur-containing aromatic polymers 20% market share (mainly PPS), aromatic polyarylether and polyketones 10% market share (mainly PEEK) and liquid crystal polymers (LCP) 6%. In the electrical and electronics industries are 41% and 24% of high-performance plastics used in the automotive industry, respectively. Thus, these are the largest consumers. All remaining industries (including chemical industry) have a share of 23%.

Based on the properties of the standard plastics some improvements of mechanical and thermal features can already be accomplished by addition of stabilizers or reinforcing materials (glass and carbon fibers, for example) or by an increase in the degree of polymerization. Further improvements can be achieved through substitution of aliphatic by aromatic units. In this way are reached operating temperatures up to 130 °C. An even higher service temperature can be reached by linking of aromatics (e.g. phenyl) with oxygen (as diphenyl ether group e. g. PEEK), sulphur (as diphenyl sulfone groups in PES or diphenyl group, for example in PPS) or nitrogen (imide group in PEI or PAI). Resulting operating temperatures might be between 200 °C in the case of PES to 260 °C in case of PEI or PAI. The increase in temperature stability by incorporating aromatic units is because the temperature stability of a polymer is determined by its resistance against thermal degradation and its oxidation resistance. The thermal degradation occurs primarily by a statistical chain scission; depolymerisation and removal of low molecular weight compounds are playing only a minor role.

High-performance plastics can be divided in amorphous and semi-crystalline polymers, just like all polymers. Polysulfone (PSU), poly(ethersulfone) (PES) and polyetherimide (PEI) for example are amorphous; poly(phenylene sulfide) (PPS), polyetheretherketone (PEEK) and polyether ketones (PEK), however are semi-crystalline. Crystalline polymers (especially those reinforced with fillers) can be used even above their glass transition temperature. This is because semi-crystalline polymers have, additional to the glass temperature  $T_g$ , the crystallite melting point  $T_m$ , which is mostly much higher located. For example, PEEK has a  $T_g$  of 143 °C but it is anyway applicable up to 250 °C (continuous service temperature = 250 °C). Another advantage of semi-crystalline polymers is their high resistance against chemical substances: PEEK possesses a high resistance against aqueous acids, alkali and organic solvents.

In general, engineering thermoplastics are defined somewhat arbitrarily as thermoplastic resins, neat or filled that maintains dimensional stability and most mechanical properties above 100 °C and below 0°C. This category of engineering materials can be further divided into low performance polymers and high-performance polymers. Here again the borderline is rather vague. For the purpose of this work, we define high-performance engineering thermoplastics as materials resisting at elevated temperatures above 150°C for an extended period of time. Quite frequently, these thermoplastics exhibit other useful attributes, such as good chemical resistance, relatively high mechanical properties, most notably high tensile strength, high impact strength, high hardness and high flame resistance. These polymers are listed in **Table 1.1**.

**Table 1.1:** High-performance engineering thermoplastics

Type of polymers	Chemical name	Acronym
Oxygen containing	Liquid crystal line polymers	LCP
	Polyether ketones	PEEK
		PEK
		PEKK
Sulfur containing	Poly(phenylene sulfide)	PPS
	Polysulfones	PSU
		PES
		PPSU
Nitrogen containing	Polyimides	PI
	Polyamide imides	PAI
	Polyether imides	PEI

Currently, the commercial high-performance engineering thermoplastics are available either as neat or reinforced by glass fibers, carbon fibers or various other fillers; they also can be compounded to exhibit electrical dissipation or conductivity, enhance flame resistance etc. Many of them are used as thermoplastic polymeric matrix in advanced fiber-reinforced composites. Some of them are available as films with special properties or coatings. Since one of the most important attribute of the high-performance thermoplastics is the resistance to elevated temperatures, the continuous service temperature in air of each of them is listed in **Table 1.2**.

Most material properties are strictly depending on the chemical substance under investigation; others depend on the processing operation, which determines the shape, dimensions and orientation within the material. Therefore, the properties of individual polymers are essentially distinguished as physical, mechanical, thermal, and electrical. There are some other attributes that are important for specific polymers or classes of polymers, which may be their specific optical properties, chemical properties, response to electric field, radiation, their barrier properties, solubility, and thermal stability.

**Table 1.2:** Continuous service temperatures in air of high-performance engineering thermoplastics

Polymer	Long-term service temperature in air [°C]
Polybenzimidazole	315
Thermoplastic polyimide (TPI)	300
Poly(ether ketone) (PEK)	260
Poly(ether ketone ether ketone ketone) (PEKK)	260
Poly(amide imide) (PAI)	260
Poly(ether ether ketone) (PEEK)	250
Liquid crystal polymer (LCP), unfilled	240
Poly(phenylene sulfide) (PPS)	240
Poly(ether sulfone) (PES)	200
Poly(phenyl sulfone) (PPSU)	180
Poly(ether imide) (PEI)	170
Polysulfone (PSU)	160

The broader classes of high-performance engineering thermoplastics included polyaryl ether ketones, polysulfones, aromatic polyamides, liquid crystal polymers and polyimides.

Poly(aryl ether ketone)s (PAEK)s are a family of semi-crystalline high-performance engineering thermoplastics. They include a variety of aromatic high-performance polymers characterised by the presence of ether bridges and ketone groups in the main chain linking together arylene groups. This class consists of several structurally different polymers and includes poly (ether ketone) (PEK), poly (ether ether ketone) (PEEK), and poly (ether ketone ketone) PEKK. Because each member of this family is composed of identical building blocks, mostly benzene groups connected by ether and ketone links, they are frequently identified by the number of bridging groups within a repeating unit, characterizing the molecular structure. The ratio and sequence ether to ketone mainly affect the glass transition temperature and melting point of the polymer, its heat resistance and processing temperature the higher the ratio of ketones, the more rigid the polymer chain. The PAEKs are currently being produced either by nucleophilic route (substitution reaction) or by electrophilic route by Friedel-Crafts reaction. The nucleophilic route promotes the formation of ether linkages in the polymerization step, while the electrophilic route promotes the formation of carbonyl groups in the polymerization step. The most widely known *polyether ketone*, *poly (ether ether ketone) (PEEK)* is produced by polycondensation of 4,4-difluorobenzophenone and a potassium salt of bisphenol. The reaction is carried out at high temperatures (up to 300°C) in a high-boiling solvent like diphenylsulfone. The remaining products bearing various sequences of ether and ketone groups bridging together arylene rings, e.g. PEK, PEKK are synthesized in similar ways.

*Polyimides* possess excellent thermal and oxidative stability, resistance to practically all kinds of radiation and to many organic chemicals. They also have good dielectric and mechanical properties. They are widely used as non-metallic materials where prolonged use at temperatures up to 300°C is required. The name of this large family of engineering thermoplastics is based on the cyclic imide

group. They can be divided by the methods used for their synthesis: condensation and addition. The former types are produced by the two-step reaction. The first step includes the formation of a well soluble prepolymer, poly(amic acid), PAA, resulting from the reaction of tetracarboxylic acid dianhydrides with primary diamines and/or their derivatives at ambient temperatures in polar aprotic solvents, such as N-methylpyrrolidone (NMP, N,N-dimethylformamide (DMF) or N,N-dimethylacetamide (DMAc). The obtained solution, with a concentration of 10-30% of PAA by weight, is the prepolymer, that can be used to cast films, form coatings or spin a fiber. In the second stage of the process, the produced prepolymer is converted into the desired form (film, fiber or coating). This stage, the imidization of the PAA, is usually induced thermally by extended heating at temperatures up to 300–400°C. *Polybenzimidazole* is prepared from aromatic tetramines and aromatic dicarbonic acids. The reactants are heated to form a soluble prepolymer that is converted into the insoluble polymer by heating at temperatures above 330°C. The polymer has a Tg of 430°C and is capable of continuous service at temperatures up to 425°C and up to 760°C. It is not available as a moulding resin, only in fiber form, shaped forms and solutions for composite impregnation. It is processed only by a high-temperature and pressure sintering process.

Due to the complexity of production, the scientific and technical commitment and the reduced number of producers, the price of these materials is quite high; currently, the cost of a commercial grade of PEEK is around € 100/kg and that of a standard PEI is rarely less than € 70/kg. The high cost of the polymer matrix currently restricts the field of application to valuable uses where the incidence of costs is not strictly binding. However, as has happened historically for many innovative materials, it is likely that as the number of technopolymers applications increases, the companies involved in the production process will also multiply and consequently there will also be a reduction in material costs. Moreover, in the current situation, the high cost of technopolymeric matrices offers the advantage of using fillers belonging to relatively high cost ranges: in fact, it would be unthinkable to be able to use a nanofiller, for example from 40 € / kg to 10% wt. in a traditional polymer, which costs an average of € 1 / kg, because it would rise 5 times the price. On the contrary, in the case of a PEEK, it would lead to a 6% price decrease. Therefore, even with the same performance, it is convenient to use the maximum possible amount of reinforcements at costs below 100 € / kg, because it produces at least a reduction in prices. This was the main aim of the present work.

## **1.2 Fiber reinforced (FR) composites**

It is reasonable to begin an introduction to composite materials by defining just what these materials are. Here we will follow a common definition that takes “composites” to be materials in which a homogeneous “matrix” component is “reinforced” by a stronger and stiffer constituent, that is usually fibrous but may have a particulate or other shape. For instance, the term “FRP” (for Fiber Reinforced

Plastic) usually indicates a thermosetting polyester matrix containing glass fibers. Fibers used in modern composites have strengths and stiffness far above those of traditional bulk materials. The high strengths of the glass fibers are due to processing that avoids the internal or surface flaws which normally weaken glass, and the strength and stiffness of the polymeric aramid fiber is a consequence of the nearly perfect alignment of the molecular chains with the fiber axis. Of course, these materials are not generally usable as fibers alone, and typically they are impregnated by a matrix material that acts to transfer loads to the fibers. The matrix also protects the fibers from abrasion and environmental attack. The matrix dilutes the properties to some degree, but even so very high specific (weight-adjusted) properties are available from these materials. Metal and glass are available as matrix materials, but these are currently very expensive and largely restricted to R&D laboratories. Polymers are much more commonly used, with unsaturated styrene-hardened polyesters having the majority of low-to-medium performance applications and epoxy or more sophisticated thermosets having the higher end of the market. Thermoplastic matrix composites are increasingly attractive materials, with processing difficulties being perhaps their principal limitation.

Many composites used today are at the leading edge of materials technology, with performance and costs appropriate to ultra-demanding applications. Materials selection has always involved a number of compromises for the engineering designer. Of course, the material's properties are extremely important, since the performance of the structure or component to be designed relies in the properties of the material used in its construction. Composites bring many performance advantages to the designer of structural devices, among which we can list:

- *Composites have high stiffness, strength, and toughness*, often comparable with structural metal alloys. Further, they usually provide these properties at substantially less weight than metals: their "specific" strength and modulus per unit weight is near five times that of steel or aluminium. This means the overall structure may be lighter, and in weight-critical devices such as airplanes or spacecraft this weight savings might be a compelling advantage.
- *Composites can be made anisotropic*, i.e. have different properties in different directions, and this can be used to design a more efficient structure. In many structures the stresses are also different in different directions;
- Many structures experience fatigue loading, in which the internal stresses vary with time: *composites often have excellent fatigue resistance* in comparison with metal alloys, and often show evidence of accumulating fatigue damage, so that the damage can be detected, and the part replaced before a catastrophic failure occurs.
- Materials can exhibit damping, in which a certain fraction of the mechanical strain energy deposited in the material by a loading cycle is dissipated as heat. This can be advantageous, for instance in controlling mechanically-induced vibrations. *Composites generally offer relatively high levels of*



*damping*, and furthermore the damping can often be tailored to desired levels by suitable formulation and processing;

- Composites can be excellent in applications involving sliding friction, with tribological (“wear”) properties approaching those of lubricated steel;
- Composites do not rust as do many ferrous alloys, and resistance to this common form of environmental degradation may offer better life-cycle cost even if the original structure is initially costlier;
- Many structural parts are assembled from a number of subassemblies, and the assembly process adds cost and complexity to the design. Composites offer a lot of flexibility in processing and property control, and this often leads to possibilities for part reduction and simpler manufacture.

Of course, composites are not perfect for all applications, and the designer needs to be aware of their drawbacks as well as their advantages. Among these cautionary notes we can list:

- Not all applications are weight-critical. If weight-adjusted properties not relevant, steel and other traditional materials may work fine at lower cost.
- Anisotropy and other “special” features are advantageous in that they provide a great deal of design flexibility, but they also complicate to design. The well-known tools of stress analysis used in isotropic linear elastic design must be extended to include anisotropy, for instance, and not all designers are comfortable with these more advanced tools.

### **1.3 Nanostructured (NS) materials**

The use of innovative materials that are able to confer particular properties is continually under research, for technological and industrial development. The speech given by Prof. R.P. Feynman at the annual congress of the American Physical Society of 1959 entitled " There's a lot of room at the Bottom " is considered the milestone for the beginning of the study of nanosciences. In the last decades the nanosciences sector is occupying a substantial part of the research and development resources, offering a wide range of applications with highly effective solutions. The purpose of nanosciences is to create and manipulate materials with dimensions ranging from a few tenths to a hundred nanometres ( $10^{-7}$ - $10^{-10}$  m), exploiting the high surface reactivity to obtain innovative characteristics and behaviours of known materials. The growing interest in nanometric materials is favoured by the development of increasingly refined tools and techniques that allow us to examine the properties of matter with a resolution close to that of individual atoms [[R.P. Feynman, 1960](#)].

When the dimensions of a material are reduced to a few nanometres, the optical, physical, chemical and electromagnetic properties of the material become closely dependent on the shape and size of

the crystalline nanostructures [Alivisatos and Endeavour, 1997; Narayanan and El-Sayed, 2004; Hines and Guyot-Sionnest, 1998; Malko et al 2004; Vargas, Socolovsky and Zanchet, 2005; Li et al., 2001]. The behaviour of nanometric materials cannot be predicted on the basis of knowledge at the macroscopic level, since quantum effects and surface and interface phenomena occur. The quantum effects and the phenomena related to the relationship between surface and volume are studied in depth and punctually in the bands theory. By applying the theory of macroscopic solid bands to nanocrystals, the behaviour of charge carriers within a bulk crystal can be described by the "free electron gas" model. As a first approximation, it is assumed that such electrons do not interact with the inner potential of the crystal, due to nuclei and to the "core" electrons; moreover, a solid of infinite dimensions is considered, in order to neglect the contribution of the superficial atoms. This latter approximation can no longer be valid in the case of a nanocrystal, in which the fraction of surface atoms with respect to the total is high and this introduces a significant contribution to the total potential of the solid. This theory has led to the development of further theories which, with various more or less complex and approximate approaches, have attempted to explain the behaviour of nanometer-sized materials. Among these we can mention Bloch's "Tight Binding", the "Wannier Functions" and "Truncated Crystal" method [Bloch and Physik, 1928; Wannier, 1937; Ramakrishna & Friesner, 1991; Rose, 1983]. For the objectives of this study, it is sufficient to understand that the different behaviour of nanometric materials compared to the corresponding macroscopic dimensions is due to the fact that the effect of surface atoms with respect to core atoms is therefore no longer negligible. Approximation used for bulk materials is no longer valid; therefore, the reactive characteristics of the material no longer depend exclusively on core atoms but are influenced, in a more or less sensitive manner, by the dispersion index  $D_i$  and the intrinsic characteristics of the material and the reactivity of the surface atoms. A first evaluation of the different behaviour of nanometric materials can be obtained by defining the dispersion index as the ratio between surface atoms and bulk atoms

$$D_i = \frac{\text{surface\_atoms}}{\text{bulk\_atoms}}$$

A value of  $D_i$  that tends to unity indicates that most of the atoms of the crystal are surface atoms and therefore highly reactive. If we consider that the atomic dimensions vary between 0.1 and 0.3 nm, it is understood that a nanocrystal with a thickness of about 1 nm has only some atoms along this dimension. In **Figure 1.2** various clusters are depicted, for simplicity supposed to simple cubic atomic packaging, for which the relationship between surface atoms and total atoms is highlighted; it is clearly seen that the cluster of 8 atoms consists of all surface atoms and therefore has a dispersion index equal to 1; in the same figure, a graph of the progress of  $D_i$  according to the number of total atoms is reported.

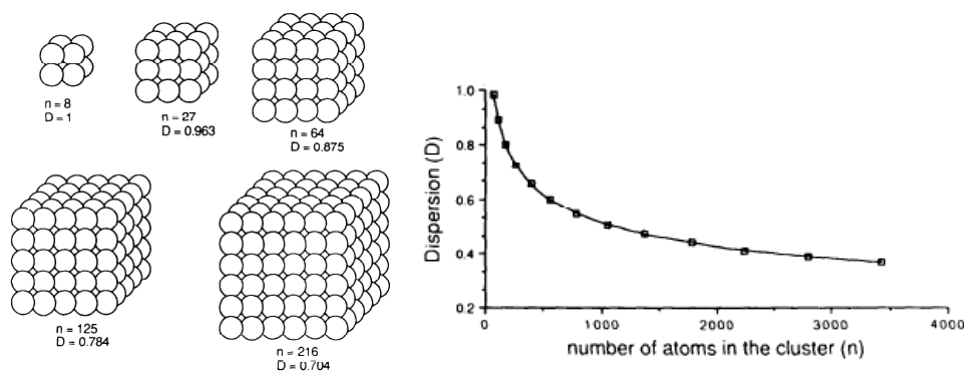


**Figure 1.2:** Trend of the dispersion index  $D_i$  as a function of the total atoms

The different behaviours of nanometric materials compared to the corresponding bulk materials make available to researchers a new category of materials that can offer endless possibilities of application and innumerable properties. The behaviour of nanometric materials in a given context is difficult to forecast, since a large quantity of variables and correlations must be taken into account; for this reason, often, a priori carried out a general evaluation of the avulsed properties of a nanomaterial, the empirical method is the most practical and effective for the definition of behaviour in the specific context. With this assumption, a study field of almost infinite size is proposed for the possible combinations that can be obtained; therefore, it is not possible to have reliable data for applications that have not been tested with an empirical process and a bibliographic availability is not foreseeable to cover all the possibilities. Being aware of general information on the use of certain materials in specific contexts can only be a summary indication to direct a specific study which will, in any case, require the experimental application. The study carried out in this thesis work must therefore first have a general approach to indicate or exclude the possibility of using certain materials in generally defined contexts; then the empirical phase will be carried out, which will allow to evaluate the behaviours of the materials chosen in the specifically defined contexts [Samorjay, 1994].

### 1.3.1 Selected families of nanocarriers

During the last decade, the plethora of commercial nanofillers available on the market has produced a specialization of these fillers for targeted uses [www.aerosil.com, www.sasol.com, Laviosa.it, www.tolsa.com; www.topy.co.jp, www.nycomineral.com, www.sachtleben.de; www.mknano.com; www.grupoantolin.com; www.solvaysolexis.asia]. Within each nanofillers family described in the following paragraphs, fillers with different characteristics and different compatibility with respect to the matrices can be found. The choice must be oriented towards nanofillers that offer the possibility of improving as many complementary properties as possible. Following these two selection

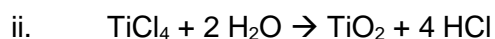
principles, some fillers must be eliminated because they do not satisfy the prerogatives and others because they do not make the necessary modifications to the properties.

**Oxides:** The oxides represent a large family of nanofillers that includes both pure metal oxides and mineral oxides, up to mixtures of oxides. Nanometer oxides are available in great variety with very different characteristics, properties and costs. For the purposes of this study, pure synthesis oxides were considered which, according to the bibliography, could satisfy the required prerogatives. Mixtures of industrial production oxides were also considered that could produce a synergistic effect. We report here (**Table 1.3**) the selected fillers, with its own this family and relative trade name.

**Table 1.3:** Selected Oxide-based fillers

COMMERCIAL NAME OF CHARGES	FAMILY	MAIN COMPONENTS
AEROSIL 300	Oxide	SiO <sub>2</sub>
AEROSIL R 7200	Oxide	SiO <sub>2</sub>
HOMBITEC RM 400	Oxide	TiO <sub>2</sub>
HOMBITEC RM 230 P	Oxide	TiO <sub>2</sub>
COK 84	Oxide mixture	SiO <sub>2</sub> – Al <sub>2</sub> O <sub>3</sub>
SIRAL 40	Oxide mixture	SiO <sub>2</sub> – Al <sub>2</sub> O <sub>3</sub>
DISPERAL 60	Oxyhydroxides	AlO(OH)
DISPERAL P2	Oxyhydroxides	AlO(OH)

From the table, it is noted that mainly used oxides are titanium oxide, silicon oxide and aluminium oxide. The titanium oxide is obtained through the process of chlorination in an oven of extractive minerals, such as ilmenite and leucosene, with the production of titanium tetrachloride, which hydrated, produces TiO<sub>2</sub> according to the reactions:



The most common forms of titanium oxide are Rutilium and Anatase, while Brookite with an orthorhombic crystalline structure has no industrial interest. Rutilium has the most stable crystalline structure, consisting of a tetragonal cell with dimensions  $a = b = 4.587\text{Å}$  and  $c = 2.953\text{Å}$ , with the octahedral arrangement shown in Figure 3.1 and is therefore the most widespread. The stability of the structure leads to a lower reactivity compared to the Anatase form, which is much more effective for uses that require a sensitive photocatalytic activity. The Anatase is characterized by a tetragonal cell with dimensions  $a = b = 3.782\text{Å}$  and  $c = 9.502\text{Å}$  with the octahedral arrangement reported again in **Figure 1.3**.

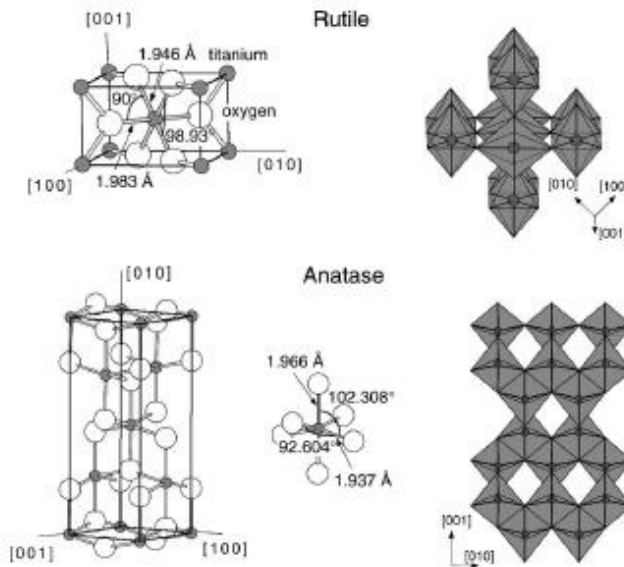


**Figure 1.3:** Crystalline structure of  $\text{TiO}_2$  (Rutilium and Anatase)

Titanium oxide is historically used as a pigment, due to the excellent ability of  $\text{TiO}_2$  to reflect the radiation, producing an unparalleled white. The thermal stability of titanium oxide suggests its use also as fillers in technopolymers that must be processed at high temperature. In particular, the two grades called Hombitec differ for the treatment of compatibilization (RM 400 sample has no treatment, while the RM 230 P type has an inorganic surface treatment for applications with high-temperature processed polymers and a crystalline doping for inhibition of photo activity).

Silicon oxide cannot fall into the metal oxide family, due to the known semiconductor behaviour of this element. Silicon is one of the most naturally occurring elements, almost always in combination with oxygen in  $\text{SiO}_2$  and  $\text{SiO}_4$  oxides, in silicates together with 42 metals, in some non-metals and rare earths; the silicon oxides and the silicates present in the minerals constitute 60% of the earth's crust. Silicon dioxide or silica may occur in three different crystalline forms which are quartz, tridymite and cristobalite; the last two are formed in the presence of high temperatures in volcanic rocks and are of little industrial interest. A particular form of silicon oxide is keatite formed in New Mexico following nuclear explosions. The quartz, in the form  $\alpha$  present in environmental thermal conditions, is very common and is present in granites and many sedimentary rocks. Silica has many properties that propose its use for various uses. The high hardness that characterizes the  $\text{SiO}_2$ , at the seventh level of the Mohs hardness scale, suggests its use for surface applications such as ceramics vitrification or as an abrasive. Silica is an excellent thermal insulator, so the use in refractories and even in the heat shield of space vehicles is very effective; it is also an electrical insulator used for the isolation of integrated circuits and transistors. The properties of transparency and chemical inertia place silica as a basic constituent for the glass industry. An abundant range of silicon oxide nanocarriers is offered in the form of particulate, colloidal solution, sol-gel, etc. with various

modifications and compatibilizations for use in various formulations. **Figure 1.4** shows the images of the crystalline structure  $\alpha$  and a TEM image of nanosilica dispersed in resin.

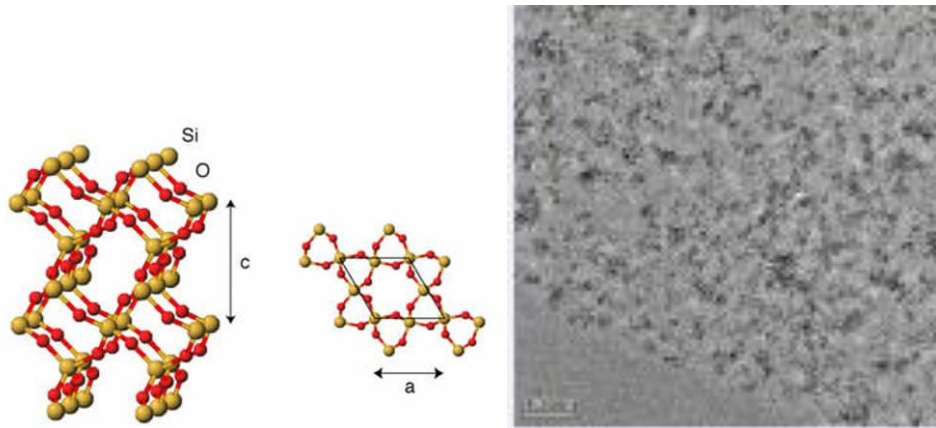


**Figure 1.4:** Crystalline structure of  $\text{SiO}_2$  and TEM image of crystalline nanosilica  $\alpha$  and a TEM image of nanosilicate dispersed in resin.

In particular, "pure" silicon oxides are called Aerosil; within the two selected types, the one marked with code 300 is not modified but it is characterized by a high surface area, estimated at  $300 \text{ m}^2/\text{g}$ . The R7200 grade has a compatibilizing treatment for the chemical characteristics of PEEK, however it does not guarantee thermal stability at the required process temperatures.

Aluminium oxide has long been used as filler to exploit its characteristics of considerable hardness; in nanometric dimensions,  $\text{Al}_2\text{O}_3$  (alumina) confirms its considerable hardness and therefore the ability to improve the mechanical properties of nanocomposites, but poses a problem of not easy solution, that is the difficulty of forming a compatible mixture, due to the lack of affinity between metal oxide and polymeric compound with consequent dispersion problems. It has been seen that an effective solution can be to use some compatibilizing additives able to create a link between the polymer molecules and the particulate oxide and, at the same time, to hinder the agglomeration and sedimentation processes. The compatibilization treatment allows the use of aluminium oxide in nanometric size, avoiding agglomeration; however, the used compatibilizers are of organic origin and undergo significant degradation to the temperatures required for the HPPs processing process.  $\text{Al}_2\text{O}_3$  showed the ability to increase many mechanical properties by forming hard "islands" inserted in the polymer matrix, without compromising toughness. Aluminium oxide is available on the market in large quantities with different purities and particle sizes compared to modest costs. **Figure 1.5** shows the structure of  $\text{Al}_2\text{O}_3$  and the conglomeration phenomenon of  $\text{Al}_2\text{O}_3$  nanoparticulate.

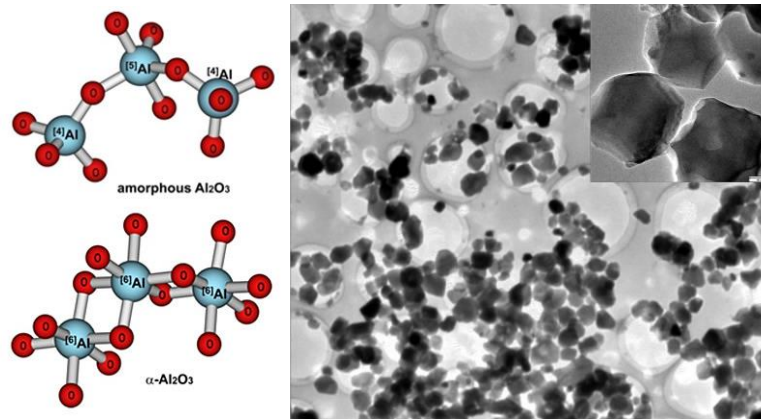


**Figure 1.5:** Alumina structure and TEM image of  $Al_2O_3$  nanometric particles

**Oxides mixtures:** The market of polymeric fillers often proposes mixtures of oxides to obtain properties mediated on those characteristics of a single oxide; sometimes, mixtures of oxides produce synergistic effects that improve dispersion and emphasize individual strengths. In particular, in our case, aluminium oxide was used in mixture with silicon oxide in two different premixed nanofillers. The product called COK 84 has a weight content of 16% of  $Al_2O_3$  and of 84% of  $SiO_2$  from fumed silica. The other selected mixture called SIRAL 40 has a weight ratio of alumina/silica of about 60/40 and it is produced by refining extractive materials.

**Hydroxides:** Hydroxides are ternary compounds formed from a metal, oxygen and hydrogen and have the general formula  $M(OH)_n$ , where  $n$  is the number of anion groups hydroxide ( $OH^-$ ) bound to the metal. The hydroxides dissolved in the water release the  $OH^-$  group and a positive metal ion. Hydroxymers are ternary compounds analogous to hydroxides, but they differ for the general formula which is of the  $MO(OH)_n$ . Hydroxides, unlike oxides, tend to have lower densities and hardness and they are generally found as secondary or alteration products. Two aluminium oxide hydroxide fillers, called Disperal 60 and Disperal P2 have been selected, obtained by refining boehmite, a bauxitic mineral with a high content of  $\alpha-AlO(OH)$ . Being of extractive origin, the two hydroxymers differ in content of the main components as well as the particulate size.

**Silicates:** Mineral fillers represent the largest family of reinforcing materials for polymer composites. The cataloguing is quite complex, because it can be carried out with multiple criteria, such as chemical composition, geological formation, geographic origin, etc. Here we will try to group the mineral fillers selected according to the most recurring names in the bibliography of polymer composite materials, neglecting the strict crystallochemical cataloguing. Fillers of mineral origin selected for this work are reported in **Table 1.4**.

**Phyllosilicates:** The phyllosilicates are silicates characterized by a stratified structure with tetrahedral symmetry, in which each tetrahedron tends to bind with three others through oxygen bridges. Members of this family generally have a lamellar or scaly appearance with well-defined flaws. They are based on  $SiO_4$  tetrahedral chains extended indefinitely side by side, joined together,

on the same plane, to form a ring link, generally of pseudo hexagonal symmetry. In three dimensions, the crystallographic structure of a phyllosilicate is constituted by two-dimensional planes of cyclic mesh tetrahedrons (T layers) superimposed on octahedral layers (O layers) consisting of bivalent and trivalent cations, mainly, Magnesium, Calcium, Sodium, Potassium, Iron and Aluminium. The atoms common between the two layers are the oxygens. An explanatory image of the crystalline structure of phyllosilicates is shown in **Figure 1.6**. **Table 1.5** shows a crystal-chemical classification of the mineral species belonging to the large family of phyllosilicates.

**Table 1.4:** Selected fillers of mineral origin

COMMERCIAL NAME OF CHARGES	FAMILY	MAIN COMPONENTS
DELLITE HPS	Phyllosilicates	Montmorillonite
PURAL MG 30	Phyllosilicates	hydrotalcite
PURAL MG 63 HT	Phyllosilicates	hydrotalcite
PANGEL S9	Phyllosilicates	Paligorskite
NYGLOS 8	Inosilicates	Wollastonite
ASPECT 4000	Inosilicates	Wollastonite
PDM 5B	Mica	Fluoroflogophite
PDM 7-325	Mica	Fluoroflogophite
TREFIL 1232	Mica	Flogophite

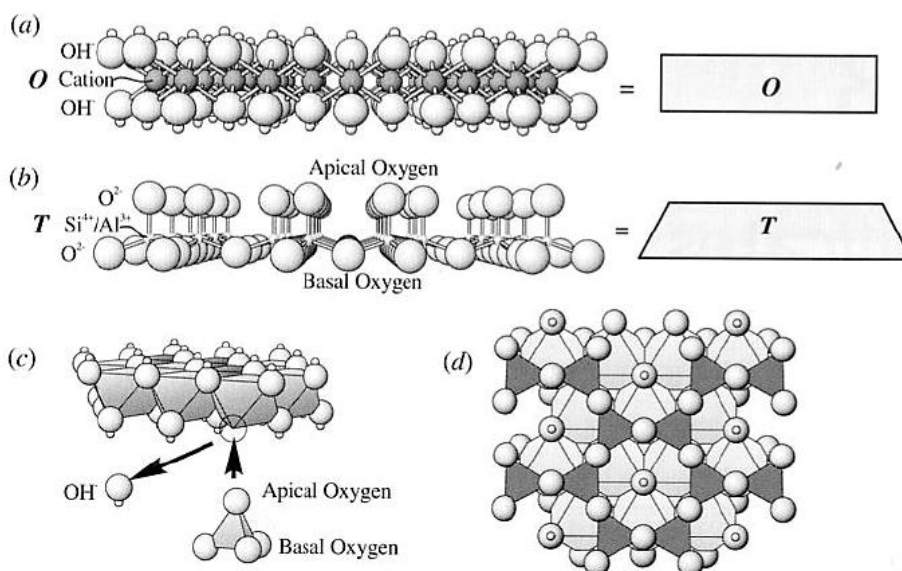


**Figure 1.6:** Crystalline structure characteristic of phyllosilicates



**Table 1.5:** Classification of mineralogical species of phyllosilicates

Caratteristiche cristalline		Gruppo	Sottogruppo	Principali specie mineralogiche
1:1 (T O)	carica elettrica del foglietto - 0	Caolinite - Serpentino	Caolinite	Caolinite dickite, nacrite, halloysite-10 Å, halloysite 7 Å,
			Serpentino (diottaedrico)	Crisotilo (orto-, clino-, para-), antigorite, lizardite
2:1 (T O T)	x ~ 0	Pirofillite - talco	Serpentino (triottaedrico)	Croenstedtite, greenalite, chamosite, amesite
			Pirofillite (diottaedrica)	Pirofillite
	x ~ 0.2 - 0.6	Smectite	Talco (triottaedrico)	Talco
			Smectiti (diottaedriche)	Montmorillonite, beidellite, nontronite, volkhonskoite
	x ~ 0.6 - 0.9	Vermiculite	Smectiti (triottedriche)	Saponite, hectorite, sauconite, leMBERGITE
			Vermiculiti (diottaedriche)	Vermiculiti diottaedriche
Vermiculiti (trioattedriche)			Vermiculiti triottaedriche	
Miche diottaedriche			Muscovite, (illite) paragonite,	
x ~ 1	Miche	Miche trioattedriche	Flogopite, biotite, lepidolite, (celadonite, glauconite)	
		Miche fragili diottaedriche	Margarite, clintonite	
2:1:1 (T O T + O)	x variabile	Clorite	Miche fragili trioattedriche	Anandite
			Cloriti diottaedriche	donbassite, sudoite
			Cloriti di-triottaedriche	cookeite, suddite, manandoite
			Cloriti trioattedriche	clinocloro, chamosite, sheridanite, ripidolite, brunsvigite, daphnite

**Montmorillonites:** In the field of the nanofillers, it is usual to refer clays as materials of sedimentary or volcanic origin that underwent geological transformations and are characterized by a generally stratified structure. Bentonite is a volcanic clay characterized by a tetrahedral symmetry layer structure; because of its heterogeneity characteristics, it is preferred for applications where extreme purities and properties are not required, such as in the building sector. Of greater interest are its components that are refined or created synthetically, finding use in many applications. Montmorillonite is one of the main components of bentonite and is characterized by a crystalline structure consisting of two silica tetrahedral layers which interlace an octahedral layer of metal oxides with shared edges. This crystalline structure represents the elementary particle of montmorillonite, characterized by a nearly two-dimensional geometry as it consists of irregularly shaped discs with thicknesses that generally do not exceed 1 nm and diameters ranging between 75 nm and 150 nm offering a contact surface of over 700 m<sup>2</sup> for every gram of product and thus conferring particular properties and behaviours. The elementary lamellae are collected in layers and held together by the forces of Van der Waals, but they can be easily separated in water. Each crystal of montmorillonite presents net negative charges on the surface and partial positive charges on the edges, due to the isomorphic substitution of some aluminium and silicon atoms with others of magnesium and aluminium respectively; these substitutions create an unbalance of charges in the crystalline structure which leaves negative charges on the surface. These negative charges are generally neutralized by sodium, calcium or magnesium ions, which are located in the lamellar interstices and are called exchangeable cations. In the case that the exchangeable cations are divalent hydrated

calcium ions, the binding with the crystalline layers of the montmorillonite is difficult to split due to the strong positive charge and it is therefore unlikely that a dispersion of the calcareous montmorillonite lamellae occurs due to simple hydration. In the event that the exchangeable cations are sodium, due to its greater size, during the hydration phase causes a swelling such as to cause exfoliation of the lamella layers. Furthermore, the hydrated ions of sodium due to the strong hydration progressively migrate into the interlamellar area, leaving the lamellae negatively charged, helping to promote separation due to electrostatic repulsion. This dispersion can be further facilitated by increasing the temperature and mechanically stirring the hydrated mixture. Being a natural product extracted from mines located in most of the terrestrial globe, montmorillonite can be distinguished in various types that differ in composition details. With the MMT the commercial prerogatives are surely satisfied, thanks to the discrete diffusion of the raw material and to the simplicity of the working processes. As regards the properties to be improved, montmorillonite shows in some cases an increase in resistance to mechanical stresses. MMT was probably the first nanofiller used for making polymer nanocomposites. Its use for a component of the transmission in the Toyota engine allowed to significantly improve the performances of traditional polymeric materials. Subsequently it was and still is one of the most investigated nanosized fillers. Therefore, montmorillonite appears to be an ideal candidate for the purposes of this study. **Figure 1.7** shows the images of an extractive montmorillonite mineral and a SEM image.

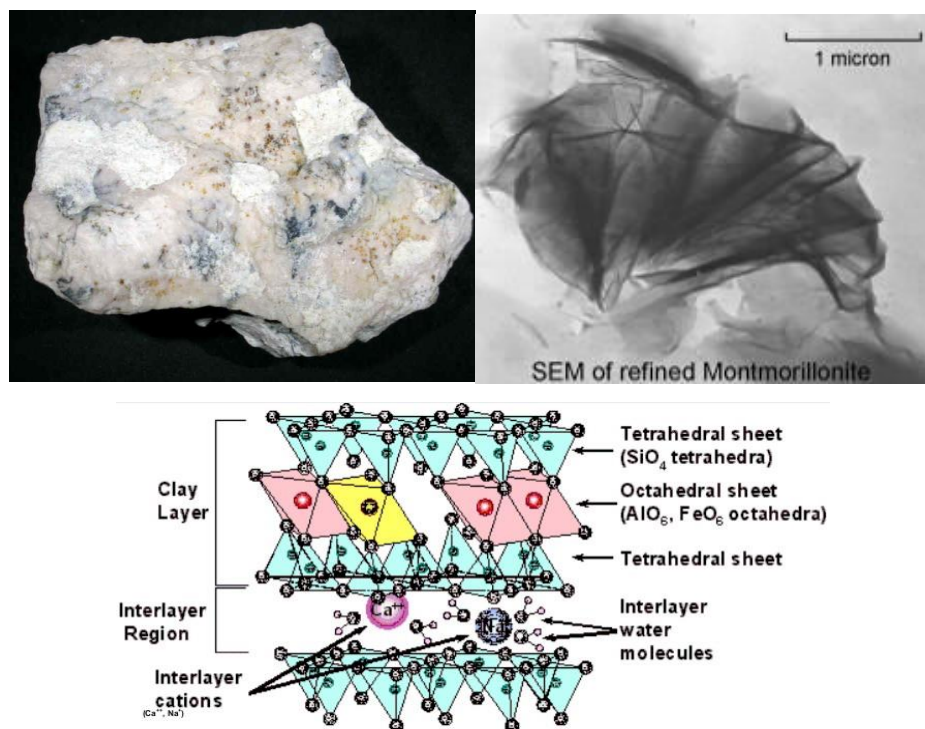


**Figure 1.7:** SEM images of the mineral and the crystalline structure of montmorillonite

The figure also shows the crystalline structure and the characteristics of self-exfoliating discoids. In particular, a MMT obtained was selected for the refining of bentonite of extractive origin of the Tuscan area without any potentially thermo degradable organic compatibilization.

**Mica:** Mica is a group of phyllosilicates with a closely related structure and characterized by a perfect flaking and similar chemical composition. These minerals crystallize all in the monoclinic system, with a tendency to form pseudo-hexagonal crystals; the characteristic flaking of the mica is linked precisely to the laminar arrangement of atoms like hexagonal sheets. The molecules of micas are formed by tetrahedrons in which a silicon atom is placed at the centre, while four oxygen atoms are arranged at the vertices, these tetrahedrons are joined by three of their vertices to form hexagonal meshes; the other chemical elements forming the micas are placed at the centre of an octahedron, while at the top of these octahedrons are atoms of oxygen or groups of hydroxyl groups; a layer of octahedrons is arranged between two layers of tetrahedrons. The vertices of the tetrahedrons and octahedrons are bound together. This set of three layers is called a "package". The alkali metals are arranged between each package. The forces that hold alkaline metals together in packets are weak, while the forces within the pack are strong. This fact would explain the flaking of the lamellar micas.

Phlogopitic mica is of particular interest for use as reinforcement fillers for polymeric composites. Both refined mineral phlogopites and modified phlogopitic structures will be tested; the latter are synthetically produced through the replacement of part of the interlamellar metals with halogenated compounds to give the fluorophlogopites. The characteristic phlogopithic packaging is shown in **Figure 1.8**.

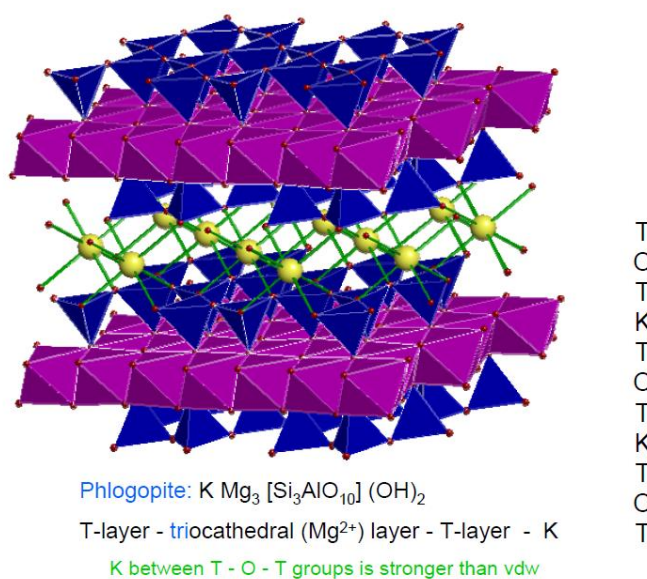


**Figure 1.8:** Crystalline structure characteristic of phlogopite mica

**Inosilicates** The inosilicates are silicates in which the tetrahedrons come together to form single or double chains, while the triple chains are very rare. The basic chemical formula for single chain fibrous silicates is of the  $\text{Si}_2\text{O}_6$  type whereas for the double chain silicates it has the  $\text{Si}_4\text{O}_{11}$  form. Two important constituents of the rocks, pyroxenes (single chain) and amphiboles (double chain), belong to the inosilicates family (**Figure 1.9**).

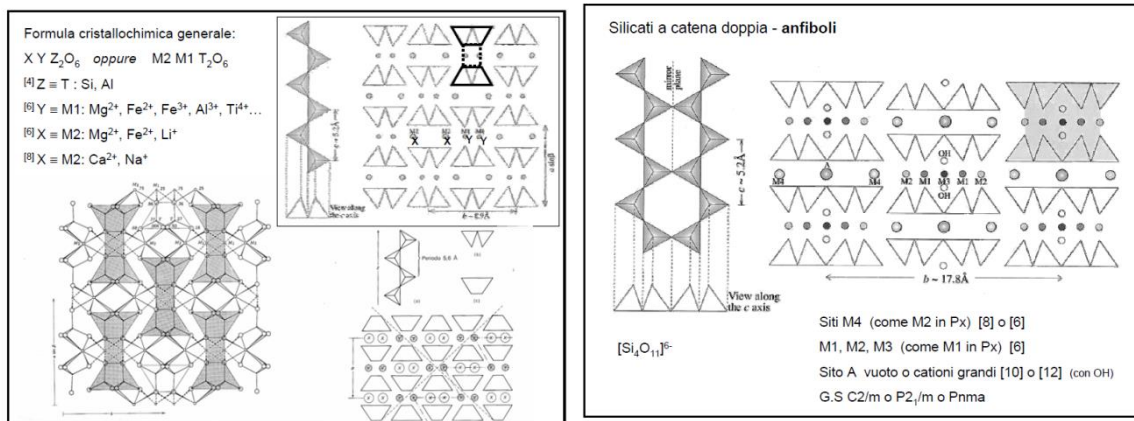


**Figure 1.9:** Rocks, pyroxenes (single chain) and amphiboles (double chain), belong to the inosilicates family

**Pyroxenes:** In their simple chain structure, each tetrahedron shares two of the four oxygens, so there is a Si:O ratio of 1: 3. The repetition period of the repeating  $\text{SiO}_3$  unit within the chain is two, that is 5.2 Å. Pyroxenes have the general formula  $\text{XYZ}_2\text{O}_6$  where:

X represents  $\text{Na}^+$ ,  $\text{Ca}^{2+}$ ,  $\text{Mn}^{2+}$ ,  $\text{Fe}^{2+}$ ,  $\text{Mg}^{2+}$  and  $\text{Li}^+$

Y represents  $\text{Mn}^{2+}$ ,  $\text{Fe}^{2+}$ ,  $\text{Mg}^{2+}$ ,  $\text{Fe}^{3+}$ ,  $\text{Al}^{3+}$ ,  $\text{Cr}^{3+}$  and  $\text{Ti}^{4+}$

Z represents  $\text{Si}^{4+}$  and  $\text{Al}^{3+}$  in the tetrahedral sites of the chains.

The most common pyroxenes can be represented by the closed system Enstatite ( $\text{MgSiO}_3$ ), Ferrosilite ( $\text{FeSiO}_3$ ) and Wollastonite ( $\text{CaSiO}_3$ ). The chemical formula of the pure elements is simplified with respect to the general formula since it becomes divisible by 2. The pyroxene structure is based on single  $\text{SiO}_3$  chains that develop parallel to the c axis. The chains contain two cationic sites, one with coordination 6 (M1) and one with coordination 8 (M2). The cations located at site M1 are all bound to the oxygens of two of the  $\text{SiO}_3$  chains, forming a t-o-t (tetrahedron-octahedron-tetrahedron) configuration. The silicon is placed at the centre of the tetrahedron, at whose vertices are four oxygen atoms united by two vertices to create indefinite chains characteristic of inosilicates. The individual chains are joined by different characteristic elements of the individual species of pyroxenes, among which we can mention: iron, magnesium, manganese and, in the centre of the tetrahedron, besides silicon, aluminium. These elements can be replaced by creating a series of innumerable isomorphous varieties. Of particular interest are the wollastonites, a particular type of

single chain inosilicate characterized by remarkable thermal stability and crystalline structure particularly suitable to form a robust interface with the polymer matrix. The long chains formed by links of three tetrahedrons joined together by a vertex improve the adhesion and constitute a fibrous reinforcement for the polymer. **Figure 1.10** shows the particular crystalline structure of wollastonite and the high aspect ratio with a TEM image.

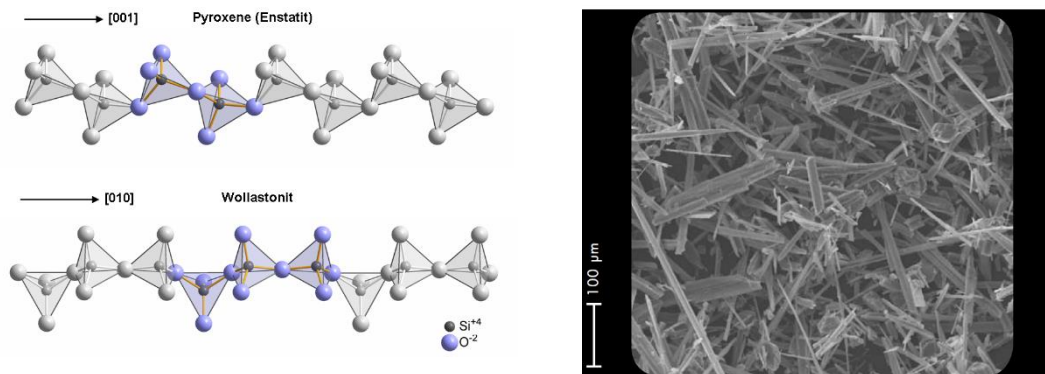


**Figure 1.10:** Crystalline structure characteristic of wollastonite and TEM image which highlights the fibrous appearance

**Paligorskiti:** Paligorskite is a mineral originating from the sedimentation of products of volcanic origin that can chemically be called a magnesium and aluminium phyllosilicate with formula  $(\text{Mg, Al})_2\text{Si}_4\text{O}_{10}(\text{OH}) \cdot 4(\text{H}_2\text{O})$ . The main characteristic is represented by the crystalline structure that can be described as a "quincunx", that is an arrangement of five objects, arranged so that four are on the sides and a fifth is in the centre of the area of the rectangle thus formed; the floors are separated by parallel free channels. This pseudo-chain structure means that the arrangement of the paligorskite is not the classic flat plates, common to other clays, but is of the needle type. The acicular structures of paligorskite have an average length between 1  $\mu\text{m}$  and 2  $\mu\text{m}$ , and a width of 0.01  $\mu\text{m}$ ; they contain open channels with dimensions of 0.36 nm x 1.06 nm, along the entire length of the "fiber" axes. These particles are arranged to form porous aggregates with a dense network of channels, which explains the high degree of porosity and its low density due to a large amount of empty spaces. The large surface area combined with the high porosity makes it possess considerable absorption properties. The product of the particularization and refining of paligorskite is called sepiolite and is widely used for its high absorption capacity. Sepiolite is fairly diffused in some sites in Spain, Africa and North America, allowing low costs and modest processing difficulties. The main effect of the sepiolite nanofiller should be found in the improvement of the mechanical characteristics since the fibrous structure of this filler tends to form cross-links that act as reinforcement for the polymer matrix; this effect microscopically should also increase resistance to shocks and fatigue cycles. Sepiolite is therefore a suitable filler to be tested for the objectives of this study. **Figure 1.11** shows the images

of a sepiolite extract mineral and a SEM image; the crystalline structure and an explanatory image of the quincunx structure are also reported.

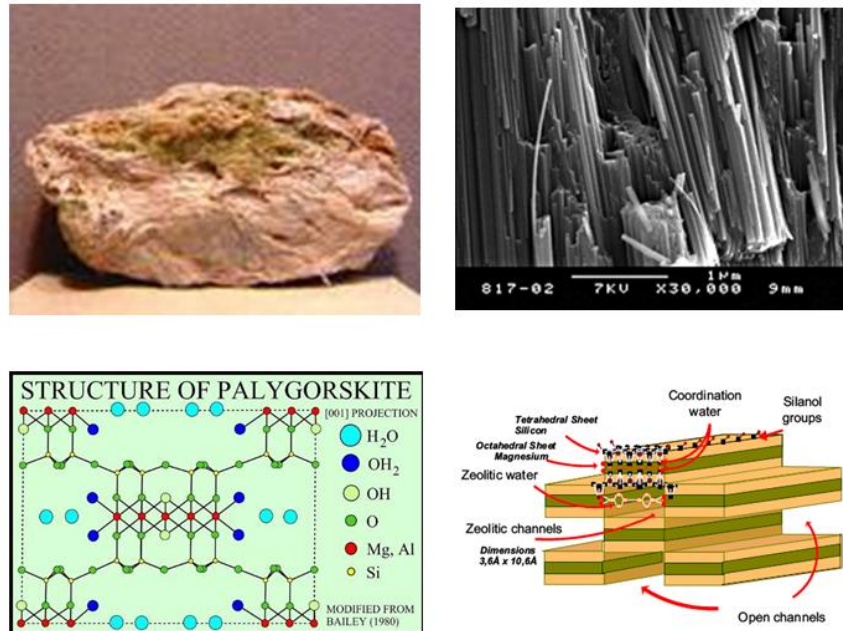


**Figure 1.11:** Images of the mineral and crystalline structure of sepiolite

#### 1.4 Fiber reinforced nanostructured (FRNS) materials

Composite materials have largely demonstrated their potential in terms of weight reduction, improved corrosion and fatigue resistance, and design flexibility. Autoclave processing of long-fiber-reinforced composites ensures the production of high quality parts that have all the above-mentioned advantages. The high cost of the equipment, raw materials, and long processing times involved have restricted the application of high performance composites to aerospace and aeronautic applications where performances and light weight are more important than the cost. Recent developments in aeronautical, transportation, and commodity applications have made this class of material comparable to metals and ceramics.

The diffusion of nanocomposites is necessary to develop new correlations and new models for the processes. Owing to the recent developing of these new materials, few data and processing model are yet available. Most of these models refer to the injection moulding of thermoplastic layered silicate nanocomposites; in this case, it has been shown that the available processing models can be slightly modified to take into account the changes in the rheological behaviour caused by the use of layered silicates, analogous attempts were made on modelling liquid moulding processes with nanocomposite resins. It has been pointed out that the most critical parameters to obtain a valid model of nanocomposite processes are the rheological behaviour, which is strongly influenced by

the presence of the nanofillers, the diffusion of the resins in the fiber bed, and the determination of the main physical properties of the nanocomposite resin. Regarding the materials, many chances of improvement exist. For high performance applications, for example, there is a need to have injectable and, at the same time, toughened resin. For low performance applications, there is the need of having fast, reliable and economic materials and compounds. But, the most important development is represented by the use of nanotechnologies applied to composites. Nanotechnologies can represent a great opportunity for composites.

In this field, there are still opened many possibilities. The current research is more dedicated to nano tailored fiber-reinforced composites that can offer multifunctional performances, whereas nanocomposite resins can provide new and improved properties to composite parts. Researchers and companies usually practice this bottom-up approach in designing, processing, and manufacturing fiber-reinforced composites. When designing a composite, the material properties are tailored for the required performance at all length scales. From the choice of the adequate matrix and fiber materials and the layup of the laminate (meter scaled) up to the design and optimization of the fiber/matrix interface and interphase (micro scaled), the integrated approach used in composites processing is a remarkable example in the successful use of the bottom-up approach. When to these levels, a nanoscale one is added, applying nanotechnology to composite materials, tremendous opportunities for innovative approaches in the processing, characterization, and analysis/modelling of this new generation of composites can be found.

Considering that nanosized particles usually tend to stay in agglomerates because of their huge surface area and, on the other hand, that the exploitation of their benefits is possible only if they are evenly dispersed into the matrix, it is clear that the most important challenge in nanocomposite development is the study of the dispersion. The development and production of fiber-reinforced composites based on nanocomposite matrices (fiber-reinforced nanocomposites, FRN) are basically performed utilizing the same techniques commonly employed for commercial FRPs.

The advantage of this approach comes from the fact that only well-established techniques are utilized for the production of nanocomposites, especially those that can produce large volume per hour material, and for the production of composite laminate. Nonetheless, this approach can lead to some problems all connected to the different rheological behaviour of a nanocomposite with respect to the neat resin, which can affect the flowing rate and the homogeneity of the impregnation effectiveness in all the techniques.

Beside the well approaches that can be considered for the improvement of mechanical properties in fiber-reinforced composites (selection of fiber reinforcements that optimized properties, toughening of the matrix, and optimization of the fiber–matrix interface to enhance the stress-transfer properties), attempts to incorporate both nanoscale and microscale reinforcements have been extensively

considered during the last two decades. Even if the replacement of FRPs by nanocomposites can be regarded as improbable because of the highly developed and well-established conventional fiber reinforcement of polymers and their still unsurpassed level of material properties, the incorporation of nanofillers to give three-phase composites is expected to improve specific mechanical properties such as fracture toughness and the compressive strength.

## **1.5 Aim of the study**

The realization of nanocomposite materials with a techno-polymer matrix is not however restricted to the economic aspect, which represents a necessary condition, but allows to obtain materials with modified properties according to the specific use for which they are intended. From the bibliography, it has been seen that, with regard to traditional polymers, it is possible to intervene with the use of nanofillers to modify some fundamental characteristics, such as elastic modulus, strength and deformation even when temperature changes, toughness, rheological, tribological properties, and other specific properties. The scarce availability of scientific articles related to the use of nanoparticles in technical polymer matrices does not allow establishing a certain correlation between the realization of the composites and the achievement of certain properties. For this reason, it is necessary an empirical approach that allows to understand the general effect of the use of some types of nanofillers. On the basis of the considerations previously expressed, the amount of potentially usable fillers is decidedly broad and can be reduced only by theorizing with the imposition of some discriminating prerogatives. For example, a prerogative is imposed by the process conditions, because the selected polymers are high melting and, if extrusion and melt intercalation processes are used, they must be processed at temperatures between 350 and 400 °C; at such temperatures, some fillers may show thermo degradation phenomena, typical of the filler or related to possible compatibilization treatments carried out to make the filler more "affine" to the traditional polymeric matrix. If the technical parameters of filler show thermal degradation phenomena at the process temperatures, then they automatically exclude the use of that filler for the application. In a similar way, a selection of the charges can be made based on the bibliography on traditional polymers that show some affinity with the techno polymer, going to exclude the types of fillers that have repeatedly and absolutely shown negative results in applications with similar characteristics. Also reinforcing materials that showed irrefutably opposite effects to those sought within this study may be excluded. This last step presupposes the definition of the characteristics to be pursued and therefore the modifications of the properties that are to be realized. With reference to the considerations previously expressed, it is possible to define some characteristics to be pursued in the realization of the technopolymer based nanocomposites. The high cost of the matrix induces to use high percentages of filler in order to reduce the costs of the material. Furthermore, an increase



in the elastic modulus with relative increase in yield strength is desirable. These general objectives are partially realized also by the companies producing masterbatches preloaded with fiberglass and carbon fiber. However, premixed matrices are marketed at prices that do not take into account the abatement that should be achieved thanks to the low cost of the additives fibers. Moreover, these composite matrices loaded with high fiber contents certainly show values of the Young modulus considerably higher than the corresponding pure matrices, but they pay this increase with a considerable loss in the field of deformations; this reduction can be related to a loss of tenacity and probably also to decrease in resistance to instantaneous loads or cyclic stresses. The almost homogeneous and micrometric order of the reinforcements also leads to suppose a high probability of induction of the damage phenomena to the composite in the interface areas attributable to pull-out / debonding or fiber fracture.

The use of nanofillers could carry out its action both in replacement and in synergy with the microfibers currently used. The use of nanocomposite materials will therefore have to be developed both on pure matrices to understand if there are more effective reinforcements than those currently in use, but also to understand the absolute effect and compatibility of the reinforcements used to evaluate their synergistic use with the pre-loaded matrices. The creation of materials that exhibit high values of the elastic modulus and, at the same time, deformations sufficiently high to show stubborn behaviour, could represent the solution for currently prohibitive uses. This realization could also tolerate compromise solutions in many ways; the quantities of micro and nanofiller could be manipulated to obtain the management of modulus and deformation, generally antithetical properties, realizing materials with characteristics tailored to specific applications. Furthermore, the cost factor should not be overlooked, so that the possibility of increasing the share of the reinforcements with a corresponding reduction in the costs of the material, even against a tolerable decrease in some properties, could be considered a positive result. Finally, the behaviour at high temperatures must be evaluated as the correlation between the properties measured at room temperature with those at temperatures of 150-200 °C is not immediate. It is reasonable to suppose that one can obtain a levelling of the properties of the composites in the measurements at high temperatures, so that the criteria for selecting the materials could be economic rather than based on a performance nature. In conclusion, it can be said that the objectives of the research in question are not absolute but rather pursue the possibility of obtaining a wide versatility and management of the properties of nanocomposite materials with a techno-polymeric matrix, that allows their use in differentiated applications. The knowledge of the effect of the various types of nanofillers could allow in this way to produce, from time to time, materials with properties for each specific use. Gaskets for hydraulic systems subject to high temperatures and contact with corrosive chemical agents or parts of moving parts or gears applied under severe working conditions for temperature and environment

can be used immediately. Many other special uses can arise precisely from the characteristics and properties of composite materials with a techno-polymer matrix.

The aims of the present study can be identified in the production and characterization of innovative materials obtained with the use of HPPs opportunely blended, reinforced and filled, in order to improve some properties for specific applications. Main properties to improve could be considered the thermal stability and the mechanical properties at high temperature in order to increase stiffness, tensile strength or toughness, especially in severe conditions like high temperature and corrosive environment. Another main aim of the study will concern the cost problems: the reduction of price of these materials could allow to access to composites based on High Performance Polymer matrices to a large range of industrial sectors that currently consider HPP not affordable.

The activities to carry out to achieve the aims involve the research of bibliographic literature about HPP matrices, reinforcement fibers, fillers, composites and nanocomposites. Then it will follow a phase of selection and finding of polymeric matrices belonging to different families like Polyaryletherketones (PAEK), Polyetherimides (PEI), Polyamide-imide (PAI), Polyimides (PI), thermoplastic polyimides (TPI), Polysulfones (PS), Polybenzimidazole (PBI), Polyamides (PA), Aromatic polyamides (PARA), Fluoropolymers (FP) and others. The selection will be done based on criteria like properties, costs, processability, versatility in applications, compatibility, etc. Afterwards a thermal characterization and other test necessary to the definition of process parameters needed for the realization of samples of HPP matrices it will be done. The samples produced will be used to perform the thermo-mechanical characterization of the matrices. The results of the tests will be used to understand the behaviour of the materials at different temperatures with particular attention to high range. The later activities will involve the study and the realization of HPPs polymeric blends and their thermo-mechanical characterization.

The next activity will be focused on investigation on the reinforcement fibers for HPPs with particular attention to the compatibility fiber/matrix. It will be necessary to make thermal characterization of the fibers or master-batches with high ratio of fibers before the production of samples of composites fiber-reinforced (FR) based on HPP matrices. These materials will be characterized in order to their thermo-mechanical properties. The same investigation procedure will be used to study the FR materials produced with HP polymeric blends.

The most relevant phase of activities will concern the introduction of nanotechnology to further improvement of material properties. After an accurate research of bibliographic literature about micro/nanofillers and nanocomposites, an adequate number of nanofillers will be selected, and a series of new polymer-based nanocomposites will be developed. Thermal characterization will be used to understand the processability of nanocomposites based on HPP matrices. After the production of nanostructured materials, the thermo-mechanical characterization will show the effect

of the nanoreinforcements on the matrices. The knowledge acquired will permit to design hybrid materials; the combined effect of blending HPP matrices, fiber reinforcing and nanostructuring the materials will allow to produce materials with various distinctive properties tailored for specific applications. Moreover, the addition of fibers and filler, at a considerably lower price respect to the matrices, could decrease the cost of the materials. The expected results at the end of the three years research will be: the development and the complete characterization of new nanocomposite thermoplastic matrices and their composites. Such materials will be able to retain their properties at higher temperatures and will be a valid and less costly alternative to current high-performance engineering plastics. Another aim of this thesis will be to put the basis for the development and optimization of the processing technologies for the production of such materials.

## 1.6 References

- Alivisatos, A.P., *Endeavour*, 21 (1997), 56-60.
- Bloch, F., *Z.Physik* 52, 555 (1928).
- Feynman, R.P. – There's plenty of room at the bottom – American Physical Society – 1960 - Caltech's Engineering and Science
- Fink, JK, High Performance Polymers, in *Plastics Design Library*, 2008, William Andrew.
- Hines, M. A.; Guyot-Sionnest, P.; *J.Phys.Chem.B* 1998, 102, 3655.
- Li, L.; Hu, J.; Yang, W.; Alivisatos, A. P. *Nanoletters* 2001, 1, 349
- Malko, A. V.; Mikhailovsky, A. A.; Petruska, M. A.; Klimov, V. I. *J.Phys.Chem.B* 2004, 108, 5250.
- Narayanan, R.; El-Sayed, M. A. *J.Am.Chem.Soc.* 2004, 126, 7194.
- Ramakrishna M.V., Friesner, R.A. *Phys.Rev.Lett.* 67, 629 (1991).
- Rose, J. B. European Patent 63, 874 (1983); *Chem. Abstr.* 1983, 98, 180081
- Samorjay, G.A. *Introduction to surface chemistry and catalysis* (1994), Wiley, New York.
- Vargas, J. M.; Socolovsky, L. M.; Zanchet, D. *Nanotechnology* 2005, 16, S285
- Wannier, G.H. *Phys.Rev* 52, 191 (1937).
- [www.aerosil.com](http://www.aerosil.com) – Fumed silica products
- [www.sasol.com](http://www.sasol.com) Internet site of "Sasol GmbH"
- [www.laviosa.it](http://www.laviosa.it) Internet site of "Laviosa Chimica Mineraria spa",
- [www.tolsa.com](http://www.tolsa.com) Internet site of "Grupo Tolsa",
- [www.topy.co.jp](http://www.topy.co.jp) – Topy Industries Limited – Japan
- [www.nycominerals.com](http://www.nycominerals.com) – Producer of wollastonite
- [www.sachtleben.de](http://www.sachtleben.de) – Sachtleben Chemie GmbH
- [www.mknano.com](http://www.mknano.com) – Quality Nano Products Supplier - MK Impex Canada
- [www.grupoantolin.com](http://www.grupoantolin.com) – Nano Fiber Producer

## CHAPTER 2: HIGH PERFORMANCE POLYMERIC MATRICES (HPPs)

### 2.1 Selected neat matrices

The high cost of technopolymeric matrices leads to the use of high charge percentages to reduce material costs. Furthermore, an increase in the elastic modulus with relative increase in yield strength is desirable. These general objectives are partially realized also by the companies producing the matrices that also market masterbatches preloaded with fiberglass and carbon fiber. However, premixed matrices are marketed at prices that do not take into account the abatement that should be achieved thanks to the low cost of the additives fibers. Moreover, these composite matrices loaded with high fiber contents certainly show values of the Young modulus considerably higher than the corresponding pure matrices, but they pay this increase with a considerable loss in the field of deformations; this reduction can be related to a loss of tenacity and probably also to behaviours related to it such as the decrease in resistance to instantaneous loads or cyclic stresses. The almost homogeneous and micrometric order of the reinforcements also leads to suppose a high probability of induction of the phenomena of damage to the composite in the interface areas attributable to pull-out/debonding or fiber fracture. The use of nanofillers could carry out its action both in replacement and in synergy with the microfibers currently used. The experimentation of nanocomposite materials will therefore have to be developed both on pure matrices to understand if there are more effective charges than those currently in use, but also to understand the absolute effect and compatibility of the charges used to evaluate their synergistic use with the pre-loaded matrices. The creation of materials that exhibit high values of the elastic modulus and at the same time deformations sufficiently high to show stubborn behaviour could represent the solution for currently prohibitive uses. This realization could also tolerate compromise solutions in many ways; the quantities of micro and nano charge could be manipulated to obtain the management of modulus and deformation, generally antithetical properties, realizing materials with characteristics tailored to specific applications. Furthermore, the cost factor should not be overlooked, so that the possibility of increasing the share of the charge with a corresponding reduction in the costs of the material even against a tolerable decrease in some properties could be considered a positive result. Finally, the behaviour at high temperatures must be evaluated as the correlation between the properties measured at room temperature with those at temperatures of 150-200 °C is not immediate. It is reasonable to suppose that one can obtain a levelling of the properties of the composites in the measurements at high temperatures, so that the criteria for selecting the materials could be of an economic rather than a performance nature [DeMeuse & Jaffe, 1988; DeMeuse & Jaffe, 1989; DeMeuse & Jaffe, 1990; Hsieh, Tiu and Simon, 2000; Demeuse, 2014; Kemmish, 2011; Mittal, 2011].

In conclusion, it can be said that the objectives of the research in question are not absolute, but rather pursue the possibility of obtaining a wide versatility and management of the properties of nanocomposite materials with a techno-polymeric matrix that allows their use in differentiated applications. The knowledge of the effect of the various types of nanofillers could allow in this way to produce from time to time materials with properties made to measure for each specific use. Gaskets for hydraulic systems subject to high temperatures and contact with corrosive chemical agents or parts of moving parts or gears applied under severe working conditions for temperature and environment can be used immediately. Many other special uses can arise precisely from the characteristics and properties of composite materials with a techno-polymer matrix

Technical polymers and polymers with high and very high performance are born to compensate for the deficiencies of traditional basic polymers (PE, PP, PS, PVC, etc); the fields of application are many and concern uses for which traditional polymers cannot be used. However, the advantages of workability, productivity, lightness, etc. Polymers compared to metal or ceramic materials are attractive for many industrial applications. In **Figure 2.1** and **Figure 2.2** some functional elements made with high performance polymers are reported.



**Figure 2.1:** Elements produced with technical polymers and HPPs

Classic examples are the uses in automotive or appliances with parts of bodywork, casing and gears of household appliances or mechanics up to more severe applications; the use of polymers in aeronautics, in the refining industry, in robotics and in aerospace has become indispensable for various reasons. In addition to those previously introduced, it is important to consider the versatility of HPPs that can withstand relatively high temperatures, in corrosive environments, can change their behaviour depending on the operating conditions (glass transition), can offer thermal insulation properties and electric, etc. The versatility of technical polymers and HPPs is progressively subtracting "market shares" to metallic, ceramic and natural materials. Below are some pictures of various elements made with HPPs for various uses (**Figure 2.2**).



**Figure 2.2:** *Tubing for special uses, gears and impeller in fiber-reinforced HPPs, gaskets, bearings, membranes and valves made with HPPs*

Thermoplastic polymers currently occupy a substantial market segment of materials with multiple applications. However, the use of the most commonly used polymers, such as polyethylene (PE, HDPE or LDPE), polypropylene (PP), polyvinylchloride (PVC), polystyrene (PS or EPS), polyethylene terephthalate (PET), is impossible in applications that require severe conditions of use, such as high temperatures or particularly corrosive environments. Recently, specific polymers have been developed for such purposes, able to preserve good mechanical properties even at relatively high temperatures and to resist to the chemical-physical attack in corrosive environments; these particular materials are called techno polymers (TP). Polyetheretherketone (PEEK), polyetherimide (PEI) and polyethersulfone (PES) belong to the technopolymer category (**Figure 2.3**).

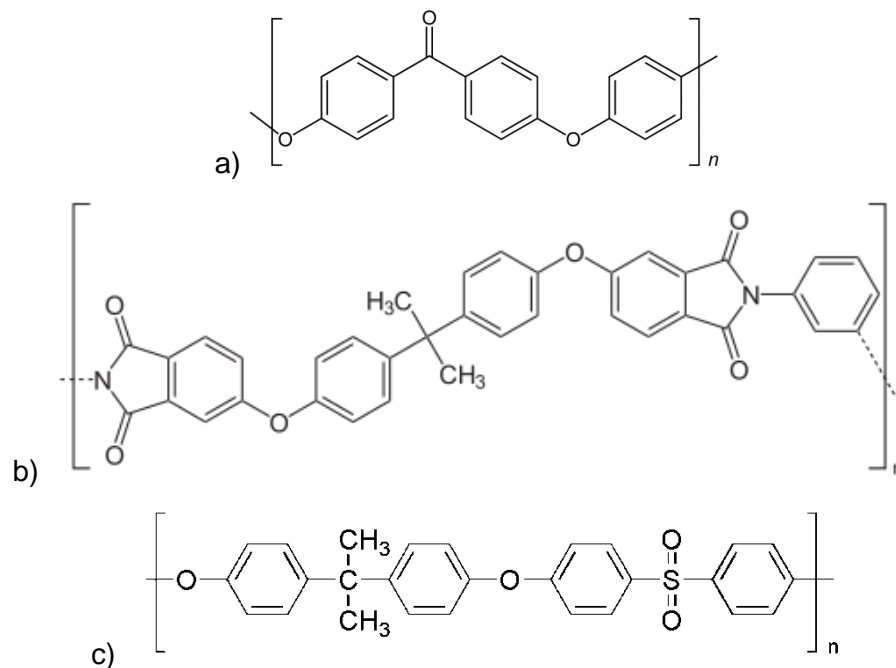


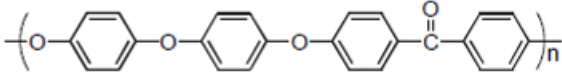
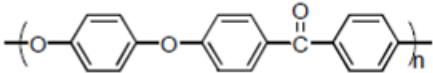
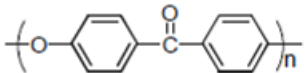
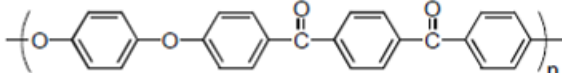
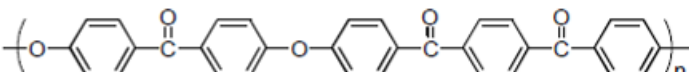
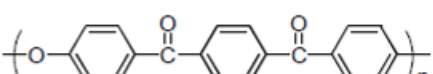
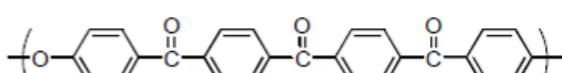
**Figure 2.3:** Molecular structure of the repeating unit of polyetheretherketone (PEEK) (a), polyetherimide (PEI) (b) and polyethersulfone (PES) (c)

### 2.1.1 Polyetheretherketone (PEEK)

The family of technical polymers to which PEEK belongs takes the name of polyaryletherketone (PAEKs). The thermoplastic polymers of this family are all unified by thermal stability, resistance to chemical attack, good mechanical resistance in a wide temperature range. In addition, PAEKs show good behaviour in fire resistance tests and good electrical performance. In general, these polymers, unlike the usually amorphous PAEKs, are semi-crystalline and therefore have a good resistance to solvents. The repetitive unit structure formulas of some technopolymers of the PAEKs family are shown in **Figure 2.4**, together with the relative glass transition and melting temperatures. [Staniland, 1989; Lakshmana, 1995; Dahl & Jansons, 1995; Harris et al., 1987; Marks, 1964; Starkweather, 1987].

These materials can also be used with exposure to corrosive agents, such as acids and strong bases or to severe conditions, such as condensation cycles, radiation and exposure to fumes. These characteristics allow the use of technopolymers in applications unthinkable for traditional polymers; many applications, nowadays prerogative of metallic or ceramic materials, could therefore be replaced by TPs with multiple advantages, such as simplicity of processing, mechanical behaviour and resistance to corrosion. The production of PAEKs requires the use of technologies and process plants with special characteristics. In fact, due to the crystallinity and the consequent low solubility, combined with the high melting temperature, make it difficult to produce polymers with a high molecular weight without considering reactions in extreme conditions.



Polymer	Structure	T <sub>g</sub>	T <sub>m</sub>
PEEEK		129	324
PEEK <sup>a</sup>		144	334
PEK <sup>b</sup>		163	361
PEEKK		154	358
PEKEKK <sup>c</sup>		173	371
PEKK		165	391
PEKKK		175	439

**Figure 2.4:** Molecular structure of the repeating unit of some TPs of the polyaryletherketone family (PAEKs)

Polyaryletherketones (PAEKs) are high-temperature, crystalline, true thermoplastics. The glass transition temperature (T<sub>g</sub>) is typically 140–180 °C, although higher values are possible by copolymerisation with rigid units (e.g., sulfone, biphenyl). Melting point (T<sub>m</sub>) values are typically 330–390 °C. At processing temperatures, viscosity is similar to many other thermoplastics, and typical thermoplastic processing techniques can be used. The materials can be 30–40% crystalline, which results in good resistance to chemicals and fatigue. PAEK offer a combination of properties that goes far beyond temperature resistance. They include resistance to wear, chemical environments, hydrolysis, sterilization and fire together with biocompatibility, purity, low smoke and toxic-gas generation and electrical performance. They are produced by a range of companies, including Arkema, Evonik, Gharda, Jilin Super Engineering Plastics, Polymics, Solvay and Victrex. The latter is the leading supplier with the longest product history. PAEK are found in almost all industry sectors, and are available as pure resins, compounds, blends, composites, films, coatings and medical grades. PAEK are commonly described in terms of an ‘E’ (ether group) and a ‘K’ (ketone group). For all *para* structures, temperature performance increases as the ratio of relatively polar and inflexible K units increases. The most common PAEK are polyetheretherketone (PEEK), polyetherketone

(PEK), polyetherketoneetherketoneketone (PEKEKK) and Polyetherketoneketone (PEKK) [Bonner, W. H. 1962; Goodman et al. 1964; Rose, 1983].

The synthesis of PEEK is generally carried out through a nucleophilic aromatic substitution reaction, as shown in **Figure 2.5**.

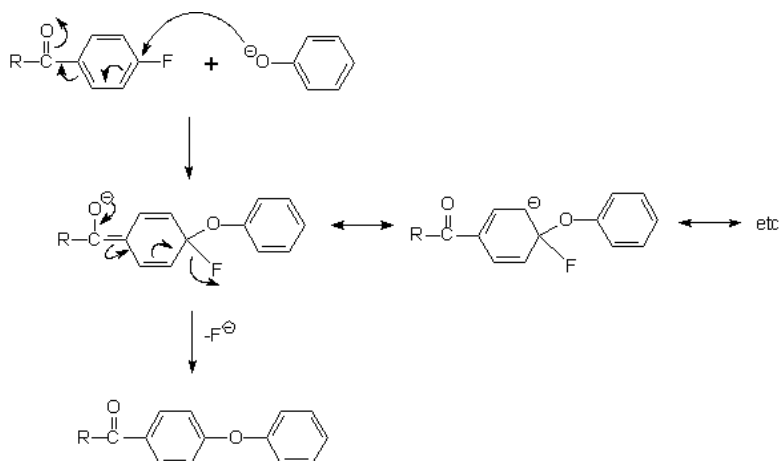


**Figure 2.5:** Nucleophilic aromatic substitution reaction scheme for the synthesis of PAEKs

Another method of synthesis is the electrophilic acylation of the aromatic ethers called Friedel-Crafts reported in **Figure 2.6**.

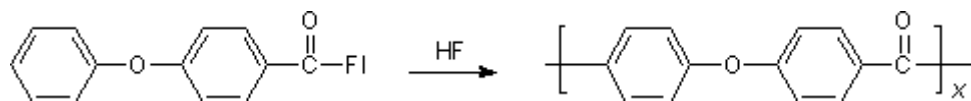


**Figure 2.6:** Friedel-Crafts reaction scheme

Other methods used to produce PEEK with high molecular weights involve the use of trifluoromethanesulfonic acid (Rose) or diphenylsulfone (Victrex), in the presence of catalysts, to obtain the reactions schematized in **Figure 2.7**, respectively at points a and b.

Other more recent methods of synthesis considered an approach that uses soluble precursors; examples of this type of method are the low-temperature ones proposed by McGrath in DMSO and by Pandya in NMP. **Figure 2.8** summarizes the reaction patterns [Percec and Clough, 1994; Percec et al., 1993; Mohanty et al. 1984].

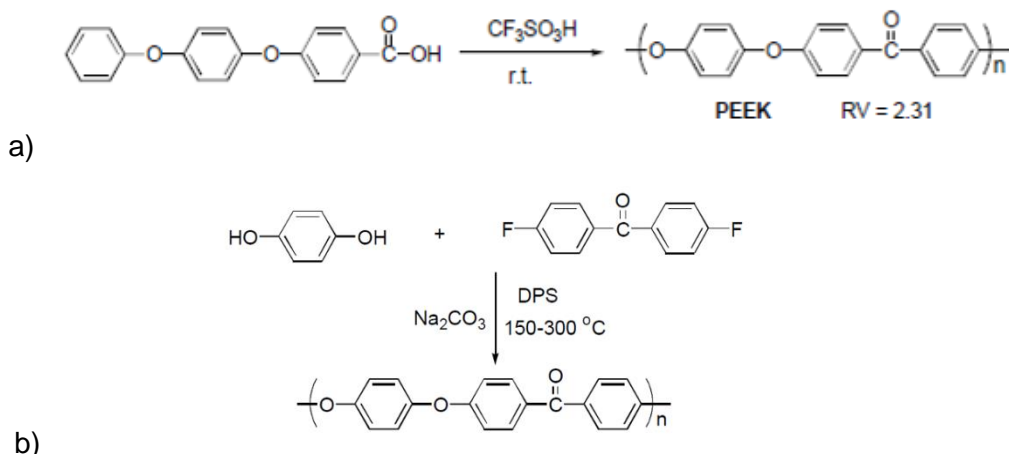


**Figure 2.7:** Reaction scheme for the synthesis of high molecular weight PEEK with Rose process (a) and Victrex process (b).

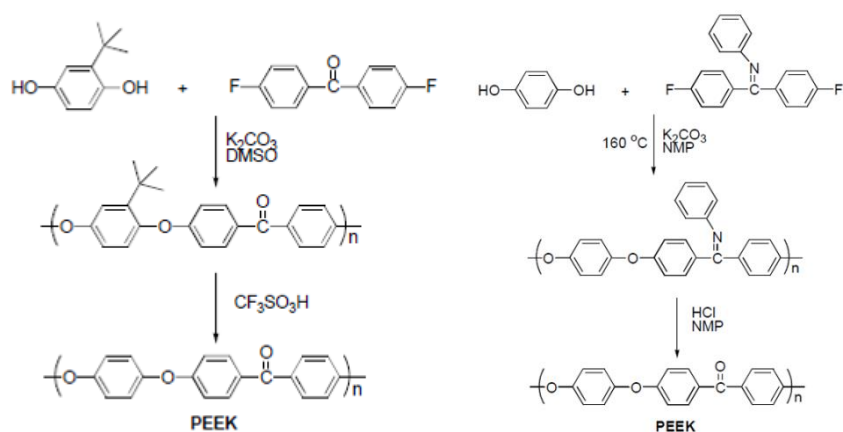


**Figure 2.8:** Scheme of reactions for the synthesis of PEEK with soluble low temperature precursors

Alternatively, PEKK can be obtained by condensation of isophthaloyl chloride and/or terephthaloyl chloride with isolated intermediates such as 4,4'-diphenoxyterephthaloylphenone and 4,4'-diphenoxyisophthoylphenone. These polymerizations yield cleaner polymers, especially in the presence of  $\text{AlCl}_3$  complexed with a basic co-agent. The copolymer was prepared by Gay and Brunette at DuPont from the isolated intermediates, 1,3-bis(*p*-phenoxybenzoyl)benzene with terephthaloyl chloride, and 1,4-bis(*p*-phenoxybenzoyl)benzene with isophthaloyl chloride. This perfectly alternating copolymer of *meta* and *ortho* phenylene group has high  $T_g$  (166°C) and low  $T_m$  (332°C), which is desirable for facile processing and high heat deformation resistance.

Various attempts have been made to use cheaper chloromonomers. For example, a recent patent describes the production of PEK from the alkali metal salt of 4,4'-hydroxychlorobenzophenone. PEKK is produced by an electrophilic process from diphenyl ether and phthaloyl chlorides. It is one of the few PAEK that would be difficult to make by nucleophilic routes because of the complexity of

the monomer required. The high  $T_m$  of linear, 100% *para* PEKK means that it is made from terephthaloyl (T) chloride and isophthaloyl chloride (I). Crystalline PEKK is typically 80:20 T/I, whereas the amorphous grades used for thermoforming are 60:40 T/I. The isophthaloyl groups limit the size of crystals and hence reduce their  $T_m$ , together with crystallisation rate and overall crystallinity. There is also an electrophilic route to PEEK from phenoxyphenoxybenzoic acid and PEKEKK has previously been made using electrophilic processes.

Product forms include powders and granules, fine powders, compounds with a wide range of fillers and reinforcements, continuous-fibre composites, films, fibres, coating dispersions, stock shapes and foams. There are a wide range of speciality products, including wear, electrostatic-dissipative, high-purity, coloured, radio-opaque, antimicrobial, laser-markable, and authentication grades. Some of these are produced by resin manufacturers, but others are available from specialty compounders (e.g., RTP, Sabic LNP). PAEK can be blended with a range of other polymers (although the blend components must have sufficient thermal stability). Most blends are immiscible, but many PAEK are miscible with polyetherimide (PEI) (Ultem) in all proportions. The addition of PEI increases the  $T_g$  and can be used to build the heat distortion temperature (HDT) while retaining crystalline chemical resistance properties. PEI can also be blended with PAEK to obtain melt adhesive effects. Blends with Extem are used to enhance thermal performance and polyimidesiloxane copolymers can be blended with PEEK to improve flexibility. Polyphenylene sulfide (PPS) is crystalline, and blends will retain a good degree of chemical resistance. Blends with polybenzimidazole (PBI) can show exceptional wear performance. Liquid crystalline polyester (LCP) blends have improved flow properties. Blends with polysulfones and PPS are immiscible. PES is amorphous and can reduce mould shrinkage and warpage. Fluoropolymers are commonly added to wear-resistant compounds. Longer-term, continuous-use temperatures (CUT) are typically 180–260 °C depending on the property measured. PAEK will degrade at elevated temperatures, especially in the presence of air and transition metal catalysts such as copper. Degradation can often be detected by changes in crystallisation rate or colour and can result in the formation of gels and carbonised black specks during melt processing.

In interpreting manufacturer's literature, it can sometimes appear that lower molecular-weight-grades have higher short-term properties (e.g., modulus). This may be due to slightly higher degrees of crystallinity in the faster-crystallising lower-molecular-weight resins or perhaps better wetting and less breakage of fillers and fibres in some production processes. However, higher-molecular-weight material may indeed show better long-term properties (e.g., fatigue resistance). Continuous carbon fibre-reinforced PAEK (which may contain ≤68% carbon fibre) has exceptional strength and stiffness properties. The wear resistance of tribological grades is excellent. Chemical resistance is generally very good and hydrolysis resistance is excellent. The semi-crystalline structure of PAEK resists

swelling and ingress of chemical environments, and the dissolution of crystals is energetically unfavourable. Material suppliers produce extensive chemical-resistance tables. These include automotive fluids, jet fuel, hydraulic fluids, refrigerants, and oilfield semiconductor manufacturing chemicals. However, performance can be limited in certain environments (e.g., halogens, very strong acids, strongly oxidative environments, high-temperature aromatics and amines). Resistance to ultraviolet radiation is limited, but resistance to hard radiation (gamma rays, and so on) can be very good. PAEK do not support combustion in air, produce little smoke, and burn in excess oxygen to produce carbon dioxide and water. However, the limiting oxygen index (LOI) is not especially high (e.g., 35% in PEEK). Fire performance can be enhanced by the addition of fillers. The extraction processes used in PAEK production can result in very pure polymers in terms of metal ions and volatile organic compounds (outgassing). PAEK are good electrical insulators in a wide range of environments and temperatures. However, the comparative tracking index can be relatively low, reflecting the ease of degradation to conducting char. The polar carbonyl groups mean that dielectric constants and dissipation factors are inferior to those of fluoropolymers. PAEK can usually be processed using virtually all the standard technologies. They can be injection- and compression-moulded, extruded into film, sheet and fibre, oriented, powder- and dispersion-coated, blow-moulded, laser-sintered, converted into thermoplastic composites, welded, metallised, adhesively bonded and machined. Although moisture does not result in chemical degradation, it can produce moulding defects, and PAEK need to be dried before processing. Melt temperatures are typically 30–60 °C above the  $T_m$ . A suitable cooling regimen is required to produce crystalline components. This will involve an injection mould temperature in excess of the  $T_g$ . Amorphous material may appear as a brown skin on the surface. This should not be confused with thermal degradation. If necessary, it can be removed by annealing, but it is better to use correct mould temperatures. Annealing is sometimes used to increase crystallinity and/or to remove residual stress.

PAEK thermoplastic composites are used less than their PPS counterparts because of cost and higher processing temperatures, but they offer higher toughness and temperature performance. Potential applications include fuselage panels, fasteners, floor beams, spars, ribs, thermals and fire barriers and stiffeners. A range of composite fasteners, bolts, nuts, inserts and brackets is made using composite flow moulding technology. In automotive applications, high-volume injection-moulded components offer greater design flexibility and are often less expensive than their metal counterparts. Transmission components include seal rings, self-lubricating (usually containing PTFE) thrust washers, bearing retainers and cages, bearings, bushings, vacuum pump vanes and vane tips, oxygen sensors, steering column sleeves, lamp sockets, fuel management components, antilock brake system tappets and plungers, and fork pads.

PAEK gear applications include worm gears for steering adjustment and gears for air conditioning, seat adjustment and electronic power steering systems. Compared with metal gears, PAEK offer

design flexibility, reduced weight, corrosion resistance, reduced fabrication cost, lower noise, and the ability to run without lubrication. Extraction of oil and gas offer many opportunities for PAEK. Oil and gas extraction can involve temperature and pressures of 200 °C and 140 MPa, respectively, combined with hydrogen sulfide, methane, brine, carbon dioxide and crude oil. The cost of equipment failure means that the industry uses the more expensive PEK, PEKEKK as well as PEEK. Typical applications include data-logging tools, sensor housings, data and power cables, electrical connectors, bearings, bushings, seals, backup rings, compressor components, radio frequency identification tags, cable ties and energy-absorbing springs for sealing systems. Recently, there has been a lot of interest in PAEK pipes that offer low permeability, low sensitivity to rapid gas decompression, erosion and wear resistance, and high strength, fatigue and creep performance. PAEK are used as liners in a range of umbilicals and, in the future, may be used as deep-ocean risers with superior buoyancy to their steel counterparts. Electronic-device applications include high-performance connectors and wiring systems.

PEEK is used in wiring for nuclear power stations because of its resistance to radiation, temperature and chemicals. Lead-free solders require high process temperatures. LCP offer the necessary temperature performance but may lack mechanical performance and weld-line strength. PPS offers high flow and dimensional stability, but it can be limited by its temperature performance. Mobile-phone applications include battery gaskets, hinges and the use of film in speakers and microphones. Office machine applications include gears, split fingers and bushings for copiers and printers, as well as lamp holders for digital projectors. PAEK film is also finding uses in flexible printed circuit boards. PAEK have important applications in the production of semiconductors and displays. This includes robotic wafer handling wands as well as wafer transport and storage devices. PEEK/PBI blends are used in robotic wands for extreme environments. Benefits include low particle generation due to wear, electrostatic discharge performance, high purity and low outgassing in vacuum, ability to handle hot wafers, no additives, and the production of complex geometries by injection moulding. The high level of purity and low wear particle generation increase device yield. PAEK are also used in chemical mechanical polishing rings because of wear life and in the plasma etch environment. PAEK test and burn in sockets survive the test environment with only very small changes in dimensions. Industrial and chemical process applications include static compressor components together with moving components which require excellent fatigue life. Examples include valve plates, bearings, piston rings, labyrinth seals, scroll compressor tip seals, star gears and rotors. The slight plastic flow compared with metal allows components to 'bed' into their environment, and thereby respond to a degree of damage and wear. PAEK can reduce noise and vibration and increase efficiency. There are many applications in textile and weaving equipment, including lubricant-free wear plates, chain belt parts, as well as yarn and thread guides with over-moulded ceramic inserts. Analytical equipment makes extensive use of the environmental resistance of PAEK. PAEK films

and membranes are used in heat exchangers and separation processes. Food-contact applications are mostly found in food processing factories (although PAEK are used in steam contact components in espresso machines). Factory applications include conveyor-belt chains, scraper blades, pump impellers, and spray cleaning heads. Consumer applications include strings for tennis racquets and violins, together with vacuum-cleaner components and portable camping stoves. Short- and long-term implantable medical devices are made from PAEK.

Short-term applications include: tubing and catheters (e.g., for stent delivery in minimally invasive surgery), heat shrinkable tubing for wiring protection, sterilisable diagnostic devices, drug-delivery and blood-management devices (e.g., dialysis equipment), laparoscopes, surgical instruments, surgical head restraints, endoscopes, endoscopy camera housings, dental tools, electrosurgical devices, analytical equipment, chromatography, and bio-hazard handling [<http://medical.vestakeep.com/product/medical/en/>]. Long-term applications include many spinal devices, bone pins, screws and plates, joint replacements (including wear-resistant surfaces), hip prostheses, dental implants, finger implant stems, cardiac pumps and pacemakers.

Some commercial grades of polyaryletherketone polymer matrices were here examined in order to make a selection. Among the possible aromatic technical polymers, polyetheretherketone (PEEK) has been identified as the polymer that shows a balanced compromise between performance aspects and commercial diffusion and economy. With regard to PEEK, it was necessary to define an evaluation criterion to make the selection of techno polymer grades that are theoretically more suitable for the realization of the nanocomposites that are to be investigated. This criterion was based on some characteristics of the materials, available in the technical sheets, provided by the producers and on some related quantities; these values, analysed overall, led to the identification of some degrees of TP. Where the information found was not sufficient to exercise the choice, it was necessary to perform specific tests and analyses to identify the discriminating for the choice. Above all, this aspect can be decisive for the development of nanocomposite materials because it allows orienting the choice by preventing the potential difficulties that could arise with the production of high-content nanocomposites. A characteristic example is the increase in viscosity (**Figure 2.9**) which could make the composite difficult to process in the face of a high starting viscosity of the matrix. Finally, factors of an economic nature, commercial and logistical availability have also affected the making of the choice.

Tables with extrapolation of some of the features taken into consideration to make the selection are reported. It can be noted that the characteristic parameters vary in type and method from one producer to another but also for different degrees of TP of the same manufacturing company. Tables from 2.2 to 2.5 show some characteristic values of the most widespread pure and preloaded PEEK matrices [<http://industrial.vestakeep.com/product/peek-industrial/en/Pages/default.aspx>].

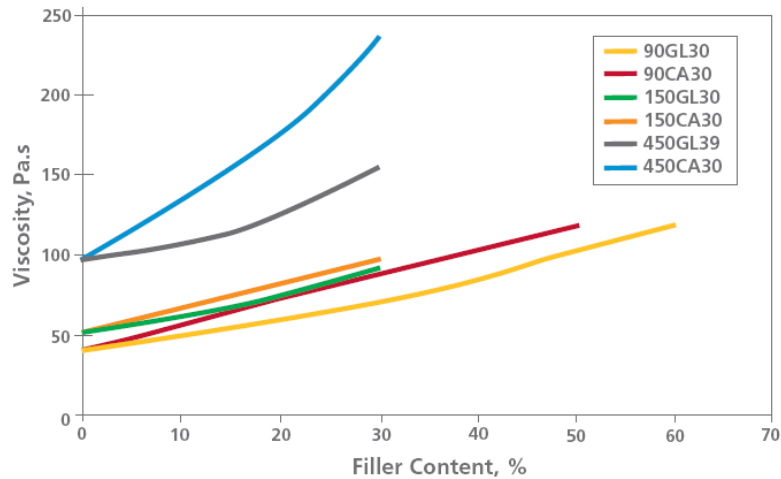


**Figure 2.9** Viscosity of some Victrex PEEK grades according to the amount and type of additives amount

**Table 2.1:** Some features of Evonik PEEK line 2000 in pure grades, with 30% glass fiber and 30% carbon fiber

Physical and thermal properties and fire behavior		Standard	Unit	2000 G	2000 GF30	2000 CF30
Density	23 °C	ISO 1183	cm <sup>3</sup> /10 min	1.30	1.50	1.39
Melting range	DSC, 2nd heating		°C	approx. 340	approx. 340	approx. 340
Melt volume-flow rate (MVR)	380 °C / 5 kg	ISO 1133	cm <sup>3</sup> /10 min	70	25*	19*
	400 °C / 21,6 kg	ISO 1133	cm <sup>3</sup> /10 min			
Temperature of deflection under load	Method A: 1.8 MPa	ISO 75-1/2	°C	155	323	330
	Method B: 0.45 MPa	ISO 75-1/2	°C	205	338	340
Vicat softening temperature	Method A: 10 N	ISO 306	°C	335	340	343
	Method B: 50 N	ISO 306	°C	310	335	340
Linear thermal expansion	23 °C - 55 °C, longitudinal	ISO 11359	10 <sup>-4</sup> K <sup>-1</sup>	0.6	0.3	0.1
Oxygen index	3.2 mm	ISO 4589	%	38	45	47
Flammability acc. UL94	3.2 mm	IEC 60695		V-0	V-0	V-0
Glow wire test	GWIT 2 mm	IEC 60695-2-12/13	°C	800	825	875
	GWFI 2 mm	IEC 60695-2-12/13	°C	960	960	960
Water absorption, saturation	23 °C	ISO 62	%	0.5	0.4	0.4
<b>Mechanical properties</b>						
Tensile test	50 mm / min	ISO 527-1/-2				
Stress at yield		ISO 527-1/-2	MPa	100		
Strain at yield		ISO 527-1/-2	%	5		
Strain at break		ISO 527-1/-2	%	30		
Tensile test	5 mm / min	ISO 527-1/-2				
Tensile strength		ISO 527-1/-2	MPa		170	240
Strain at break		ISO 527-1/-2	%		2	1.7
Tensile modulus		ISO 527-1/-2	MPa	3700	10600	22000
CHARPY impact strength	23 °C	ISO 179/1eU	kJ/cm <sup>2</sup>	N	55 C	45 C
	-30 °C	ISO 179/1eU	kJ/cm <sup>2</sup>	N	65 C	45 C
CHARPY notched impact strength	23 °C	ISO 179/1eA	kJ/cm <sup>2</sup>	5 C	10 C	8 C
	-30 °C	ISO 179/1eA	kJ/cm <sup>2</sup>	6 C	8 C	8 C



**Table 2.2:** Some characteristics of Evonik PEEK line 4000 in pure grades, with 30% of glass fiber and 30% of carbon fiber

Physical and thermal properties and fire behavior		Standard	Unit	L 4000 G 4000 GHP	4000 GF30	4000 CF30
Density	23 °C	ISO 1183	cm <sup>3</sup> /10 min	1.30	1.50	1.40
Melting range	DSC, 2nd heating		°C	approx. 340	approx. 340	approx. 340
Melt volume-flow rate (MVR)	380 °C / 5 kg	ISO 1133	cm <sup>3</sup> /10 min	12		
	400 °C / 21,6 kg	ISO 1133	cm <sup>3</sup> /10 min		32	22
Temperature of deflection under load	Method A: 1.8 MPa	ISO 75-1/2	°C	155	312	325
	Method B: 0.45 MPa	ISO 75-1/2	°C	205	335	335
Vicat softening temperature	Method A: 10 N	ISO 306	°C	335	340	343
	Method B: 50 N	ISO 306	°C	305	335	340
Linear thermal expansion	23 °C - 55 °C, longitudinal	ISO 11359	10 <sup>-4</sup> K <sup>-1</sup>	0.6	0.3	0.1
Oxygen index	3.2 mm	ISO 4589	%	36	45	47
Flammability acc. UL94	3.2 mm	IEC 60695		V-0	V-0	V-0
Glow wire test	GWIT 2 mm	IEC 60695-2-12/13	°C	825	825	850
	GWFI 2 mm	IEC 60695-2-12/13	°C	960	960	960
Water absorption, saturation	23 °C	ISO 62	%	0.5	0.4	0.4
<b>Mechanical properties</b>						
Tensile test	50 mm / min	ISO 527-1/-2				
Stress at yield		ISO 527-1/-2	MPa	95		
Strain at yield		ISO 527-1/-2	%	5		
Strain at break		ISO 527-1/-2	%	25		
Tensile test	5 mm / min	ISO 527-1/-2				
Tensile strength		ISO 527-1/-2	MPa		160	240
Strain at break		ISO 527-1/-2	%		2	2
Tensile modulus		ISO 527-1/-2	MPa	3500	10800	23000
CHARPY impact strength	23 °C	ISO 179/1eU	kJ/cm <sup>2</sup>	N	70 C	60 C
	-30 °C	ISO 179/1eU	kJ/cm <sup>2</sup>	N	75 C	60 C
CHARPY notched impact strength	23 °C	ISO 179/1eA	kJ/cm <sup>2</sup>	7 C	11 C	11 C
	-30 °C	ISO 179/1eA	kJ/cm <sup>2</sup>	6 C	9 C	9 C

**Table 2.3:** Some features of neat Victrex PEEK in the 150 line

## VICTREX® PEEK 150PF

➤ **Product Description:**

High performance thermoplastic material, unreinforced PolyEtherEtherKetone (PEEK), semi crystalline, fine powder for compression moulding, easy flow, FDA food contact compliant, colour natural.

➤ **Material Properties**

	CONDITIONS	TEST METHOD	UNITS	TYPICAL VALUE
<b>Mechanical Data</b>				
Tensile Strength	Yield, 23°C	ISO 527	MPa	100 *
Tensile Elongation	Break, 23°C	ISO 527	%	15 *
Tensile Modulus	23°C	ISO 527	GPa	4.1 *
Flexural Strength	23°C	ISO 178	MPa	170 *
Flexural Modulus	23°C	ISO 178	GPa	3.9 *
Izod Impact Strength	Notched, 23°C	ISO 180/A	kJ m <sup>-2</sup>	4.5 *
	Unnotched, 23°C	ISO 180/U		n/b *
<b>Thermal Data</b>				
Melting Point		ISO 11357	°C	343
Glass Transition (Tg)	Onset	ISO 11357	°C	143
	Midpoint			147
<b>Flow</b>				
Melt Viscosity	400°C	ISO 11443	Pa.s	130

**Table 2.4:** Some features of Victrex PEEK pure and with 30% glass fiber from the 450 line

## VICTREX<sup>®</sup> PEEK 450G

➤ **Product Description:**

High performance thermoplastic material, unreinforced PolyEtherEtherKetone (PEEK), semi crystalline, granules for injection moulding and extrusion, standard flow, FDA food contact compliant, colour natural/beige.

➤ **Typical Application Areas:**

Applications for higher strength and stiffness as well as high ductility. Chemically resistant to aggressive environments, suitable for sterilisation for medical and food contact applications.

➤ **Material Properties**

	CONDITIONS	TEST METHOD	UNITS	TYPICAL VALUE
<b>Mechanical Data</b>				
Tensile Strength	Yield, 23°C	ISO 527	MPa	98
Tensile Elongation	Break, 23°C	ISO 527	%	45
Tensile Modulus	23°C	ISO 527	GPa	4.0
Flexural Strength	At 3.5% strain, 23°C	ISO 178	MPa	125
	At yield, 23°C			165
	125°C			85
	175°C			19
	275°C			12.5
Flexural Modulus	23°C	ISO 178	GPa	3.8
Compressive Strength	23°C	ISO 604	MPa	125
	120°C			70
Charpy Impact Strength	Notched, 23°C	ISO 179/1eA	kJ m <sup>-2</sup>	7.0
	Unnotched, 23°C	ISO 179/U		n/b
Izod Impact Strength	Notched, 23°C	ISO 180/A	kJ m <sup>-2</sup>	8.0
	Unnotched, 23°C	ISO 180/U		n/b
<b>Thermal Data</b>				
Melting Point		ISO 11357	°C	343
Glass Transition (Tg)	Onset	ISO 11357	°C	143
	Midpoint			150
Coefficient of Thermal Expansion	Along flow below Tg	ISO 11359	ppm K <sup>-1</sup>	45
	Average below Tg			55
	Along flow above Tg			120
	Average above Tg			140
Heat Deflection Temperature	As moulded, 1.8 MPa	ISO 75-f	°C	152
	Annealed 200°C / 4h, 1.8MPa			160
Thermal Conductivity	Along flow, 23°C	ISO 22007-4	W m <sup>-1</sup> K <sup>-1</sup>	0.32
	Average, 23°C			0.29
Relative Thermal Index	Electrical	UL 746B	°C	260
	Mechanical w/o impact			240
	Mechanical w/impact			180
<b>Flow</b>				
Melt Viscosity	400°C	ISO 11443	Pa.s	350

## VICTREX<sup>®</sup> PEEK<sup>™</sup> 450GL30

➤ **Product Description:**

High performance thermoplastic material, 30% glass fibre reinforced PolyEtherEtherKetone (PEEK), semi crystalline, granules for injection moulding and extrusion, standard viscosity, FDA food contact compliant, colour natural/beige.

➤ **Typical Application Areas:**

Applications for higher strength in a static system. Low coefficient of thermal expansion. Chemically resistant to aggressive environments, suitable for sterilization for medical and food contact applications.

➤ **Material Properties**

	CONDITIONS	TEST METHOD	UNITS	TYPICAL VALUE
<b>Mechanical Data</b>				
Tensile Strength	Break, 23°C	ISO 527	MPa	180
	Break, 125°C			120
	Break, 175°C			60
	Break, 275°C			35
Tensile Elongation	Break, 23°C	ISO 527	%	2.7
Tensile Modulus	23°C	ISO 527	GPa	11.8
Flexural Strength	23°C	ISO 178	MPa	270
<b>Flow</b>				
Melt Viscosity	400°C	ISO 11443	Pa.s	560

A discriminating characteristic for the choice was certainly the type of process necessary for the realization of the nanocomposites and for the final production; all the matrices that did not show an easy possibility of dispersion of the fillers in the polymer melt and that could be worked by injection were excluded. Another decisive factor, in many aspects related to the previous one, has been the rheological characterization of the polymer melt, with reference to the viscosity in the various evaluation approaches. The visco-elastic behaviour of the fused matrix is, in fact, one of the discriminating characteristics, both in the dispersion phase of the nanofiller and the subsequent workability of the composite. From the information that can be extrapolated from the technical datasheets we note that, in general, viscosities are found in the characteristic range of traditional polymers, but for some degrees of PEEK for injection moulding, they are significantly lower, even one order of magnitude, compared to others; it can be thought that the degrees of PEEK with lower viscosity may be more suitable for the application in question, as they guarantee the processability of the nanocomposite melt even in the case of a substantial increase in viscosity. It is necessary to reiterate that the information found in some cases are not comparable and to carry out a comparative assessment, specific tests have to be used; in particular, it can be noted that the TDS of Evonik products show the Melt Volume Flow Rate that certainly provides a comparative parameter between the various PEEK (VestaKeep) grades considered, but is insufficient for the understanding of rheological behaviour. In this way, it is understood that the VestaKeep 2000 P (VK2000) shows a MFVR of an order of magnitude higher than the VestaKeep 4000 P (VK4000) and probably possesses better viscosity characteristics for the use of the study in question. With similar considerations, it can be seen from the tables and the graph, among the grades of pure PEEK produced by Victrex, the most suitable seems to be 150 PF grade. The comparison assessment between Victrex and Evonik PEEK grades, in relation to rheological behaviour, is difficult to be done only with product data. For this reason, a rheological characterization was necessary to compare products with information obtained through equivalent tests.

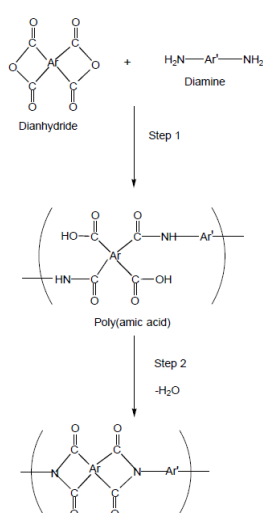
### **2.1.2 Polyimide (PI) and Thermoplastic Polyimide (TPI)**

Aromatic polymers, in general, consist of five members' imide heterocyclic units and aromatic rings. The structure of these "chain" systems makes cyclic polyamides insoluble/intractable and, therefore, is not susceptible to traditional solution/fused polycondensation reactions. The first attempts made at DuPont R & S in 1950 using direct reaction of dianhydrides and aromatic diamines in the molten material or in solution resulted in intractable low molecular weight polyimide precipitation. However, in 1956, Dr. A. Endrey at DuPont had successfully experimented with the invention of obtaining polyimides for reaction of intermediate / processable soluble known as poly (friendly acid)s. This type of reaction consists of two phases: the polycondensation solution of an aromatic diamine and a

dianhydride to form poly (friendly acid) that can be transformed into a useful form, followed by cyclodehydration diamide acid to form polyimide [[www.pi84.com](http://www.pi84.com)].

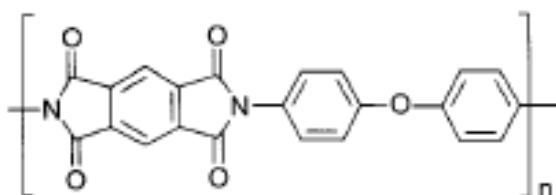
*Classic two-step method of polyimide synthesis:* In the classical two-step method of sintering of aromatic polyimides, the initial step consists in preparing an aromatic diamine solution in a polar aprotic solvent, such as N-methylpyrrolidone (NMP), to which a tetracarboxylic dianhydride is added. The formation of poly (friendly acid) takes place during this phase at room temperature and is complete in 24 hours, depending on the reactivity of the monomer. The high molecular weight poly (friendly acid) produced is completely soluble in the reaction solvent and, therefore, the solution can be thrown into a film on a suitable substrate. The second step in this synthesis method is the cyclodehydration (imimidization) reaction which is performed by heating the film at elevated temperatures, or incorporating a dehydrating chemical agent. The general reaction scheme for the two-step method is shown in the diagram reported in **Figure 2.10**.

Polyimides are known as reliable high temperature polymers with superior mechanical and electrical properties. The properties of polyimides are affected by internal rotation around bond in molecules, sweep volume, free volume, molecular packing, and molecular ordering. These factors are mainly dependent on the structure of polyimides, but also on the preparation condition. In particular, the molecular packing and the molecular ordering of some polyimides were reported to be extremely dependent on the preparation condition (preparation procedure, imidation conditions, annealing conditions and film thickness, etc). In future, high performance polyimides are expected to be developed on the basis of knowledge about the effect of the structures and the preparation conditions on properties, taking into consideration the polyimide characteristic, the cost, the convenience of operation and the environment.



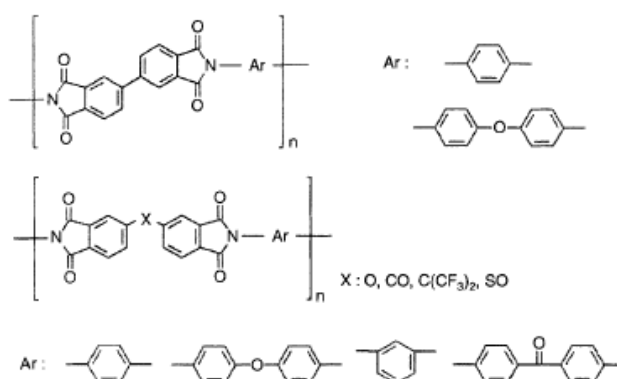
**Figure 2.10:** Two-step method of polyimide synthesis

The most familiar polyimide is poly-N,N'-(oxydi-p-phenylene)pyromellitimide, which is synthesized from bis(4-aminophenyl) ether and pyromellitic dianhydride, and is widely known as Kapton (**Figure 2.11**). Polyimides are stable over a wide range of temperatures from very low temperatures to temperatures above 300°C, so they are suitable for severe space environments. Polyimides were originally developed for the aerospace industry, are now also used in airplanes and in machinery for various other industries and are indispensable in the electronics industry as heat-resistant insulators suitable for soldering processes.



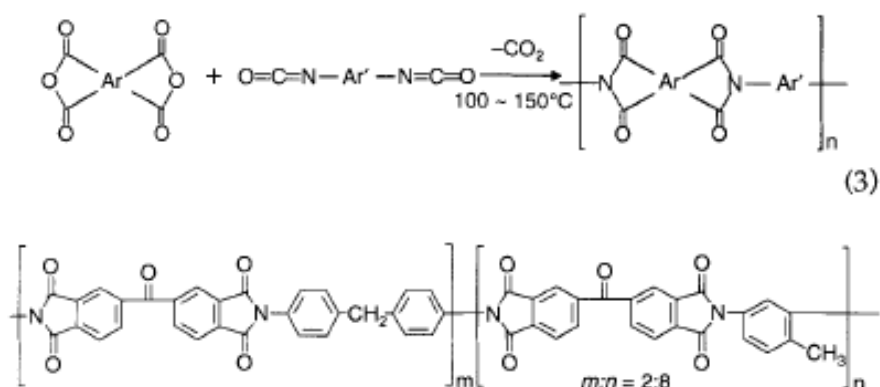
**Figure 2.11** Kapton-type polyimide.

With the rapid development of electronics, devices such as semiconductors, displays and the computers, the characteristics demanded from the electronic parts progressed, and it became necessary for polyimides to have other characteristic properties, such as processability, low dielectric constants ( $\epsilon$ ), low water absorption (WA), low coefficients of thermal expansion (CTE), and high radiation resistance, as well as their excellent thermal stability and good mechanical properties. After the marketing of the Kapton-type polyimide, many other polyimides, such as biphenyl-type polyimides and polyimides with a connecting group (-X-) between the phthalimides, were developed (**Figure 2.12**). More types of polyimides have been synthesized to investigate the relationship between their structures and these properties. The methods of synthesis for polyimides and the relationship between their structures and properties are under intensive study.



**Figure 2.12:** Biphenyl-type polyimides and polyimides with a connecting group (-X) between the phthalimides

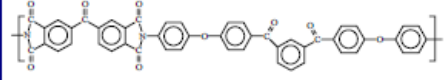
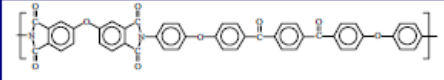
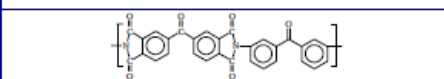
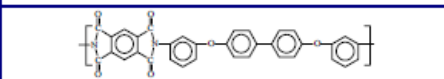
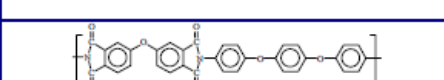
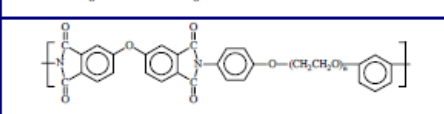
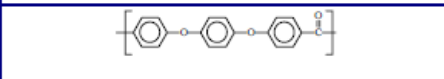
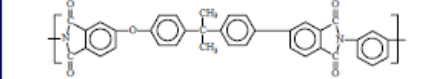
Most polyimides are insoluble in organic solvents, but some are soluble. Soluble polyimides can be synthesized in one-step. The polyimide solution is obtained by reacting a diamine with a tetracarboxylic dianhydride in a high boiling point solvent (phenolic solvent, for example, m-cresol) at 150-200°C. As the polyamic acid is formed and converted to the polyimide in solution, the water formed during imidation is removed as an azeotrope with toluene to obtain high molecular weight polyimide. prepared in one-step procedure were higher than those of polyimides prepared in two-step procedure and the polyimides prepared in one-step procedure showed higher strength than those prepared in two-step procedure, and the one-step procedure is thought to be more suitable for the synthesis of soluble polyimides. The solubility of some polyimides prepared by the one-step procedure was reported to be higher than that of polyimides prepared by two-step procedure in spite of the same structures. Thermoplastic polyimides and polyimide adhesives are prepared by this method. Soluble polyimides are also synthesized by using diisocyanates instead of diamines. The polyimide solution is obtained by reacting a diisocyanate with a tetracarboxylic dianhydride in NMP or DMAc at 100-150°C. The soluble polyimide "PI-2080" (**Figure 2.13**) is produced by the one-step procedure using diisocyanate. Synthesis using tetracarboxylic dithioanhydrides instead of tetracarboxylic dianhydrides and the high-pressure synthesis from nylon-salt-type monomers composed of diamines and tetracarboxylic acids have also been reported.



**Figure 2.13:** Synthesis route for PI-2080 soluble polyimide

New-TPI (New-Thermoplastic Polyimide) originally developed and licensed by Mitsui Toatsu Chemicals, has probably been the most popular system in attracting the attention of several research groups. Before New-TPI though, several other systems which showed varying degree of promise were developed by workers at NASA, and they were LaRC-CPI (Langley research centre -crystalline polyimide), LaRC-CPI-2 (second generation) and LaRC-TPI. The structures of these polyimides and their glass transitions and melting points are shown in **Table 2.5**.

**Table 2.5:** Chemical structure and  $T_g$  and  $T_m$  of various semicrystalline polyimides. The structures and values for ULTEM, an amorphous polyetherimide, and PEEK are also shown

Chemical Structure	Name	$T_g$ (°C)	$T_m$ (°C)
	LaRC-CPI	220	360
	LaRC-CPI-2	217	334 & 364
	LaRC-TPI	240	330-350
	New-TPI	250	385
	TPEQ-OPDA	238	420
	Ethylene Glycol based diamine-ODPA	112 n=3 145 n=2 177 n=1	268 n=3 304 n=2 340 n=1
	PEEK	143	334
	Ultem®-PEI	215	ND

It is important to mention that for each of these polyimides, there were several different grades that essentially differed in their molecular weight or sometimes the nature of the end capping. The crystallization ability of the different grades is different. Most of these polyimides display the essential characteristics of  $T_g$  (>200°C) and high  $T_m$ 's (>350°C) and thus are candidates for high temperature and high performance applications from this standpoint [Kido et al. 2000; Chun & Weiss, 2004].

The AURUM PL450C Thermoplastic Polyimide grade and their blends with glass fiber and carbon fiber have been selected for our work. AURUM PL450C is a high performance thermoplastic polyimide for precision injection moulded components and extruded products. A member of the AURUM family of advanced engineering resins, unfilled AURUM PL450C offers a unique balance of mechanical and thermal properties for superior performance in demanding automotive, business machinery, industrial equipment, aerospace, and semiconductor equipment applications [www.mitsuichem.com; www.dupont.com].

AURUM exhibits outstanding resistance to chemicals and radiation, a low coefficient of thermal expansion, ultrahigh purity, low outgassing in a vacuum, excellent electrical properties, and flame resistance. AURUM PL450C can be conventionally extruded to produce high performance wire &

cable insulation, thin-wall tubing, and fiber. The grades containing glass fiber (AURUM® JGN3030) and carbon fibers (AURUM® JCN3030) have been selected for the purpose of the present work.

### 2.1.3 Polyetherimide (PEI)

It is an amorphous polymer (**Figure 2.14**) belonging to the family of polyamides. It falls into the category of super engineering plastics because it has very specific technical characteristics: it is inherently self-extinguishing (V0 according to UL94), also regarding the thermal resistance (continuous use temperature of 170 °C and Vicat softening point > 200° C) and chemical resistance (contact with chemical agents), a rare performance for amorphous polymers. The linear thermal expansion (CTE) in the formulations with glass fiber is very low, it also possesses good tribological properties (low friction and wear). It is particularly suitable for the evaluation of metal replacement [[www.sabic.com](http://www.sabic.com)].

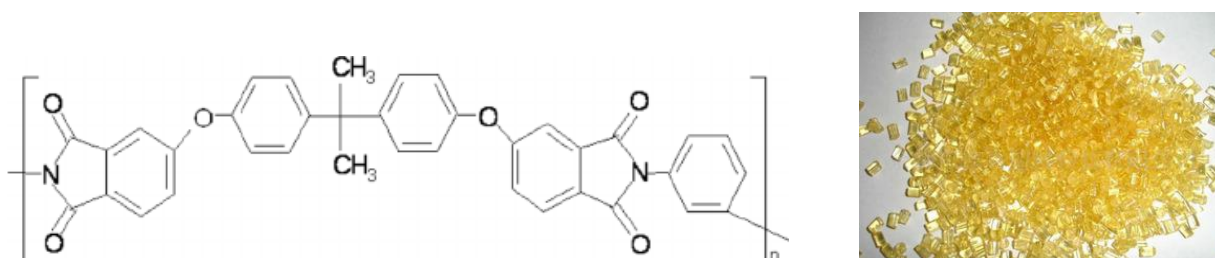


**Figure 2.14:** PI chemical structure and appearance

Relative to PEEK, PEI is cheaper, but is lower in impact strength and usable temperature. Because of its adhesive properties and chemical stability, it became a popular bed material for FDM 3D printers. Ultem is a family of PEI products manufactured by SABIC as a result of acquiring the General Electric Plastics Division in 2007, developed by Joseph G. Wirth in the early 1980s. Ultem resins are used in medical and chemical instrumentation due to their heat resistance, solvent resistance and flame resistance. Ultem 1000, selected for the present work, (standard, unfilled polyetherimide) has a high dielectric strength, inherent flame resistance, and extremely low smoke generation. Ultem has high mechanical properties and performs in continuous use to 340 °F (170 °C).

### 2.1.4 Polyamide-imide (PAI)

PAI (polyamide-imide) combines the exceptional performance of thermoset polyimides with the melt-processing advantage of thermoplastics. Wear-resistance grades offer unsurpassed performance in both dry and lubricated environments. High-strength grades retain their toughness, high strength



and high stiffness up to 275 °C (525 °F), making PAI the industry's highest performing thermoplastic. Its broad chemical resistance includes strong acids and most organics.

PAI exhibits greater compressive strength and higher impact resistance than most advanced engineering plastics. High creep resistance and an extremely low coefficient of linear thermal expansion (CLTE) provide excellent dimensional stability.

Polyamide-imides are used extensively as wire coatings in making magnet wire. They are prepared from isocyanates and TMA (trimellitic acid-anhydride) in N-methyl-2-pyrrolidone (NMP). A prominent distributor of polyamide-imides is Solvay Specialty Polymers, which uses the trademark Torlon [<https://www.solvay.com/en/markets-and-products/featured-products/torlon.html>].

The currently popular commercial methods to synthesize polyamide-imides are the acid chloride route and the isocyanate route. The earliest route to polyamide-imides is the condensation of an aromatic diamine, such as methylene dianiline (MDA) and trimellitic acid chloride (TMAC) (**Figure 2.15**).

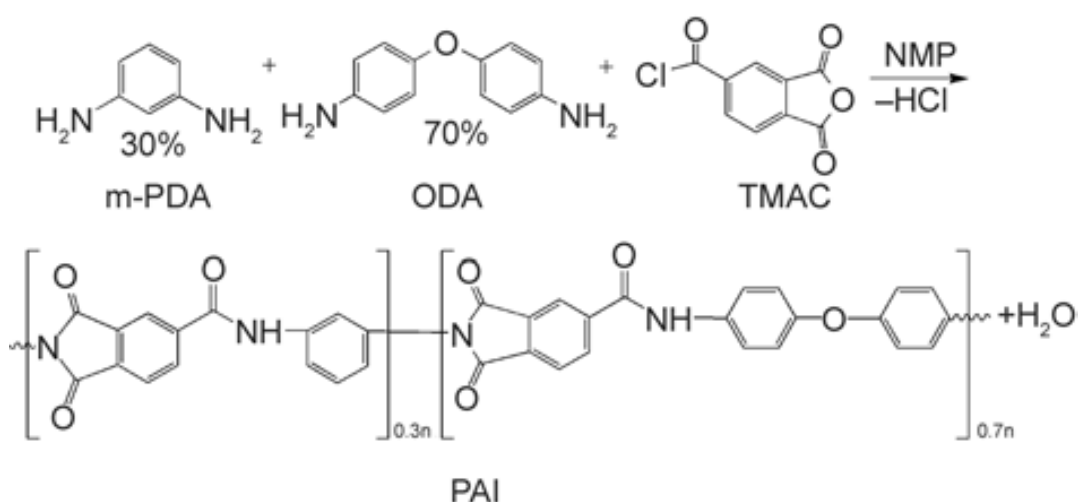


**Figure 2.15:** PAI chemical structure (synthesis route by TMAC)

Reaction of the anhydride with the diamine produces an intermediate amic acid. The acid chloride functionality reacts with the aromatic amine to give the amide bond and hydrochloric acid (HCl) as a by-product. In the commercial preparation of polyamideimides, the polymerization is carried out in a dipolar, aprotic solvent such as N-methylpyrrolidone (NMP), dimethylacetamide (DMAC), dimethylformamide (DMF), or dimethylsulfoxide (DMSO) at temperatures between 20-60 °C. The byproduct HCl must be neutralized in situ or removed by washing it from the precipitated polymer. Further thermal treatment of the polyamideimide polymer increases molecular weight and causes the amic acid groups to form imides with the evolution of water.

The high temperature and chemical resistance of polyamide-imides make them ideal candidates for membrane-based gas separations. The separation of contaminants such as CO<sub>2</sub>, H<sub>2</sub>S, and other impurities from natural gas wells is an important industrial process. Pressures exceeding 1000 psi demand materials with good mechanical stability. The highly polar H<sub>2</sub>S and polarizable CO<sub>2</sub> molecules can strongly interact with the polymer membranes causing swelling and plasticization due to high levels of impurities. Polyamide-imides can resist plasticization because of the strong intermolecular interactions arising from the polyimide functions as well as the ability of the polymer chains to hydrogen bond with one another as a result of the amide bond. Although not currently used in any major industrial separation, polyamide-imides could be used for these types of processes where chemical and mechanical stability are required.

Torlon® PAI offers the highest strength and stiffness of any thermoplastic up to 275 °C (525 °F). Its outstanding wear, creep and chemical resistance make it ideal for severe service environments (**Figure 2.16**)

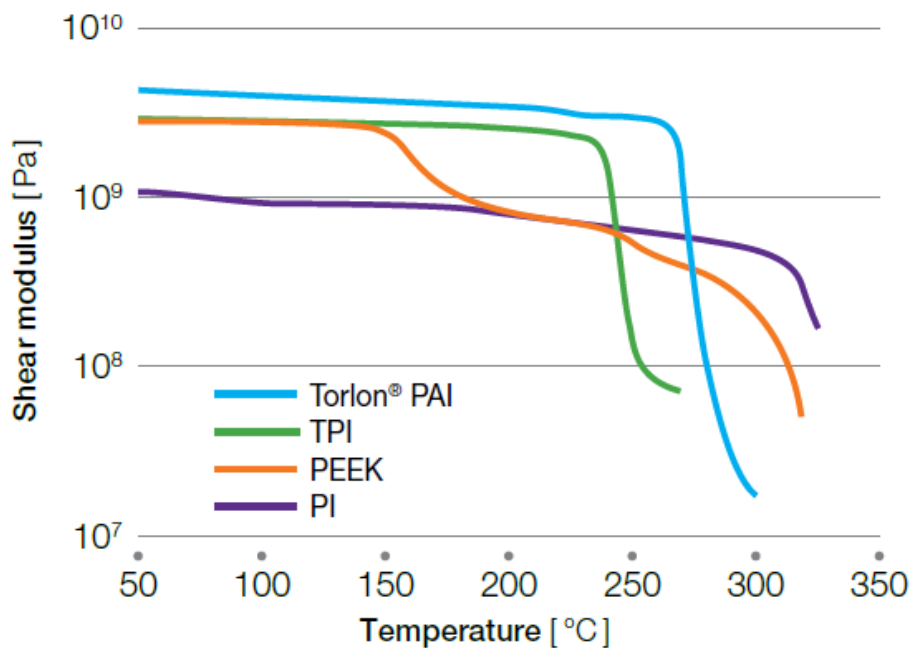


**Figure 2.16:** DMTA results for PAI in comparison with TPI, PEEK and PI

High-strength grades deliver metal-like performance and are routinely specified for precision components used in repetitive-use, load-bearing operations. Glass fiber and carbon fiber filled grades retain their strength and stiffness at high temperatures with the added benefit of low creep and excellent fatigue resistance. Wear-resistant grades offer select combinations of mechanical and tribological properties. Their inherent heat and chemical resistance, makes them an effective alternative to metal in high-temperature friction and wear applications—even when lubrication is

marginal or non-existent. Select grades can perform in lubricated environments at exceptionally high pressures and velocities.

### 2.1.5 Polybenzimidazole (PBI)

Development work on aromatic polybenzimidazole (PBI) polymer was done in the early 1960s. Later, NASA and the Air Force Materials Lab sponsored work on PBIs as a non-flammable and thermally stable textile fiber for aerospace and defence applications. In the 1970s NASA used PBI as part of the astronaut's clothing on Apollo and other space shuttle flights. In 1983 the Celanese Corporation commercialized PBI fibers, spun from solutions of the polymer, and subsequently started development of other PBI forms, including films, papers, microporous resins, sizings, coatings, moulding resins, as well as reinforced composites [www.pbiproducts.com].

PBI was introduced to the Fire Service as an outer shell protective fabric, typically 40% PBI/60% para-aramid. In the 1990s shortcut PBI fiber was introduced for use in automotive braking systems as a friction formulation material. Also, staple fiber was introduced into the aircraft market as a seat fire blocking layer material, and lightweight fabrics were developed for electric utility and petrochemical applications. During the early 2000s enhanced and next-generation fibers were continuously commercialized and introduced in firefighter turnout gear. In 2005, Celanese sold its PBI business to PBI Performance Products PBI high temperature polymers and blends 175 Inc, an affiliate of the InterTech Group of North Charleston, SC, and the world's only commercial producer of PBI polymer (**Figure 2.17**).

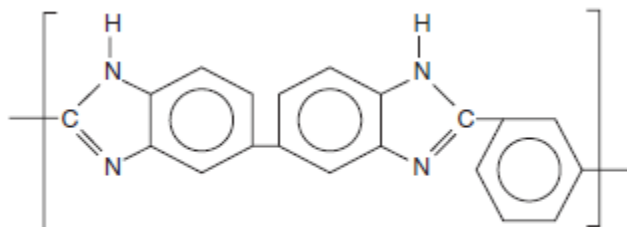


**Figure 2.17:** Structure of PBI polymer

PBI does not burn in air, has high heat resistance (does not melt), possesses the highest compressive strength and mechanical property retention over 205°C of any unfilled resin, and it is hydrolytically stable to high pressure steam or boiling water. In an inert atmosphere, such as nitrogen, the high temperature weight loss occurs at 600°C. For example, for a ~10-min exposure time, the suggested maximum temperature is ~650°C. Long-term temperature aging can lead to rapid loss of mechanical properties, due to oxidative degradation, and thus ~320°C is the maximum temperature capability for exposures exceeding 200 h.

PBI is typically resistant to organic acids, chlorinated solvents, alcohols, and weak organic bases, but can be affected by polar aprotic solvents and strong acids and bases. PBI is also known to be

hygroscopic with an equilibrium moisture content of ~15% by weight, the uptake primarily due to water forming hydrogen bonds with the hydrogen on the imidazole ring of the polymer chain. Thus, sample materials are generally dried at ~180°C for several hours in a vacuum oven prior to testing and usage. The polymer also absorbs acid (pKa ~ 5.5), a vital characteristic for fuel cell membranes and other proton-conducting applications. Due to the several attractive properties of PBI such as commercial availability, high glass transition temperature (T<sub>g</sub>, 425–435°C), chemical resistance in hostile environments, and retention of good mechanical properties at both high and cryogenic temperatures, it has been and continues to be examined in high performance polymer blends. Thus, blending with other high temperature-resistant polymers targets the high T<sub>g</sub> provided by PBI and the improved processability afforded by the component polymers.

### 2.1.6 Polyarylamide (PARA)

Polyarylamide is a semi-crystalline polymer that offers very high rigidity for a polymeric material due to its glass transition temperature of approximately 85 °C (185 ° F). Other key properties are its high strength (flexural strength as high as 400 MPa), very low creep (deformation of less than 1% after 1000 hours under 50 MPa), excellent surface finish, ease of processing and slow rate of water absorption (**Figure 2.18**).

Polyarylamide has good resistance to most common solvents, aqueous solutions and engine oils. However, it is degraded by strong and concentrated mineral acids, powerful oxidants and strong bases. It is sensitive to certain organic acids and to some solutions of metallic salts. Also, it is recommended that their use should be carefully considered where the product is continuously in contact with water.

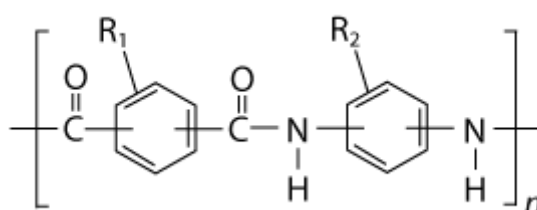


**Figure 2.18:** Structure of PARA polymer

Polyarylamide has replaced metal in many fields of application.

- Automotive and transportation: fuel pumps, cam covers, vandal-proof seats, rear-view mirror housings, clutch parts, wiper controls, oil filter bodies, headlamp control pivots, door handles, seat adjustment mechanisms, headlamp surrounds.

- Electrical & electronics: connectors, chassis and housings for electrical and electronic equipment, sliding parts in video recorders, safety switches, disk supports in CD players, induction motor supports, telecommunications parts.
- Domestic appliances: electric razor heads, electric iron parts, vacuum cleaner motor supports, sewing machine parts.
- Other markets: leisure industry applications, machine tools, furniture, medical.

Solvay Advanced Polymers is the world's only producer of polyarylamide. The Ixef resins are produced in the USA and compounded at Oodenarde, Belgium, in a 10,000 tpa compounding plant

## **2.2 Compounded matrices**

Polymer blends are being used in an increasing number of industrial applications. Sectors ranging from the automotive to the aircraft industry have expressed an interest in developing these materials for specific applications. In fact, for some time, research in blends has been one of the biggest areas of polymer research, in both the industrial and academic world. Recently, requirements for materials in certain areas have become increasingly severe. Temperatures in excess of 200°C for times of hundreds of hours have become stated requirements for some materials. Particularly severe in this regard are requirements from the aircraft industry for engine components where high service temperatures for long periods of time are often normal. The commercial activity in high temperature blends has been somewhat limited. As already alluded to, one of the major driving forces for higher temperature performance has involved military and aerospace applications. Other emerging application needs have developed, but at a slower rate. Continued needs for high temperature materials will be present in the aerospace as well as in the transportation area where under-the-hood components, High Temperature Polymer Blends friction and wear applications continue to require more demanding performance. Electric and electronic needs will also continue at a high rate of growth requiring higher temperature performance. Finally, high temperature polymer needs will emerge in advanced composites research, which often requires blend technology to optimize the performance of available materials. One approach to meeting these material requirements is to synthesize new polymers. Another method to tailor the properties of materials is through blending of two polymers. In this approach, the goal is to highlight the positive features of both materials while attempting to eliminate the negative features. This book will address various aspects of high temperature polymers and highlight the advantages of producing such blends.

The physical state of mixing which is present in polymer blends can be categorized in three ways: miscible, partially miscible or immiscible. A miscible polymer blend is a homogeneous, single-phase material. In many respects, a miscible blend behaves as if it is a single polymer. If the two

components in the blend are miscible only within a certain composition range, the polymers are deemed partially miscible. An immiscible blend contains two distinct phases and is heterogeneous in nature. The philosophy of blending two polymers is to produce a material which has properties that are tailored to a certain performance level. Since the morphology and resultant physical properties are controlled to a large extent by the miscibility and phase behaviour, it is quite easy to understand why there is so much interest in controlling the phase structure in blends. Introduction to high temperature polymer blends. In fact, this topic has evolved into a central area of polymer research during the last 40 years. One of the first ideas, that as a rule polymer blends are immiscible, needs to be re-evaluated due to the increasing number of miscible or partially miscible polymer pairs reported in the literature.

One of the issues with miscible polymer blends in general is the temperature range of their miscibility. If such materials are to be processed in the melt state as miscible blends, there must be a temperature window between the glass transition temperature and the phase separation temperature which is large enough for melt processing. If this processing window is too small, the blends will either phase separate or have too high a viscosity for melt processability. In the case of the PBI blends discussed above, phase separation takes place a few degrees above the glass transition temperature for most blend compositions.

This suggests that the miscibility which is observed is a metastable phenomenon which is controlled by kinetic factors. The observed phase separation also indicates that it will be difficult to melt process the blends in the miscible state, due to the reasons already discussed. There have been several miscible high temperature polymer pairs defined in the literature. Several of these pairs are miscible from solution but are immiscible when processing is attempted in the melt state. These results indicate that the blends phase separate when heated above their glass transition temperature. This further shows that kinetic factors as well as thermodynamic factors are important in the observed miscibility. Also, the role of the solvent in the observed miscibility needs to be better understood. One of the current technical challenges is to widen the temperature range between the glass transition temperature of the blend and its phase separation temperature, to allow miscible blends to be processed in the melt state.

### **2.2.1 PEEK/PBI**

Victrex plc and PBI Performance Products have introduced a new T-Series family of products, a range of proprietary polymer blends featuring PolyEtherEtherKetone (PEEK) and PolyBenzImidazole (PBI). This innovative new product series is designed to perform in the most demanding applications requiring high thermal, strength, and wear resistance. Comprised of four grades, TU-60, TL-60, TF-60V, and TF-60C, the new T-Series products expand the current mechanical and tribological capability of existing products with enhanced stiffness, wear, hardness,

and temperature performance that are made possible with the blending of PEEK (polyetheretherketone) polymer and Celazole PBI. T-Series polymers are a great replacement for metals and non-melt-processable high-temperature plastics.

T-Series polymers are the most thermally stable thermoplastics on the market, offering excellent mechanical performance at high temperatures up to 300°C (572°F). This semi-crystalline material retains mechanical properties well above the polymer's glass transition temperature. T-Series polymers are currently the highest performing melt processable thermoplastics for use in applications requiring physical property retention and wear resistance at elevated temperatures. They are a great replacement option for metals and non-melt processable high temperature plastics (i.e., polyimides). PEEK-PBI polymers are inherently lubricious with a very smooth surface finish. They are low sloughing and offer exceptional abrasion resistance. In high temperature exposure to organic chemicals, moulded parts made with T-Series PEEK-PBI polymers offer outstanding chemical resistance and property retention, even after extended exposures. They have excellent resistance to a range of extreme environments that degrade most plastics. Other properties: excellent wear and strength at high temperatures for long-lasting components; excellent thermal insulator (does not melt); excellent hardness (25% increase in Rockwell A Scale); creep resistant (up to 30% better than other PEEK materials); increased design and processing flexibility, superior chemical resistance versus metals and other high performance polymers.

They can be divided in:

- TU-60 (Unfilled, unreinforced (neat) PEEK-PBI blend suitable for high performance in high-temperature and high-strength applications)
- TF-60V (Glass reinforced PEEK-PBI polymer blend for even greater rigidity and dimensional stability while maintaining many of the useful characteristics of the unfilled grade). The glass reinforcement yields a product with an exceptional strength-to-weight ratio and increased tensile strength;
- TF-60C (Carbon reinforced PEEK-PBI polymer blend for highest strength, stiffness and dimensional stability while maintaining many of the useful characteristics of the unfilled grade).

These grades were selected for the purpose of our work.

### **2.2.2. PEEK/PI**

High temperatures or frictional wear at high speeds and loads often circumscribes the use of ordinary engineering plastics; hence, advanced high-performance polymers have taken their place in demanding applications. Plastics processors can use polyimides — which exhibit remarkable heat stability and creep resistance, even at elevated temperatures of 250°C or higher — where ordinary plastics would sooner melt or decompose. Processing semi-finished parts made of polyimide is often

a difficult undertaking, and the raw material is sometimes not available commercially, prompting some polyimide polymer producers to sell the machined parts at high prices, affordable in many cases only in niches.

In addition, some polyimides are known to be highly brittle and thus cannot be used in applications that call for high quality of edges and surfaces and good impact strength. To overcome the above-mentioned limitations, Evonik Fibres GmbH is now offering Polyimide P84®NT in powder or granulate form, which is processable by employing common sinter technologies such as hot compression moulding or direct forming. The high mechanical stability and the impact resistance of P84®NT parts ensure good machinability with standard tools. Parts made of Polyimide P84®NT are excellent performers in thermally and mechanically stressed applications. This novel material features a high glass transition temperature of 337–364°C and a rigid structure (3705 MPa flexural modulus, 188 MPa strength in a three-point-bending experiment), combined with a high elongation at break of over 11 % (**Figure 2.19**).

Polyimide powder P84NT from Evonik was considered as second blend component for PEEK. It shows typical properties of polyimide, such as high temperature stability up to 350°C, chemical resistance, high mechanical strength, a low friction coefficient and minimal abrasion.

Using sinter technology, polyimide powder (**Figure 2.20**) can be manufactured into semi-finished products and components. Industrial applications using this material range from automotive industry and aerospace to industrial applications and office machines. Properties like friction coefficient, coefficient of thermal expansion, electrical conductivity or thermal conductivity can be adjusted by using compounds with functional fillers.

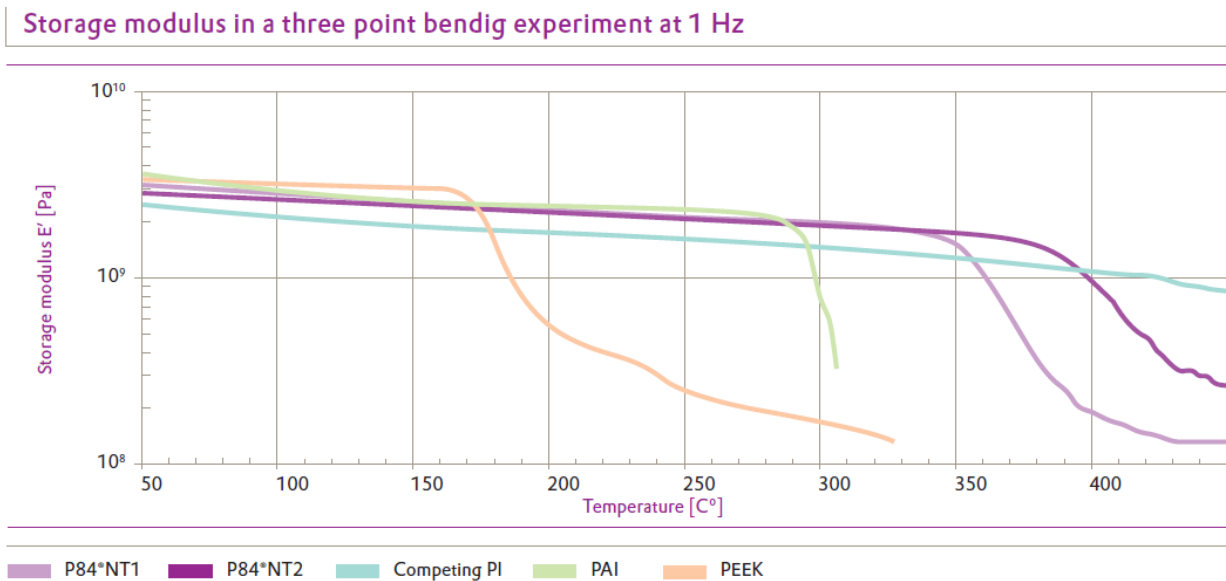


**Figure 2.19:** Storage modulus in a three-point bending experiment at 1 Hz



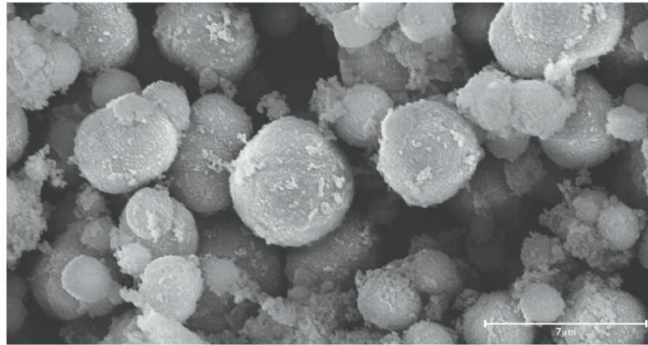


**Figure 2.20:** Scanning electron micrograph (SEM) at 4000x magnification. Spherical particles of Polyimide P84®NT with smooth surface.

### 2.2.3 PEK/PBI

GAZOLE™ 6000 Series blends are the most thermally stable available thermoplastics in the market, offering excellent mechanical performance at high temperatures up to 300°C. The semi-crystalline material retains its mechanical properties well above the polymer's glass transition temperature. They are inherently lubricious with very smooth surface finish. They show low sloughing and offer exceptional abrasion resistance and have excellent wear resistance properties, superior to any Engineering Thermoplastic.

The addition of glass fiber & carbon fiber reinforcement greatly increases the general mechanical properties at a given temperature. The glass fiber & carbon fiber filled composites are thermally stable thermoplastics with excellent mechanical performance at very high temperatures up to 300°C. Carbon fiber filled grades of GAZOLE™ 6000 series have much reduced thermal expansion coefficients making them ideal for metal replacement application. The blends filled with milled carbon fiber gives fixed electrostatic dissipative control with extremely low warpage.

The tensile properties of PEK/PBI blend polymer surpass those of most engineering thermoplastic polymers at elevated temperatures (**Figure 2.21**).

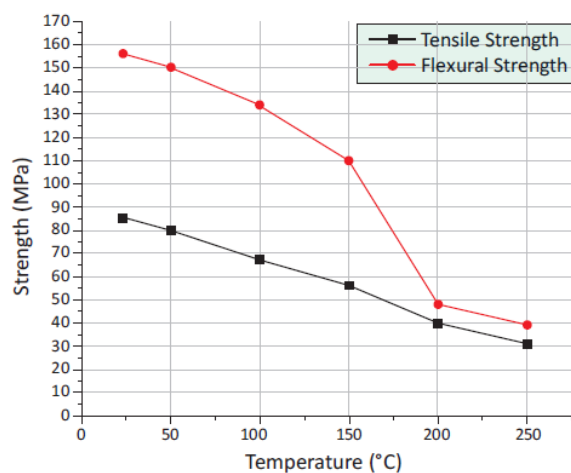


**Figure 2.21:** Tensile strength versus temperature for GAZOLE 6200G polymer

## 2.3 References

- Bonner, W. H. US Patent 3,065,205 (1962).
- Chun, Y.S., Weiss R. A. (2004) Journal of Applied Polymer Science, DOI 10.1002/app.21032.
- Dahl, K. J.; Jansons, V. In Polymers and Other Advanced Materials: Emerging Technologies and Business Opportunities, Prasad, P. N. ed., Plenum Press: New York, 1995, pp 69-81.
- DeMeuse, M.T. Jaffe, M., Molec. Cryst. Liq. Cryst., 157 (1988) 535.
- DeMeuse, M.T. Jaffe, M, Polym. Prepr. 30 (1989) 540.
- DeMeuse, M.T. Jaffe, M, in R.A. Weiss and C.K. Ober, editors, Liquid Crystalline Polymers, ACS Symposium Series No. 435 (1990) 439.
- Demeuse, M.T. High Temperature Polymers Blends (2014), Ed. M.T. Demeuse, ISBN: 978-1-84569-785-3, 2014 Woodhead Publishing Limited
- Goodman, I.; McIntyre J. E.; Russell, W. Brit. Patent 971, 227 (1964); Chem. Abstr. 1964,61
- Harris, J. E.; Robeson, L. M. J. Polym. Sci., Polym. Phys. Ed. 1987, 25, 311.
- Hsieh, T.T., Tiu, G. Simon, G.P. Polymer 41 (2000) 4737–4742.
- Kemmish, D.J. (2011) Practical Guide to High Performance Engineering Plastics, iSmithers – A Smithers Group Company,
- Lakshmana, V. R. J. Mater. Sci. 1995, 35, 661.
- Marks, B. M. US Patent 3,441,538 (1964).
- Mittal, V. (2011) High Performance Polymers and Engineering Plastics Ed. Vikas Mittal, Scrivener Publishing LLC
- Mohanty, D. K.; Sachdeva, Y.; Hedrick, J. L.; Wolfe, J. F.; McGrath, J. E. Am. Chem. Soc.Div. Polym. Chem. Polym. Prepr. 1984, 25, 19
- Staniland, P. A. Poly(ether ketone)s in Comprehensive Polymer Science; Allen, G.; Bevington, J. C., eds.; Pergamon Press: New York, 1989, Vol. 5, pp 484-497.
- Starkweather, H. W. In Encyclopedia of Polymer Science and Engineering, John Wiley and Sons: New York, 2nd ed., 1987, vol. 10, pp 369-373.
- Rose, J. B. European Patent 63, 874 (1983); Chem. Abstr. 1983, 98, 180081
- Percec, V.; Clough, R. S. Macromolecules 1994, 27, 1535.
- Percec, V.; Clough, R. S.; Grigors, M.; Rinaldi, P. L.; Litman, V. E. Macromolecules 1993,
- [www.sabic.com/](http://www.sabic.com/)
- [www.pbiproducts.com/](http://www.pbiproducts.com/)
- <http://industrial.vestakeep.com/product/peek-industrial/en/Pages/default.aspx>
- <http://medical.vestakeep.com/product/medical/en/>.
- <http://mitsuichem.com>.
- <https://www.solvay.com/en/markets-and-products/featured-products/torlon.html>

## CHAPTER 3: PROCESSING AND CHARACTERIZATION OF HPPS MATRICES

### 3.1 Processing

The preparation of polymeric nanocomposites is critical, due to the hydrophobic nature of the polymer with respect to the hydrophilic nature of many types of nanofillers. Furthermore, shape, size, surface morphology and distribution of the nanofiller in the polymer matrix determine the basic properties of the nanocomposite. The fundamental requirement lies in the so-called "principle of maximum heterogeneity" or "nanoheterogeneity": the nanofiller particles must be individually dispersed in the polymer matrix so that the heterogeneous nature of the material is revealed only for nanoscale sampling. In theory, each nanometer particle should contribute the same to the overall properties of the composite. The first problem lies in the preparation of the filler, which can be "nano" on one dimension (lamella), two dimensions (fibers) or three dimensions (spherical nanoparticles). For example, to have the maximum reinforcing effect, it is necessary to use lamellar particles or fibers, since the efficiency of the strengthening depends on the length / thickness ratio. The nanofiller must then be made chemically similar to the polymer ("compatibilized") to increase its hydrophobicity and favour its adhesion and dispersion in the matrix. The second problem lies in the synthesis of the nanocomposite which can be carried out according to three methodologies:

**In situ polymerization:** it was the first method used to make PA6-clays nanocomposites, but it is also the most widespread for thermosetting matrix nanocomposites. The first step provides that the filler is added to the monomer, possibly using agitation / sonication methods that favour the fine dispersion of the clay in the monomer, and that is allowed to swell (swelling) in the monomer for a certain period of time, to a certain temperature.

**Intercalation of the polymer in solution:** it foresees the use of polar solvents, able to originate nanocomposites intercalated. An organically modified filler, generally clay, is dispersed in a polar solvent such as toluene, N, N-dimethylformamide, etc. A system similar to that of a gel is obtained, due to a rather marked swelling process of the clay. Then the polymer is dispersed, allowing the polymer to intercalate between the galleries of the clay particles. Finally, the solvent is removed, usually under vacuum. With this method, nanocomposites based on high-density polyethylene (HDPE), polyamides, epoxy resins, nematic polymeric liquid crystals, and also nanocomposites with unsubstituted clays, using deionized water as solvent, were synthesized. The driving force of solution intercalation is the increase in entropy deriving from the desorption of solvent molecules, able to compensate the decrease in conformational entropy of the intercalated polymer chains. Moreover, this method has the advantage of being able to use polymers with low or no polarity, even if it is difficult to industrial application, due to the large quantities of solvent required.

**Polymerization by direct intercalation of the melted polymer:** it consists of mixing a melted thermoplastic with an organically modified filler, to optimize the inorganic polymer-filler interactions. The mixture is then brought above the glass transition temperature of the polymer to form the nanocomposite. In this case, it is believed that the substantial decrease in conformational entropy that the polymer chains undergo in the intercalation process is compensated and overcome by the enthalpy contribution of the polymer-filler interactions, which are carried out in the mixing and cooling. This method has great potential for industrial exploitation, also because it has been obtained by extruding several thermoplastics, such as polyamides and polystyrene; polyolefins, on the other hand, present some problems to interlayer according to this way, even if in some cases nanocomposites have been obtained. This production system is the most economically advantageous, because it does not use solvents and it is compatible with commonly used industrial processes, such as moulding or extrusion. The process typically involves the use of suitable instruments for optimal dispersion and distribution of the fillers in the polymer, such as twin-screw extruders. Through this process, the plastic in the form of granules or powder is introduced into a heated mixer (extruder), where rotating screws homogenize the whole. The particulate of micro or nano metric size is mixed with the polymer matrix in a molten state. Under these conditions, if the surfaces of the layer are sufficiently compatible with the chosen polymer, the polymer can diffuse between the layers and form either a flaked nanocomposite or an intercalated or simply dispersed nanocomposite. By heating and applying shear stresses during mixing, intercalation and in some cases delamination of the charge may occur, depending on the degree of penetration of the polymer in the silicate. The critical factor that directs the formation of the hybrid towards one or the other form is not known, but it is probably linked to thermodynamic factors. From a thermodynamic point of view, in this case there is no entropic gain, due to the desorption of the solvent. The intercalation of the polymer is made possible, from the thermodynamic point of view, by other factors. If we consider a compatibilized clay, when the polymer diffuses between the laminae of the modified clay, the spacing of the clay increases and therefore increases the conformational energy of the compatibilizing chains, due to the dimensional increase of the silicate tunnels later on when the polymer is inserted. This entropic gain compensates for the entropic decrease, due to polymer confinement. The intercalation process is therefore isentropic. In order to maintain the condition of spontaneity, it is necessary to look for the driving force in the enthalpy, i.e. a negative enthalpy variation is necessary due to the increase of the interaction energy between the host species (the polymer) and the host species (the charge). This condition is realized in the establishment of weak bonds such as hydrogen bonds, dipole-dipole interactions and Van der Waals. These bonds are extremely weak, but they are also very widespread interactions in the silicates and therefore overall this contribution is not negligible. It is precisely the enthalpy contribution that makes the energy of the system smaller and therefore makes the intercalation process possible. Exfoliation leads to an

increase in entropy due to the loss of order by the system. The main advantage of this technique is that for the processing of the thermoplastic nanocomposites thus obtained the traditional processing techniques with which thermoplastic polymers are processed (extrusion and injection) can be used, while the fundamental disadvantage is the difficulty of finding crystal-compatible systems. In some cases, even if from a thermodynamic point of view, it is possible to intercalate and exfoliate the clay, the processing times are too long and can lead to the deterioration of the polymer. It is evident that preparing nanocomposites by intercalation, exfoliation and melt dispersion is far more interesting from an industrial point of view, since it releases the phase of obtaining the nanocomposite material from that of polymer synthesis, and mixing occurs in mass in the absence of flammable solvents. Furthermore, the process is potentially transferable on most plants that process plastics currently in use, and therefore within the reach of a large number of industrial entities, even of limited size. The process of preparation by mixing in the molten state is by far the most studied for its practical implications of applicability and scalability at the industrial level, but also the one that most easily can lead to partial or irreproducible results if not properly optimized.

### **3.1.1 Extrusion, melt compounding and injection moulding**

The need to obtain phenomena that facilitate the dispersion of fillers suggests using extrusion process with ample mixing times that imply the realization of masterbatches or the use of extrusion machines which also provide a compounding device inside. The processing of the materials object of the present study was carried out with a corotating twin-screw micro-extruder produced by DSM mod. Xplore 15 Microcompounder. It is called micro extruder because it allows to work with small quantities of material (up to 15 cm<sup>3</sup>), allowing a considerable saving of material and expanding, at the same cost, the possibilities of screening the possible composites. This particular laboratory machine is characterized by a remarkable versatility, allowing a wide flexibility of the process parameters and the geometry of the extrusion cycle; in the specific case, it can be used simultaneously as a mixer and as an extruder for the production of materials. In order to carry out the compounding, it is sufficient to divert the flow of the polymer melt into an appropriate recirculation channel through a mechanical switch and the mixing is obtained for the desired time until, once again, the material exiting the extrusion head is directed again.

**Figure 3.1** shows the used micro extruder and details of the extrusion chamber with the switch for the deviation of the flow. The realization of the specimens is possible thanks to a micro injection press produced also by DSM mod. Micro 10cc Injection Moulding Machine; being able to operate in a coordinated way with the micro-extruder, it allows to produce samples of various shapes for injection moulding. **Figure 3.2** shows the press and the complete compounding, extrusion and injection system.



**Figure 3.1:** DSM microextruder used detail of the extrusion chamber with mixing switch



**Figure 3.2:** Micro press and complete compounding, extrusion and injection system

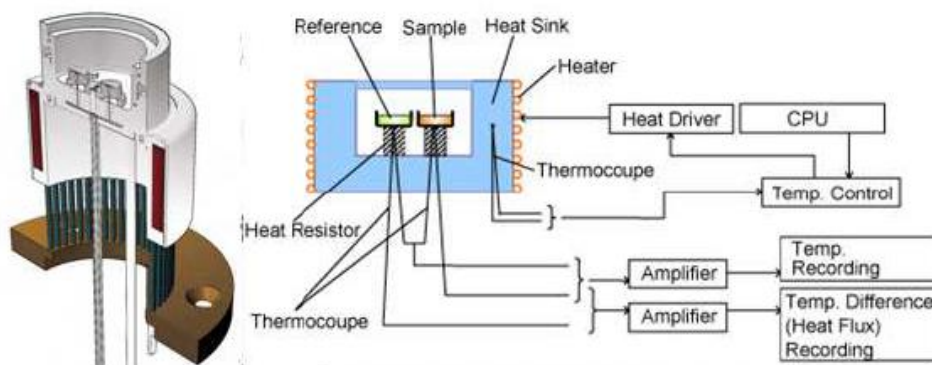
## 3.2 Thermal characterization

### 3.2.1. Differential scanning calorimetry (DSC)

DSC is the most frequently employed thermal analysis technique and it can be used to analyse nearly any energetic effects occurring in a solid or liquid during the thermal treatment used to design, manufacture, and test products. This technique is based on the energy registration required to establish a zero-temperature difference between the sample and an inert reference, as a function of time or temperature. The difference in energy recorded by the instrument is equal to the thermal energy absorbed or dissipated during the transition of the material. At that moment, displacements from the baseline are recognized for different physical or chemical changes, whose area is

proportional to the enthalpy change associated to this transition. The biggest advantage of DSC is its ease and speed to determine transitions in different materials.

**Figure 3.3a** shows the diagram of a DSC cell which comprises the sample and reference holders, the heat resistor, the heat sink, and the heater. The heat from the heater is supplied into the sample and the reference through the heat sink and heat resistor.



a)



b)

**Figure 3.3.** DSC cell diagram (a) and Q200 TA Instrument (b)

Analyses were performed with a differential scanning calorimeter (DSC) produced by TA Instruments model Q200, with the possibility of MDSC configuration (modulated DSC) (**Figure 3.3b**). The thermal investigations carried out on the polymers allow defining the melting range of the polymer matrices by analysing the curve of the heat flow as a function of the temperature. The knowledge of the characteristic points of the melting phase makes it possible to identify the thermal parameters of the polymer melt extrusion process. These analyses allow, depending on the temperature, also evaluating the weight variation that is generally related to the thermal degradation phenomena; it follows that the process limit times, in relation to the adopted temperature, are identified.

### 3.2.2 Thermo Gravimetric Analysis (TGA)

TGA is defined as a thermal technique in which the sample mass is monitored against time or temperature while the temperature of the sample, in a specified atmosphere, is programmed<sup>20</sup>.

**Figure 3.4** and **Figure 3.5** shows, respectively, the diagram of a TGA equipment with horizontal balance and the instrument produced by the Seiko Exstar 6300 model connected to the gas (nitrogen or oxygen) supply line.

TGA tests are based on a pan containing the sample supported by a precision balance. During the experiment, the pan resides in a furnace where it is heated. A sample purge gas controls the sample environment, which can be inert or a reactive one, and flows over the sample. TGA instruments can be used to quantify the loss of water, solvents or plasticizers; to monitor decarboxylation, pyrolysis, oxidation and decomposition reactions; to determine the % weight of a filler, ash or the amount of metallic catalytic residues remaining on carbon nanotubes.

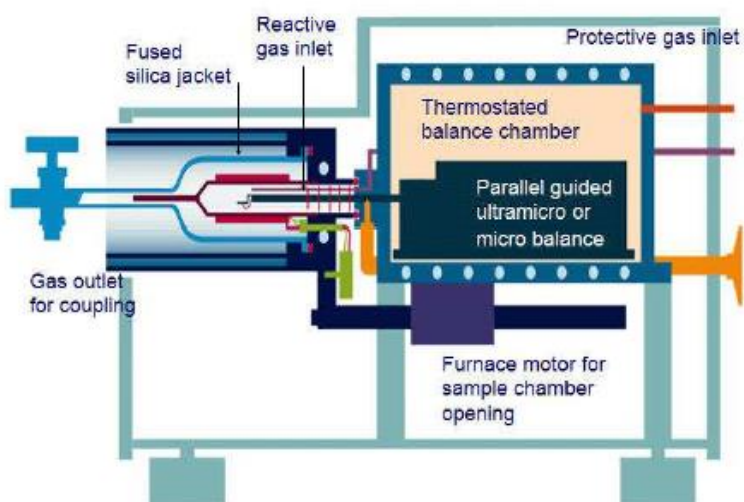


**Figure 3.4.** TGA equipment with horizontal balance



**Figura 3.5:** Thermogravimetric analyzer model Seiko Exstar 6300



In the present work, TGA was used for the study of the thermal stability of neat systems and polymeric nanocomposites/blend formulations. For all tests, inert N<sub>2</sub> atmosphere was used to ensure that samples only react to temperature during decomposition. Results from TGA analysis have been considered to fix the range for evident thermo-degradation phenomena; this information provides another important element for the evaluation of the type and parameters of the production process of the nanocomposites being studied.

### **3.2.3 Heat Deflection Temperature (HDT)**

The heat deflection temperature or heat distortion temperature (HDT, HDTUL, or DTUL) is the temperature at which a polymer or plastic sample deforms under a specified load. This property of a given plastic material is applied in many aspects of product design, engineering, and manufacture of products using thermoplastic components. The heat distortion temperature is determined by the following test procedure outlined in ASTM D648. The test specimen is loaded in three-point bending in the edgewise direction. The outer fiber stress used for testing is either 0.455 MPa or 1.82 MPa, and the temperature is increased at 2 °C/min until the specimen deflects 0.25 mm. This is similar to the test procedure defined in the ISO 75 standard. Limitations that are associated with the determination of the HDT are that the sample is not thermally isotropic and, in thick samples in particular, will contain a temperature gradient. The HDT of a particular material can also be very sensitive to stress experienced by the component which is dependent on the component's dimensions. The selected deflection of 0.25 mm (which is 0.2% additional strain) is selected arbitrarily and has no physical significance.

An injection moulded plastic part is considered "safe" to remove from its mould once it is near or below the HDT. This means that part deformation will be held within acceptable limits after removal. The moulding of plastics by necessity occurs at high temperatures (routinely 200 °C or higher) due to the low viscosity of plastics in fluid form (this issue can be addressed to some extent by the addition of plasticizers to the melt). Once plastic is in the mould, it must be cooled to a temperature to which little or no dimensional change will occur after removal. In general, plastics do not conduct heat well and so will take quite a while to cool to room temperature. One way to mitigate this is to use a cold mould (thereby increasing heat loss from the part). Even so, the cooling of the part to room temperature can limit the mass production of parts.

Choosing a resin with a higher heat deflection temperature can allow manufacturers to achieve a much faster moulding process than they would otherwise while maintaining dimensional changes within certain limits.

VICAT softening temperature or Vicat hardness is the determination of the softening point for materials that have no definite melting point, such as plastics. It is taken as the temperature at which

the specimen is penetrated to a depth of 1 mm by a flat-ended needle with a 1 mm<sup>2</sup> circular or square cross-section. For the Vicat A test, a load of 10 N is used. For the Vicat B test, the load is 50 N. Standards to determine Vicat softening point include ASTM D 1525 and ISO 306, which are largely equivalent. The Vicat softening temperature can be used to compare the heat-characteristics of different materials.

### 3.3. Mechanical characterization

#### 3.3.1 Tensile tests at T room and high Temperature

The tensile tests were performed according to standard ISO 527-1 (Plastic materials - Determination of tensile properties, General principles), in ISO 5893 (Tools for tensile, flexural and compression tests - at constant speed of the cross beam) and in ASTM D 638 (Standard test methods for tensile properties of plastics). Tensile tests were carried out using a universal electronic dynamometer produced by LLOYD Instruments, mod. LR30K, shown in **Figure 3.6**, operating with a 30KN load cell with full scale connected to a PC for data acquisition.



**Figure 3.6:** LR30K dynamometer used for tensile tests

The tensile tests were carried out using the controlled deformation method; the instrument has been set to have a rate of 5 mm per minute. This model of dynamometer is equipped with an environmental conditioning chamber that allows also performing temperature-controlled tests with a range from -80 to +250 ° C.

### 3.3.2 Impact test

The Charpy Test, Charpy V-notch Test, Izod Test and other Impact Testing determine the toughness or impact strength of different materials in the presence of a flaw or notch and fast loading conditions. This destructive test involves fracturing a notched impact test specimen and measuring the amount of energy absorbed by the material during fracture.

In this thesis two different destructive tests (Charpy Test and Izod Test) are used to characterize the materials. It is one of the most popular impact testing methods due to the relative ease of creating samples and obtaining results. The test apparatus consists of a weighted pendulum, which is dropped from a specified height to make contact with the specimen. The energy transferred to the material can be inferred by comparing the difference in the height of the pendulum before and after the fracture. Charpy impact testing is most commonly performed to ASTM E23, ASTM A370, ISO 148, or EN 10045-1. While the test is most commonly performed on metals, there are also several standards that exist for plastics and polymers, including ASTM D6110 and ISO 179.

The test apparatus and specimen design are very similar to Charpy impact, with some notable differences, including the orientation of the specimen, which is clamped into the apparatus vertically with the notch facing toward the pendulum. The pendulum then impacts the sample at a specified area above the notch. One of the main differences from Charpy impact is that Izod impact testing can be performed on either plastic or metallic specimens. Common Izod impact test methods include ASTM D256, ASTM E23, and ISO 180. Specifically, both impact tests entail striking notched specimens with a swinging weight or pendulum at a series of temperatures to show the relationship of ductile to brittle transition in absorbed energy. Where they differ is in the dimensions of the specimens and the positioning of the specimens in the test machine. **Figure 3.7** shows the instrument, Charpy e Izod Plásticos PIT-25, used in this thesis.

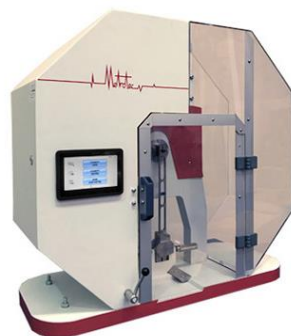


*Figure 3.7: Charpy e Izod Plásticos PIT-25*

### 3.3.3 Dynamical Mechanical Thermal Analysis (DTMA)

Dynamic mechanical analysis (DMA) is a thermal analysis technique that measures the properties of materials as they are deformed under periodic stress. Specifically, in DMA a variable sinusoidal

stress is applied, and the resultant sinusoidal strain is measured. If the material being evaluated is purely elastic, the phase difference between the stress and strain sine waves is  $0^\circ$  (i.e., they are in phase). If the material is purely viscous, the phase difference is  $90^\circ$ . However, most real-world materials including polymers are viscoelastic and exhibit a phase difference between those extremes. This phase difference, together with the amplitudes of the stress and strain waves, is used to determine a variety of fundamental material parameters, including storage and loss modulus,  $\tan \delta$ , complex and dynamic viscosity, storage and loss compliance, transition temperatures, creep, and stress relaxation, as well as related performance attributes such as rate and degree of cure, sound absorption and impact resistance, and morphology.

DMA measurements are made using a single frequency and constant deformation (strain) amplitude while varying temperature (dynamic mechanical analysis in temperature, DMTA).

**Figure 3.8** shows the instrument, *Rheometric Scientific, ARES N2*, used in this work.

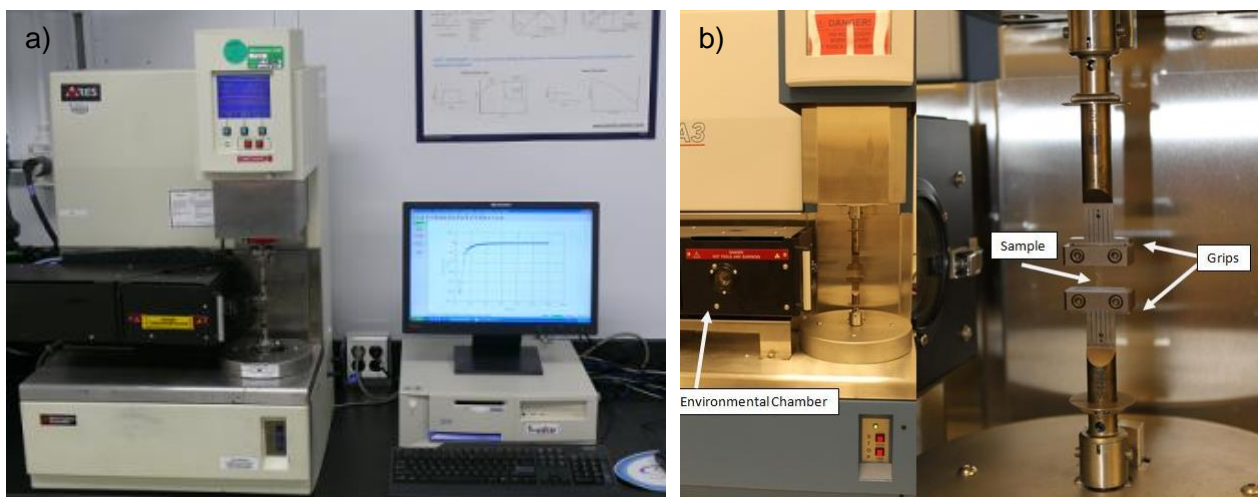


**Figure 3.8:** DMA, Rheometric Scientific, ARES N2 (a), a typical DMA tester with grips to hold sample and environmental chamber to provide different temperature (DMTA) conditions (b).

### 3.4 Morphological characterization

A field emission scanning electron microscopy (FESEM) (**Figure 3.9**) is a microscope that works with electrons instead of light and it could be classified as a high vacuum instrument (less than  $1 \times 10^{-7}$  Pa in the gun zone). These electrons are liberated by a field emission source, being a versatile, non-destructive technique that reveals detailed information about the morphology and the composition of materials. Electrons are liberated from a field emission source and accelerated in a high electrical field gradient. Within the high vacuum column these so-called primary electrons are focused and deflected by electronic lenses to produce a narrow scan beam that bombards the object. As a result, secondary electrons are emitted from each spot on the object. The angle and velocity of these

secondary electrons relates to the surface structure of the object. A detector catches the secondary electrons and produces an electronic signal. This signal is amplified and transformed to a video scan-image that can be seen on a monitor or to a digital image that can be saved and further processed. Polymer samples are usually sputtered with gold in order to increase their electrical conductivity and then analysed.

**Figure 3.9** shows the image of FESEM used in this work (FESEM, Supra 25-Zeiss, Germany).



**Figure 3.9:** FESEM, Supra 25-Zeiss, Germany.

A morphological evaluation campaign of nanocomposite materials was performed. The observation of the morphology can in fact provide important information with respect to the dispersion of the fillers in the matrices and the possible interactions of the technopolymer with the charge. The analysis of the morphology of the bonds at the matrix-fillers interface allows us to understand the affinity between the components and the goodness of the production process.

### **3.5 Rheological characterization**

An examination of the rheological characteristics allows to analyse how the viscosity varies as a function of the shear rate, both for the neat matrices and for the loaded systems. Therefore, a comparison of rheological curves provides key elements for assessing the effect of nanofillers on workability. The parameters that will be analysed are the viscosity values and the dependence on the shear rate. In order to evaluate rheological curves, tests were performed with a rotational rheometer produced by Rheometric Scientific model Ares using a test geometry with parallel flat plates of 25mm diameter. **Figure 3.10** shows the used tool.

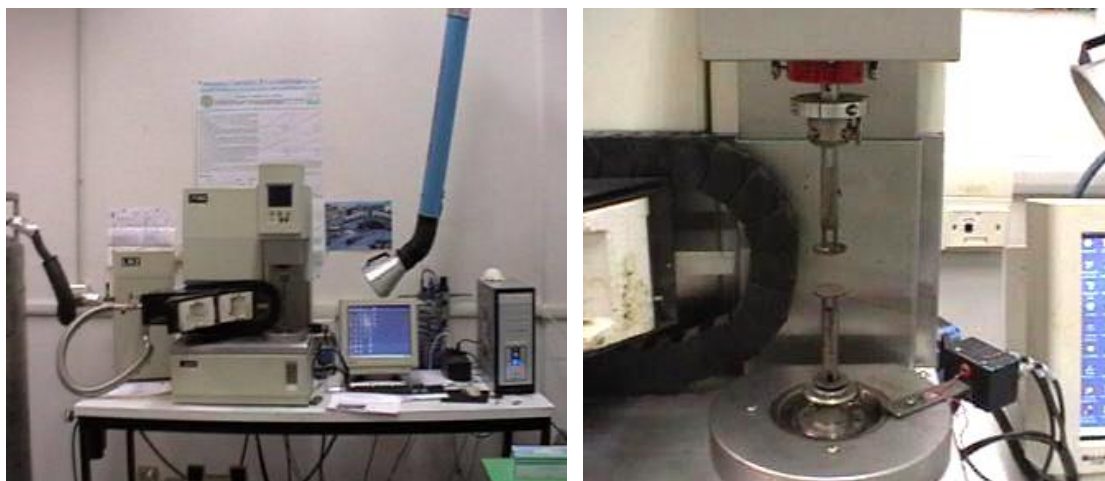


**Figure 3.10:** Parallel flat plate rheometer Ares model produced by Rheometric Scientific with a detail of parallel plates tool

The measurements were performed at a constant temperature of 400 °C under oscillatory test conditions. The Dynamic Strain Frequency Sweep Test mode was used with increasing oscillation frequency in the range 0.1 - 100 rad / sec. This range has been selected to evaluate the widest possible spectrum of properties. In addition to the viscosity curves, the trends of the storage and loss moduli were also analysed.

### 3.6 References

- <http://www.fis.unipr.it/dokuwiki/lib/exe/fetch.php?media=lmn:brochure.pdf>  
<https://www.zeiss.com/microscopy/int/products/scanning-electron-microscopes/sigma.html>
- <http://www.tainstruments.com/products/microcalorimetry/differential-scanning-calorimetry/>
- <https://scientificservices.eu/item/thermogravimetrydifferential-thermal-analyzer-tgdt-a-seiko/1605>
- <http://www.tainstruments.com/ares-g2/>
- <http://www.metrotec.es/>

## CHAPTER 4: NEAT MATRICES AND FIBER REINFORCED COMPOSITES

### 4.1 Neat matrices and fiber reinforced composites

The advanced fibre reinforced polymer (FRP) composite market is dominated by materials based on thermoset polymer (TS) matrices such as epoxy, polyimides, bismaleimides and cyanate esters which have found many applications in aeronautic, space and military usages whose extreme environments demand high-performing materials (**Figure 4.1**).

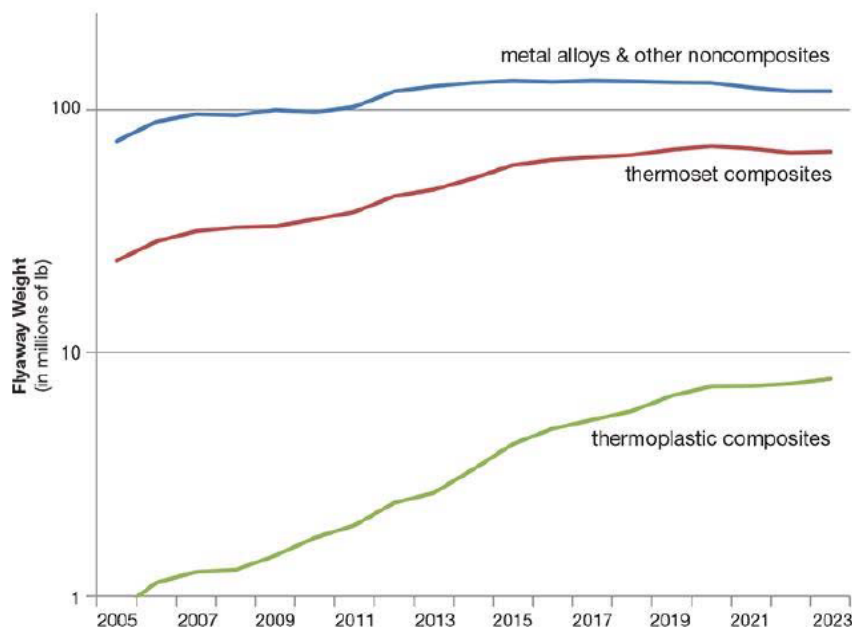


**Figure 4.1:** Trend for thermoplastic in aerospace composites [Red, C., *The Outlook for Thermoplastics in Aerospace Composites, 2014-2023, in High-Performance Composites. 2014, Gardner Business Media, Inc.: Cincinnati, Ohio. p. 54-63*].

However, thermosets have limitations in terms of storage, hydrothermal ageing, insufficient toughness and have constraints in processing since long and strict multi-step processing by autoclave are needed. Therefore, the replacement of TS matrices by thermoplastic polymers is an area of intense research with primarily use in short fibres reinforced composites. Currently, TP-based matrix composites associated with continuous fibres are growing rapidly and the TP used as matrix potentially present major competitive advantages over thermosets because of their ease of implementation and their intrinsic characteristics such as an extremely long shelf life as well as their recycling possibilities. Thermoplastics are usually high molecular weight, linear polymers which form bulk material by non-covalent bonds like hydrogen bonding, dipole-dipole, van der Waals and  $\pi$ - $\pi$  interactions, and linear structures with network possibility. When high performance applications are targeted, thermoplastics with high thermal stability are required.



HPPs aroused a strong interest as an alternative polymer for thermoset matrices replacement to the extent where it has sufficiently good properties to be compatible with severe conditions.

The reinforcement of thermoplastics with the high modulus fibers to improve strength and rigidity has been in practice from many years. HPPs have the excellent properties of the thermoplastics and they also offer a high strength over a wide temperature range. To maximize the usefulness of these resins, they are often available as reinforced composites.

In this context, we aimed to investigate the thermo-mechanical behaviour of commercial fiber reinforced HPPs, in particular we studied the general performance of composites mainly based on PEEK, PBI and TPI and their composites containing 30% wt. of Carbon and Glass Fiber. In order to efficiently advance with the characterization of the systems that could justify their utilization as fiber reinforced matrices in a nanocomposite approach, we proceed starting with the basic thermomechanical and rheological characterization of commercial products, listed in table (**Table 4.1**):

**Table 4.1:** Commercial HPPs and their fiber reinforced products containing glass and carbon fibers

NAME	TYPE	FIBER REINFORCE	NOMENCLATURE
AURUM (PL450C)	TPI	- - -	TPI
AURUM	TPI	30%GF	TPI30GF
AURUM	TPI	30%CF	TPI30CF
ULTEM	PEI	- - -	PEI
TORLON (4203L)	PAI	- - -	PAI
TORLON	PAI	30%GF	PAI30GF
POLYIMIDE (P84NT)	PI	- - -	PI
CELAZOLE (TU60)	PBI	- - -	PBI/PEEK
CELAZOLE (TF60V)	PBI	30%GF	PBI/PEEK30GF
CELAZOLE(TF60C)	PBI	30%CF	PBI/PEEK30CF
VESTAKEEP (2000P)	PAEK (PEEK)	- - -	PEEK
VESTAKEEP	PAEK (PEEK)	30%GF	PEEK30GF
VESTAKEEP	PAEK (PEEK)	30%CF	PEEK30CF
VESTAKEEP (4000P)	PAEK (PEEK)	- - -	PEEK4
VESTAKEEP	PAEK (PEEK)	30%GF	PEEK430GF
VESTAKEEP	PAEK (PEEK)	30%CF	PEEK430CF
LARAMID (PPA)	PARA	- - -	PARA
LARAMID	PARA	30%GF	PARA30GF

The main problem that we had to face in the processing of the neat and fiber reinforced HPPs was the adjustment of the extrusion/moulding equipment already available in our laboratories, that was

originally set to process polymeric matrices with relative low melting profiles. Specifically, we should proceed with the following modifications: (i) adjustment of the controlling instrument software to follow the temperature profiles; (ii) regulation of the heating systems by adding new resistances in the injection mould/chamber and in the extruder to reach the high melting temperatures of the selected HPPs; (iii) use of a new compression system (15 bars instead of 9 bars) to permit the injection of HPPs with high viscosities profiles (**Figure 4.2**).



**Figure 4.2:** Required adjustments of the processing equipments for the preparation of HPPs and fiber reinforced HPPS

The greatest difficulties have emerged in the search for optimal process parameters which involved numerous tests and attempts at the limits of the instruments settings. The most difficult composites to be extruded and injected were the fiber-reinforced products (and the nanomodified ones), difficulties due to the higher viscosity that the glass fiber (and the nanocarriers) generated. These formulations carried the extruder to high forces and on some occasions even the momentary blockage of the machinery. On the contrary, in the injector the lower fluidity of the fiber-reinforced composite made it difficult to fill the mould. For this reason, the optimization of the process parameters (temperature profile, rotation rate of the screws, injection pressures, mould temperature) was carried out: the optimized parameters were obtained through a semi-empirical feedback process, to obtain the best possible results compatible with the potential of the lab instruments. This semi empiric optimization procedure with loop feedback, which necessarily involves sacrificial attempts, has led to the use of laboratory instruments at the upper use limit.

In conclusion, despite the objective limits of the lab-scale devices, it was possible to produce all the established formulations and characterize them from a thermo mechanical perspective.

#### **4.2 Thermal characterization of neat matrices and fiber reinforced composites**

Analyses were performed with a differential scanning calorimeter (DSC) produced by TA Instruments model Q200, with the possibility of MDSC configuration (modulated DSC). The neat polymer and the granules of masterbatches loaded with 30% glass fiber and carbon fiber were subjected to a thermal ramp at a speed of 10 °C/min. The DSC profiles and the related thermal characteristics are reported in the following Figure (**Figure 4.3**).

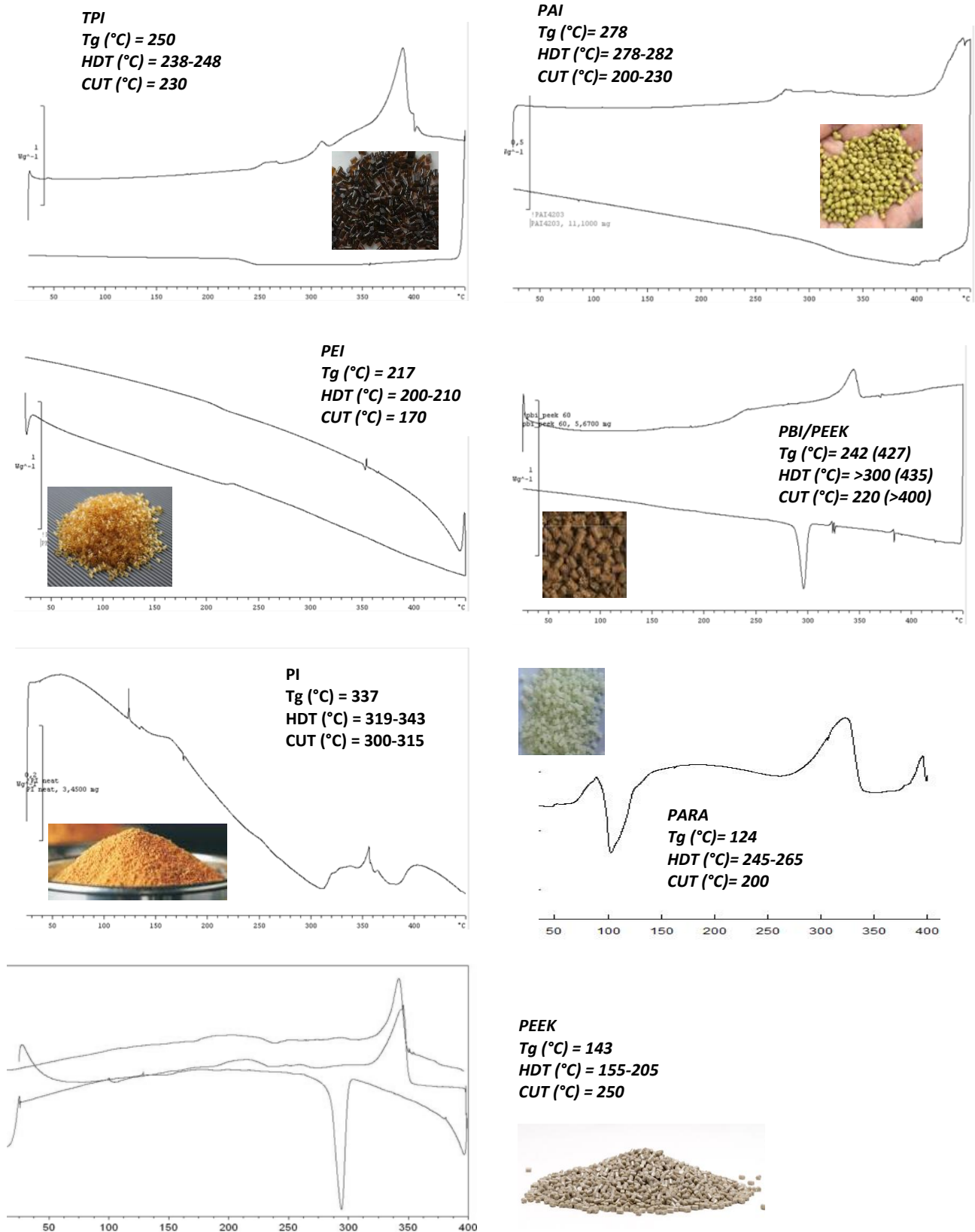


**Figure 4.3:** DSC profiles for neat HPPS matrices (neat grade), with indication of their colour, glass transition, HDT and CUT temperatures

Cooling scans for P84NT (PI) and LARAMID PPA (PARA) are not reported in Figure 4.3, since we realized that no significant information could be extrapolated from a further thermal scan in cooling conditions for these two specific matrixes. No substantial differences, in terms of melting profiles, were found for the fiber filled compounds, such as the HDT characterization (**Figure 4.4**) (boiling medium = silicone oil,  $T_b \approx 260^\circ\text{C}$ ), that confirmed unaltered or slightly modifies values for fiber reinforced PEEK based compounds (VK2000GF30 and VK2000CF30), fiber reinforced PBI/PEEK based compounds (TF60V and TF60C) and TPI based compounds (JGN3030 and JCN3030). We noted only that a rearrangement of the polymeric structure was evident, with few differences in the melting profile, in the case of composites containing thermally conductive carbon fibers. This phenomenon should be considered during the production phase of the samples to be tested and subsequently produced, since the phenomenon can influence the characteristics of the reinforced products [Goodwin and Simon, 1995].

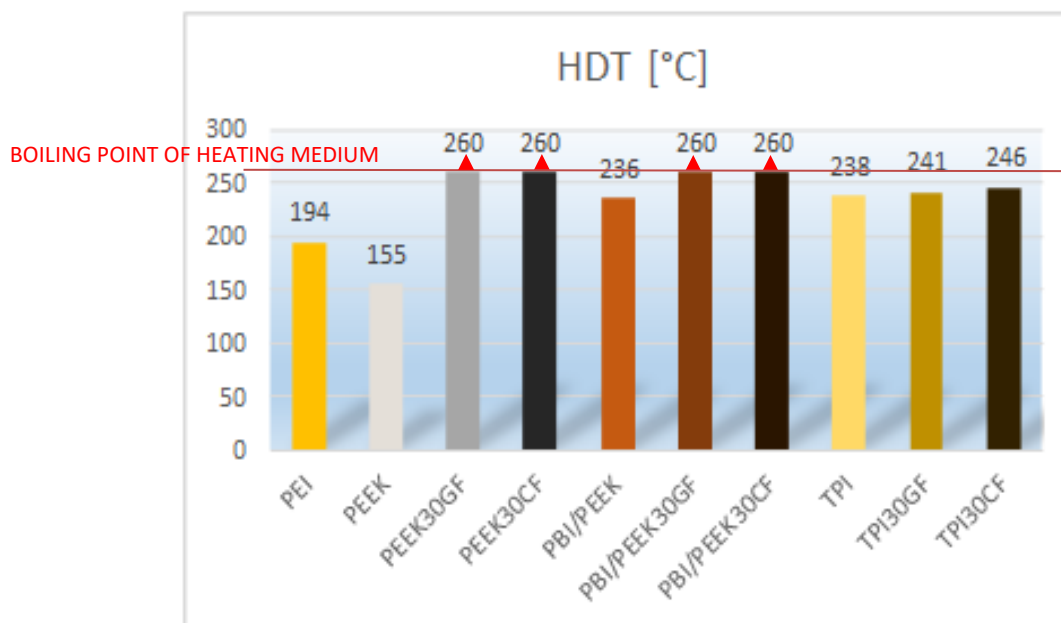


**Figure 4.4:** Detected HDT temperatures for neat HPPs matrices (neat grade) and fiber reinforced compounds

The HDT characterization (HDT/VICAT TESTER METROTEC, ASTM D648) was useful and necessary for the evaluation of suitable temperatures to be adopted in case of assessment of mechanical stresses at different frequency rate (impact, torsion) or at different testing temperatures (tensile characterization at high temperature). Here, we have reported the results of impact characterization made at room temperature and  $T = T_{\text{HDT}} - 40^\circ\text{C}$  (**Figure 4.5**).

The results confirmed how amorphous polymeric systems (TPI) performed better than semicrystalline (PEEK) and (PBI/PEEK) blends in terms of impact response, and in general the results well correlated with the presence of fibers in composites systems. In the case of characterization made

at high temperature, it is evident how the viscoelastic behaviour of the polymeric matrix had the main role.

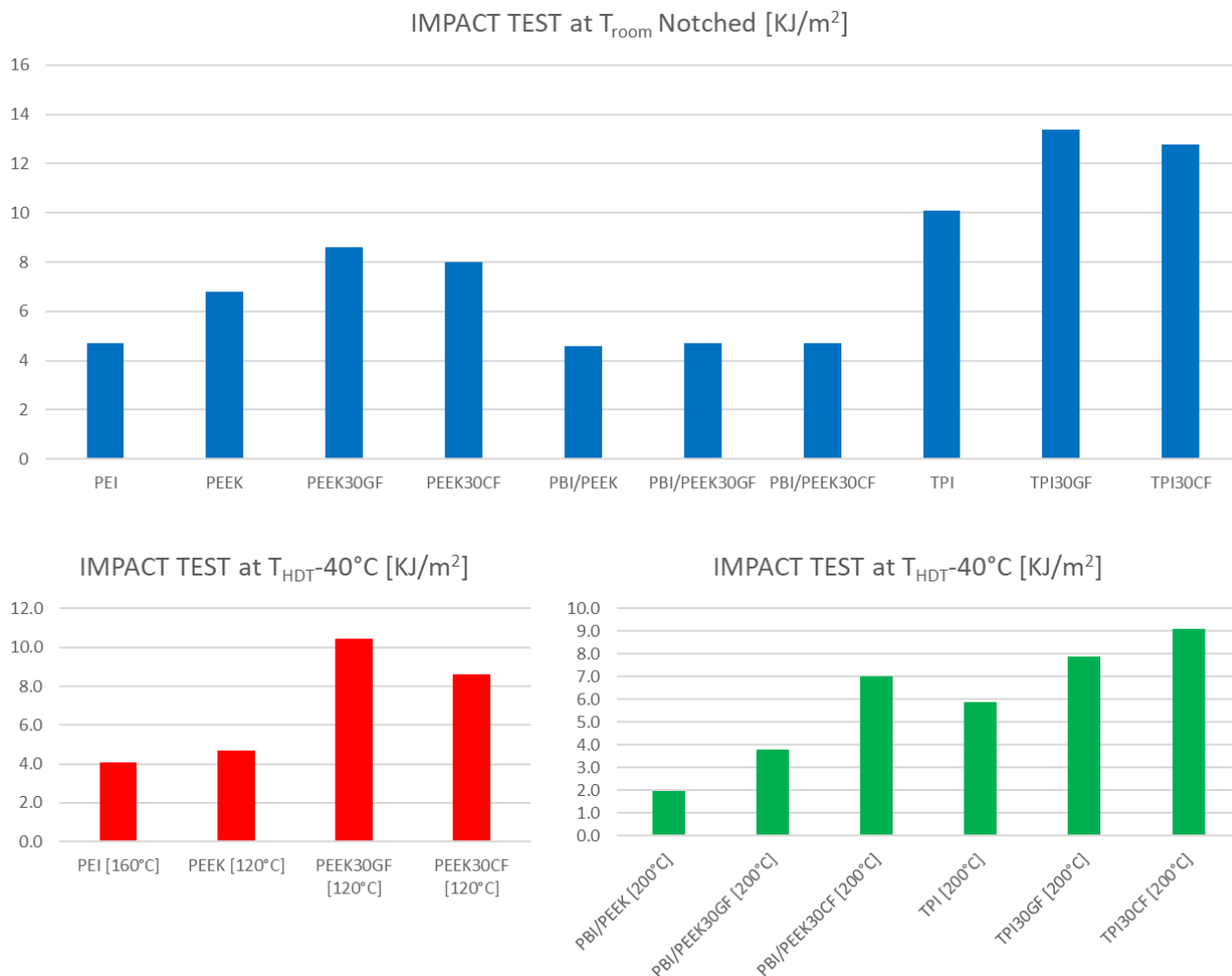


**Figure 4.5:** Results of impact tests for neat HPPs matrices (neat grades) and fiber reinforced compounds

To study the thermal stability of the selected systems, TGA dynamic scans at the heating rate of 10 °C/min were carried out for each material, with a test temperature range in the range from 30 °C to 900 °C. In each test, a flow of pure nitrogen was used to eliminate volatile thermo-oxidative products caused by the degradation process, and samples of size 5-6 mg were used. The DTG was simultaneously considered to highlight weight loss peaks. Test results are shown in **Figure 4.6**.

It can be seen that, with the selected heating mode, there are no evident thermo-degradation phenomena up to temperatures close to 500 °C; considering the shift of the curve due to the rapid heating, it can be affirmed, with good probability that important degradation phenomena will not occur in a short time with temperatures lower than 400 °C. This information provides another important element for the evaluation of the type and parameters of the production process of the nanocomposites being studied.

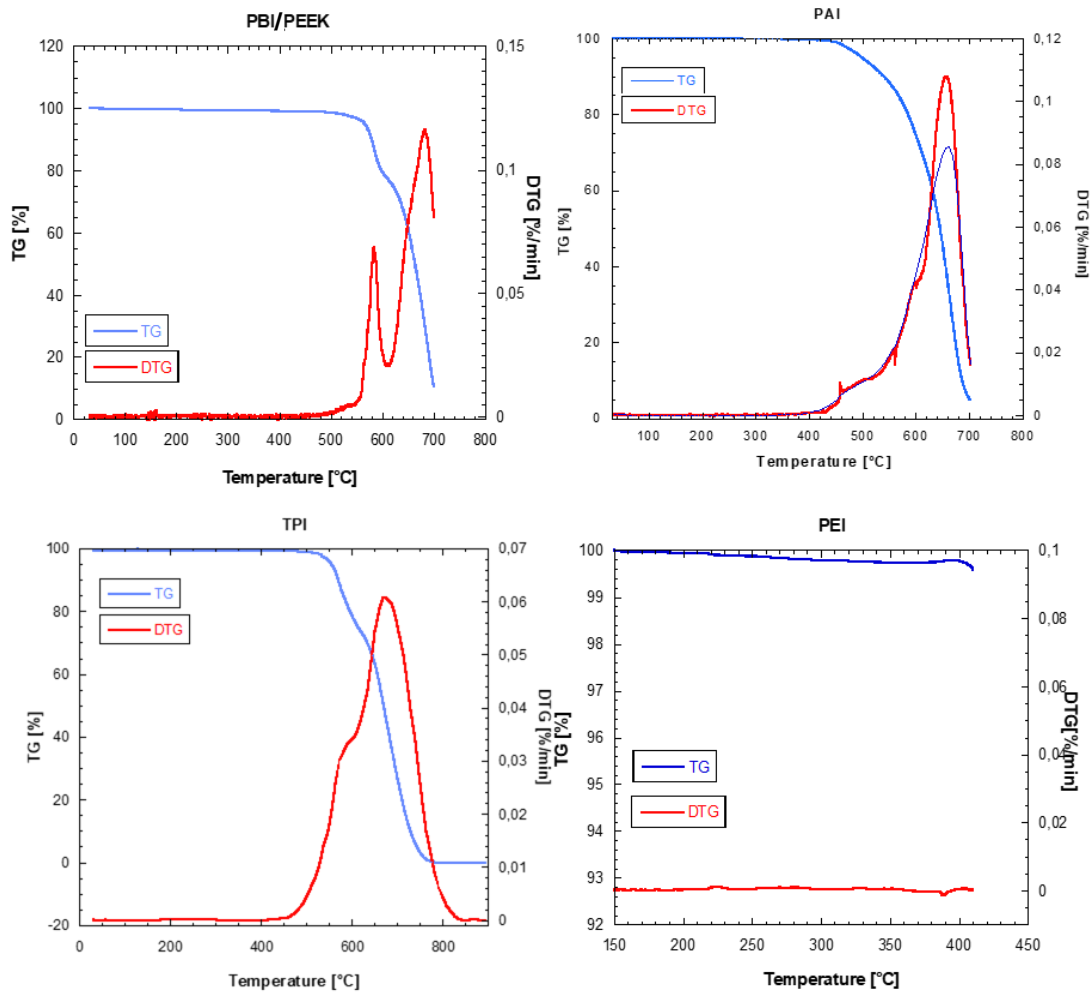


**Figure 4.6:** TG and DTG of some representative samples

### 4.3 Thermomechanical characterization of neat matrices and fiber reinforced composites

After this preliminary thermal characterization, we performed further DMTA test to evaluate the thermomechanical response of produced materials. We reduced the initial number of samples, based on processing difficulties and/or limited applicability of proposed commercial products. In details, the PARA sample was eliminated, since it was considered as the less stable from the thermal point of view (incipient degradation at 400°C, see Figure 4.6), while PI was eliminated due to limited processability (it was practically impossible to extrude the material without any other additive), while we were obliged to eliminate even the PAI system, due to limited features of our lab processing extruder (i.e. PAI requires specific extrusion system/geometries). On the basis of these perspective, we continue in the DMTA characterization of PEEK, TPI and PBI/PEEK blends and their related glass and carbon fiber composites [Saleem, Fromann, and Iqbal, 2007; Chun and Weiss, 2004].  $G'$  and  $G''$  profiles, such as  $\tan \delta$  curves for the cited systems are reported in **Figure 4.7a**, **Figure 4.7b** and **Figure 4.7c**.

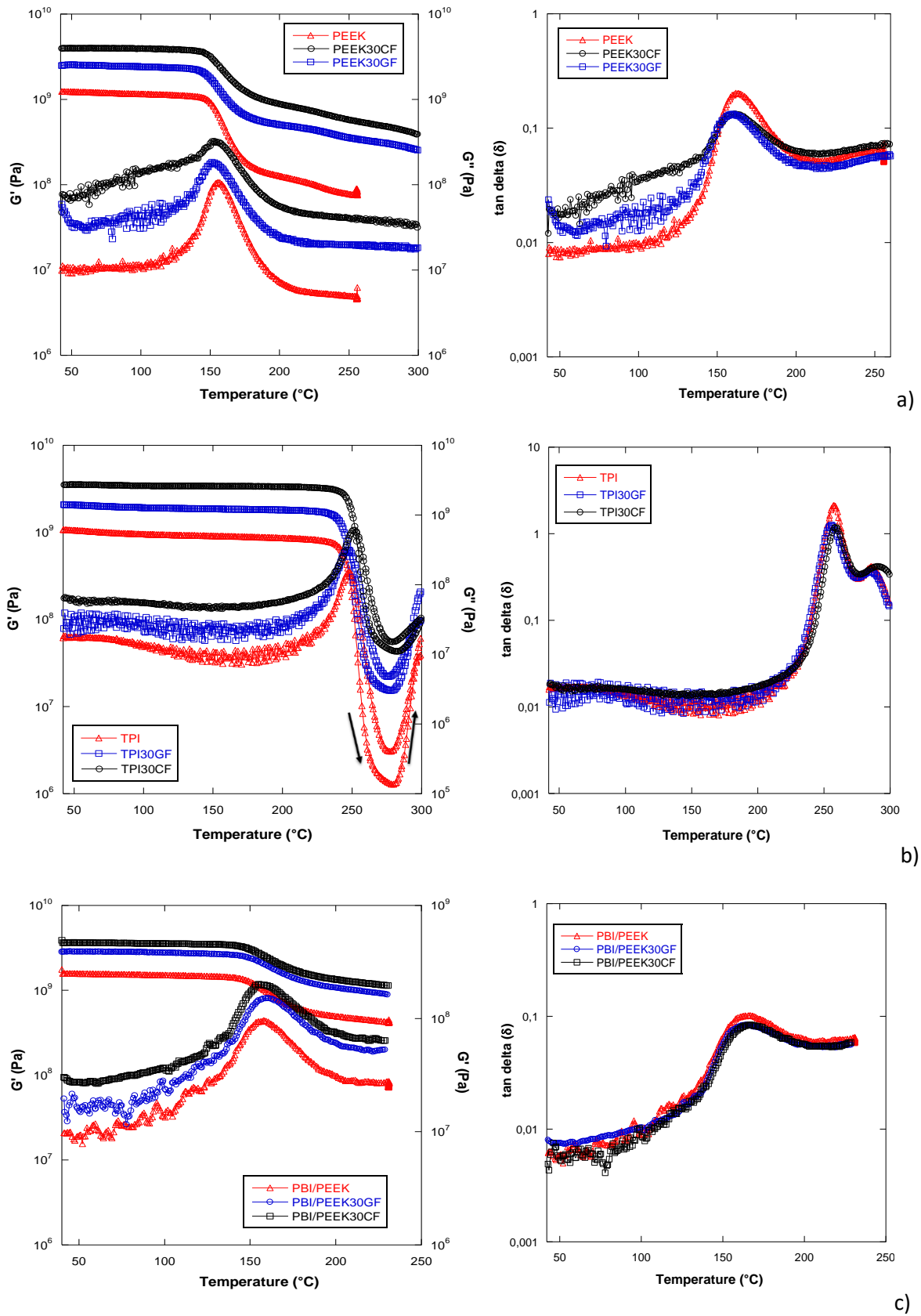


**Figure 4.7:**  $G'$ ,  $G''$  and  $\tan \delta$  profiles for neat HPPs matrices (neat grades) and fiber reinforced compounds: PEEK based (a), TPI based (b) and PBI/PEEK based (c) composites

The analysis of DMTA results for the cited systems gave us some important information about the thermomechanical performance of the neat matrices and the role of reinforcements in the evolution of  $G'$  and  $G''$  in a temperature range. In details, it was evident the increased values for  $G'$  in the case of carbon reinforced composites in comparison with both glass fiber reinforced materials, that was maintained almost for all the three different compounded systems, while a notable event was registered in the case of TPI based materials. Specifically, a further increase of the storage and loss moduli was registered, essentially due to a crystallization phenomenon that appeared after surpassing the typical glass transition for TPI (range between 250 and 270°C) [Hsiao, Sauer and Biswas, 1994].

We were able to identify this behaviour even by using an instrument equipped with a camera (Figure 4.8a) able to register the evolution at high temperature. In Figure 4.8c, the evolution of transparency to opacity during the sample specific heating scan is reported. This behaviour essentially confirms what already observed in DSC analysis (Figure 4.8b).

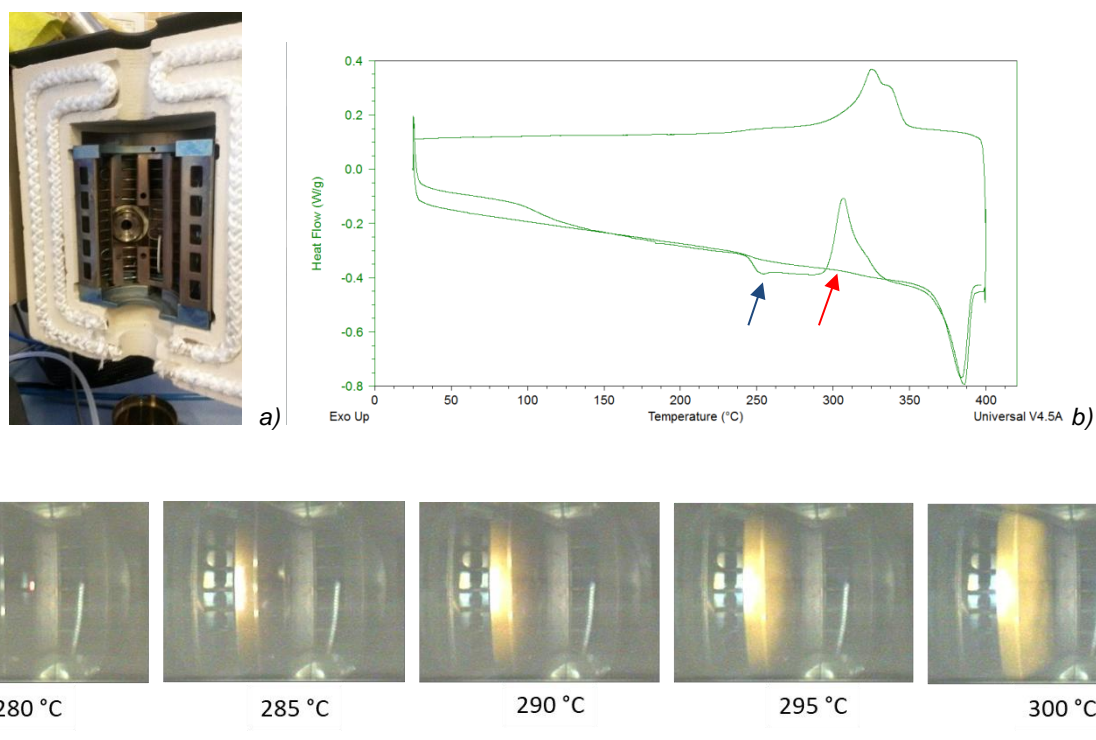


**Figure 4.8:** DMTA equipped with a camera (a), DSC profile for TPI heated between 25 and 400°C at 10°C/min (b) and Evolution of TPI transparency to opacity during the specific heating scan (c).

The direct comparison of all the materials (Figure 4.9) let us identify specific features for these materials: as expected, amorphous TPI is able to maintain stable the storage modulus up to  $T_g$ , while dropped in the case of semicrystalline PEEK when  $T_g$  is surpassed. The PBI/PEEK blend



showed an “averaged” behaviour between the two respective systems, confirmed in all the three different cases (unmodified, glass and carbon fiber reinforced compounds).

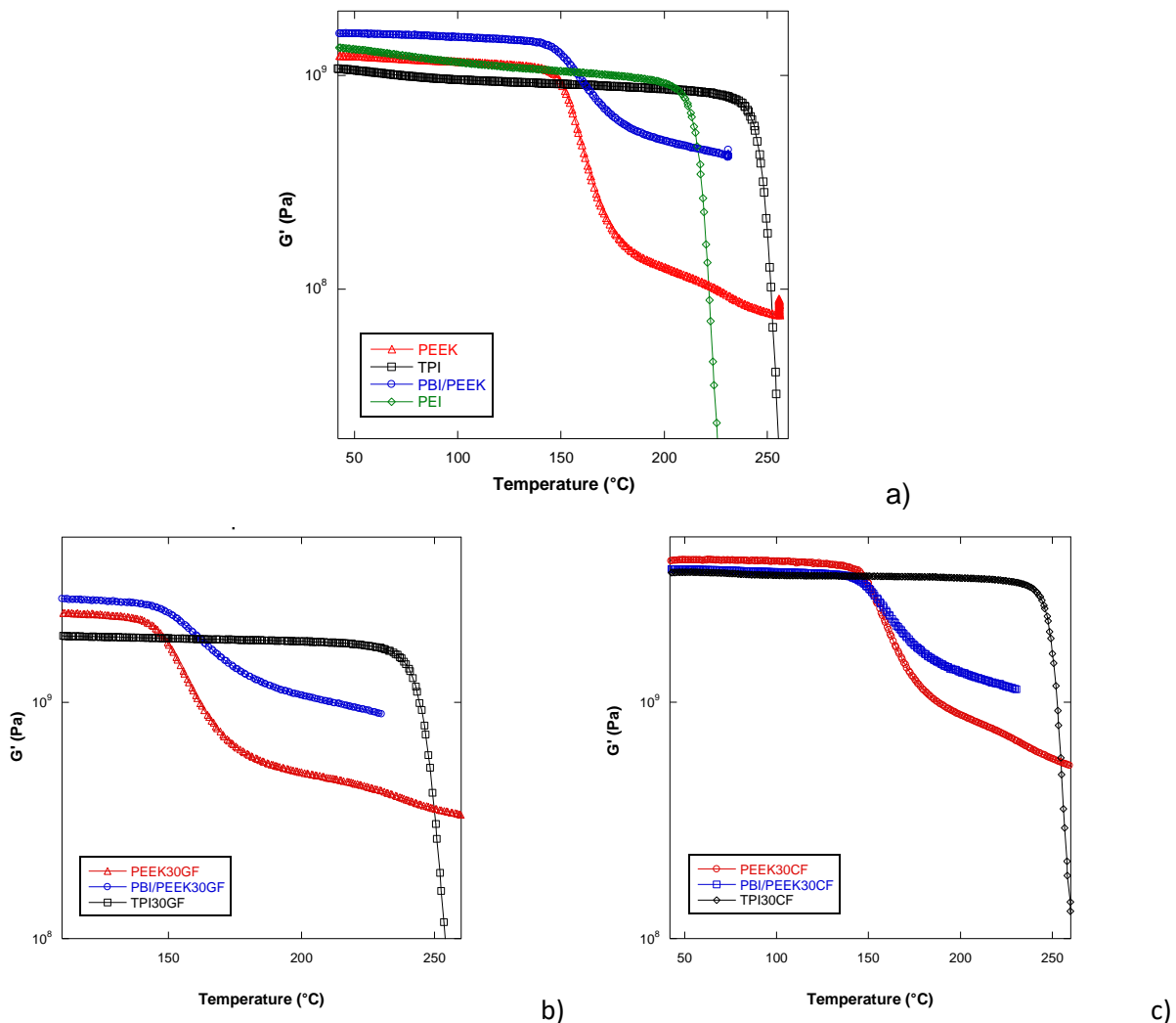


**Figure 4.9:**  $G'$  profiles for neat HPPs matrices (neat grades) (a) and fiber reinforced compounds: comparison of glass reinforced (b) and carbon reinforced (c) systems

#### 4.4 Morphological characterization of neat matrices and fiber reinforced composites

A morphological evaluation campaign of neat HPPs matrices (neat grades) and fiber reinforced compounds was performed. The observation of the morphology can in fact provide important information with respect to the possible interaction of the technopolymer with the technical fiber. In particular, the analysis of the morphology of the bonds at the matrix-fillers interface allows us to understand the affinity between the components and the goodness of the production process.

**Figure 4.10** shows the FESEM images of neat HPPs at two different magnifications (a) and the micrographs related compounds with glass and carbon fibers at 30% wt.

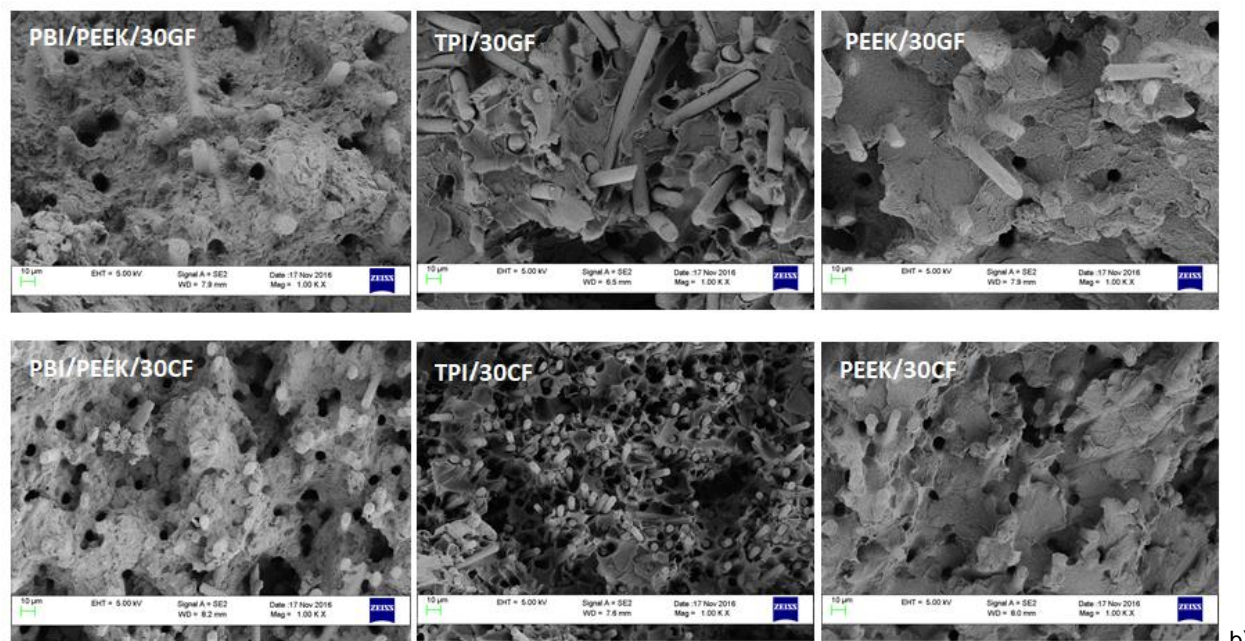
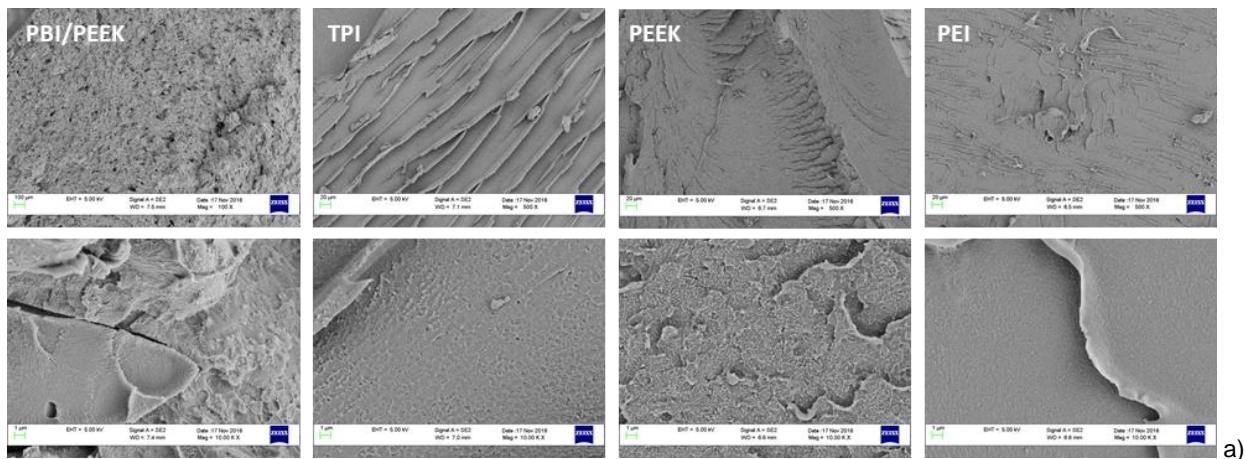


**Figure 4.10:** FESEM images of neat HPPs at two different magnifications (a) and micrographs of compounds with glass and carbon fibers at 30% wt. (b)

The results confirmed the typical surfaces of amorphous fragile (TPI) and semicrystalline ductile (PEEK) materials, while the PBI/PEEK surface well represents a balanced morphology between these two HPPs. In the cause of fiber reinforced compounds, it is evident how the quality of the interphase is extremely good in the case of PEEK matrix, while it is noticeably weak in the case of TPI. As in the case of images for neat grades, the fiber reinforced blend (PBI/PEEK/30GF and PBI/PEEK/30CF) showed a “middle” interphase morphology.

#### 4.5 References

- Saleem, A., Frommann, L., Iqbal, A. (2007) High Performance Thermoplastic Composites: Study on the Mechanical, Thermal, and Electrical Resistivity Properties of Carbon Fiber-Reinforced Polyetheretherketone and Polyethersulphone, *Polymer*, 10.1002/pc.20297.
- Yong Sung Chun, R. A. Weiss (2004) Thermal Behavior of Poly(ether ketone ketone)/Thermoplastic Polyimide Blends, *Journal of Applied Polymer Science*, 94, 1227–1235.
- A. A. Goodwin\* and G. P. Simon (1996) Glass transition behaviour of poly(etherether ketone)/poly(ether imide) blends, *Polymer*, 37 No. 6, pp. 991-995, 1996
- Hsiao, B.S., Sauer, B.B. and Biswas, A. J. *Polym. Sci. Part B* 1994, 32, 737.

## **CHAPTER 5: NANOSTRUCTURED AND FIBER REINFORCED PEEK COMPOSITES**

### **5.1 PEEK based nanocomposites**

In the light of the information found in the consulted bibliography, it was necessary to evaluate the interaction between the selected nanofillers and the PEEK matrices; therefore, it was decided to carry out a first phase of screening using only the pure degree as a reference matrix. In fact, in order to compare the effects of the nanofillers, it is necessary to eliminate as far as possible the variables of the produced systems. The starting dosage of the used nanofillers has been extrapolated from the bibliography, based on similar experiences and deductions of a chemical-physical nature; in most cases, the result can be shown immediately satisfactory. In general, in order to evaluate the real effect of the nanofillers on the selected matrices, it was decided to use intermediate charge percentages to avoid exceeding the solubility limits. These limits can often only be assessed empirically through a study approach of incremental levels of dispersion of fillers in matrices. The empirical approach will also allow evaluating the resistance to thermal degradation of the compatibilized fillers, in consideration of the high processing temperatures necessary for this type of matrices. Using this approach, it will be possible to optimize the formulations by working in feedback, i.e. by testing the results obtained and reformulating the mixtures in the light of the previous results.

The tests carried out with the differential calorimeter and with the thermogravimetric apparatus have provided important indications on the usable working process: the results of the DSC experiments showed melting between 350 and 400 ° C for the PEEK, while the results of the TGA show a good thermal stability of PEEK far beyond the melting step. The need to obtain phenomena that facilitate the dispersion of fillers suggests resorting to the extrusion process with ample mixing times that imply the realization of masterbatches or the use of extrusion machines which also provide a compounding device inside. As regards the aspects connected to the rheological behaviour of the matrix, it can be noted that the extrusion compounding processes are compatible with the measured parameter values, even if the PEEK preloaded with carbon fiber is reached, values are found near the higher processability limits and may require particular attention in the management of process parameters. The tests on the viscoelastic behaviour of the matrices have also suggested the use of sufficiently high mixing speeds: in this condition, high shear forces are obtained that favour the dispersion of the fillers but at the same time a lower viscosity is obtained which allows a better diffusion of the fillers.

#### **5.1.1 Definition of the working parameters**

All the considerations made in the light of the information found and the results of the tests carried out lead to identify the compounding for melt intercalation and the subsequent extrusion, possibly following blending, of the micro and nano-techno-polymer matrix composites. The test results also indicate, as starting parameters, a temperature profile between 350 and 400 °C, a mixing speed

between 50 and 150 rpm and residence times as long as possible, compatibly with the risk of degradation and with the subsequent industrial processability: from the information possessed it can be said that possible times could be from 2 to 20 minutes of mixing for the PEEK matrices. There are various methods that are exclusively analytical-instrumental and semi-empirical for the evaluation of the most appropriate mixing times; in this case, it was decided to use the evaluation method with an experimental approach going to produce samples of material at different mixing times and then evaluate the parameters related to the degradation and dispersion that are obtained from the mechanical characterization of the specimens. This method allows taking into account both the possible degradation actions induced by the phenomena that occur during mixing and the degree of dispersion of the fillers that can be reached when the mixing time parameter ( $T_{mix}$ ) is changed. In this way it will be easier to upscale the industrial process because it will impose process conditions very close to those of mass production. The temperature profile has been chosen on the three permitted points, taking into account the fact that during the mixing phase the solidification of the polymer melt must be avoided at the outlet of the recirculation outlet but at the same time the premature fusion of the matrix in the feed hopper must be avoided; for this reason the temperature in the feeding area must fall within the PEEK melting chamber as much as possible in the lower end. The temperature in the extrusion head must be such as to ensure complete melting of the matrix and possess a temperature gradient such as to guarantee sufficient thermal inertia for carrying out the injection operations. Finally, the intermediate temperature is dictated by the interpolation of the two temperatures imposed by the system with the only thermophysical limitation of the machine geometry. The chosen profile was therefore 355 - 375 - 395 ° C with the option of reducing as far as possible the maximum temperature in order to limit the degradation phenomena. The rotation speed ( $V_r$ ) of the maximum screws in the selected range was chosen, i.e. 150 RPM, reserving the possibility of possible reductions in case of blockage due to overfeeding of the machine due to the high viscosity of pre-loaded PEEK matrices.

We proceeded to produce samples of material to be submitted to mechanical characterization tests. In order to have an effective characterization, it was decided to also subject the matrices chosen to the extrusion process so as to confer the same "thermal history" of the composites that will subsequently be realized. The PEEK VK 2000 P was used as the first matrix and it was seen that the head temperature could be reduced by 5 °C, defining the new temperature profile 355 - 375 - 390 °C, keeping the  $V_r$  at 150 RPM. As previously mentioned, the degradation phenomenon has been verified semi empirically, going to produce samples of material with mixing times at the ends of the identified range, i.e. at 2 and 20 minutes. With these different materials only for the  $T_{mix}$ , dumbbell samples were produced for tensile tests to be subjected to mechanical characterization. The specimens were made with the micropress previously described using the injection chamber

temperature of 390 ° C and the mould temperature of 190 ° C and the injection timing-pressure profile as follows: 0.1 s - 9 bar; 0.1 s - 9 bar; 12 s - 9 bar.

In this phase of the study it was decided to use as a matrix only Vestakeep 2000 P; this choice is motivated by the desire to be able to make a comparison of the effects of nanofillers by eliminating, as far as possible, the variables of the produced systems. This method allows identifying which fillers are potentially more effective for the realization of optimized nanocomposites.

The starting dosage of the used fillers has been extrapolated from the bibliography, based on similar experiences and deductions of a chemical-physical nature; in most cases, the result was immediately satisfactory. In some cases, however, we wanted to investigate the possibility of modifying filler percentages because the results of the mechanical tests showed that there could be possibility for increasing the reinforcement dose. One of these cases was the Aerosil 300, which in the initial formulation was used at 3%. As will be seen below, from the results of the mechanical tests, we saw an increase in the elastic modulus while leaving unchanged the other mechanical parameters. Elongation at failure has remained on average above 75%, which is considered a value extending above the minimum for many applications. It was therefore decided to produce a mixture with 6% of Aerosil 300, assuming to sacrifice a portion of elongation at break in favour of a further increase of Young's modulus. In this phase, the samples of nanocomposites of PEEK were defined with the same process parameters used for the silicon oxide-based formulations. The list of formulations is shown in **Table 5.1**.

**Table 5.1:** List of produced PEEK-based formulations, to be tested for characterization of mechanical properties (commercial denomination, weight percent and abbreviated code)

TRADE NAME	NAME	CLASS	MAIN COMPONENT	SILICATES	% IN WEIGHT
Dellite HPS	HPS	Phyllosilicate	Montmorillonite	HPS	5
Pural MG30	MG30	Phyllosilicate	Idrotalcite	MG30	6
Pangel S9	S9	Phyllosilicate	Paligorskite / Sepiolite	S9	5
Mica PDM-5B	P5B	Phyllosilicate	Mica F-flogophite	P5B	8
Nyglos 8	N8	Inosilicati/pyroxene	Wollastonite	N8	10
Aerosil 300	A300	Metal oxide	Silica		
Cok 84	CK84	Mixed metal oxides	Silica / Alumina		
Disperal P2	P2	Bohemite	Aluminium oxide hydroxide		
Hombitec HM230P	HT230	Metal Oxide	Titania		
				OXIDES	% IN WEIGHT
				A300	6
				CK84	7
				P2	6
				HT230	16.5

Fillers content was considered on a weight base since volume characteristic could be too strictly related to packing conditions and a proper and significant comparison on a volume basis could be

misleading for data results interpretation. Nevertheless, we selected mineral fillers that are in the common density range. The results of the mechanical characterization of the nanocomposites are shown below (**Figure 5.1**). Tests were carried out on samples stabilized in the environment at a temperature of 23 ° C with U.R. 50% for at least 48 h.

The results of mechanical tensile tests on nanocomposite materials made at  $T_{room}$  show that almost all the mixtures produced an improvement of the elastic modulus. To this improvement, in some cases an improvement of the yield strength is also added, which indicates good compatibility and dispersion efficiency of the matrix-filler system.

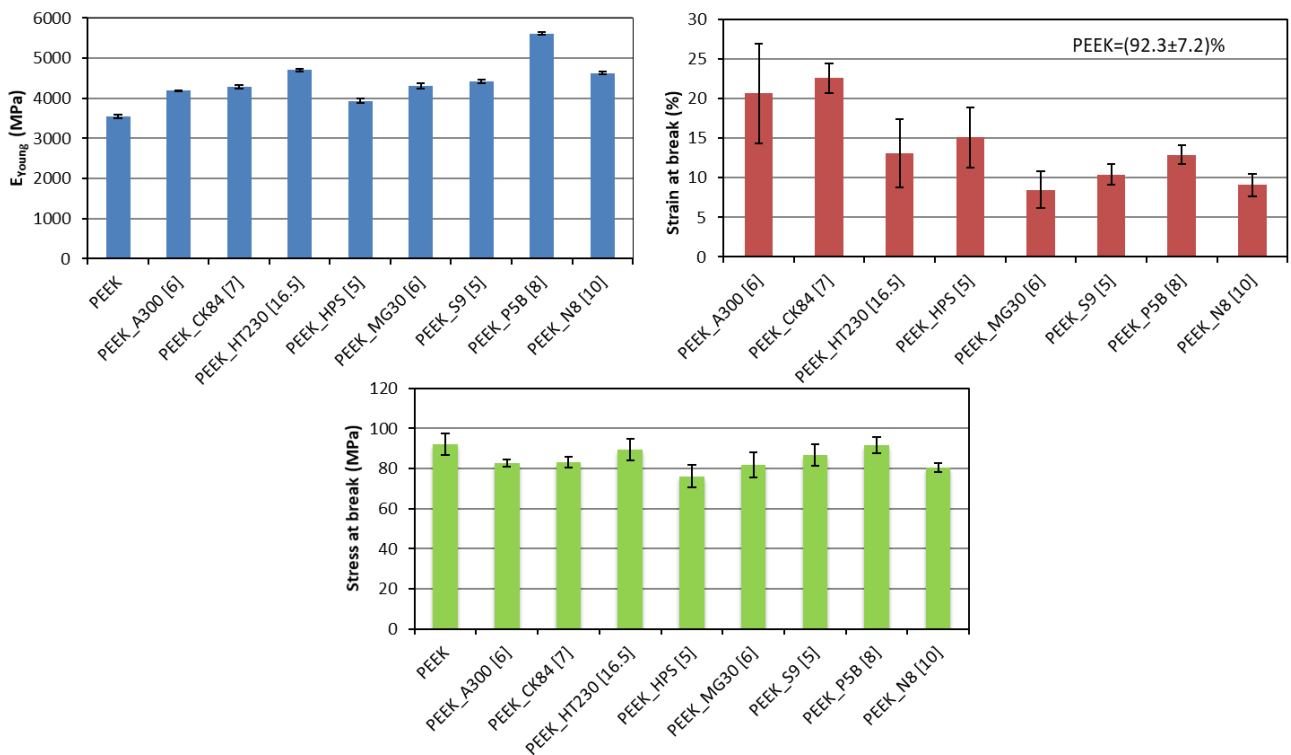


**Figure 5.1:** Results of tensile tests on specimens of nano composite materials based on PEEK

Almost all the nanocomposite products show values of elongation at break significantly higher than the failure strains measured for commercial matrices pre-loaded with glass fiber and carbon fiber; this result appears to be significantly positive because it indicates that the produced nanocomposite materials have comparable characteristics and, in some cases, better than those of the materials currently used for industrial production.

It can also be noted that, in the face of an increase in the Young's modulus, the elongation at break is still quite high; this consideration suggests that there is a further margin of improvement that can be applied by improving the formulation in terms of nano-reinforcement content. Aerosil 300 shows a general improvement of the mechanical properties, preserving a mean percentage value of the

failure of 77.5%, which suggests being able to significantly increase the content of silicon oxide in the mixture. A similar evaluation can also be applied to the mixture with 4% of Cok 84 which requires optimization reformulation. The reformulations decided on for Hombitec RM 230 P and for Disperal P2 (Bohemite) have a different explanation. In the case of Disperal P2, it was seen in the extrusion phase that the degassing phenomenon appeared intense and probably due to the treatment of the charge with acid additives used to promote the dispersion of the particles. Therefore, it was decided to carry out a pre-dispersion of the particulate in deionized water and then carry out the drying and calcination of the filler in the oven. The dissolved and calcined Disperal P2 was then used again to make another mixture to verify if, by breaking down the degassing phenomena, they could further improve the mechanical properties. Finally, a mixture was also tested with an increase in the content of non-compatibilized titanium dioxide, which showed the most promising mechanical performance and margins for intervention on the last elongation. The optimization reformulated systems given in **Table 5.2** have therefore been added to the techno-polymeric materials produced.

**Table 5.2:** List of PEEK-based mixtures reformulated after the mechanical properties characterization tests.

MATRIX	Wt. %	FILLER	NAME
PEEK	6	AEROSIL 300	PEEK_A300[6]
PEEK	7	COK 84	PEEK_CK84[7]
PEEK	25	HOMBITEC RM230P	PEEK_HT230[25]
PEEK	6	DISPERAL P2 (H <sub>2</sub> O+Calc.)	PEEK_P2[6] H2O+Calc

Even with these composites, the specimens were produced which were then subjected again to the mechanical characterization tests. The values of the module and stress-strain parameters are shown in **Table 5.3**. For convenience, the values of the previous formulations have also been reported to make an immediate comparison.

It can be seen from the results reported in **Table 5.3** that the new formulation realized with the de-acidification treatment of the Disperal P2 has led to an improvement of the modulus; however, the increase in rigidity produced an embrittlement of the composite, which does not allow the occurrence of the yielding phenomenon, leading to brittle failure at low elongation. The reformulation was therefore theoretically correct, but the filler showed objective limits of compatibility with the PEEK matrix. As for the other three optimized reformulations, improvements in terms of increase of the Young's module are evident without compromising the other mechanical parameters; the elongations at break remain above the values of the commercial composites, confirming the effectiveness of the production process and suggesting a good tenacity of the materials. It should also be noted that



many of the realized PEEK nanocomposite materials show significantly improved mechanical properties of the products currently on the market. In particular, silicon oxide (Aerosil 300) and silicon-aluminium oxide (COK 84), wollastonites (Nyglos 8 and Aspect 4000), fluorine mica (PDM-7-325 and PDM-5B) and titanium oxide not organically compatibilized (Hombitec RM 230 P) showed significantly improved mechanical properties

**Table 5.3:** Results of tensile tests on specimens of PEEK nanocomposites reformulated for the optimization of the mechanical properties.

SAMPLE	YOUNG MODULUS [MPa]	YELD STRENGHT [MPa]	YELD STRAIN [%]	FAILURE STRENGHT [MPa]	FAILURE STRAIN [%]
PEEK	3544	93.3	5.01	92.3	92.3
PEEK_A300[3]	3988	94.6	4.54	93.2	77.5
PEEK_A300[6]	4186	97.3	4.63	82.2	20.7
PEEK_CK84[4]	4032	94.6	4.73	95.5	81.5
PEEK_CK84[7]	4287	96.7	4.39	83.1	22.6
PEEK_P2[6]	4156	97.0	4.63	80.0	8.4
PEEK_P2[6] H <sub>2</sub> O+CALC	4322			67.0	1.9
PEEK_HT230[16.5]	4702	103.0	4.22	89.5	13.1
PEEK_HT230[25]	5150	102.7	4.05	99.4	5.6

## 5.2 Nanostructured and Fiber Reinforced PEEK based composites

Considering the results obtained from the tests on the nanocomposites, the fillers that showed the most sensitive improvements on the properties of main interest were then identified. Fillers based on silicon and aluminium oxide, wollastonites, fluorides and titanium oxide have proved particularly effective. So, we decided to select the fillers named Cok 84, Nyglos 8, PDM-5B, Hombitec RM 230 P and Pangel S9 to continue to develop the optimization of the mixtures. It was also decided to use, within the same type of nanofiller, the most performing filler within the same group (according to this, we excluded PDM-7-325 for the modified synthetic micas and Aspect 4000 for the wollastonitic pyroxenes in this phase of optimization of the formulations). In the light of the information produced with the activities carried out, it was therefore possible to elaborate more complex formulations using the preloaded matrices based on glass fiber and carbon fiber. We then proceeded to the production of matrices with reinforcing content in various percentages, to be able to carry out a characterization of the effect of the reinforcement. This further work has become particularly useful to optimize the content of fillers on pre-loaded matrices.

The PEEK matrices were then produced with 5%, 10% and 15% glass fiber and carbon fiber, exploiting the possibility of working in dilution for polymeric melts. The processing parameters for these formulations have been kept unchanged in comparison with the nanocomposites based on neat matrix. The considerations made during the thermal analysis phase regarding the increase of thermal conductivity of the pre-loaded matrices were considered negligible in the compounding phase of the composite material.

The tables with the formulations of the techno-polymeric composites produced with the pre-loaded matrices for the screening phase are shown below (**Tables** from **5.4** to **5.6**).

**Table 5.4:** Specimens of pre-loaded matrices with glass fiber and carbon fiber with increasing content produced for the characterization of mechanical properties

MATRIX	REINFORCEMENT	FILLER	NAME
PEEK	PEEK30GF	5 %	PEEK5GF
PEEK	PEEK30GF	10%	PEEK20GF
PEEK	PEEK30GF	15 %	PEEK15GF
PEEK	PEEK30GF	30 %	PEEK30GF
PEEK	PEEK30CF	5 %	PEEK5CF
PEEK	PEEK30CF	10%	PEEK10CF
PEEK	PEEK30CF	15 %	PEEK15CF
PEEK	PEEK30CF	30 %	PEEK30CF

**Table 5.5:** Formulations of the nanocomposites made with the matrices preloaded with 15% of glass fiber

MATRIX	REINFORCEMENT	NANOFILLER	NOMENCLATURE
PEEK + PEEK30GF	PEEK15GF	15% HOMBITEC 230	PEEK15GF_HT230[15]
PEEK + PEEK30GF	PEEK15GF	5% PANGEL S9	PEEK15GF_S9[5]
PEEK + PEEK30GF	PEEK15GF	10% NYGLOS 8	PEEK15GF_N8[10]
PEEK + PEEK30GF	PEEK15GF	8% COK 84	PEEK15GF_CK84[8]
PEEK + PEEK30GF	PEEK15GF	8% PDM-5B	PEEK15GF_P5B[8]

**Table 5.6:** Formulations of the nano composites made with the matrices preloaded with 15% of carbon fiber

MATRIX	REINFORCEMENT	NANOFILLER	NOMENCLATURE
PEEK + PEEK30CF	PEEK15CF	15% HOMBITEC 230	PEEK15CF_HT230[15]
PEEK + PEEK30CF	PEEK15CF	5% PANGEL S9	PEEK15CF_S9[5]
PEEK + PEEK30CF	PEEK15CF	10% NYGLOS 8	PEEK15CF_N8[10]
PEEK + PEEK30CF	PEEK15CF	8% COK 84	PEEK15CF_CK84[8]
PEEK + PEEK30CF	PEEK15CF	8% PDM-5B	PEEK15CF_P5B[8]

Results of the tensile tests on the specimens of pre-loaded matrices with glass fiber and carbon fiber with increasing contents are reported in **Figure 5.2**.

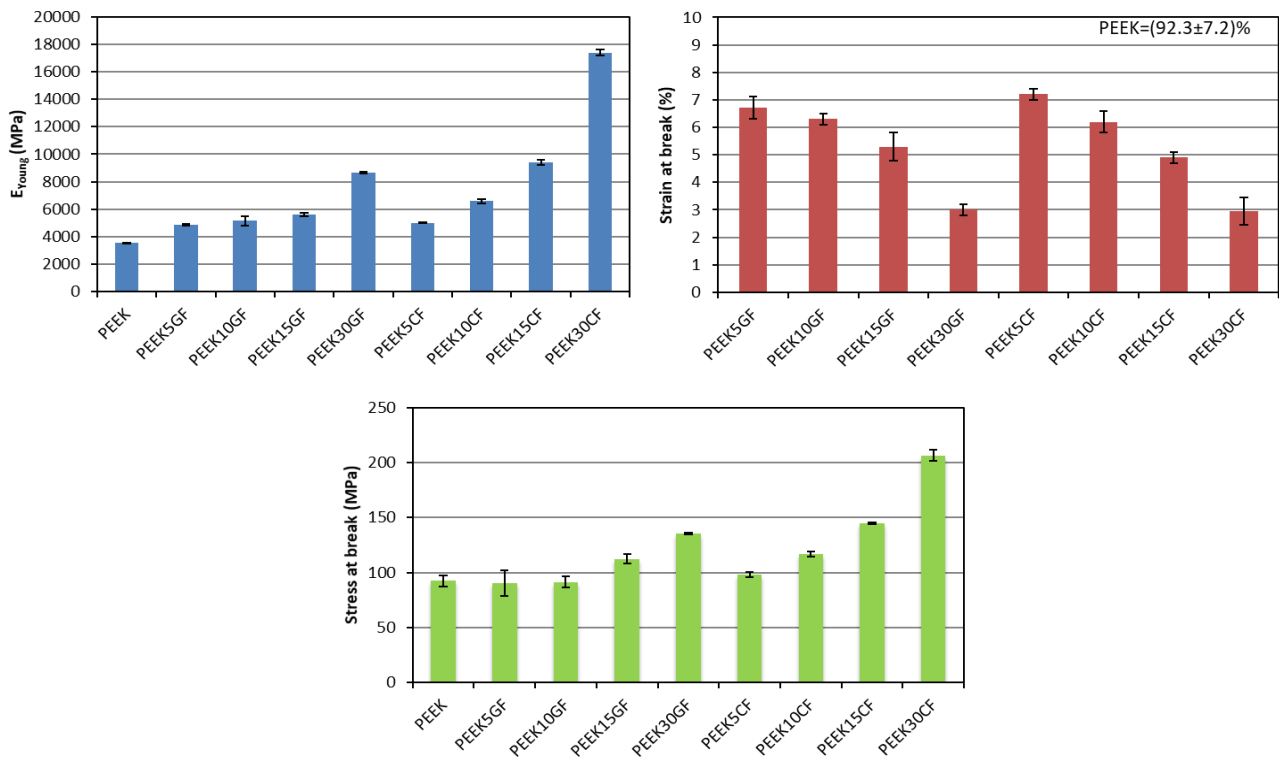


**Figure 5.2:** Results of the tensile tests on the specimens of pre-loaded matrices with glass fiber and carbon fiber with increasing contents

From the data shown in Figure 5.2, the progressive effect of increasing the stiffness of the material with the increase of the reinforcement content is evident; the increasing amount of the reinforcing fibers progressively increases the elastic modulus and, at the same time, decreases the values related to the toughness (failure strain). In the case of matrixes with Glass Fiber, it is useful to note that the trend of the mechanical parameters is uniform and suggests the use of preloaded matrix with 15% wt. of glass fiber to make the nanocomposite. In fact, with such a preloaded content, a

good compromise of the mechanical properties is achieved in terms of resistance to stresses and damage, leaving however margin for the effective use of further fillers. It is concluded that the optimized mixtures based on matrix preloaded with fiberglass will be mainly those with 15% of GF. For the matrices with Carbon Fiber also, a uniform trend of the mechanical parameters was detected; however, unlike the glass loaded matrices, there are noticeably higher values of the properties and progressively increasing effectiveness for the higher contents. These considerations suggest making the formulations of the nanocomposites with the preloaded CF matrixes at 15% wt., then increasing the reinforcement up to 20%, essentially in cases where the characterization tests offer margins for increasing the total reinforcement. Results of tensile tests on specimens of nanocomposite materials with pre-loaded matrices (15% wt. glass fiber) are shown in **Figure 5.3**.

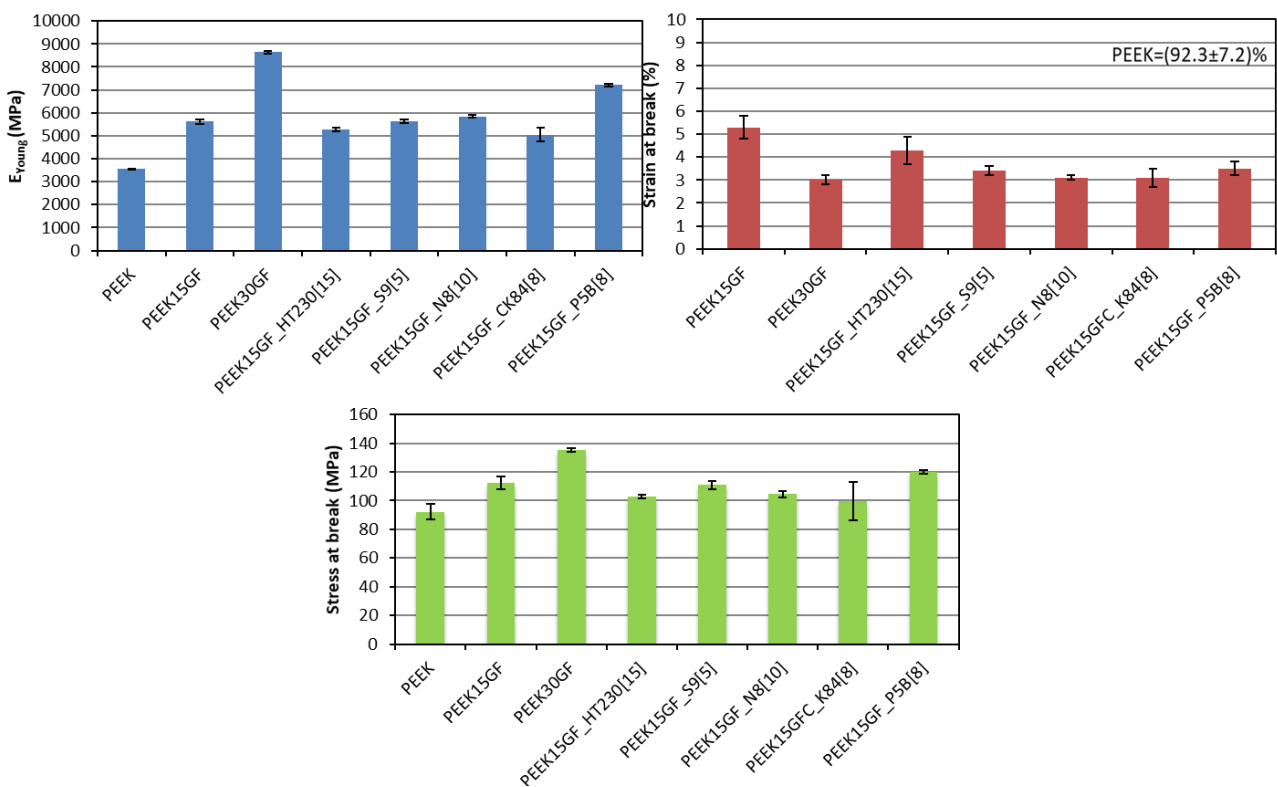


**Figure 5.3:** Results of tensile tests on specimens of nano composite materials with pre-loaded matrices with glass fiber.

The tests carried out on the nanocomposites with a preloaded 15% wt. of GF show a fragile fracture behaviour, not showing the yielding phase, which also occurred in matrices preloaded with glass even at higher levels; however, it is conceivable that this behaviour occurs only at low temperatures (close to the  $T_{room}$ ), while a tough behaviour can occur at operating temperatures ( $T = 150-200\text{ }^{\circ}\text{C}$ ). It should instead be noted that the composites with Cok 84 and titanium dioxide show lower Young modulus with respect to the corresponding 15% GF preloaded matrix, while for all the other formulations the elastic modulus increased in comparison with respect of original matrix; this improvement is also evident in the case of stress at break in the mixture added with fluorine, whereas

in the case of sepiolite the value is absolutely comparable. These results can be considered unequivocally positive, as they fully correspond to the objectives set for the work that is to improve the properties or the conservation of properties in the face of a reduction in costs. The above results and considerations have suggested that 2 additional optimized formulations should be carried out to be submitted, in addition to the previous 5, to mechanical characterization tests to be made in temperature [Parvaiz et al., 2010]. These formulations follow:

- PEEK + 20% GF + 8% PDM-5B
- PEEK + 15% GF + 10% PDM-5B

Similarly, the mechanical characterization at room temperature of the pre-loaded matrix nanocomposites with carbon fiber was carried out. The results of the tensile tests on the specimens of materials made with 15% wt. of Carbon Fiber preloaded matrix are summarized in **Figure 5.4**.

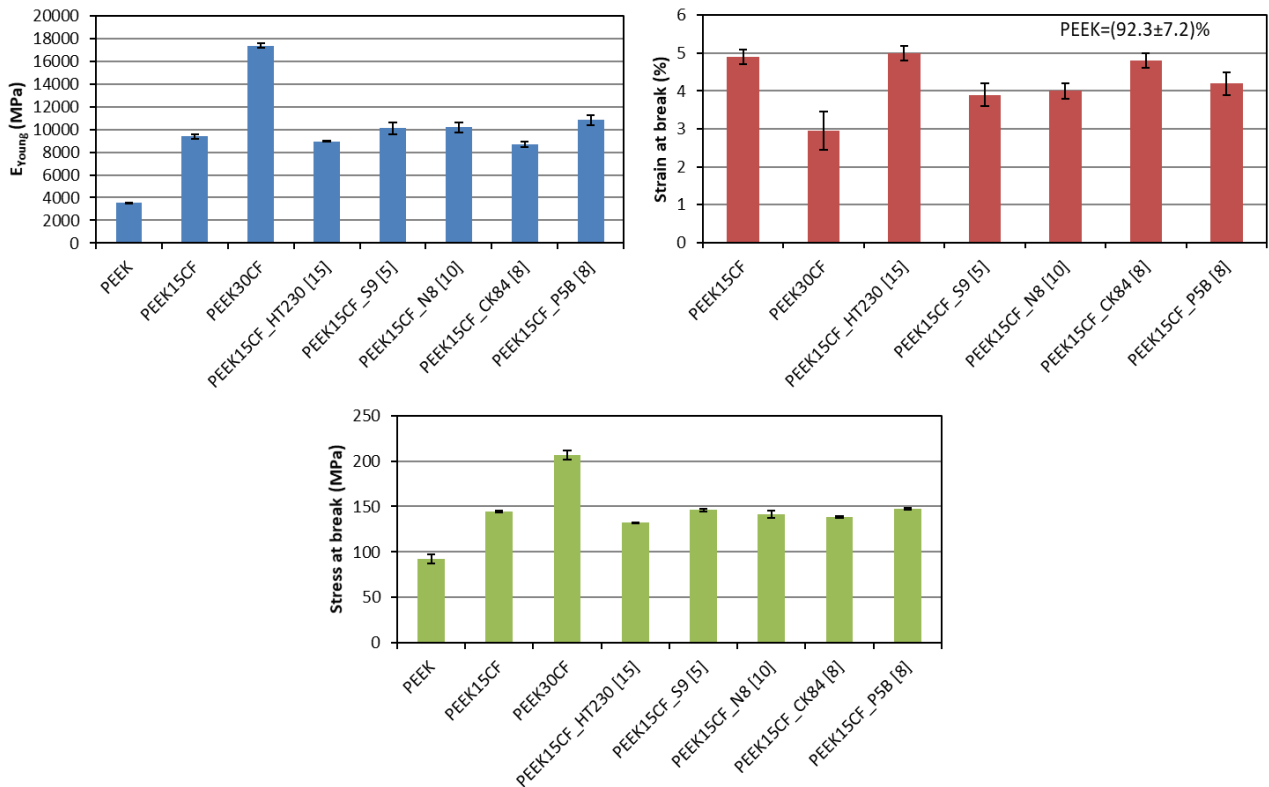


**Figure 5.4:** Results of tensile tests on specimens of nanocomposite materials with pre-loaded carbon fiber matrices.

It should be noted that the composites with Cok 84 and titanium dioxide show lower Young modules with respect to the pre-loaded 15% wt. CF corresponding matrix, while all the other formulations increase the elastic modulus with respect to the starting matrix. The values of yield strength and strength at break in mixtures showing improved Young's modulus are absolutely comparable, and

sometimes higher than the corresponding preloaded matrix. Even these results can be considered positive, since they fully correspond to the objectives set for the project and are relevant, as they show high performance values even on the most performing materials.

The results and the considerations above reported have suggested the realization of 6 further optimized formulations, in addition to the 6 previous ones, to be tested in temperature. These formulations include both increased amount of both fiber and filler reinforcement, as follows:

- PEEK + 15% CF + 15% Nyglos 8
- PEEK + 15% CF + 20% Nyglos 8
- PEEK + 20% CF + 10% Nyglos 8
- PEEK + 30% CF + 10% Nyglos 8
- PEEK + 20% CF + 8% PDM-5B
- PEEK + 30% CF + 10% PDM-5B

The samples were then mechanically characterized in temperature with the 8 additional optimization formulations proposed (2 with GF matrix and 6 with CF matrix).

### **5.3 Tensile tests at high temperature**

High temperature tensile tests were carried out to analyse the response of the samples even under severe environmental conditions. To carry out this type of test, it was necessary to store the samples produced in a climatic chamber at 200 °C until an equilibrium condition with the measuring instrument is reached. The instrument was a Lloyd LR30 dynamometer equipped with a conditioning chamber, that allows performing measurements of mechanical characterization in the temperature range from -80 ° C to + 250 ° C. The realization of this kind of test requires relatively long times, since the achievement of the equilibrium conditions at 200 ° C must take place with slow transients in order to allow the samples and the instrumental components to adapt them to the severe environmental conditions. The risk associated with a too rapid climate control would be to have effects of measuring drift of the load cell, caused by non-calculable thermal expansions and/or to carry out tests on samples that are not completely above the glass transition temperature. In this specific case, the transients necessary to reach the optimal measurement conditions were also close to 1 hour per sample. The behaviour of polymers and polymer matrix composites above the glass transition temperature is generally very different from those observed at temperatures below the T<sub>g</sub>, since the polymer chains have greater mobility; the properties can change substantially, reducing stiffness and increasing deformations. The results of tensile tests at 200 °C, carried out on the formulations

preloaded with various levels of glass fiber and carbon fiber, are reported in **Figure 5.5**. It can be seen from this comparison how, in general, the values of the Young's modulus are decidedly reduced, when compared to the tests made at room temperature, highlighting a significant reduction in the stiffness of the techno-polymeric material above the  $T_g$ . An increase in the deformation at break is also immediately noticed, which in the matrices preloaded at 15% appears clearly high, if compared to 30% commercial preloaded matrices. This consideration suggests that the choice of using pre-loaded matrices with a lower content than the commercial one can lead to the elaboration of materials with high toughness, especially in high-temperature operating conditions.

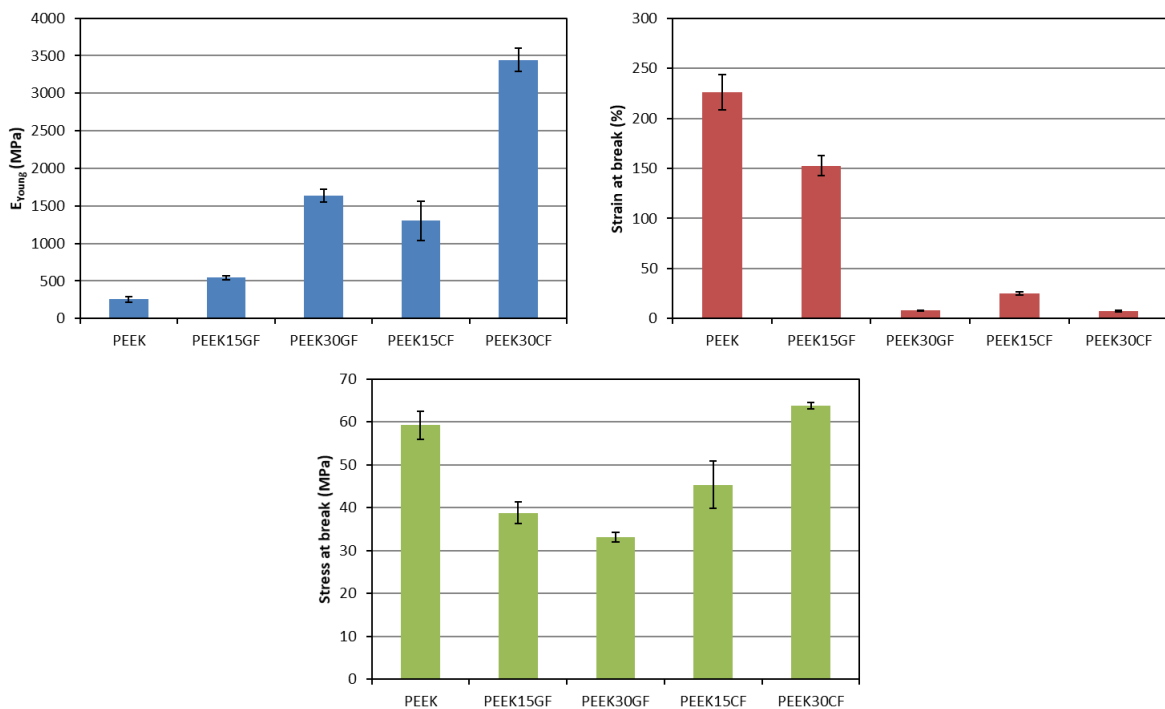


**Figure 5.5:** Tensile test results at  $T = 200^{\circ}\text{C}$  on specimens of matrices preloaded with glass fiber and carbon fiber with increasing content

This hypothesis is also confirmed by the fact that, while the commercial preloaded systems show fracture phenomena at  $200^{\circ}\text{C}$ , the "diluted" 15% wt. matrices exhibit yielding phenomena that can be correlated with tough behaviours. **Figure 5.6** and **Figure 5.7** show the results of tensile tests carried out on formulations with a preloaded matrix of 15% of optimized Glass Fibers; in this way it is easier to make a comparison between the glass-based materials tested at room temperature and at  $200^{\circ}\text{C}$ , respectively.

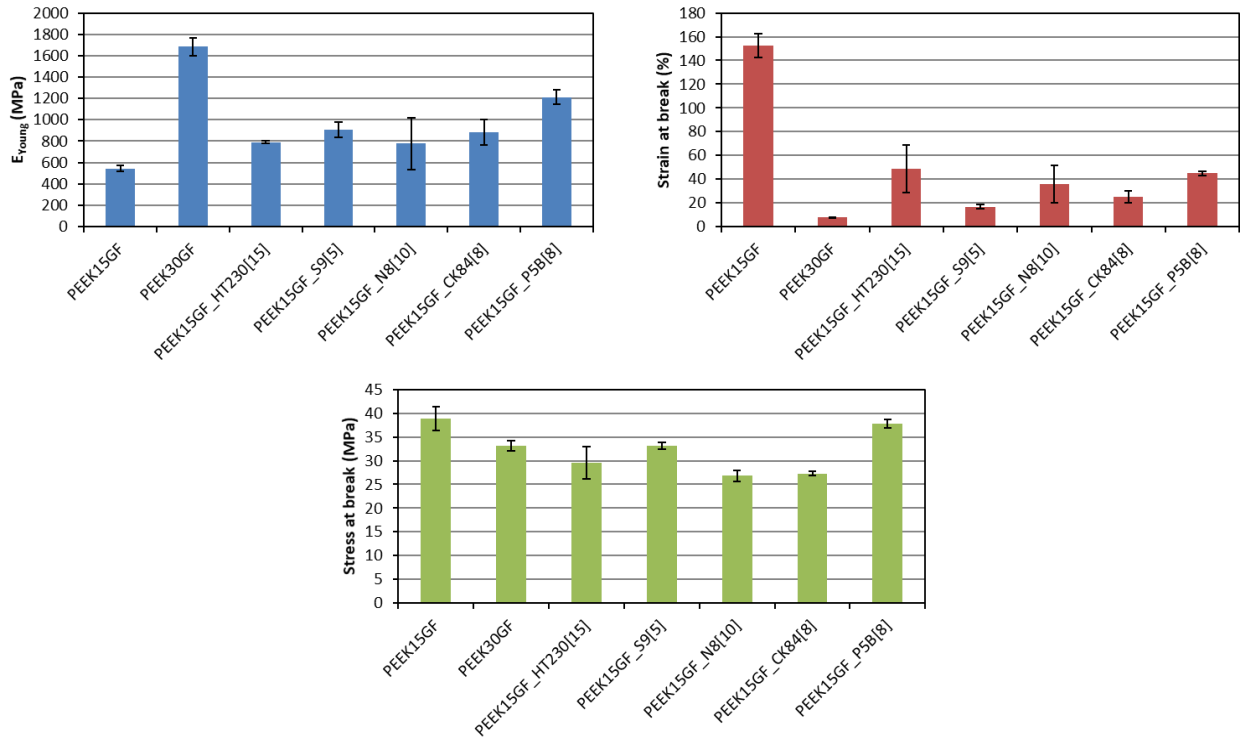


**Figure 5.6.** Results of tensile tests on specimens of nanocomposite materials with pre-loaded fiberglass matrices at  $T = 200^{\circ}\text{C}$

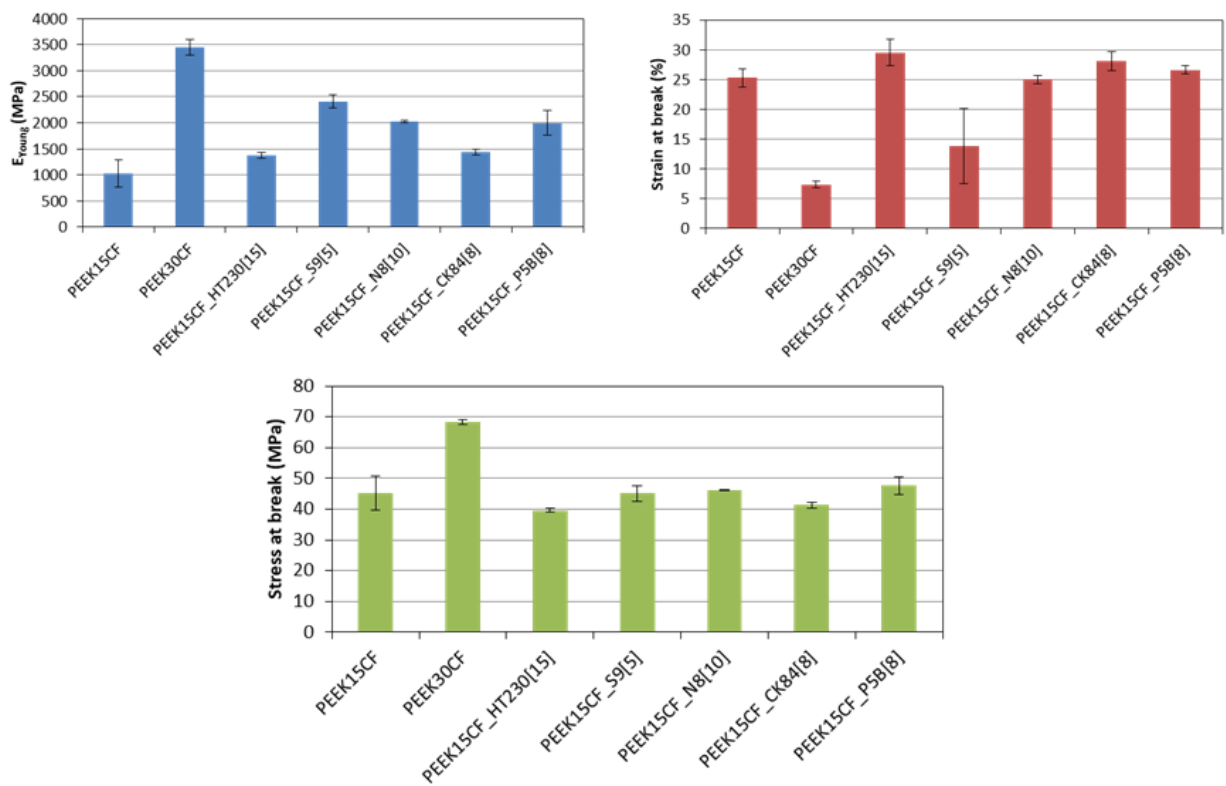
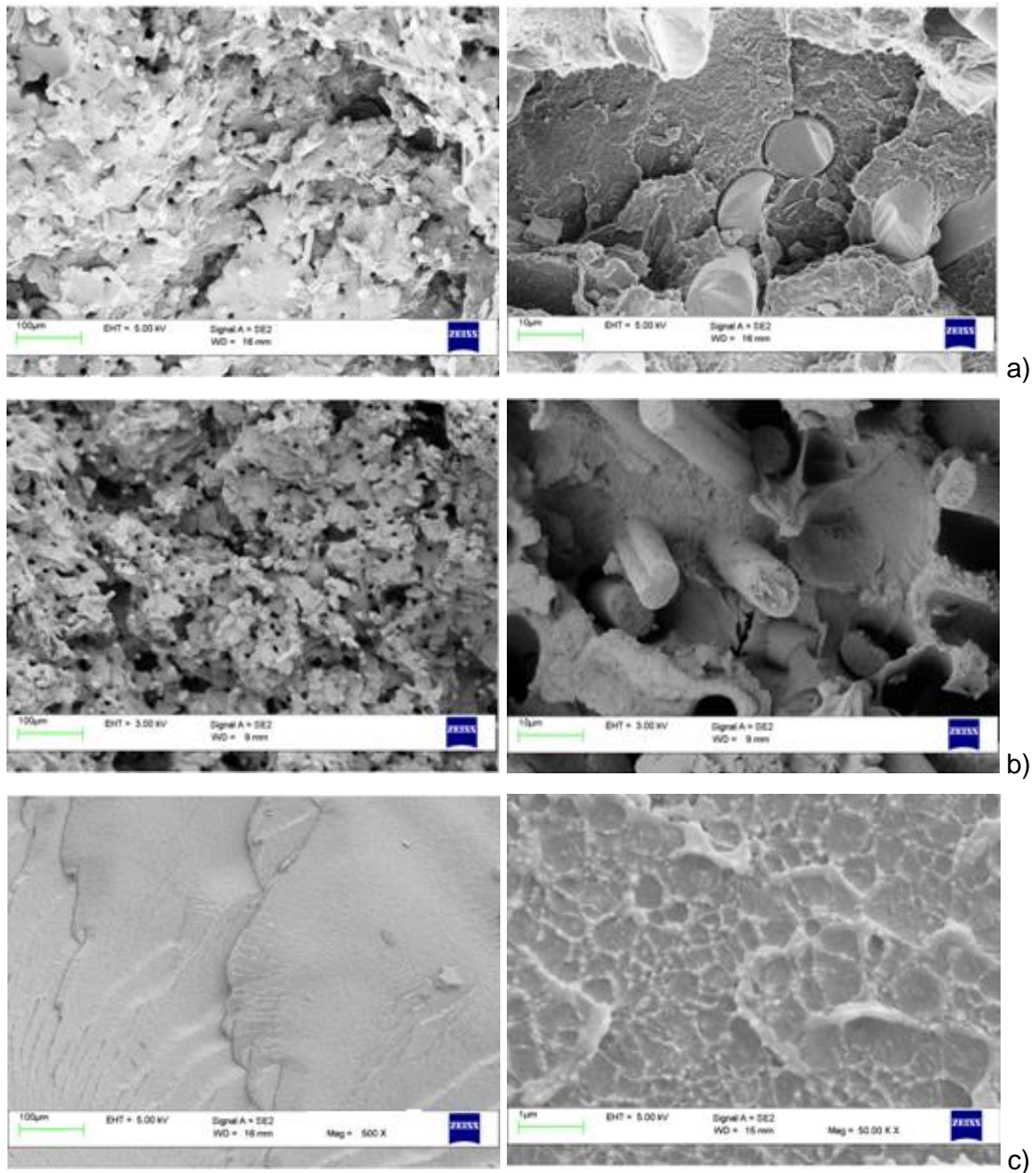


**Figure 5.7.** Results of tensile tests on specimens of nanocomposite materials with pre-loaded carbon fiber matrices at  $T = 200^{\circ}\text{C}$



## 5.4 Morphological analysis

A morphological evaluation campaign of nanocomposite materials was also performed, to support the results obtained with the mechanical characterization. The observation of the morphology can, in fact, provide important information with respect to the dispersion of the fillers in the matrices and the possible interactions of the technopolymer with the nanofiller. In particular, the analysis of the morphology at the matrix-fillers interface allowed us to understand the affinity between the components and the quality of the production process. Some representative images are reported in **Figure 5.8**.



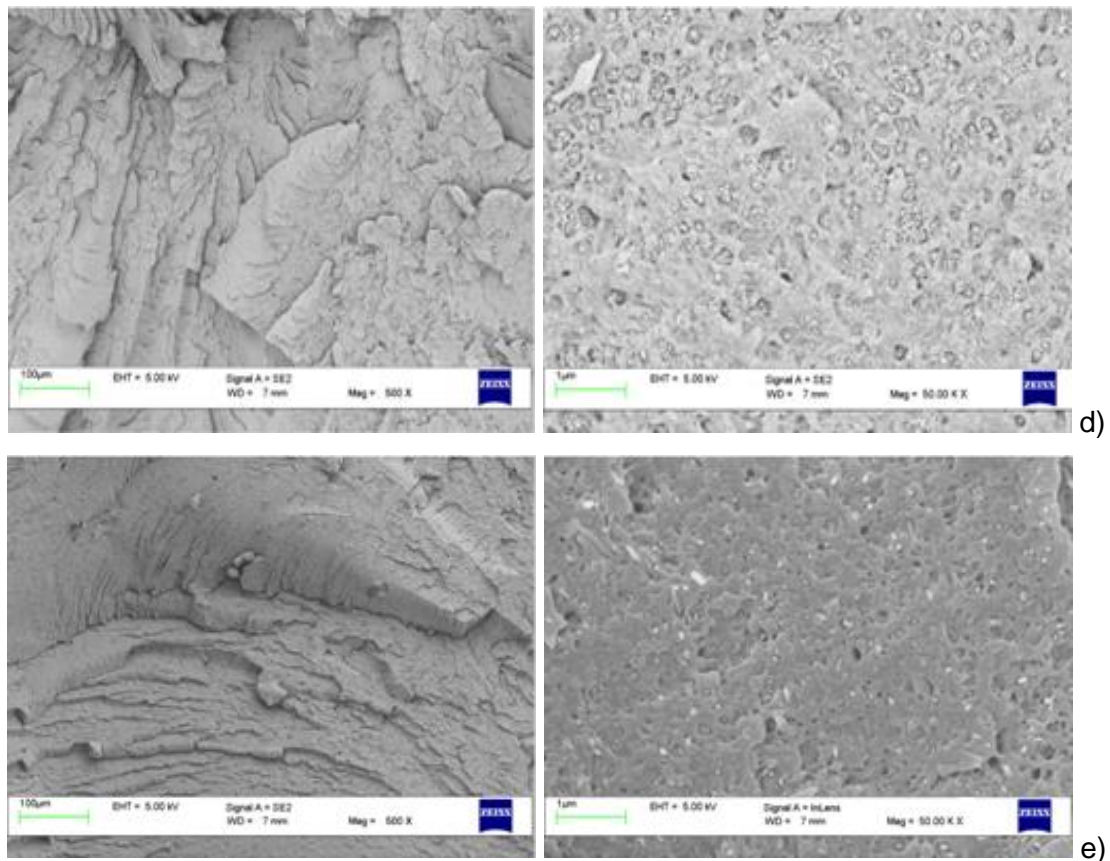


**Figure 5.8:** Micrographs of the fragile fracture surface on a sample of matrices preloaded with glass fibers (a), carbon fibers (b), nanocomposite with Aerosil300 (c) and nanocomposite with COK84 (d), nanocomposite with Pangel S9 (e).

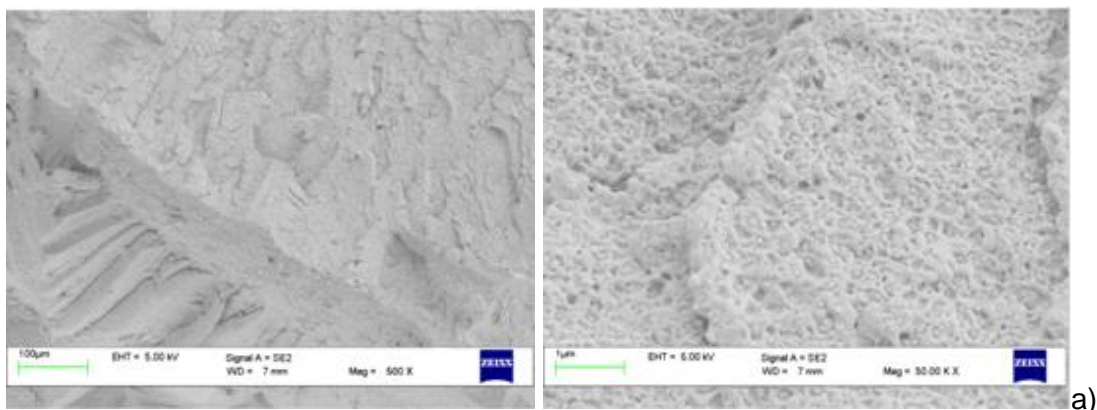
The uniform dispersion of the glass fiber is evident, which causes a fracture arranged on several levels. In the second image, it is possible to observe the bonding at the matrix-fiber interface that appears uniform and dense even if with a gap, due to the not perfect compatibility between organic part (TP) and inorganic reinforcement (GF). It is possible to notice an excellent dispersion of the reinforcements which guarantees a fragile, non-planar fracture, an index of the effectiveness of the reinforcement. In the micrograph at the highest magnification it is possible to observe the perfect junction at the interface between the matrix and organic reinforcement. Unlike the previous case, there is no gap on the bonding surface, or effects of trabecular junctions; the result of the excellent dispersion and compatibility is found in the excellent mechanical properties. On the other hand, considering the interface conditions and the properties of the reinforcement, it is possible to understand the extreme stiffness of the composite material which limits its toughness [Blundell and Osborn, 1983].

In the case of nanofilled systems, a uniform but not completely planar fracture surface can be observed, indicating good dispersion and effectiveness of the reinforcement (no micrometric sized agglomerates can be detected).

The similarity of the fracture surface between COK84 containing material (Figure 5.8d) and the previous one (Aerosil base) is evident (Figure 5.8c); the level of the fracture planes appears to be increased in number and size, which corresponds to improved mechanical performances. It is also possible to notice the presence of small particle agglomerates of  $Al_2O_3$ , that reveal the extreme difficulty of dispersion of the nanometric alumina without compatibilizing additives.

The material reinforced with Pangel S9 (Figure 5.8e) also shows a good fracture surface, arranged on staggered and oriented planes. The orientation of nanometer-sized reinforcements only in two dimensions is the result of the effect of the injected polymer flow. The acicular conformation of the sepiolite is intuited in the micrograph at the greatest magnification. In the second image, in some cases, agglomerations of a few sepiolite needles and a discrete bonding gap are visible; these two morphological phenomena indicate a uniform but not perfect dispersion, and a limited matrix-filler compatibility. As already hypothesized above, in the case of paligorskite it is not possible to fully exploit the potential of this type of filler without the use of compatibilizers; unfortunately, the silanization treatments undergo heavy degradation when exposed to the extrusion temperatures of the used technopolymers.

The fracture surface of the nanocomposite with titanium oxide (**Figure 5.9a**) reveals a good similarity with that reinforced with Cok 84. The effect of the metal oxide bases its main action on hardness at the expense of the non-perfect compatibility between the organic nature matrix and the inorganic reinforcement. In the image at the highest magnification it is possible to observe again the similarity with the other matrix containing the aluminium oxide; however, in this case, the gap effect at the interface due to the considerable presence of oxide and the lack of compatibilizers is emphasized.



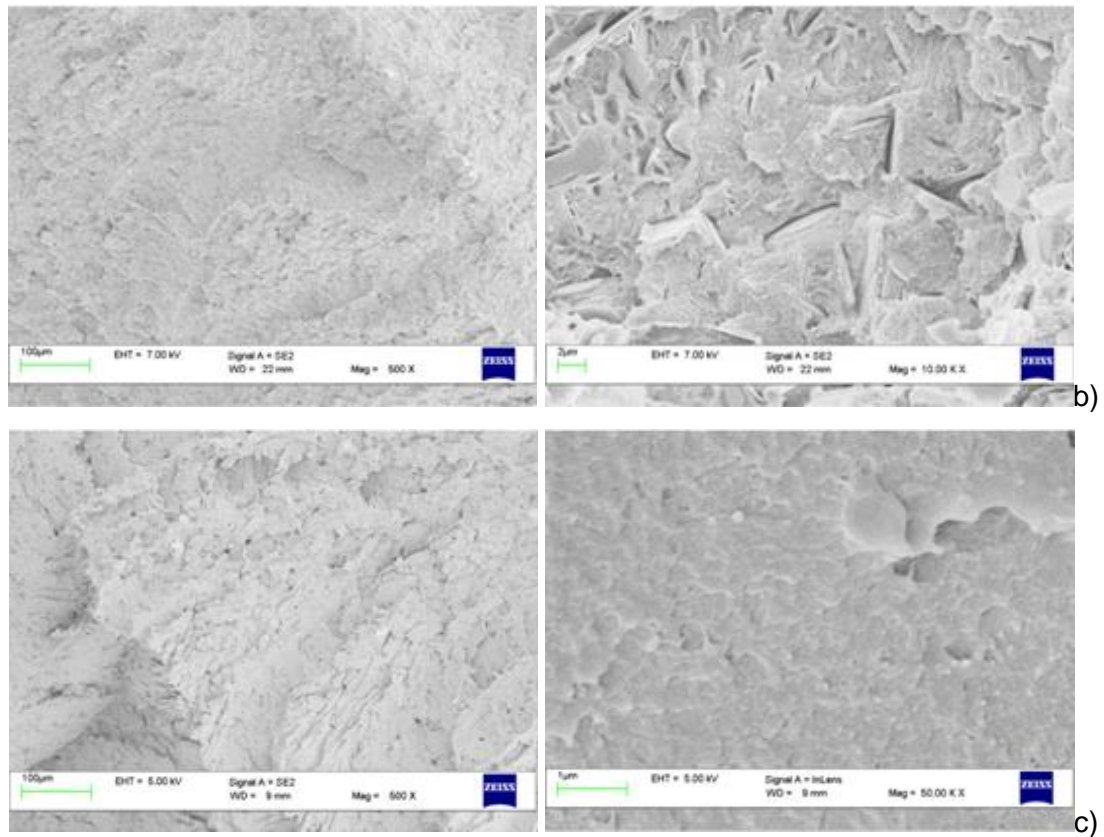


**Figure 5.9:** Micrographs of the fragile fracture surface for nanocomposites material with Hombitech RM 230 P (a), Nyglos 8 (b) and PDM-5B (c).

However, the good dispersion found in the absence of micro agglomerates, associated with the physical characteristics of the oxide, proved to be sufficient to give the composite improved properties with respect to the reference matrix. The micrographs for samples containing Nyglos 8 (Figure 5.9b) show a morphology with a multi-planar and micro cross-dense fracture; both elements are characteristic of composite materials with good homogeneity, strength and good matrix-filler compatibility index. In the image with greater magnification, the largest crystals of the granulometric distribution of wollastonite are easily identifiable; a small bonding gap can be seen, which indicates a good compatibility between polymer and reinforcement. From this image it can be also useful to detect the dimensional heterogeneity of this nanofiller which, together with the good dispersion and interface bonding, allows the use of nanofiller levels well above the traditional quantities. These characteristics confirm the correctness of the choice to carry out further optimization formulations with some fillers in high dosages. In conclusion, the morphological considerations find full correspondence in the detected mechanical properties. The fracture surface shown in the micrographs (Figure 5.9c) produced on the fluorine-reinforced sample appears to be multi-planar and with angles oriented at a live angle; this particular morphological appearance is generated by the characteristic lamellar conformation of the selected reinforcement. Furthermore, this morphology confirms the fracture behaviour of a homogeneous composite material characterized by good

compatibility. The coplanar orientation of the PDM-5B platelets according to the lines of the polymeric flow is inferred from the micrograph at greater magnification and it is, with good probability, a further reason for the effectiveness of this reinforcement. Thanks to the morphological considerations, it is conceivable that reinforcement synergies were created between the fluorine-phlogopite lamellar fillers and the pre-loaded matrix fibers, making this filler very effective; in the light of these considerations, the choice of producing further optimized formulations with this filler was correct. In general, the morphological analysis confirmed and strengthened the mechanical characterization performed on produced nanocomposite materials.

## 5.5 Optimized formulations

As previously commented, it was decided to use different nanofillers in preloaded composites at 15% wt. with both glass fiber and carbon fiber. The results of these previous tests showed that intermediate levels are the most effective for the realization of hybrid nanocomposites. The consideration also derives from the fact that an excessive presence of nanoreinforcement could give the risk of overcoming the saturation of the matrix, compromising the toughness and producing defects in the composite material. **Table 5.7** and **Table 5.8** show the results of mechanical properties of the optimized mixtures containing GF and CF at 15% wt. in the presence of the selected nanofillers at room temperature.

*Table 5.7: Tensile properties of optimized GF samples at room temperature*

SAMPLE	YOUNG MODULUS [MPa]	YELD STRENGHT [MPa]	YELD STRAIN [%]	FAILURE STRENGHT [MPa]	FAILURE STRAIN [%]
PEEK	3544	93.3	5.01	92.3	92.3
PEEK15GF	5613	116.2	3.56	112.3	5.3
PEEK30GF	8258	135.4	2.99	135.3	3.0
PEEK15GF_HT230[15]	5270			102.8	4.3
PEEK15GF_S9[5]	5644			111.0	3.4
PEEK15GF_N8[10]	5839			104.4	3.1
PEEK15GF_CK84[8]	5049			99.5	3.1
PEEK15GF_P5B[8]	7211			120.0	3.5

**Table 5.8:** Tensile properties of optimized CF samples at room temperature

SAMPLE	YOUNG MODULUS [MPa]	YELD STRENGHT [MPa]	YELD STRAIN [%]	FAILURE STRENGHT [MPa]	FAILURE STRAIN [%]
PEEK	3544	93.3	5.01	92.3	92.3
PEEK15CF	9384	148.0	3.81	144.5	4.9
PEEK30CF	16625	184.5	2.27	180.2	2.6
PEEK15CF_HT230[15]	8960	134.7	3.63	132.3	5.0
PEEK15CF_S9[5]	10090	148.0	3.68	146.0	3.9
PEEK15CF_N8[10]	10178	143.5	3.44	141.5	4.0
PEEK15CF_CK84[8]	8698	139.7	3.99	138.3	4.8
PEEK15CF_P5B[8]	10813	148.2	3.39	147.7	4.2

High temperature tensile tests were carried out on these specimens, the results are shown in **Figure 5.10** and **Figure 5.11**. Observing the results reported in the two figures, it can be noted that all the formulations of the realized nanocomposites confirm the trend. In particular, it can be seen that at high temperatures all the materials produced show an increase in the elastic modulus, while maintaining an acceptable value of the deformation at break. The most surprising result is achieved with the nanocomposite containing fluorine mica; in fact, this material retains the yielding phenomenon with values of the Yield strength higher than the relative preloaded matrix, against a value of the acceptable failure strain, up to allow margins for increased charge. All this against a significant improvement of Young's modulus compared to the 15% preloaded glass fiber matrix. The proposed considerations suggest that this material may represent a satisfactory improvement over the commercial products currently in use. The hypothesis of testing the two further optimized formulations based on glass fiber and fluorine mica is also correct.

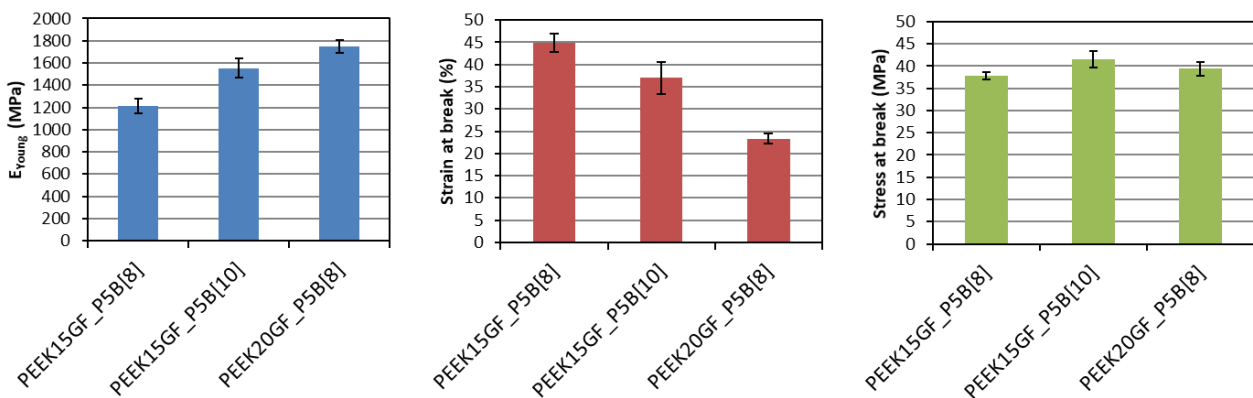


**Figure 5.10:** Tensile properties of optimized GF samples at T = 200°C

From the reported results we see even that both the further GF optimized formulations bring improvements with respect to the previous formulation. In fact, it can be noted that for the last two formulations a further increase of the elastic modulus and of the yielding and break stresses is obtained. These increases do not penalize the deformations that remain acceptable and, in the case of 15% GF + 10% PDM-5B, comparable with the first optimization formulation. The last two formulations show interesting qualities in terms of mechanical behaviour at high temperature, with attention to the nanocomposite PEEK15GF\_P5B [10] for which, in addition to the improvement of all the parameters evaluated, we cannot neglect the reduced cost, due to the presence of additional nanoreinforcement.

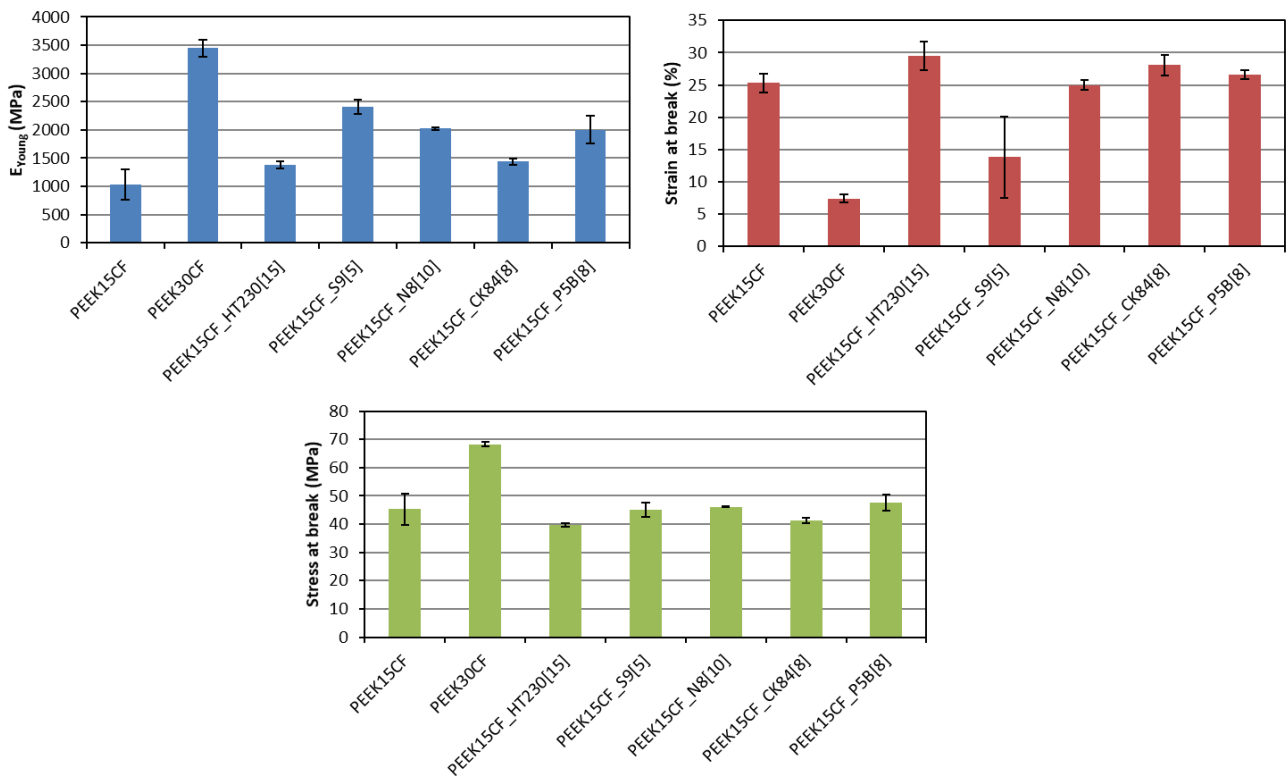


**Figure 5.11:** Tensile properties of optimized CF samples at  $T = 200^{\circ}\text{C}$

In a similar manner, results of the tests carried out at 200 °C on the optimized mixtures based on carbon fiber preloaded matrix show an increase in the deformation at break with respect to the commercial preloaded matrix to 30% of carbon fiber. Furthermore, in all the formulations produced, the yielding phenomenon is present, which, associated with the previous consideration, suggests an improvement in the tough behaviour of the nanostructured composites. However, the values of the elastic modules are significantly lower than the 30% CF matrix, so some use may be compromised, such as some high-pressure applications [Werner et al. 2004; Diez-Pascual et al. 2009; Hou, Shan and Choy, 2008].

A notation of good importance concerns the possibility of further increasing the filler levels for almost two types of filler, as the values of the failure strain are largely above the acceptability. The decision to produce further optimized formulations for composites containing wollastonite and fluoro mica is therefore correct. It is also apparent that the palygorskite-based formulation, although possessing satisfactory mechanical properties, seems to have reached the saturation limit, not allowing further improvements. On the other hand, formulations based on titanium dioxide and silicon oxide and aluminium oxide show potential margins for increasing the filler level; however, starting from values of the Young's modulus, that are significantly lower than the commercial reference, it is unlikely that comparable results can be achieved with the reference commercial product. In conclusion, it was decided to devote resources to investigate the most "promising" materials, for which further optimizations were produced. The results of the high temperature mechanical characterization for the last formulations are shown in **Table 5.9**.

**Table 5.9:** Tensile properties of optimized CF samples at  $T = 200^{\circ}\text{C}$  – second optimization

SAMPLE	YOUNG MODULUS [MPa]	YELD STRENGHT [MPa]	YELD STRAIN [%]	FAILURE STRENGHT [MPa]	FAILURE STRAIN [%]
PEEK15CF_N8[15]	2027	35.1	7.04	43.4	22.0
PEEK15CF_N8[20]	1767	34.3	7.00	41.5	19.0
PEEK20CF_N8[10]	2360	39.5	6.68	52.4	18.4
PEEK30CF_N8[10]	3660	58.4	8.00	62.8	11.3
PEEK20CF_P5B[8]	2433	48.5	10.9	55.0	19.2
PEEK30CF_P5B[10]	3457	58.6	8.50	62.6	11.9

The values shown in **Table 5.9** clearly show the effect that the two fillers produce on the mechanical properties of the composite exposed to high temperature. It is seen that an increase in the content of wollastonite at 15% wt., while maintaining the quantity of carbon fiber, does not produce significant effects on the elastic modulus, but slightly decreases the parameters correlated to the tough behaviour. This aspect is even more evident when the wollastonite percentage rises to 20% and the CF is kept at 15%; in this case, in fact, there is a fall of the value for elastic modulus without improvements of the other parameters. It can be deduced that the 10% wt. represents the threshold for the nanofiller for saturation in the mixture.

On the contrary, keeping the content of pyrossene based nanofiller fixed at 10% wt. and increasing the organic level, a progressive increase of the elastic modulus is obtained without compromising the values correlated with the toughness. With the mixture containing 30% wt. of carbon fiber and 10% wt of Nyglos 8, are reached values for moduli above the reference matrix, obtaining, however,



significantly better toughness parameters than commercial products. The behaviour at high temperature also confirms this hypothesis, showing the characteristic yielding phenomena of a material not subjected to a brittle fracture.

According to this, the proposed objectives of realizing a nanocomposite material with a techno-polymer matrix that showed greater toughness, preserving the mechanical stiffness at lower costs, are thus achieved. Similar considerations can also be carried out for the formulations containing the PDM-5B; in fact, also in this case, a margin of increase of reinforcement contents was detected in the mixture 20% CF + 8% PDM-5B. By increasing both the carbon and the nanofiller amount, Young's modulus values higher than the reference product are reached.

It can be said that even the formulation containing 30% CF + 10% PDM-5B completely meets the requirements that were intended to be pursued. The mixture with higher levels of carbon fibers and nanofiller shows a decrease in properties, indicating that the synergistic effect has limited potential and that probably saturation was reached with the formulation of the first optimization. It is important to note that a series of reference materials has been produced, able to provide "tailor-made" solutions for different applications, in which it is necessary to manage the mechanical parameters. Thus, improved materials have been obtained compared to those currently on the market and a range of materials with intermediate properties adaptable to specific application solutions. In an equally important manner we have obtained reference information, related to a theory, regarding the creation of nanocomposite materials with a techno-polymer matrix that open perspectives for a greater future use of these types of products.

Concluding, modifying the levels of the additives, we could produce a series of properties trend with the variation of the formulations. Hybrid formulation containing 20% of glass fiber and 8% of fluoro mica (PDM-5B) has values of the Young's modulus higher than the reference commercial products, also showing parameters that can be correlated to a more tough behaviour; similar behaviour is also found for the formulation with 15% GF + 10% PDM-5B, which also meets the objective of cost reduction thanks to 10% wt. of filler additive. Equally relevant results have been obtained with the hybrid nano composites with a preloaded matrix with carbon fiber. Formulations containing 30% of carbon fiber and 10% respectively of Nyglos8 and PDM-5B show values of the elastic modulus higher than the reference matrix. Both also present the yielding phenomenon and stress and strain values that can be correlated with a more tough behaviour of commercial materials. In this case also, the objectives set by the research project are completely achieved, also satisfying the economic aspect with a significant reduction in material costs [ [Werner et al. 2004](#); [Diez-Pascual et al. 2009](#); [Hou et al. 2008](#); [Ding and Bikson, 2010](#)].

In addition to the creation of nano-composite materials with a techno-polymer matrix that fully meet the expected objectives, it is important to note the achievement of a parallel objective. The quantity

of tested materials and the method of approach make it possible to formulate a theory concerning the effects that the tested fillers induce on the characteristics of the materials in question. This information allows us to "manage" some properties of these materials by acting appropriately on the formulations, to produce nanocomposite materials with a techno-polymer matrix that possess characteristics tailored to each individual use. In this way, the goal of creating materials with the prerogatives of a technopolymer and the desired properties optimized for specific applications, allowing for broad prospects for future use, has also been achieved (**Figure 5.12**).

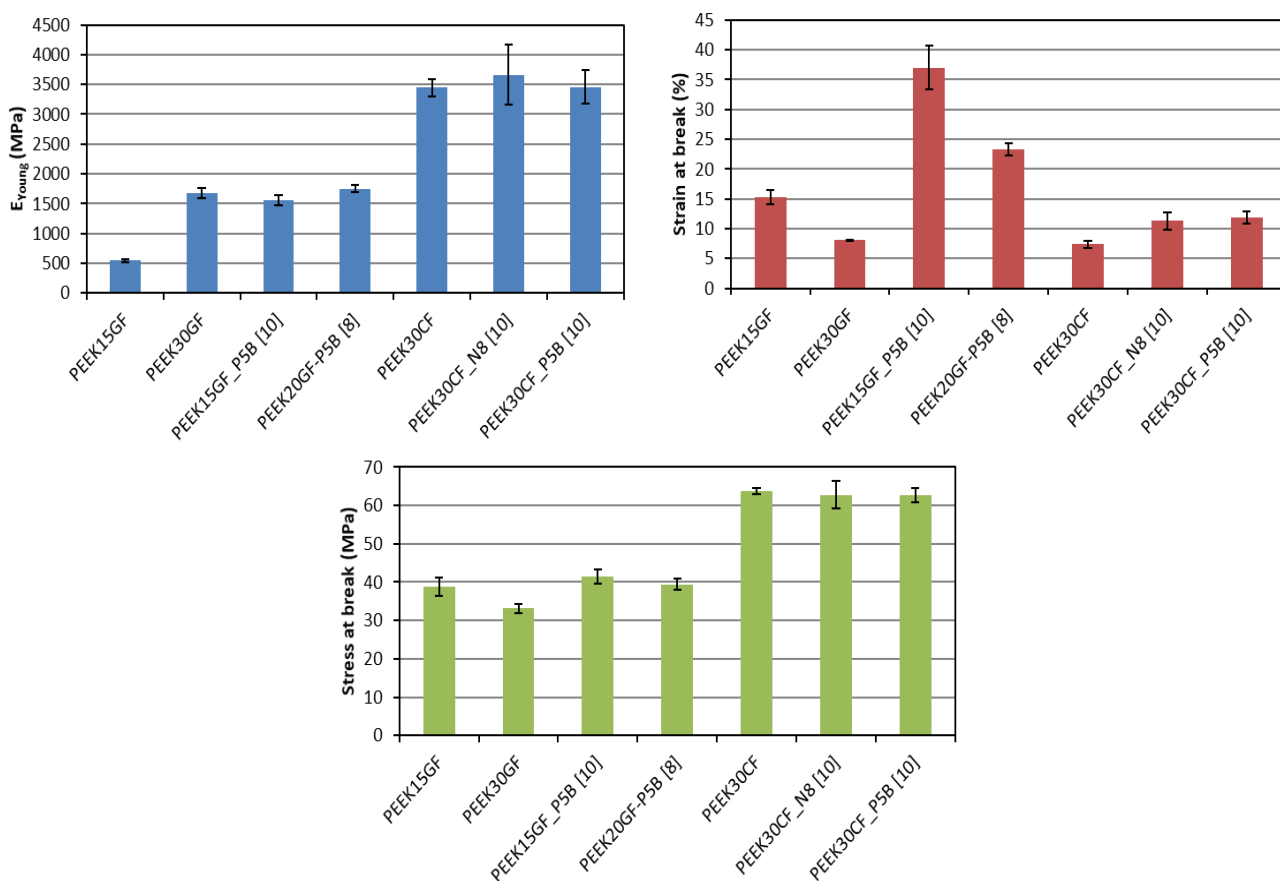


**Figure 5.12:** Best nanostructured and fiber reinforced PEEK based formulation

It has thus been demonstrated that it is possible to modify the mechanical properties of a techno polymer such as polyetheretherketone, by making nanocomposites by intercalation in the polymer melt. The mechanical characterization of the composites was carried out with test at room and high temperature. Among the future developments of the work, the evaluation of the tenacity of the materials produced with specific impact tests at various temperatures is certainly of interest. Although the effect of different charge families has been tested, the possibilities of expanding this study with additional types of fillers appear almost limitless. In a similar way it would be interesting to evaluate the possibility of creating blends of polymeric matrices. In effect the PAEEKs are widely

compatible with each other and with other technical polymers such as some polyimides or polysulfones. By suitably creating blends, the advantages of semi-crystalline polymers such as PEEK and the properties of amorphous polymers such as PEI could be obtained at the same time.

## 5.6 References

- Kido et al. 2000, US006103806A, Patent Number: 6,103,806, POLYIMIDE RESIN COMPOSITION
- D. J. Blundell and B. N. Osborn POLYMER, 1983, Vol 24, August 953
- P. Werner, V. Altstadt, R. Jaskulk et Al Wear 257 (2004) 1006–1014
- A.M. Diez-Pascual, M.Naffakh, M.A. Gomez, C. Marco, G. Ellis1 et Al.— Nanotechnology 20 (2009) 315707
- Xianghui Hou, C.X. Shan, Kwang-Leong Choy - Surface & Coatings Technology 202 (2008) 2287–2291
- Yong Ding, Benjamin Bikson - Journal of Membrane Science 357 (2010) 192–198- P. Werner, V. Altstadt, R. Jaskulk et Al Wear 257 (2004) 1006–1014
- A.M. Diez-Pascual, M.Naffakh, M.A. Gomez, C. Marco, G. Ellis1 et Al., Nanotechnology 20 (2009) 315707
- Xianghui Hou, C.X. Shan, Kwang-Leong Choy urface & Coatings Technology 202 (2008) 2287–2291

## CHAPTER 6: NANOSTRUCTURED AND FIBER REINFORCED COMPOSITES

### 6.1 PEEK - PI based NS and FR composites

A set of composite materials was produced using a blend of PEEK and PI as a matrix. The polyimide P84 NT1 (PI) supplied by Evonik is characterized by remarkable thermal stability and excellent mechanical properties even at high temperatures. Unfortunately, it cannot be processed by extrusion alone, but only by thermal compression in the mould which is a low productivity batch process. In appropriate formulations with PEEK, it can be processed by extrusion, increasing productivity and exploiting the excellent thermal-mechanical properties. The presence of PI in mixture can confer thermal stability, especially when the material exceeds the glass transition temperature of PEEK and a significant reduction of the mechanical properties of the semi-crystalline polymer occurs [Dominguez et al, 2015; Clair, 1990; Hergenrother and Havens, 1989].

Mixtures with 30, 40 and 50% in wt. of PI were made to understand which mixing ratio could be more suitable for the production of composite materials. Samples of these materials were produced by melt mixing and injected into suitable moulds to undergo thermomechanical characterizations. A microcompounder DSM Xplore 5 & 15 cc was used, setting the three temperature (top-middle-bottom) zones at 355 – 375 – 390 °C mixing at 90 revolutions per minute for a residence time of 180 seconds. The injection was performed with a DSM injection machine setting the temperature of the injection chamber at 395 ° C and the mould at 200 ° C and making the injection with the profile pressures-times 12-0.2; 11-0.2; 11- 9.6 in bar-s.

#### 6.1.1 Mechanical characterization by tensile test

The specimens were tensile tested according to ASTM D638, with a dynamometer Lloyd instrument LR30K at a speed of 5 mm/min at room temperature. The values of the characteristic parameters of the tensile test are shown in **Table 6.1**.

*Table 6.1: Results of tensile tests on PEEK-PI blends*

Sample	Young Modulus [MPa]	Stress at Yield [MPa]	Strain at Yield [%]	Stress at Break [MPa]	Strain at Break [%]
PEEK	3921±158	98.5±1.78	4.75±0.39	70.9±3.56	15.9±3.20
70PEEK–30PI	3860±172	100±1.33	5.78±0.73	91.8±8.32	11.6±4.28
60PEEK–40PI	3864±6	101±1.50	6.28±0.22	102±0.51	7.18±0.98
50PEEK–50PI	3886±133	102±0.58	6.10±0.08	102±0.14	6.99±0.32

Stress-strain diagram curves representative of the behaviour of the tested materials are shown in **Figure 6.1**.

The graph shows that the addition of 30% of PI increases the tensile strength; the elastic modulus remains substantially unchanged and the elongation at break has a slight decrease, which does not affect the performance of the material. The samples with 40% and 50% of PI do not show improvements of elastic modulus and tensile strength, while there is a noticeable decrease in the deformation at break. Since the PI matrix is more expensive and less effective at the interface with the reinforcements, it was considered that the blend made with 70% wt. of PEEK and 30% wt. of PI (70PEEK-30PI) was more suitable for making composites.

Stress-strain diagram curves representative of the behaviour of the tested materials are shown in **Figure 6.1**.

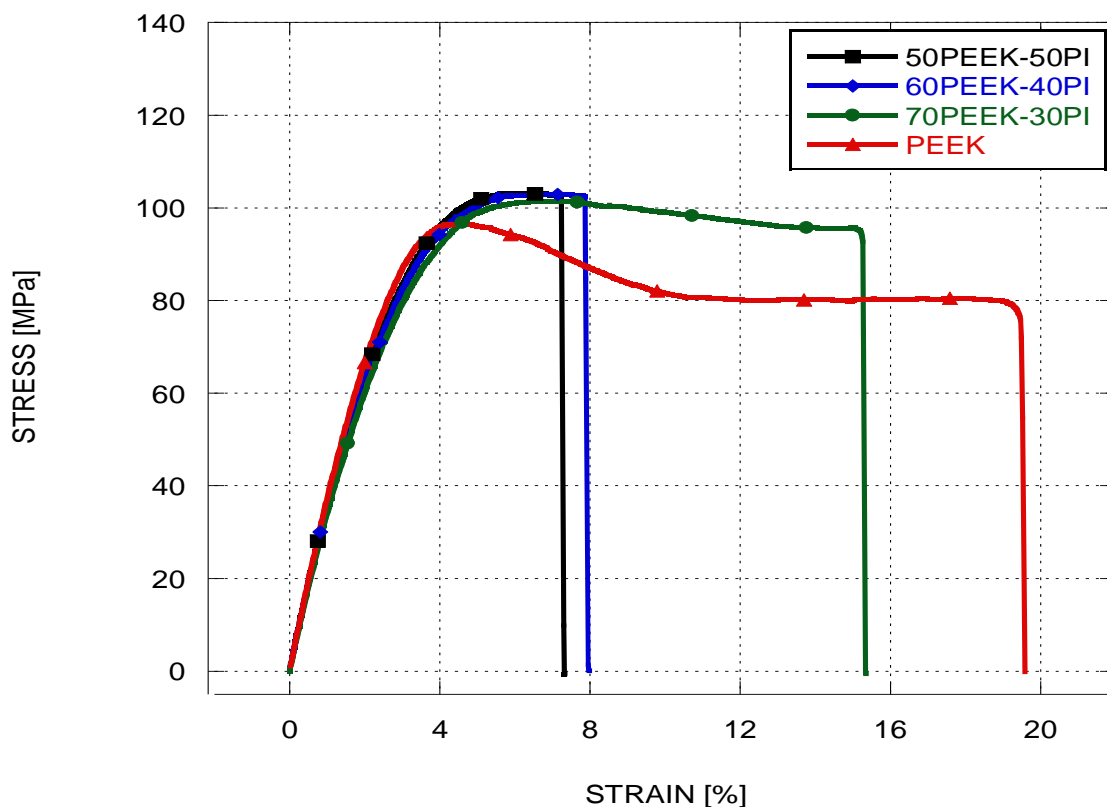


**Figure 6.1** Stress-Strain curves of PEEK-PI blends

Based on considerations concerning thermal stability and compatibility with the matrix available in literature, three nanoreinforcements were considered for the production of nanostructured composites: a fumed titanium dioxide characterized by a specific surface area (SSR measurement with BET method) of 70-110 m<sup>2</sup>/g under the trade name Aeroxide TiO<sub>2</sub> P90 (TP90) and fumed aluminium oxide Aeroxide Alu 130 (C130) with SSR of 110-150 m<sup>2</sup>/g, both supplied by Evonik

Industries AG. The third micro/nanosized reinforcement is a wollastonitic calcium inosilicate mineral characterized by acicular morphology with aspect ratio of 19:1, supplied by Nyco Minerals as Nyglos8 (N8). The tetrahedral arrangement within the chains in pyroxenes compared to wollastonite structure and a TEM image of Nyglos8 is reported in **Figure 6.2a** and **Figure 6.2b**, respectively.

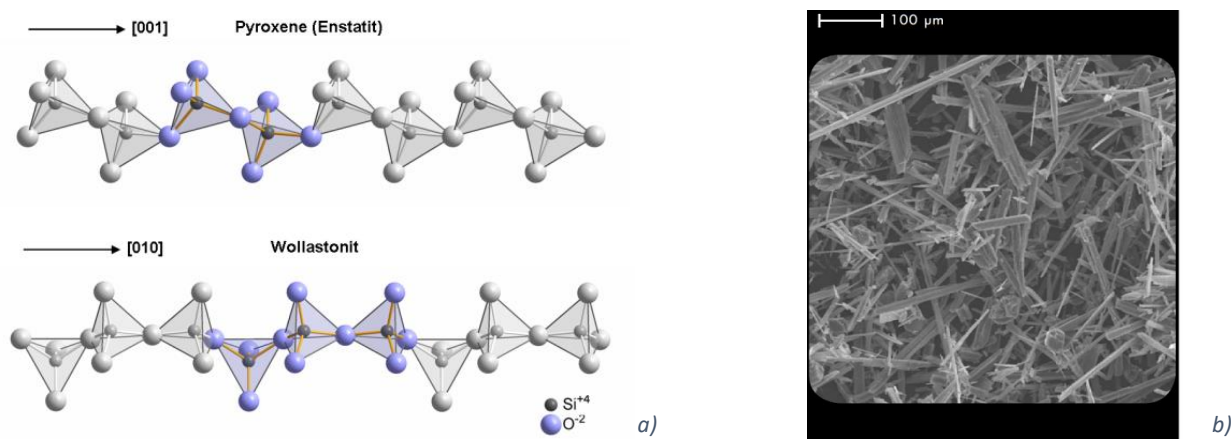


**Figure 6.2** Nyglos8 structure (a) and TEM micrography (b)

Three nano composites were produced with the formulations shown in **Table 6.2**, with the aim of evaluating the effect of the nanofillers on the 70PEEK-30PI matrix. The production of nano reinforced composites was carried out using the same process and the same parameters described for the production of PEEK-PI blends. The mixing of the two types of polymer also took place simultaneously to the filler dispersion, to obtain a better mixing and bonding of the reinforces with the matrices and to optimize the process in one step. In addition to the formulations of the nanostructured composites with the three selected charges, three other formulations were produced using also glass fiber to evaluate the synergistic effect of the two types (fibrous and nanometric) of reinforcement: Finally, two other formulations were produced, in which the amount of glass fiber and the amount of nanofiller that had yielded the best results in the previous formulations were alternately halved. This approach was aimed at understanding the effect of the different reinforcements on the thermo-mechanical properties of the composite materials considered. The list of formulations produced, including the benchmarks, is shown in Table 6.2.

A first characterization of the mechanical properties of the nanostructured composites was carried out with tensile tests using the same method described previously. The values of the main parameters are shown as histograms in **Figure 6.3**.

The graphs show that all the used nanofillers produce a general increase in the elastic modulus. Titanium dioxide causes the reduction of tensile strength with wide dispersion of values. This result is probably due to a poor compatibility with the matrix and / or to an irregular dispersion of the nano

filler. Both the other two nano fillers produce an improvement in tensile strength with good uniformity of results. Even the last deformations of these two reinforcements, although decreasing with respect to the matrix, remain above acceptable values without falling below 5%. Also for this aspect the composite with the TiO<sub>2</sub> is less satisfying. However, all the reinforcements have produced effects that do not exclude their use together with the reinforcing fibers.

Then the fiber-reinforced and nano-structured materials produced, together with the benchmark materials, were also tensile tested. **Table 6.3** shows the results of the tensile tests carried out at room temperature.

**Table 6.2** Formulation of composites based on PEEK-PI blend matrix

NAME	PI %	GLASS FIBER %	NANO FILLER NAME	NANO FILLER %
100PEEK	-	-	-	-
70PEEK-30PI	30	-	-	-
60PEEK-40PI	40	-	-	-
50PEEK-50PI	50	-	-	-
PEEK-30PI-7TP90	30	-	TP90	7
PEEK-30PI-6N8	30	-	N8	6
PEEK-30PI-7C130	30	-	C130	7
PEEKGF30-30PI	30	30	-	-
PEEKGF30-30PI-7TP90	30	30	TP90	7
PEEKGF30-30PI-6N8	30	30	N8	6
PEEKGF30-30PI-7C130	30	30	C130	7
PEEKGF30-30PI-3.5C130	30	30	C130	3.5
PEEKGF15-30PI-7C130	30	15	C130	7

\* The percentage in weight of PI, glass fiber and fillers are calculated on the weight of PEEK

**Table 6.3:** Result of tensile test on fiber reinforced and nanostructured composites at room temperature

Sample	Young Modulus [MPa]	Tensile Stress [MPa]	Strain at Break [%]
100PEEK	3921±158	98.5±1.78	15.9±3.20
70PEEK-30PI	3860±172	100±1.33	11.6±4.28
PEEKGF30-30PI	8164±626	143±4.90	3.89±0.28
PEEKGF30-30PI-7TP90	7940±557	129±15.9	2.91±0.39
PEEKGF30-30PI-6N8	8165±270	131±2.23	3.18±0.66
PEEKGF30-30PI-7C130	8646±196	142±3.00	2.92±0.03
PEEKGF30-30PI-3.5C130	7747±296	123±22.3	2.38±0.79
PEEKGF15-30PI-7C130	6442±506	123±6.28	3.20±0.07



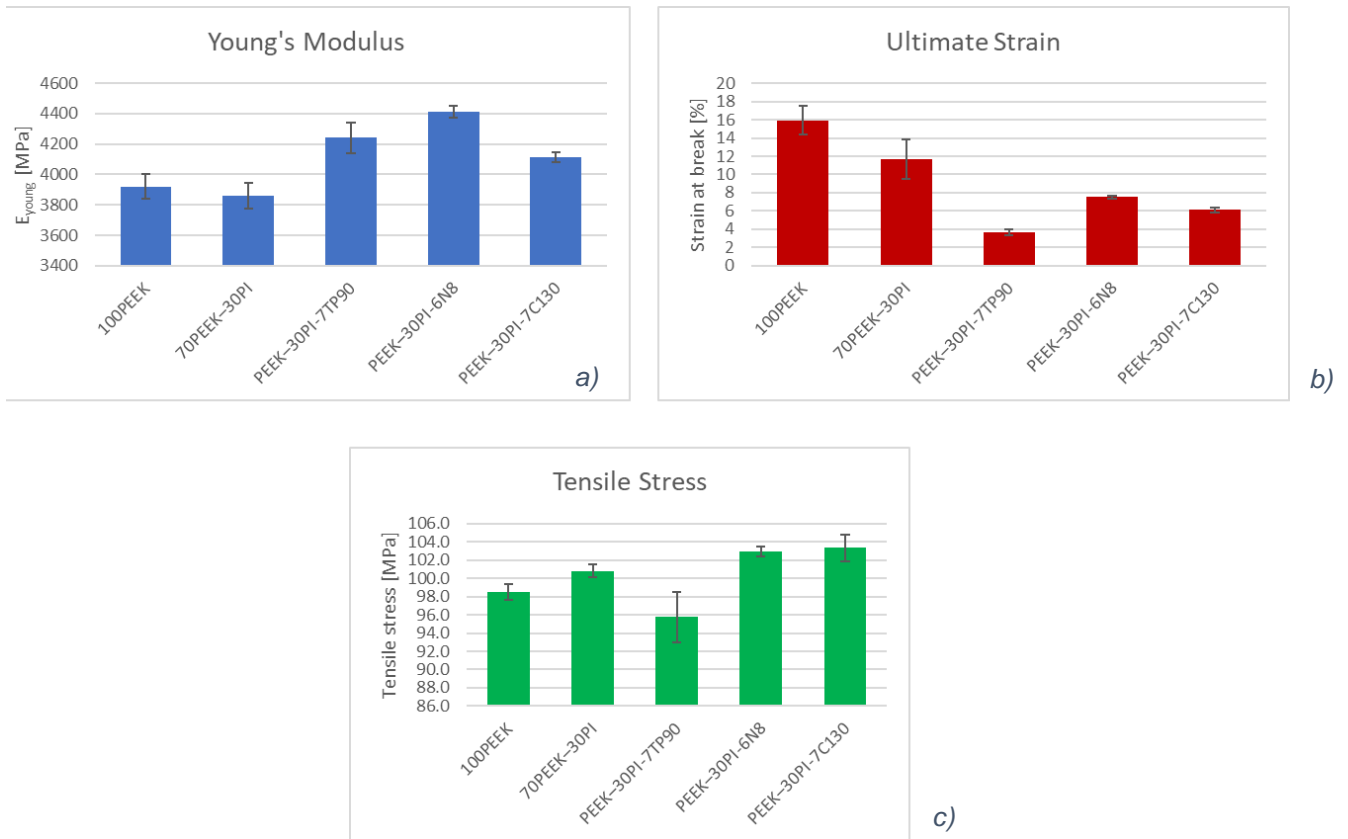


**Figure 6.3** Result of tensile test on nanostructured composites: Elastic moduli (a), Strain at break (b) and Stress resistance (c)

The values of the elastic modules show that there are no differences between the PEEK neat matrix and the blend with PI; an appreciable increase in stiffness is seen when 30% wt. of glass fiber is added. In the case of composites with 30% wt. of GF nanostructured with TP90 and N8 the variations of E are maintained within the deviations, while the formulation with 7% wt. of C130 shows a slight increase. The formulated materials having GF and C130, as expected, show a decrease in stiffness. The use of reinforcing materials in the composites, parallel to the increase in stiffness, produces a reduction in the deformation at break, that for all the composites does not show significant variations and it is always kept below 5%.

The tensile stress is maintained constant with the addition of PI at room temperature. The 30% wt. GF composite shows an increase in strength of about 40%. This value is also equalled by the formulation PEEKGF30-30PI-7C130, while the other composites show a slight decrease in resistance to stress. In particular, the formulations produced by reducing the two types of reinforcements alternately show equal values; the only difference between the two systems is given by the greater homogeneity of the PEEKGF15-30PI-7C130 found in the lower value of the standard deviation. The same materials were tested at high temperature in tensile mode, by using a climatic

chamber. It was decided to test the materials at 200 °C because this temperature is significantly above the glass transition temperature of PEEK ( $T_g \approx 143$  °C) and it is an extreme temperature for the use of these polymers. Then the specimens were subjected to air conditioning at 200 °C for a period of time sufficient to ensure the achievement of thermal uniformity within the sample and then subjected to tensile testing at  $T_{high} = 200$  °C. The results of the high temperature tests are reported in **Table 6.4**. At  $T = 200$  °C, there is a general decrease of the elastic modulus, which however does not collapse, thanks to the semi-crystalline nature of the PEEK matrix and the very high  $T_g$  of the PI ( $T_g = 337$  °C); in this case, the contribution of PI in mixture is evident with respect to PEEK, both in the value of the modulus and in the tensile strength.

**Table 6.4:** Result of tensile test on fiber reinforced and nanostructured composites at 200°C

Sample	Young Modulus [MPa]	Tensile Stress [MPa]	Strain at Break [%]
100PEEK	256±35.2	16.9±2.1	226±33.9
70PEEK–30PI	400±55.1	23.9±0.49	203.7±36.4
PEEKGF30–30PI	1699±124	36.8±0.82	7.75±0.13
PEEKGF30–30PI-7TP90	1947±471	45.9±5.16	7.85±0.17
PEEKGF30–30PI-6N8	2060±20.7	42.8±2.90	5.77±0.94
PEEKGF30–30PI-7C130	2146±82.4	50.6±1.37	9.80±0.65
PEEKGF30–30PI-3.5C130	1782±244	43.9±3.23	8.51±0.47
PEEKGF15–30PI-7C130	1355±180	41.2±0.34	13.1±2.35

It has been revealed that the value of the Young's modulus of the composite with the glass fiber is significantly higher than the reference matrix of more than 3 times. All nanostructured composites with 30% wt. GF show improved  $E_{young}$  values, even when compared to PEEKGF30-30PI. In particular, the PEEKGF30-30PI-7C130 composite shows an increase of the elastic modulus of more than 25%, when compared to the fiber-reinforced mixture. Only the composite with 15% wt. of GF undergoes a reduction of the elastic parameter, due to the halved quantity of fiber; however, the presence of the nano reinforcement produces a strength resistance value higher than the composite with 30% wt. reinforcing fiberglass.

Furthermore, the PEEKGF15-30PI-7C130 shows a greater deformation at break than the PEEKGF30-30PI, which can be correlated with an improvement of the toughness. The elongations at break of all the fiber-reinforced and nanostructured composites never fall below 5%, revealing non-particularly fragile behaviour. The tensile stress values of nanostructured composites show significant improvements even compared to the fiber-reinforced composite with 30% wt. GF.

Compared to the fiber-reinforced benchmark, the nanocomposite with TP90 shows an increase of strength of 25%, while for the PEEKGF30-30PI-7C130 formulation, an increase of more than 37% was measured. These results appear to be relevant for the design of composite materials for high temperature applications.

In addition, it can be noted that the choice of the quantities and types of fibers and nano fillers can be appropriately managed to design composite materials with specific properties for each particular application. **Figure 6.4** shows the stress-strain diagrams of the tests carried out at 200 °C for some of the materials produced.

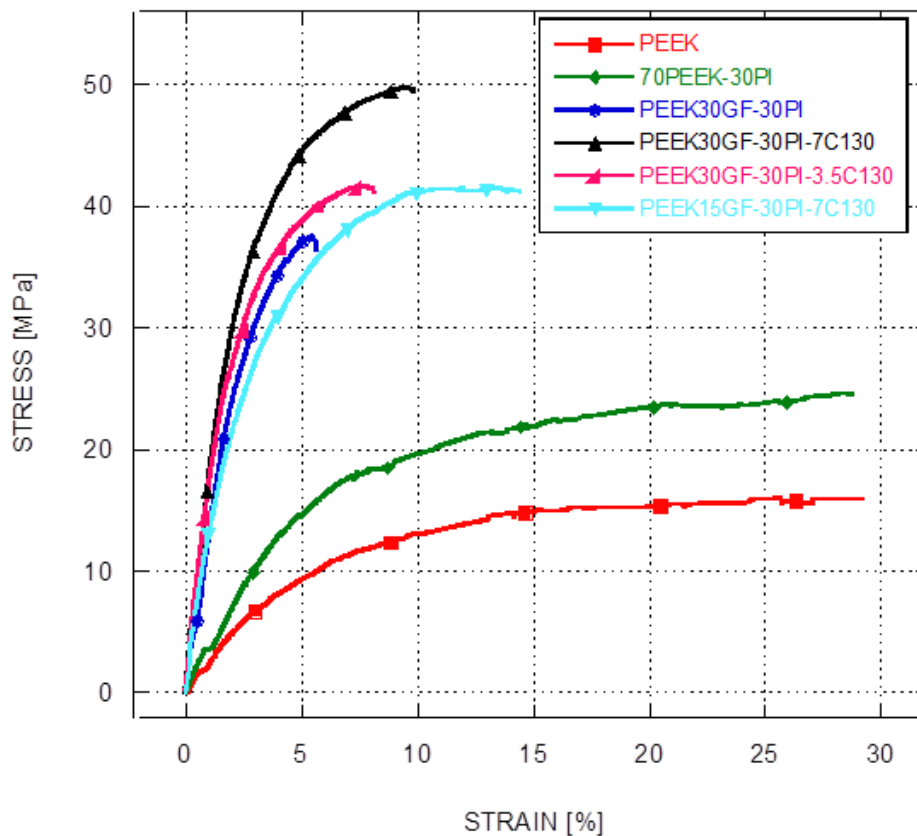


**Figure 6.4:** Stress-strain diagram of the tests at  $T=200$  °C

It appears evident that the composite materials offer mechanical performances superior to the reference matrices, but also that it is possible to make materials with greater rigidity or resistance to stress or toughness depending on the potential use of the application to which they are intended.

Furthermore, it must be considered that all the reinforcements used have costs of at least one or two orders of magnitude lower than the matrices, so their use involves a considerable saving on the costs of the materials; the one-step melt compounding method further reduces costs by avoiding multiple melt blending steps of masterbatches.

### 6.1.2 DSC thermal characterization

The thermal characterization with the differential scanning calorimeter was carried out with a DSC mod. Q200 from TA Instruments. The tests were carried out with a temperature ramp at 10 °C / min from 25 to 400 °C with two heating cycles and a cooling.

The main data have been summarized as graphs to highlight the characteristics of interest. The considerations relating to the results obtained are shown below (**Figure 6.5** and **Figure 6.6**).

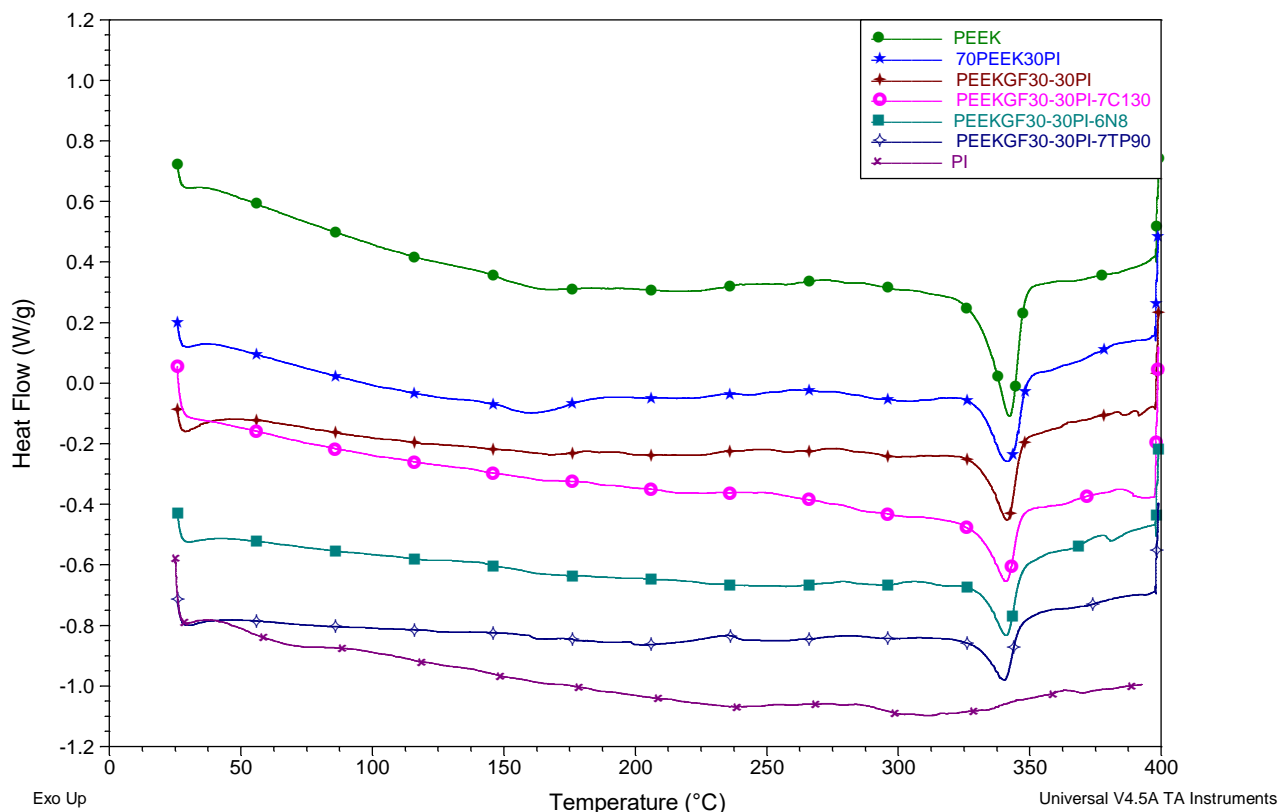


**Figure 6.5:** DSC curves at the second heating of the composites

The DSC analysis carried out on the two matrices used to produce the blend confirms the characteristic temperatures reported in the technical data sheets. In particular, the PEEK shows a rather narrow melting peak, indicative of the semi-crystalline nature of this neat polymer, with melting peak at 343 °C. The glass transition temperature is less evident, but still identifiable around 143 °C. The polyimide graph shows a transition peak with temperatures between 320 and 380 °C, with a maximum of around 350 °C. These results are in perfect agreement with the values provided by the technical data sheet, which identifies the glass transition temperature and the Heat Deflection Temperature (HDT) , respectively, at 345 °C at 337 °C.

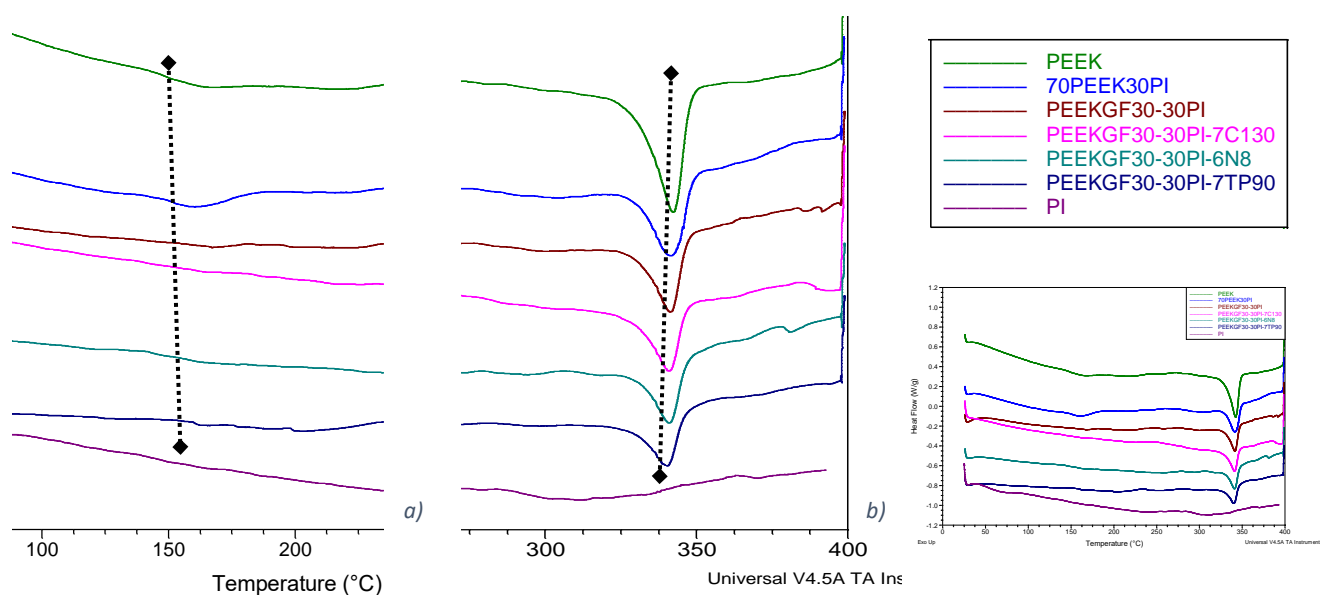


**Figure 6.6:** Details of the DSC curves at the second heating: glass transition zone (a) and melting zone (b)

The DSC scans performed on the 70PEEK-30PI samples show a good compatibility between the matrices, without highlighting the separation of the characteristic peaks. At the substantial permanence of the melting peak in the range of temperatures detected for the pure PEEK corresponds a slight increase in the glass transition temperature. The relative expansion of the latter suggests an improvement in thermal stability and in HDT compared to pure PEEK. The test performed on the same blend with the addition of reinforcing glass fibers showed no evident differences, to confirm that the glass fibers improve the mechanical properties without affecting the thermal characteristics. The material produced with the 30% wt. glass fiber and PEEK-PI blend with 7% of titanium dioxide shows the same characteristic temperatures detected for the corresponding material without nanometric additives. The only note that could be of relevance can be found in the shape of the curve that is more rounded, probably due to the thermo-capacitive effect of the metal oxide content. This feature could be useful in preventing thermal shocks for cyclic applications. The scan carried out on the PEEK30GF-30PI-6N8 is substantially superimposable to the corresponding non-nanostructured composite, confirming the good thermal stability and compatibility of this filler with the used polymers. For the nanocomposites made with the aluminum oxide, the considerations already produced for the material with the  $\text{TiO}_2$  can be confirmed, both in terms of characteristic temperatures and trend of the curve. A consideration concerning the material with 15% wt. of GF and 7% wt. of C130 is necessary: it is possible to notice a lowering, even if of only 3-4 °C, of the melting peak. This phenomenon could be due to the method of realization of this mixture: in fact, in order to reduce the glass fiber amount, a dilution in polymer melt was carried out starting from a masterbatch with 30% wt. of GF with pure PEEK. However, the effect does not seem to be of great

importance and in any case it is negligible in the context of research of increased toughness. It can be stated that the materials selected for the realization of nanostructured formulations accurately meet the information reported in the technical documents. In particular, the polymer matrices show the same transition temperatures described in the relative datasheets; the selected fillers show no transition phenomena that reveal the presence of organic additives, potential sources of degradation phenomena during the production process of the samples.

The polymer blends produced, with and without reinforcement fibers, showed the same range of melting temperature compared to an effective increase in glass transition temperatures. This change leads us to assume a consistent increase in the characteristic temperatures of use, conferring an improvement both in terms of deflection temperature (HDT) and of the temperature in continuous use (CUT). Furthermore, it does not seem necessary to overturn the process parameters traditionally used for peek processing while maintaining the same production lines. Also the nanostructured and fiber-reinforced materials confirm the same thermal behaviour of the matrices in the blend; this suggests that improvements to thermal stability are also effective for the nanocomposites produced. The presence of nanofillers does not affect the characteristic temperatures of the materials and hopefully improves other properties.

### **6.1.3 Thermogravimetric characterization**

The thermogravimetric measurements were performed with a TGA produced by the Seiko model Exstar 6300. The thermal stability of the materials treated in this work was studied; dynamic scans at the heating rate of 10 °C/ min were carried out, with a ramp test temperature in the range of 30°C to 400°C. The experimental values were then sent to the computer connected to the thermogravimetric scale and subsequently processed with software. In each test an air flow was used to simulate the extrusive process conditions with degassing in the atmosphere. The DTG was simultaneously considered, to highlight possible weight loss peaks. The data obtained from the tests carried out with the thermogravimetric device were placed in the form of graphs reporting abscissa temperatures in °C and in ordinate weight loss and the rate of mass variation in mg/min (DTG). The selected nano fillers were dynamically tested to evaluate thermal stability even beyond the temperature range of the process. The results are reported in **Figure 6.7**. The two metal oxides and the mineral charge showed remarkable thermal stability well beyond the temperature of 400 °C; this behaviour is evident both in the practically negligible weight loss and in a more evident way from the thermogravimetric derivative, which appears practically constant at the process temperatures. Although not directly related to the case study, it was seen that wollastonite appears thermally stable even at temperatures close to 550 °C, where a slight weight loss begins. It can also be noted that charges resist high temperatures for relatively long times when it is considered that at least three minutes are required to bring the samples from 370 to 400 °C. This method of analysis confirms that

at the temperatures in question a residence time of a few minutes does not produce significant thermal degradation phenomena on the selected nano reinforces. The TGA and DTG scans carried out on the samples of the PEEK-PI materials (**Figure 6.8**) show a negligible weight loss in the first section which is exclusively attributable to drying of the sample. Subsequently there are no significant weight losses up to temperatures above 400 °C. At 480 °C the losses appear to be consistent in the order of a few percentage points to end in a progressive and heavy weight loss between 500 and 700 °C. It can be concluded that the polymer blend offers considerable guarantees of thermal stability even at temperatures higher than those achieved for the most severe applications.

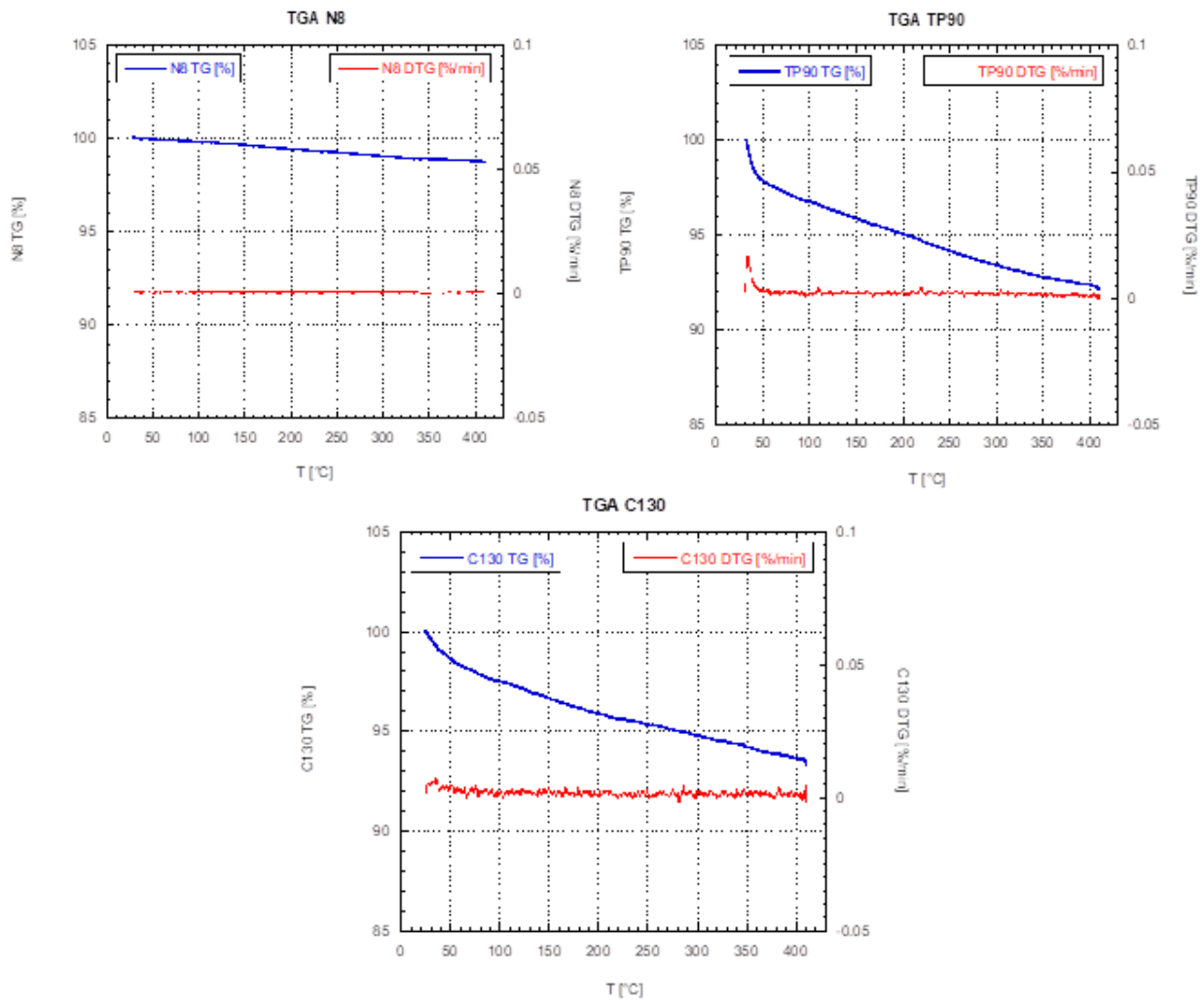


**Figure 6.7:** Results of dynamic TGA test on nano fillers

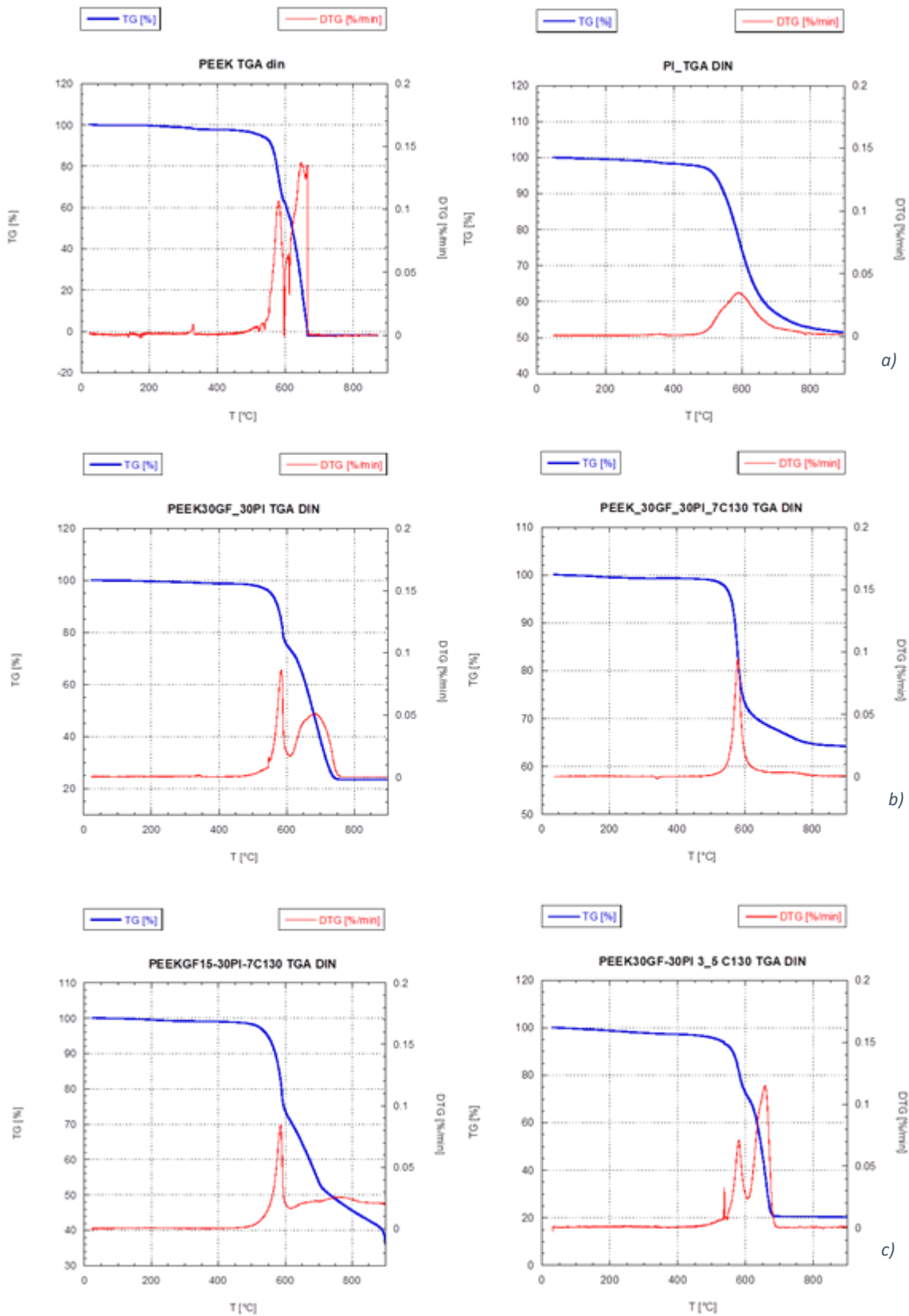


**Figure 6.8:** Results of dynamic TGA test on fiber reinforced and nanostructured blends



The formulation with 30% wt. glass fiber and 7% wt. C130 is practically superimposable to the starting blend. The only detectable difference with respect to the matrix consists in a slight delay of the degradation, but in a greater speed of weight loss above 500 °C; both phenomena could depend on thermal capacity of the metallic oxide, which initially absorbs heat, protecting the polymers, but subsequently works as a heat accumulator, emphasizing the effects of thermal degradation. The same behaviour is also observed for the material with 3.5%wt. aluminium oxide. In the graph shown in Figure 6.8c, the discrete events that cause the thermal degradation of the material are evident. Even if it is difficult to establish with certainty the phenomena that occur during the sudden loss, it can be said that there is a first step with a peak at about 540 ° C and two further consistent steps with a maximum of around 570 and 670 ° C. The observation of the thermal analytical graph of the mixture with 15% wt. of GF and 7% wt. of aluminium oxide shows a similar trend to the other mixtures with the same components. It must however be noted that the first reduced peak of the previous case is not perceived, probably due to a lower presence of glass fiber or some additive related to it. The peak at 570 °C is emphasized with respect to the previous case, and this suggests that this peak is related to a greater presence of PEEK. In fact, it turns out that the ignition temperature of PEEK is just 570 °C, reaching the maximum loss rate for 600 °C. The nano-structured materials based on titanium oxide and wollastonite show behaviour similar to the formulation with 3.5% of aluminium oxide.

A comparison of the TG curves of the composite materials can be observed in **Figure 6.9**. It can be seen that the composites have a good thermal stability.

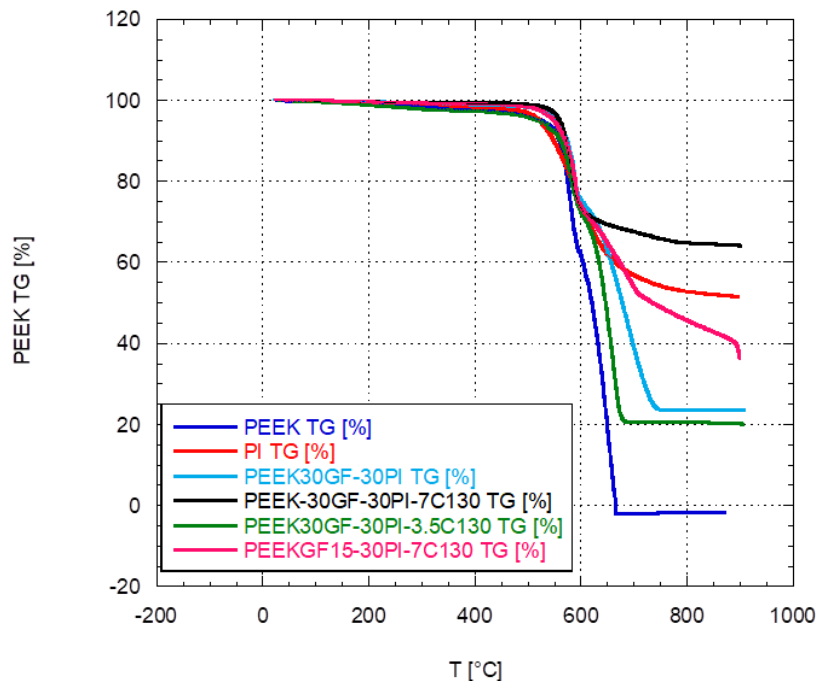


**Figure 6.9:** TG comparison of composite materials based on PEEK-PI blend

The results obtained from the thermogravimetric analysis can be considered very positive. In general, all the materials used to produce the nanostructured mixtures have shown thermal stability, appropriate characteristics for the intended use, with temperatures and residence times typical of a polymer melt dispersion processing. All the materials produced showed excellent thermal stability, even at temperatures well above the range of conventional operating temperatures for reference matrices. The formulation PEEKGF30-30PI-7C130 shows a high thermal stability even at high temperatures.

#### 6.1.4 Morphological characterization

The morphology of the fractured surfaces for the composite materials was observed with a field emission electronic microscope mod. Supra 25 of Zeiss. For each material, two micrographs at 500 and 5000 magnifications have been reported.

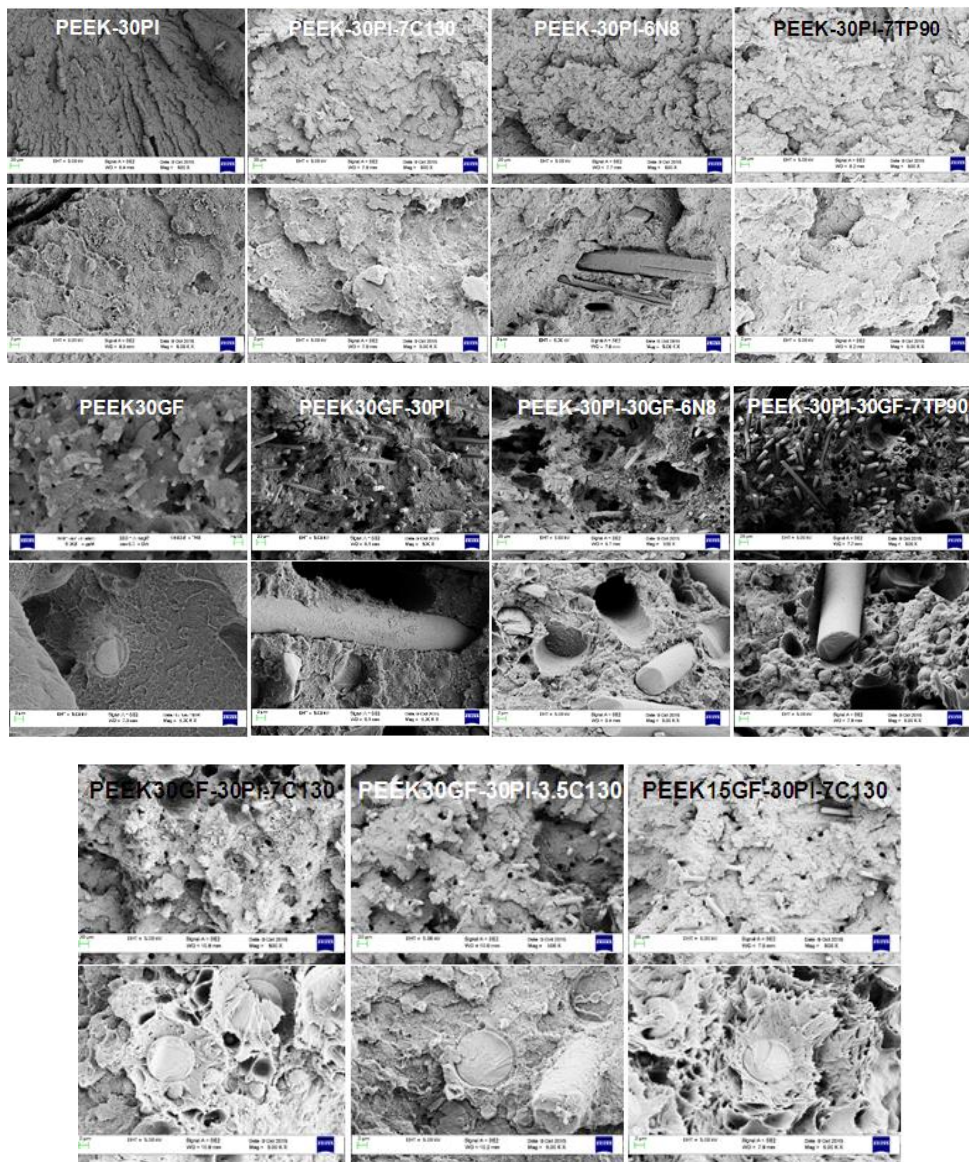


Figure 6.10: SEM micrographs of the produced composites

In the first SEM image it is possible to appreciate the good compatibility between the matrices. SEM micrographs of nanostructured materials generally show good compatibility between nanofillers and matrix. The plasticized PI particles immersed in PEEK are almost completely indistinguishable. All fracture surfaces appear to be tough, very similar to the starting blend. The composite with wollastonite shows some adhesion defects at the interface, with the larger fillers probably due to the lower dimensional uniformity of the mineral filler. The PEEK-30PI-7C130 composite has a morphology very similar to the PEEK-30PI matrix and it is distinguished only by the presence of deformations of a tough nature close to the particles, representative of a good bonding at the matrix-reinforcement interface. The comparison between the PEEK matrix and the PEEK-PI blend reinforced with 30% wt. glass fiber shows that the presence of PI negatively slightly affects adhesion to the interface. This deterioration is also noted in the FR and NS composites with N8 and TP90, albeit to a lesser extent; probably the presence of the nano fillers slightly improves the adhesion during the mixing phase. The fiber-reinforced and nanostructured composites with C130 show a compact and tough fracture surface. The adhesion of the matrix to the glass fibers seems to be improved by the presence of the nano-charge in all three formulations. These considerations on the morphology of the materials produced are consistent with the mechanical characterizations performed, confirming the good quality of the composites produced.

#### **6.1.5 Dynamic Thermo Mechanical Analysis**

The tests of thermo mechanical characterization in dynamic regime were performed with a rheometer mod. Ares by Rheometric Scientific with DMTA test grips. A dynamic thermal-mechanical analysis was carried out to study the behaviour of composite materials produced in a wide range of operating temperatures. The samples were subjected to torsional and oscillatory stress applied by the instrument through an internal motor connected to the lower clamp; the upper transducer recorded how the samples of composite material transmit the stress as the temperature increases. The temperatures range from 25 to 220 °C was considered with a ramp rate of 3 °C/min with rectangular torsion geometry and a frequency of 6.2832 rad/s. DMTA tests provide some characteristic parameters including the storage module  $G'$  related to the elastic behaviour, the loss module  $G''$  correlated to the plastic behaviour and the parameter  $\tan \delta$ . The DTMA curves of the tests performed on the nanocomposite materials are shown in **Figure 6.11a** and **Figure 6.11b**.

The results of the DMTA tests performed on nanostructured composites without FR show a general increase of the mechanical characteristics with respect to the matrix in the whole temperature range of the test. These results are coherently correlated with the Young's modules measured with the tensile tests reported in

**Figure 6.3a.**

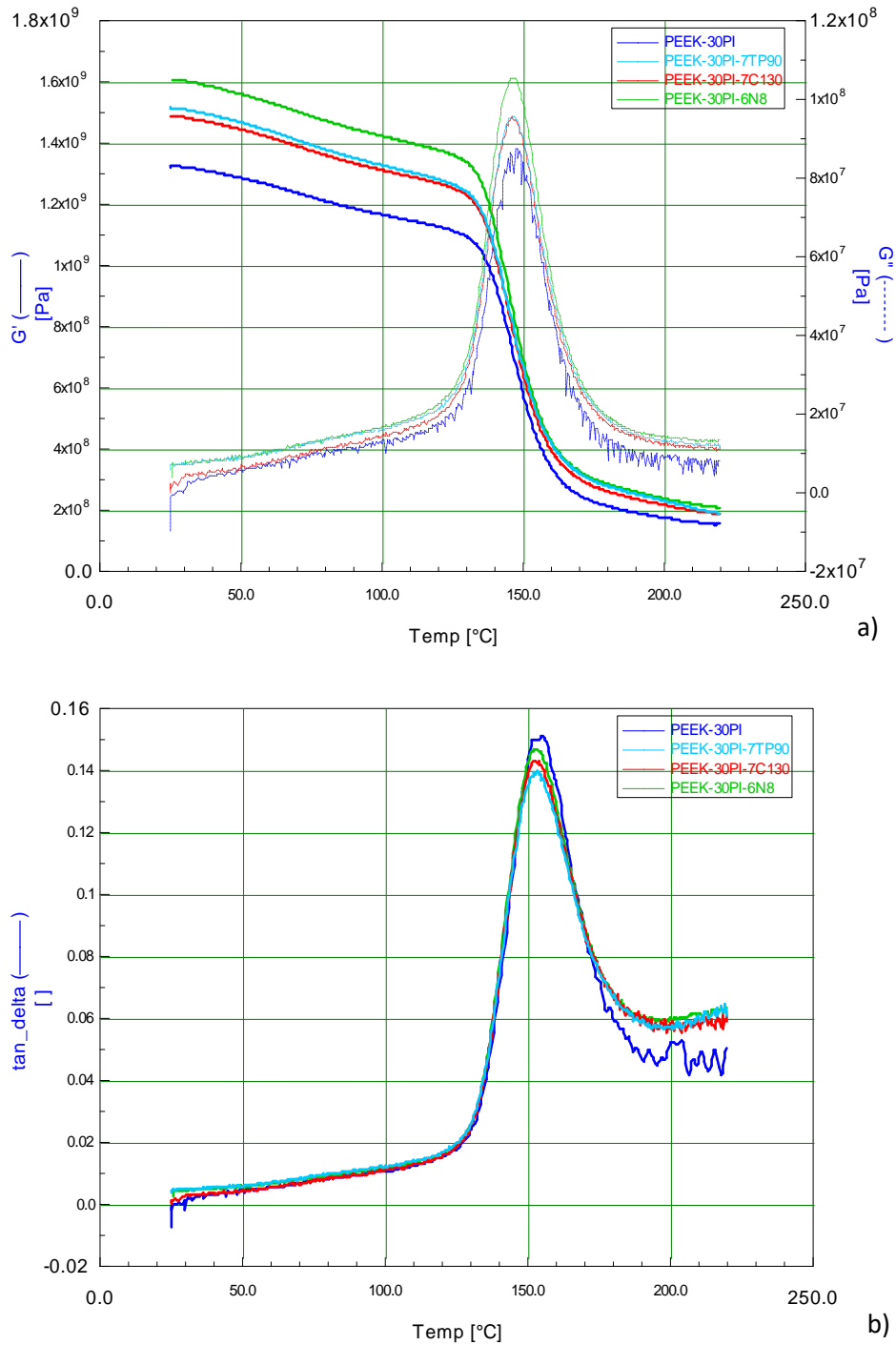


**Figure 6.11:** Graph of the DTMA curves of the nano-structured composites based on PEEK-PI:  $G'$  and  $G''$  (a) and  $\tan \delta$  (b)

The  $\tan \delta$  peaks do not show significant variations in the glass transition temperatures of the composites. In this set of composite materials, the micro-nano charge N8 appears to be the most effective for increasing the storage module. The results of this test provide indications on the interaction of the matrix blend with the nano reinforcements before the addition of the glass fibers.

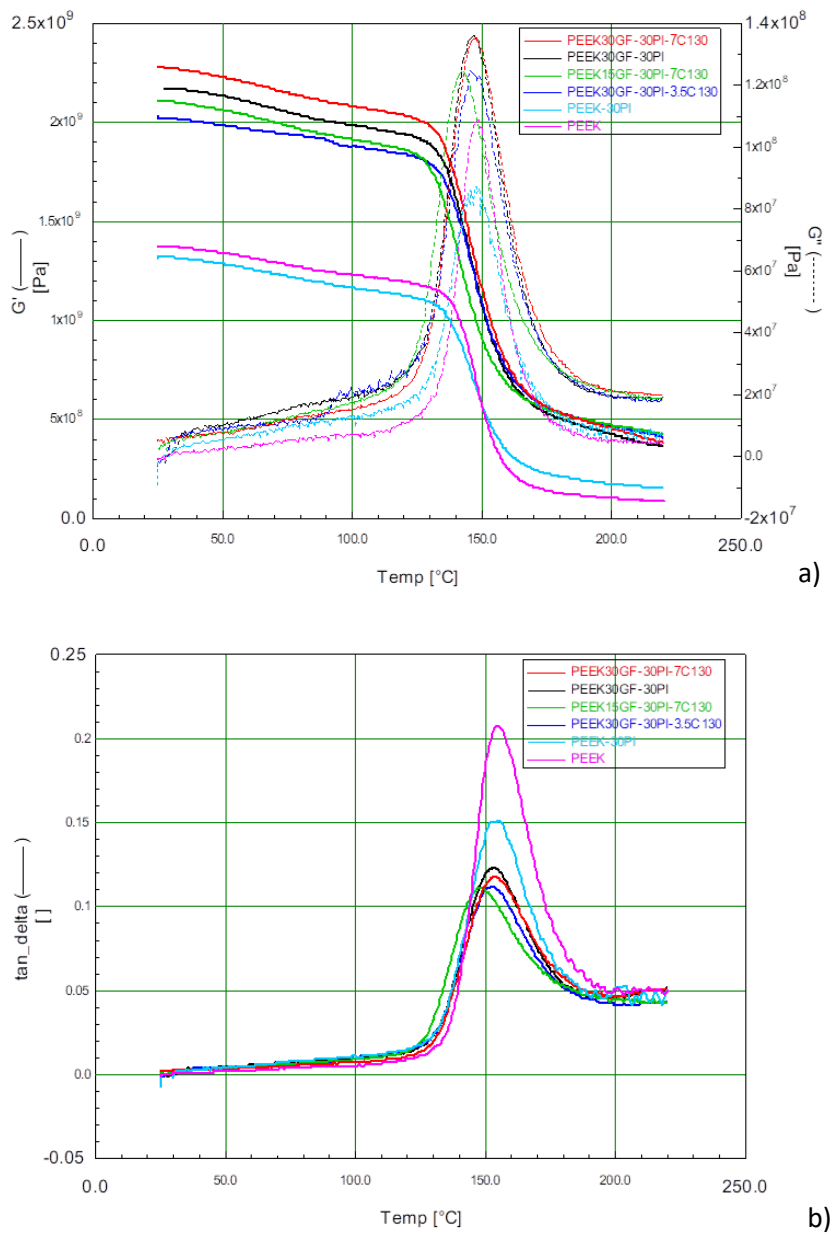


**Figure 6.12:** DTMA curves of fiber reinforced and nanostructured composites based on PEEK-PI:  $G'$  and  $G''$  (a) and  $\tan \delta$  (b)

**Figure 6.12a** and **Figure 6.12b** show the representative curves of the DTMA results for FR and nanostructured materials with C130. This comparison makes it possible to understand the effect of the presence and of the quantitative variation of the two types of reinforcement (fibrous and nanometric). The DTMA curves of the reinforced fibrous and nanostructured composites based on PEEK-PI show the effectiveness of the reinforcements in increasing the storage modulus. The improvement obtained with the composites occurs in the whole range of tested temperatures, assuming particular importance at high temperatures, as shown in **Figure 6.13**.

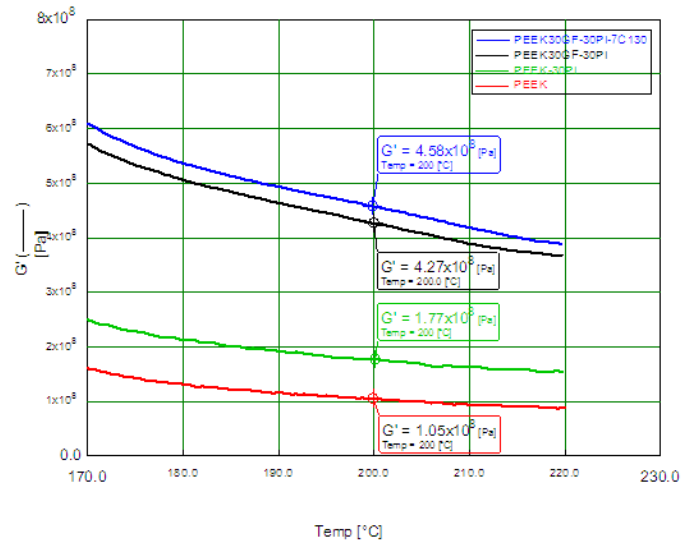


**Figure 6.13:**  $G'$  values at 200 °C obtained from the DTMA curves

With reference to **Figure 6.12a**, it is noted that below the  $T_{g_{PEEK}}$ , the formulations with the two reinforcement types show values of  $G'$  lower than the composite with only GF. However, the PEEKGF30-30PI-7C130 formulation shows values of  $G'$  higher than all other materials produced in the entire test range. This behaviour may depend on the presence of the nanofiller on the interface between matrix and fiber. From the micrographs it is noted that, even if the C130 improves adhesion to the GF surface when compared to the other two fillers, the best interface is obtained with glass fiber alone. Another reason for explaining this behaviour lies in the structure of PEEK in the presence of nanoreinforcements, that can act as nucleating agents, increasing crystallinity and /or as blocking agents of the amorphous phase, producing an intermediate amorphous rigid phase between the other two. In this case, the ratio between quantity of fiber and nanoreinforcement is decisive for achievement of a balance between the phases. In this case, the formulation PEEKGF30-30PI-7C130 seems to achieve the best balance of formulation of the composites made. Above the  $T_g$ , at high temperatures, where the amorphous phase of the matrix loses significantly mechanical properties, the effect of the nanofillers seems to prevail over the reinforcement contribution brought by the glass fibers. This behaviour seems to confirm the theory that nanofillers in PEEK contribute to form a rigid phase with mechanical properties and thermal stability higher than the amorphous phase. However, the absolute effect of the nanofillers consisting of a rigid solid phase must not be neglected.

## 6.2 References

- Parvaiz, R.M., Mohanty, S., Nayak, S.K., Mahanwar, PA (2010) Polyetheretherketone (PEEK) Composites Reinforced with Fly Ash and Mica, *Journal of Minerals & Materials Characterization & Engineering*, 9(1), 25-41.
- S. Dominguez, C. Derail, F. Léonardi, J. Pascal b, B. Brulé. Study of the thermal properties of miscible blends between poly(ether ketone ketone) (PEKK) and polyimide, *European Polymer Journal* 62 (2015) 179–185
- St, Clair, T.L. in *Polyimides* Eds. Wilson, D., Stenzenberger, H.D. and Hergenrother, P.M., 1990, Chapman and Hall, New York, pg. 58.
- Hergenrother, P.M. and Havens, S.J. in *Polyimides: Materials, Chemistry and Characterization* Eds. Ferger et. al. Elsevier, New York, 1989.

## CHAPTER 7: CALCIUM TEREPHTHALATE TRIHYDRATE SALTS (CATS)

### 7.1 Synthesis and characterization of CATS and anhydrous CATS

The positive results obtained with the composite materials based on high temperature matrices studied up to now has suggested the further search for other suitable nanofillers to be used for this study. The usefulness of nanoreinforcements has a double advantage: both for the performance aspect and from an economic point of view, contributing to lower costs and expanding the market for this class of materials. However, the identification of reinforcements suitable for the production of thermoplastic composites with high temperature matrices is rather complex.

There are many problems that must be faced to satisfy the prerogatives of using fillers. The main characteristics to be found can be summarized in thermal stability, physical-chemical compatibility with matrices, nanometric size and low cost. In order to have a good productivity, continuous processes must be used, such as extrusion, and the method used to produce the composites turns out to be melt blending; for this reason, the reinforcements must possess thermal stability up to the characteristic process temperatures for the matrices used for the time necessary for the dispersion in the melt, usually of 370-400 °C for 2-3 minutes.

In this case, the filler/matrix compatibility must be intrinsic since the traditional compatibilization treatments used for reinforcements in thermoplastic matrix composites (e.g. silanization or maleic grafting) cannot be applied, due to thermal degradation. The research must therefore be directed towards nanoreinforcements that can theoretically be mixed with matrices at high temperatures and capable of forming good quality bonds. The nanometric dimension is important to obtain the reactive phenomena characteristic of this innovative class of materials, both in terms of effectiveness on the properties of the composites and in terms of realization in the process phase. Finally, the cost of the filler is decisive for the competitiveness on the market of composite materials based on HPP matrices. Even if the costs of the matrices are so high that even the use of relatively expensive fillers is convenient, the reduction in costs is a fundamental parameter to make these materials affordable to wider industrial sectors; therefore, the realization of composites with high percentages of low cost fillers that preserve the characteristic properties is to be considered important, at least as much as the improvement of the performances.

A search was made taking into account these criteria and the family of **terephthalate salts** was found interesting, because it seemed to satisfy all the required criteria. Moreover, there are no examples in the scientific literature of these salts used for the production of thermoplastic composites. The terephthalate salts can be obtained by the reaction of terephthalic acid with different metal oxides to obtain the terephthalate salts of the metal used in the reaction. Many different



terephthalate salts, sodium, potassium, aluminium, magnesium, calcium and other metals salts may be obtained [Panasyuk et al., 2002a; Panasyuk et al., 2002b; Panasyuk et al., 2002c]. Electronic micrographs of some terephthalate salts are shown in **Figure 7.1**.

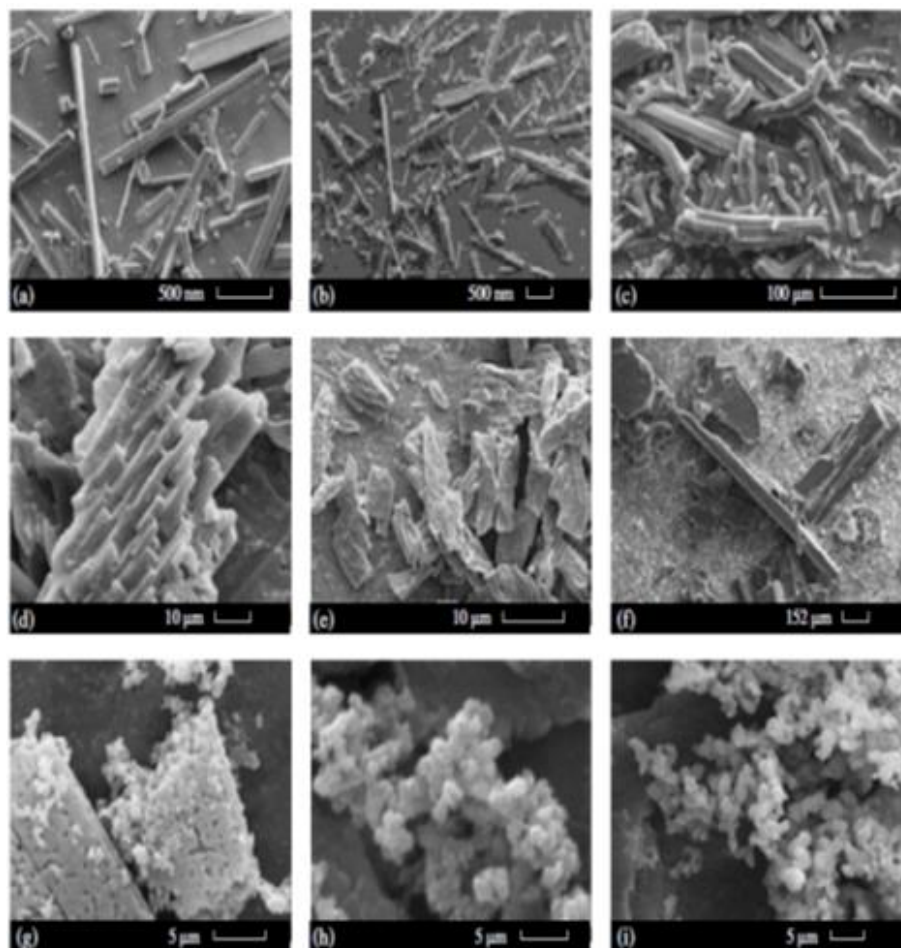


**Figure 7.1:** SEM micrographs for terephthalate salts of K (a), Na (b), Li (c), Ca (d-e) and Al (f-i)

For example, the reaction of terephthalic acid with calcium oxide in the presence of water for the production of calcium terephthalate trihydrate salts is reported in the following Formula:



*Reaction of terephthalic acid to give calcium terephthalate trihydrate salts*

Many of these salts show good thermal stability in the range of temperatures characteristic of the extrusion process of the matrices under study. **Figure 7.2** shows some graphs of thermogravimetric analysis performed on some terephthalate salts. For some it is evident the good thermal stability below 400 °C.

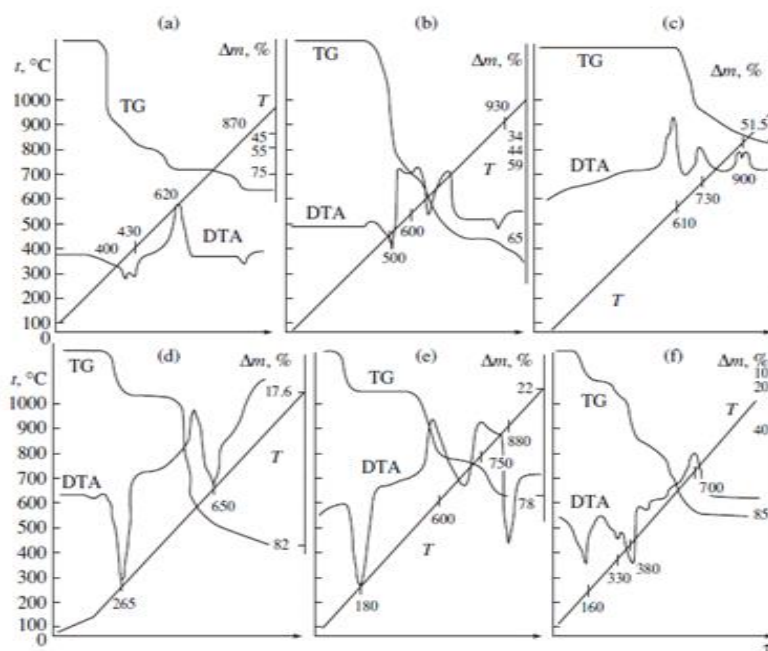


**Figure 7.2:** Thermal analysis of  $\text{NaOOC}_6\text{H}_4\text{COOH}$  (a),  $\text{KOOC}_6\text{H}_4\text{COOH}$  (b),  $\text{NaOOC}_6\text{H}_4\text{COONa}$  (c),  $\text{Mg}(\text{OOCC}_6\text{H}_4\text{COO}) \cdot \text{H}_2\text{O}$  (d),  $\text{Ca}(\text{OOCC}_6\text{H}_4\text{COO}) \cdot 3\text{H}_2\text{O}$  (e), and  $\text{Al}_2(\text{OOCC}_6\text{H}_4\text{COO})_3 \cdot 8\text{H}_2\text{O}$  (f)

The characteristic benzene ring suggests that there may be good compatibility between the terephthalate salts and the polymer molecules for temperature applications, which are also rich in stable aromatic rings. Furthermore, the bound water molecules of some salts, such as magnesium, calcium and aluminium salts, can probably offer further bonds if properly removed. In applications that use terephthalate salts for making batteries, it has been shown that nanometer crystals are used [Kaduk JA., 200; Jones et al. 2014]. The production of salts with nano-sized lamellar structure can be obtained with appropriate controls of the reaction parameters. The cost effectiveness of the materials is given by the low cost of the raw materials, the simplicity and the exothermic nature of the reaction. The acid could be obtained from the recycling processes of polyethylene terephthalate to make the system more environmentally friendly and the metal oxides as the  $\text{CaO}$ , commonly known as quicklime, are very cheap and common chemical compound, as shown in **Figure 7.3**.



**Figure 7.3:** Recycled and cheap raw materials used for the production of terephthalate salts

The calcium terephthalate salts have been selected to be used as fillers for the good thermal stability above 400 °C. The possibility of removing the bound water molecules to form bonds with the polymeric molecules and the particular structure formed by the terephthalic acid ions with the calcium ions suggests the possibility of a good compatibility, with formations of strong bonds between fillers and polymers. The structural characteristics of terephthalate calcium salts are shown in **Figure 7.4**, where the chemical bonds between the terephthalate ion, the calcium ion and the three water molecules are highlighted [Matsuzaki & Iitaka, 1972; Amin Alavi and Morsali 2011].

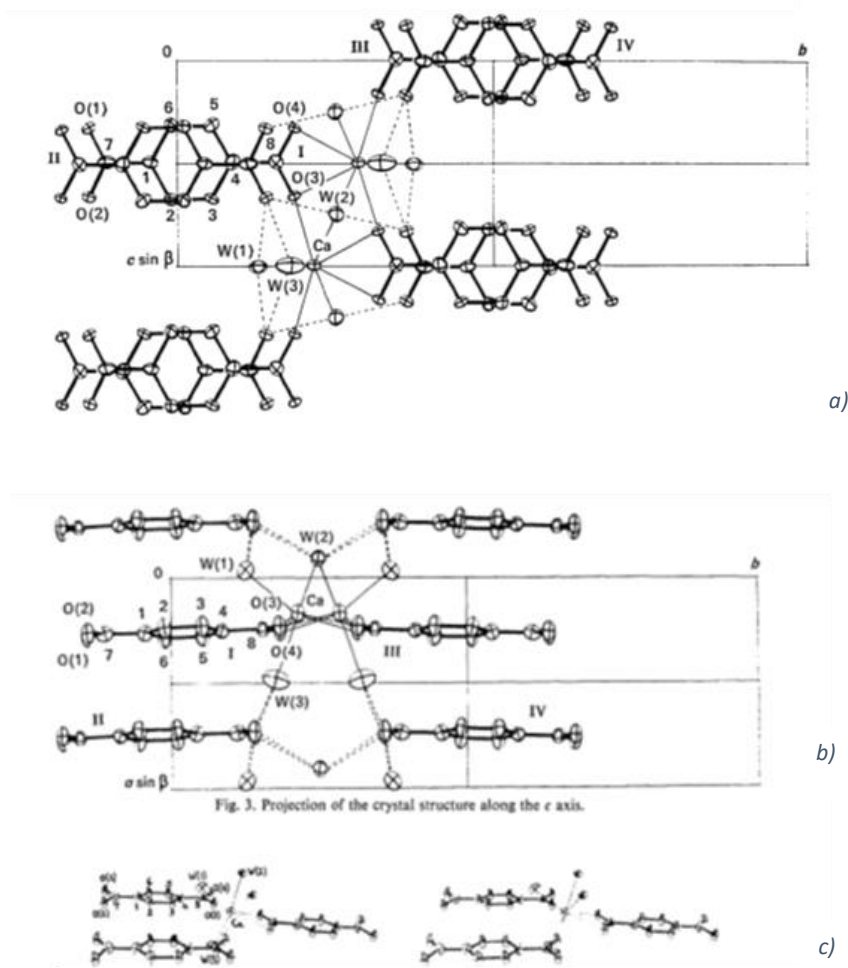


**Figure 7.4:** Projection of the crystal structure along the *a* axis. Roman numbers denote the symmetry operations I:  $x, y, z$ ; II:  $1-x, -y, 1-z$ ; III:  $x, \frac{1}{2}y, -\frac{1}{2}z$ ; IV:  $1-x, \frac{1}{2}y, \frac{1}{2}z$ . Broken lines indicate hydrogen bonds and solid thin lines indicate coordinations around calcium ions (a). Projection of the crystal structure along the *c* axis (b). Stereoscopic drawing of the crystal structure showing the coordination of the oxygen atoms around the calcium ion (c).

Another reason is the relative simplicity of the production of nanometer-sized platelets. The reaction between terephthalic acid and calcium oxide in water was carried out to produce trihydrate calcium salts terephthalate. The production process required an appropriate monitoring of reaction conditions, by acting on the kinetics and using appropriate additives to obtain the nanometric

structures. Some attempts have been made to optimize the characteristics of the fillers. Finally, calcium terephthalate trihydrate salts (CATS) were obtained by precipitation being insoluble in water. A SEM micrograph of the salts obtained with the optimized reaction parameters is shown in **Figure 7.5**. The nanometric size of the lamella thickness can be appreciated.

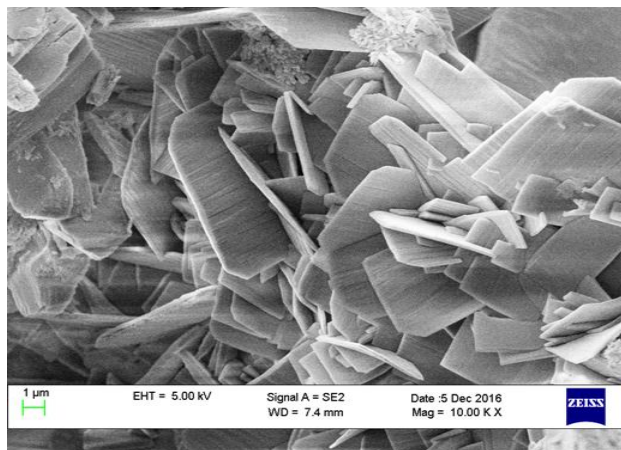


**Figure 7.5:** SEM micrograph of calcium terephthalate trihydrate salts (CATS) produced in our laboratories

In order to evaluate the thermal stability and compare the results with the values found in the literature, a thermo-gravimetric analysis was performed on the obtained salts. The salt sample was tested with dynamic TGA with a temperature ramp at 10 °C/min from 30 to 900 °C. The results of mass loss (TG) and derivative weight loss (DTG) are shown in **Figure 7.6**.

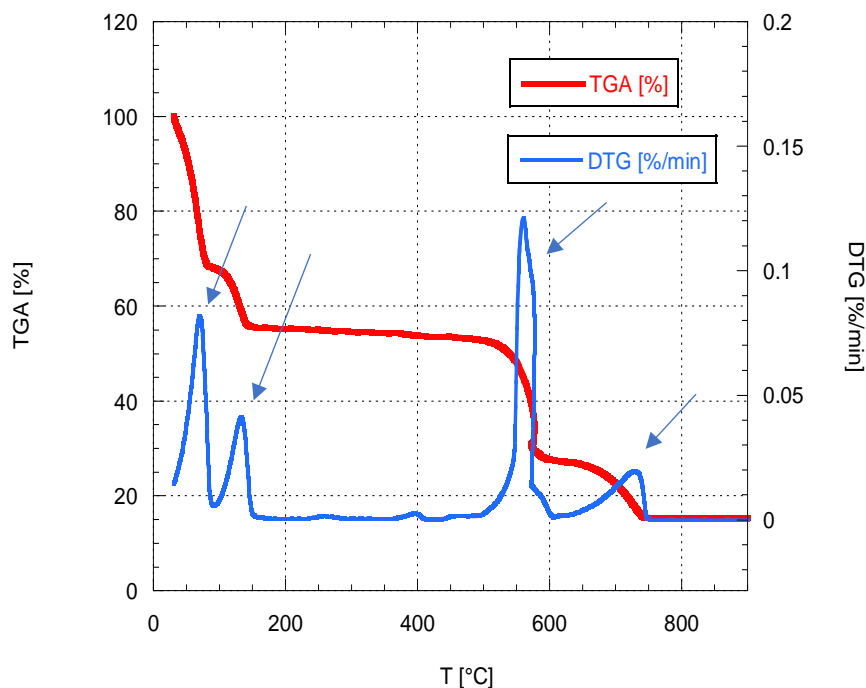


**Figure 7.6:** Results of TGA and DTG analysis on CATS samples

The four mass loss zones shown in the TG curve correspond to the four peaks highlighted in the DTG curve. The first peak, at a temperature lower than 100 °C, refers to the loss of hygroscopic water and any volatile additives present during the reaction. The second peak, at a temperature between 100 °C and 170 °C, refers to the loss of molecular water since a weight loss of 22% corresponds to three water molecules per formula unit. The decomposition of the acid salts involved the breaking of the carboxyl groups, the formation of carbonates and the release of gaseous products. The subsequent mass losses are due to thermo-oxidative destruction of organic ligands and subsequent oxidation of the residue over 600 °C.

FTIR measurements (**Figure 7.7a**) of CATS salts before and after dehydration confirmed the results already reported in the literature (**Figure 7.7b**): absence of characteristic absorption peaks of terephthalic acid ( $C_8H_6O_4$ ) (e.g.  $1671\text{ cm}^{-1}$  and  $1420\text{ cm}^{-1}$ ) demonstrates a complete reaction in our synthesis procedure. Strong bands at  $1557$  and  $1437\text{ cm}^{-1}$  are assigned to asymmetric and symmetric stretching vibration of carbonyl groups, respectively. Bending vibration of  $\delta(\text{Ca-O})$  presents a band at  $515\text{ cm}^{-1}$ . The bands of  $\delta(\text{Ca-O})$  in  $\text{CATS} \cdot 3\text{H}_2\text{O}$  at  $515\text{ cm}^{-1}$  splits into double peaks ( $530\text{ cm}^{-1}$  and  $504\text{ cm}^{-1}$ ) in CATS, presumed that the coordination environmental for  $\text{Ca}^{2+}$  is changed [Mou et al, 2015 Wang et al. 2015; Mazaj et al. 2013].

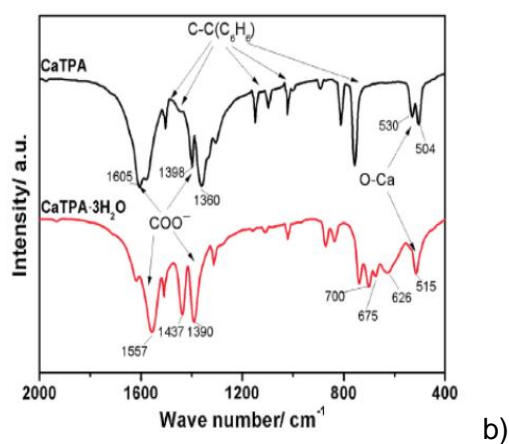
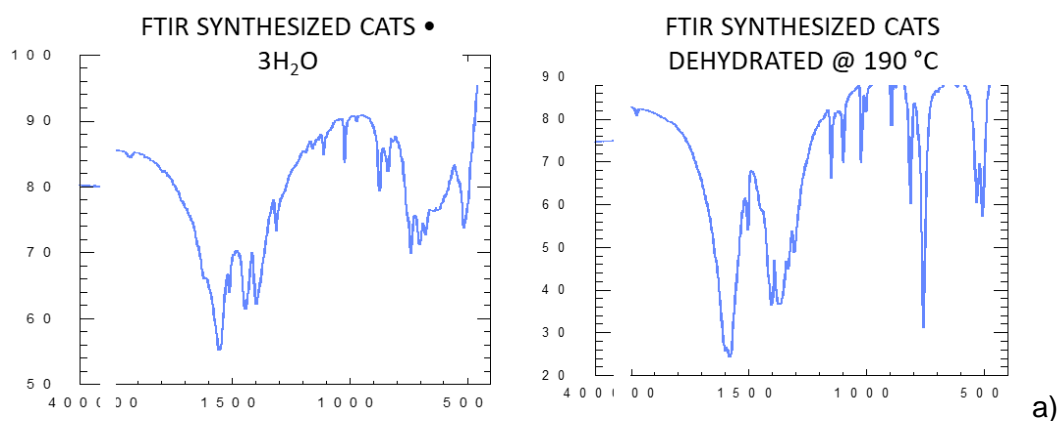


**Figure 7.7:** Infrared spectra of  $\text{CATS} \cdot 3\text{H}_2\text{O}$  and CATAS (a) and  $\text{CaTPA} \cdot 3\text{H}_2\text{O}$  and  $\text{CaTPA}$  (b)

Morphologies of CATS · 3H<sub>2</sub>O and CATAS powders are also included (**Figure 7.8**), confirming the nature of the obtained salts: it can be seen that CATS · 3H<sub>2</sub>O has a plate shape with smooth surface and the thickness of the plate is about 50 nm. After the dehydration (T>190°C), the anhydrous salts have cracks with rough surface, revealing that volume contraction happens in the hydration process. Approaching T=450°C, it is visible that the salt morphology still remains unaltered, so it is reasonable to use these nanofillers in a high temperature melting polymers. Only after 500°C, as already commented in TGA analysis, the fillers started to degrade and a visible change in morphologies (from platelets to particles) can be found.

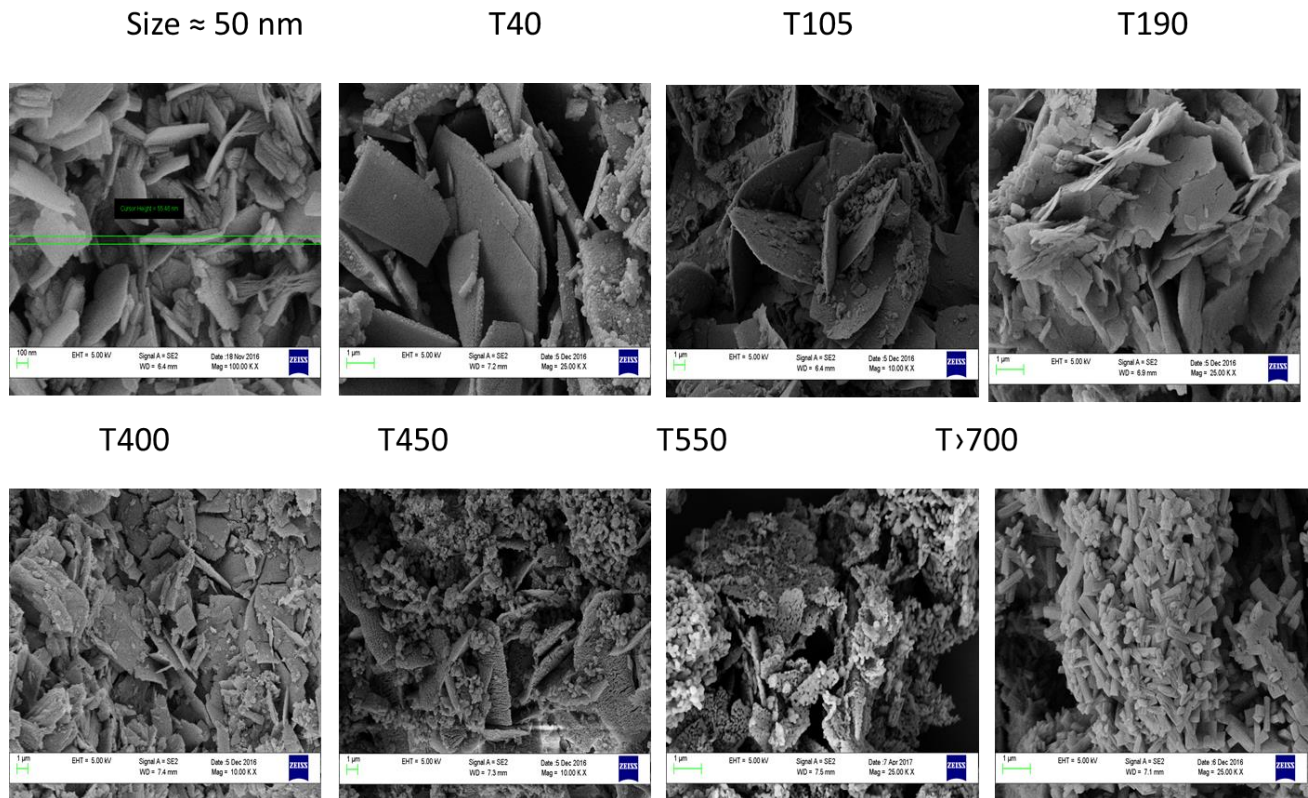


**Figure 7.8:** FESEM morphologies of CATS · 3H<sub>2</sub>O (T 105) and CATAS (from T190 up to T > 700)

## 7.2 References

- T. Matsuzaki and Y. Iitaka. *Acta Cryst.* (1972). B28, 1977-1981 - Mou, C., Wang, L., Deng, Q. et al. *Ionics* (2015) 21: 1893. - Liping Wang, Chengxu Mou, Yang Sun, Wei Liu, Qijiu Deng, Jingze Li. *Electrochimica Acta*, Volume 173, 2015, Pages 235-241.
- Matjaž Mazaj, Gregor Mali, Mojca Rangus, Emanuela Žunkovič, Venčeslav Kaučič, and Nataša Zabukovec Logar, 2013, *J. Phys. Chem. C*, 117 (15), pp 7552–7564
- Mohammad Amin Alavi, Ali Morsali Chapter 9 Alkaline-Earth Metal Carbonate, Hydroxide and Oxide Nano-Crystals Synthesis Methods, Size and Morphologies Consideration, *Nanotechnology and Nanomaterials* » "Nanocrystal", book edited by Yoshitake Masuda, ISBN 978-953-307-199-2, Published: June 28, 2011
- Panasyuk, G.P., Mishal Khaddaj, Privalov, V.I., and Miroshnichenko, I.V., *Plast. Massy*, 2002, no. 2, pp. 27–31.
- Panasyuk, G.P., Azarova, L.A., Budova, G.P., and Izotov, A.D., *Inorg. Mater. (Engl. Transl.)*, vol. 38, no. 4, pp. 385–389].
- Panasyuk, G.P., Azarova, L.A., and Mishal Khaddaj, *Structural Transformation of Terephthalic Acid in Water Fluids*, *Proc. VIII Meet. on Supercritical Fluids*, 2002, p. 225.
- Panasyuk, G.P., Azarova, L.A., Khaddaj, M. et al. *Inorganic Materials* (2003) 39: 1292.
- Kaduk JA. *Acta Crystallogr B*. 2000 Jun;56 (Pt 3):474-85.
- Peter G. Jones, Jerzy Ossowski, Piotr Kus, and Ina Dix. *Zeitschrift für Naturforschung B*. Published Online: 2014-06-02 Three Crystal Structures of Terephthalic Acid Salts of Simple Amines

## CHAPTER 8: NANOSTRUCTURED AND FIBER REINFORCED COMPOSITES WITH TEREPHTHALATE SALTS

### 8.1 Composites based on PEEK

Terephthalate calcium salts (CATS) have been used to make new nanostructured composites. In the previous chapter, it was shown that, it is necessary to carry out a heat treatment to eliminate the molecular water and then obtain calcium terephthalate anhydrous salts (CATAS). In order to understand the effect of CATAS, a first study was carried out by using PEEK as a reference matrix. Assuming good compatibility between matrix and filler, it was decided to produce composite samples with 10, 20 and 30% of CATAS reinforcement. Using a semi-crystalline matrix, it was decided to study also the possible effects on the crystallinity of the matrix. In fact, some nanofillers have a nucleating effect on the semi-crystalline structure, increasing the value of  $X_c$  and improving some correlated properties. The ordered crystalline structure has higher thermal and mechanical properties than the random molecular arrangement of the amorphous phase. Moreover, the fillers, especially if of nanometric size, can modify the semi-crystalline structure, going to increase the transition zones between the amorphous phase and the crystalline rigid phase. This intermediate phase is called the rigid amorphous phase (RAF) and produces an improvement of the thermo-mechanical properties when it replaces the amorphous phase. **Figure 8.1** shows a typical arrangement of polymer chains in a semi-crystalline polymer.

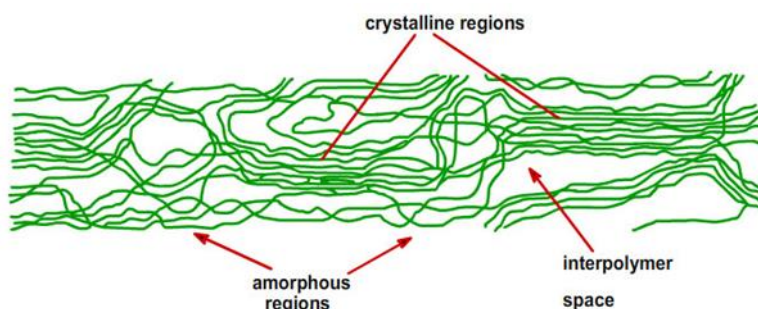
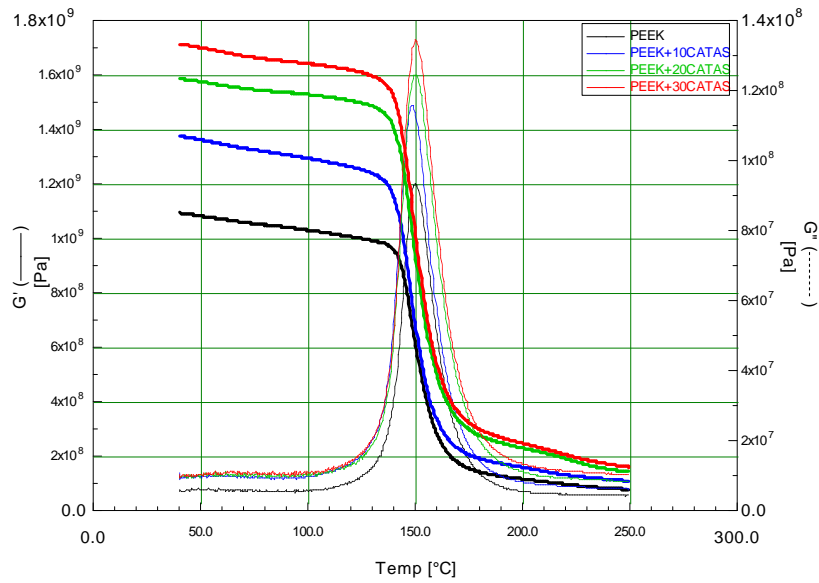


**Figure 8.1:** Arrangement of polymer chains in a semi-crystalline polymer as PEEK

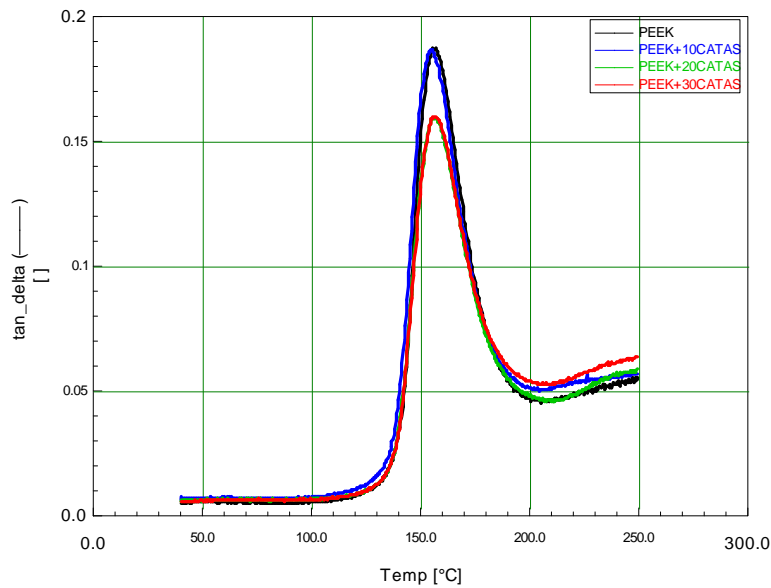
A thermomechanical characterization with DMTA was performed to evaluate the behaviour of the new composites with respect of PEEK. In order to make a comparison with the other nanostructured materials, the tests were carried out with the same parameters previously considered. The results are shown in form of a graph in **Figure 8.2a** and **Figure 8.2b**. The graphs show that, as the quantity of CATAS increases, there is a progressive increase of the storage module  $G'$ . This trend is maintained throughout the test temperature range. However, there are no variations on the peaks of the tan delta curves, which indicate changes in the glass transition temperatures; the  $G''$  module



also remains substantially unchanged, even if it respects the progressive growth with the increase in the percentage of nanofiller.



a)



b)

**Figure 8.2:** Results of DMTA test on CATAS reinforced composites:  $G'$  and  $G''$  (a) and  $\tan \delta$  (b)

In order to have a numerical comparison, in **Figure 8.3** the values of the  $G'$  modules at 100 °C and 200 °C for the matrix and the nanostructured composites with 10, 20 and 30% of CATAS were reported. The choice of these two temperatures also makes it possible to evaluate the effect of the reinforcements below and above the  $T_g$ , with the main aim of clarifying their influence on the amorphous phase of the matrix.

**Table 8.1:** Values of  $G'$  at 100 °C and 200 °C of PEEK-CATAS nanostructured composites

NANOCOMPOSITE		$G'$ [MPa] @100°C	$G'$ [MPa] @200°C	% $\Delta G'$ 100 vs PEEK	% $\Delta G'$ 200 vs PEEK
PEEK		1.03E+09	1.15E+08		
PEEK	10CATAS	1.29E+09	1.59E+08	+25.24	+38.26
PEEK	20CATAS	1.53E+09	2.29E+09	+48.54	+99.13
PEEK	30CATAS	1.64E+09	2.48E+09	+59.22	+115.65

The calculated  $G'$  values have been reported in **Table 8.1** and the percentage variation of the storage module has been calculated. From the table, it can be seen that at 100 °C the presence of nanoreinforcement produces an increase in the value of  $G'$  which varies from 25% with 10% by weight of CATAS, an increase of about 48% with the intermediate amount of filler, up to an improvement of almost 60% for the PEEK-30CATAS formulation. The effect of nanofillers on  $G'$  values measured at 200 °C is even more relevant. Above the PEEK  $T_g$ , where the amorphous phase contributes in a reduced way to the mechanical properties, the  $G'$  increments of the composites with the three percentages of CATAS are respectively 38%, 99% and 115% with respect to the matrix. The noticeable improvement of  $G'$  over the PEEK  $T_g$  suggests that there has been a variation involving the amorphous phase. Other possible causes of thermo-mechanical variations could be sought in the possible nucleating effect of the nanofillers that cause a variation of crystallinity degree.

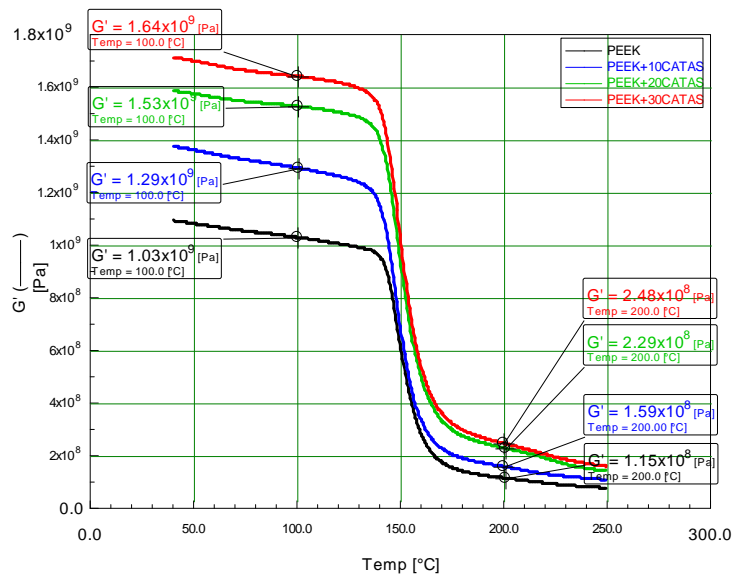


**Figure 8.3:** Values of the  $G'$  modules of CATAS composites at 100 °C and at 200 °C

To better investigate this phenomenon, a thermal characterization with DSC instrument was performed. A first heating, cooling and second heating scans cycle was carried out between 25 and 400°C at 10 °C/min for matrix and composites. The second heating was performed to guarantee that the materials have the same “thermal history” and that the crystallization phenomena depend only on the different formulations. The degree of crystallinity  $X_c$  was calculated using as a melting heat reference value for a 100% crystalline PEEK of  $\Delta H_m^0 = 130$  J/g. The evaluation of the amorphous phase was made considering a value of the thermal capacity variation for a 100% amorphous PEEK of  $0.350 \text{ Jg}^{-1}\text{K}^{-1}$ . This value was obtained considering a not-amorphous phase  $X_{f_{\min}} \approx 0.12$  at the maximum degree of quenching equal to  $\Delta C_p \text{ MAX} = 0.308 \text{ Jg}^{-1}\text{K}^{-1}$  for a PEEK quenched in liquid nitrogen. We considered:

$$X_c = \Delta H_m / \Delta H_m^0 ; \quad X_f = 1 - (\Delta C_p / \Delta C_p^a) ; \quad X_{raf} = (X_f / w_{\text{peek}}) - X_c ; \quad w_{\text{peek}} = 1 - \% \text{wt. filler}$$

*Formulas used for the calculation of the phases in nanostructured composites with CATAS*

**Figure 8.4** shows the results of the scan for a PEEK matrix and for a composite with 30% of CATAS, where the values of the phases for all the transformations have been calculated.

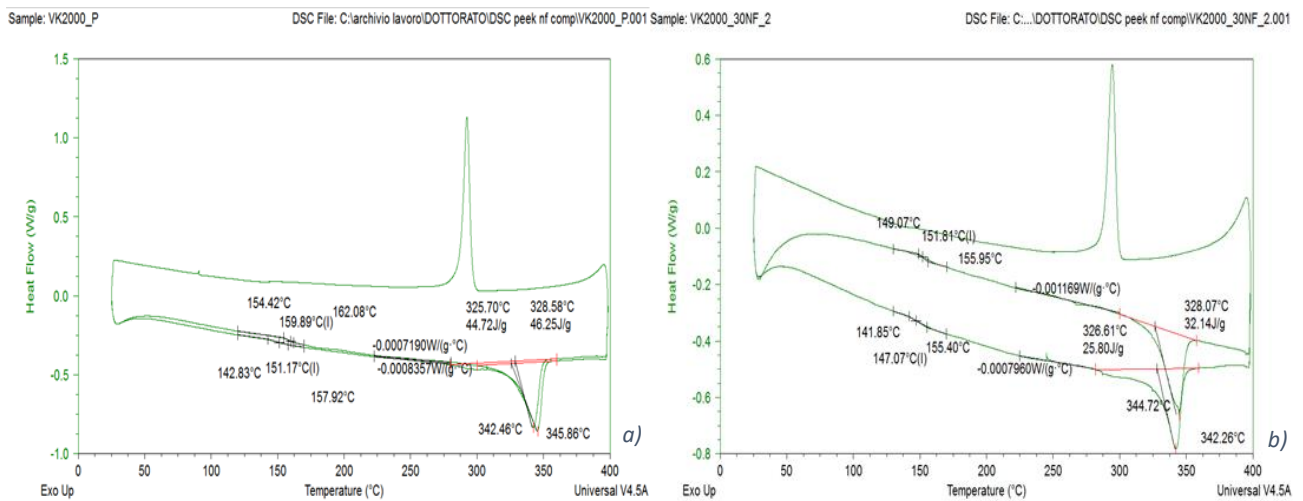


**Figure 8.4:** DSC scan for evaluation of rigid amorphous phase of PEEK (a) and PEEK-30CATAS (b) composites

The results of the calculations for amorphous, crystalline and amorphous-rigid phases fractions are reported in **Table 8.2**. The reported values show that, even at the first heating, where the thermal history related to the production of the material influences the crystallization kinetics, a more elevated fraction of the rigid amorphous phase with respect of amorphous phase can be measured [Vasconcelos et al., 2010; Jonas and Ivanov, 1998].

**Table 8.2:** Evaluation of the phase fractions obtained from the DSC analysis of the PEEK matrix and of the composite with 30% of CATAS

SAMPLE	HEATING	Xc	Xa	Xraf
PEEK	I° heating	0.357	0.472	0.171
	cooling	0.346	0.463	0.191
	II° heating	0.356	0.520	0.124
PEEK-30CATAS	I° heating	0.353	0.396	0.251
	cooling	0.366	0.122	0.513
	II° heating	0.369	0.171	0.459

This trend is also confirmed for the crystallization during the cooling cycle, where it becomes more marked. The most consistent information is obtained from the fractions calculated for the second heating, where the trend is confirmed. A reduction in the amorphous phase, which becomes blocked, giving rise to a consistent fraction of a rigid amorphous phase, is observed. It can be noted that, on the second heating scan, a substantial inversion of the relationship between Xa and Xraf is achieved, passing from PEEK to PEEK-30CATAS. The crystalline fraction undergoes a very slight increase with the addition of terephthalate salts, confirming the nucleating effect of these fillers negligible. The evaluation of phase fractions on composites with 10 and 20% of nanometric salts gave similar results, with lower Xraf fractions compared to PEEK-30CATAS [Lee and Kim, 1996].

The morphology of the fractured surfaces for the composite materials was observed with a field emission electronic microscope mod. Supra 25 of Zeiss. For each material three micrographs at 500, 5000 and 25000 magnifications have been reported in **Figure 8.5**.

Micrographs show uniform fracture surfaces with homogeneous dispersion of nanometer-sized fillers. A wide heterogeneity of salts is observed, probably due to the fracture during compounding, however most of the fillers still have a lamellar appearance. With 30% of CATAS a good filling is achieved but the composite does not seem to have reached full saturation.

Because of these positive results it was decided to evaluate the effect of CATAS also together with the use of reinforcing fibers. It has been hypothesized that these nanofillers could go to form a rigid amorphous phase that could distribute the tensions of the crystalline and fiber-reinforced zones in a more progressive way up to the predominantly amorphous zones. Moreover, it has been seen that during the process the CATAS did not produce sensible variations in the viscosity of the polymer melt, suggesting its use in synergy with the other nano fillers which had reached limit quantities in the previously optimized formulations.

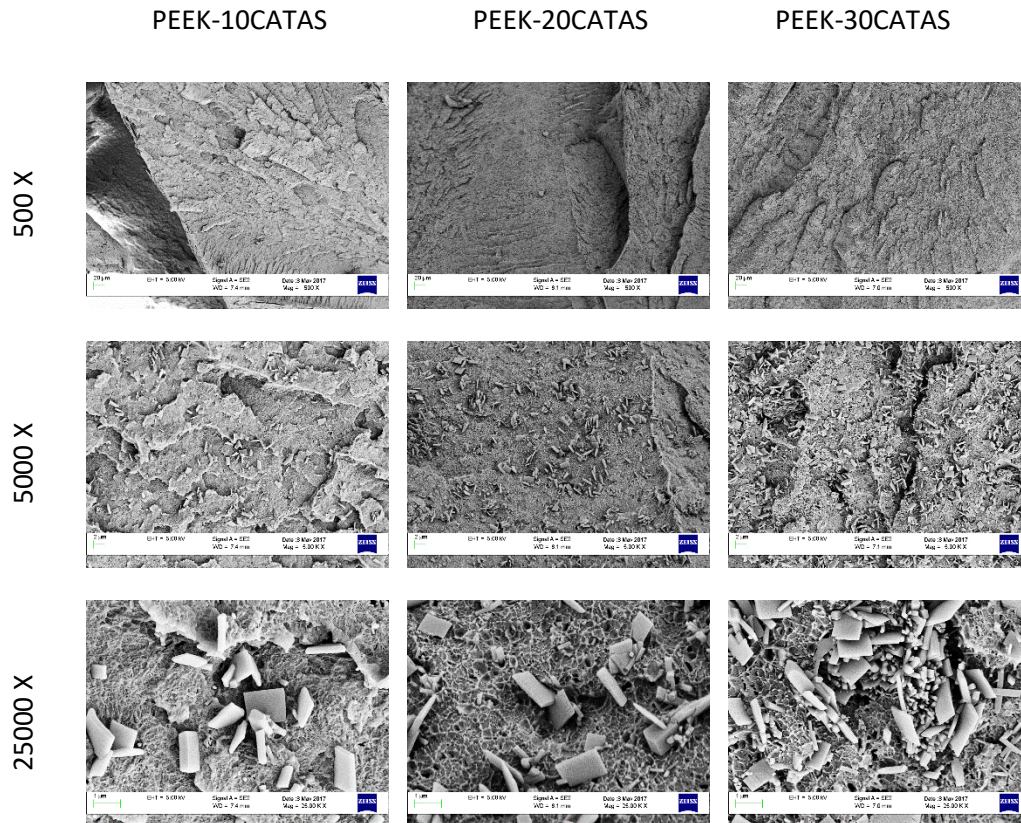


**Figure 8.5** Micrographs of the fragile fracture surface on sample of composites with CATAS

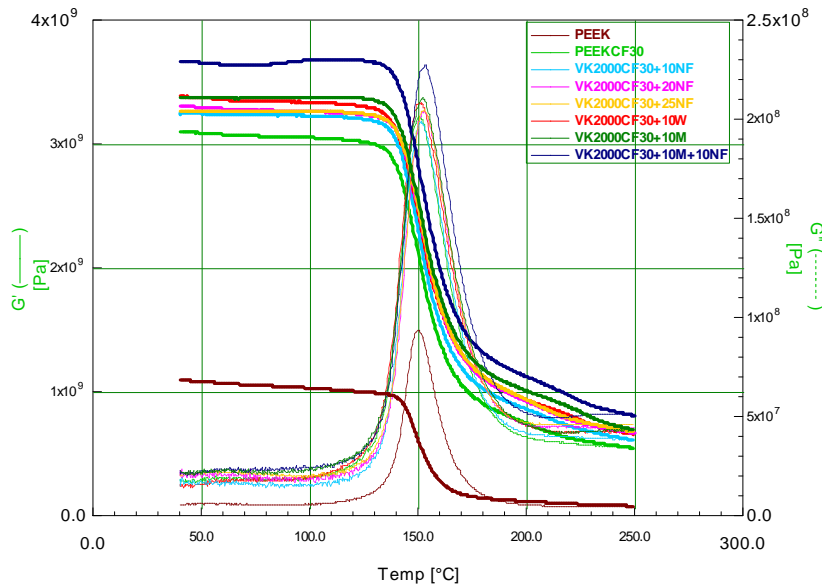
## 8.2 Effect of CATAS on hybrid FR and NS composites

Some composites were reinforced with carbon fiber and nanostructured with CATAS to evaluate the synergistic effect of the two reinforcements on the thermo-mechanical properties of the materials. Thanks to the facilitating behaviour of the extrusion process of calcium terephthalate salts, it was possible to add the salts also to the previously formulated formulation with 30% of CF and 10% of P5B, which seemed to have reached the viscosity limits for the processability. The list of formulations of hybrid composites reinforced with carbon fiber and with CATAS and other nano-reinforcements is shown in **Table 8.3**.

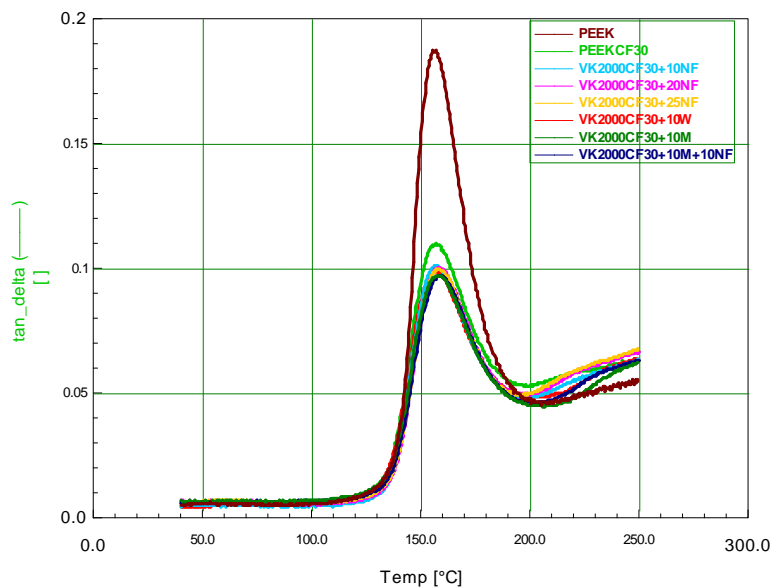
**Table 8.3:** New hybrid composite formulations with carbon fiber and CATAS

MATRIX	FIBER REINFORCEMENT [%] wt.	NANOFILLER 1 [%] wt.	NANOFILLER 2 [%] wt.	SAMPLE NAME
PEEK	30CF	10CATAS	---	PEEK30CF10CATAS
PEEK	30CF	20CATAS	---	PEEK30CF20CATAS
PEEK	30CF	25CATAS	---	PEEK30CF25CATAS
PEEK	30CF	10CATAS	10 P5B	PEEK30CF10CATAS10P5B

The samples of materials made with the formulations reported in **Table 8.3** and the related reference materials were produced and tested with DMTA using the same parameters previously set. The curves obtained by DMTA characterization are shown in the graph in **Figure 8.6a** and **Figure 8.6b**. The graph also shows the curves of the reference materials and of the two best carbon-fibers reinforced and nanostructured composite materials described in Chapter 5.



a)



b)

**Figure 8.6:** Graph of the DMTA curves of the carbon fiber reinforced and nano-structured composites based on PEEK:  $G'$  and  $G''$  (a) and  $\tan \delta$  (b)

**Figure 8.6a** shows that the carbon fiber reinforcement increases twice the value of the storage module with respect to the PEEK matrix below the  $T_g$  and that this increase is even greater at higher temperatures. Since 30% by weight of carbon fiber approaches an upper limit for a thermoplastic

material for injection, the use of nanocarriers provides the possibility of improving performance decreasing the matrix content. However, there is a limit beyond which even the nano reinforcements have no effect or can be harmful. All nano reinforcements shown in Figure 8.5 produce an increase in  $G'$  compared to PEEK30CF. The DMTA curves of the composite materials made with 30CF and 10, 20 and 25% wt. of CATAS show that, by passing from 10 to 20% of salts, there is an increase of  $G'$ , while there are no substantial differences between storage moduli of 20 and 25%wt. of nanofiller. Probably these quantities represent an upper limit for the use of CATAS in PEEK reinforced with 30% of CF. The optimized formulations discussed in Chapter 5 realized with 30% of CF and 10% of N8 or 10% of P5B show higher  $G'$  values compared to FR and NS composites with CATAS. However, the use of greater quantities of wollastonite or mica was harmful with 30% of CF. By considering the easy processability of CATAS, it was possible to produce a composite with 30% carbon fiber, 10% P5B and 10% CATAS. The DMTA curve of the storage module of this material shows a double increase compared to that produced by previously optimized CF and NS formulations. This result suggests that terephthalate salts can also be used as complementary materials in reinforced fibrous and nanostructured composites.

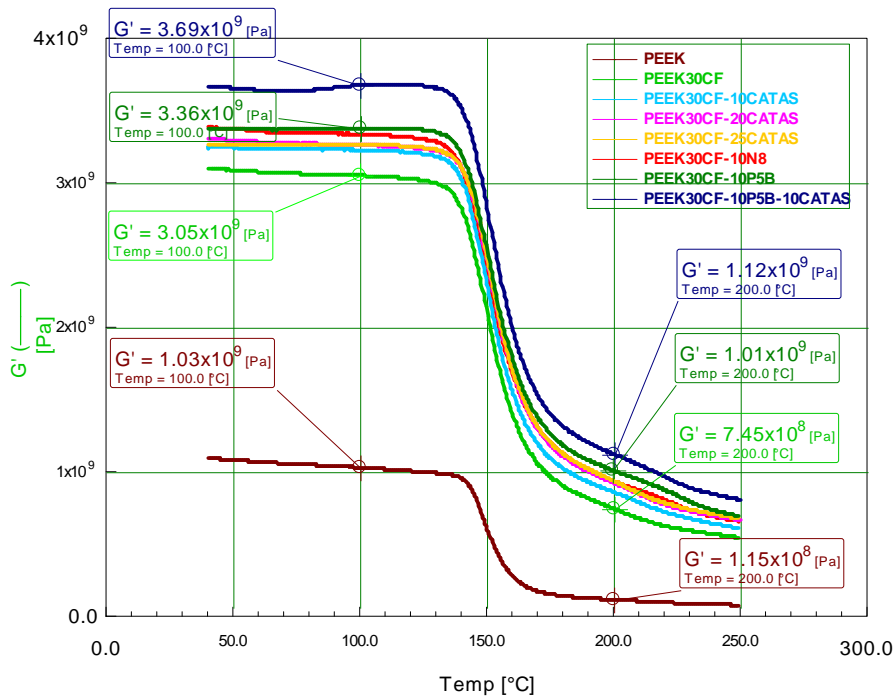


**Figure 8.7:** Graph of the DMTA curves with values of  $G'$  at 100 °C and 200 °C

**Figure 8.7** shows the values of  $G'$  at 100 °C and at 200 °C for the two benchmark materials and for the two best reinforced composites with 30% of CF and nanostructured with 10% P5B and with 10% P5B-10% CATAS. The measured  $G'$  values are shown in **Table 8.4** and compared with the benchmark materials.

From **Table 8.4**, it can be seen that at 100 °C the G' value of the composites undergoes an increase of over 200% compared to PEEK. At this temperature, the addition of mica increases the storage module by 10% compared to the material reinforced with only carbon fibers. The formulation with the P5B and CATAS fillers produces a further increase of over 20% compared to PEEK30CF. At 200 °C, the effectiveness of the reinforcements is even more important, since a 35% increase is obtained with the P5B charge and 50% with the synergistic use of nano-mica and calcium terephthalate anhydrous salts. **Table 8.5** summarizes the weight content of reinforcements used in composites, which correspond to reduced matrix costs.

**Table 8.4:** G' values of DMTA at 100°C and at 200°C for CF and nanostructured (NS) composite materials compared to the matrix

COMPOSITE				G' @100°C [MPa]	G' @200°C [MPa]	% ΔG' 100 vs PEEK	% ΔG' 100 vs PEEK30CF	% ΔG' 200 vs PEEK	% ΔG' 200 vs PEEK30CF
PEEK				1.03E+09	1.15E+08				
PEEK	30CF			3.05E+09	7.45E+08	+196.1		+547.8	
PEEK	30CF	10P5B		3.36E+09	1.01E+09	+226.2	+10.16	+778.3	+35.57
PEEK	30CF	10P5B	10CATAS	3.69E+09	1.12E+09	+258.3	+20.98	+873.9	+50.34

**Table 8.5:** summary of the reinforcing weight content in the produced composites

COMPOSITE				CF [%] wt.	P5B [%] wt.	CATAS [%] wt.	TOTAL REINFORCEMENT % wt.
PEEK				0	0	0	0
PEEK	30CF			30	0	0	30
PEEK	30CF	10P5B		30	10	0	40
PEEK	30CF	10P5B	10CATAS	30	10	10	50

The presence of large quantities of reinforcements positively affects the final price of the material. In fact, if we consider a cost for PEEK MATRIX 80 ÷ 100 € / Kg, carbon fiber of 9 ÷ 11 € / Kg, P5B of 8 ÷ 12 € / Kg and CATAS of 1 ÷ 2 of € / Kg, we can make an estimation of the cost savings for raw materials. We can consider that the preparation of the composites could be carried out in a single step, the cost of the process itself can be neglected. A cost estimation could be given by the cost reduction of around 26% for the PEEK30CF. The use of 10% of nano-mica along with 30% of carbon fiber would lower costs by about 35% and the simultaneous use of reinforcements in the formulation PEEK30CF10P5B10CATAS would result in a cost saving of 45%.



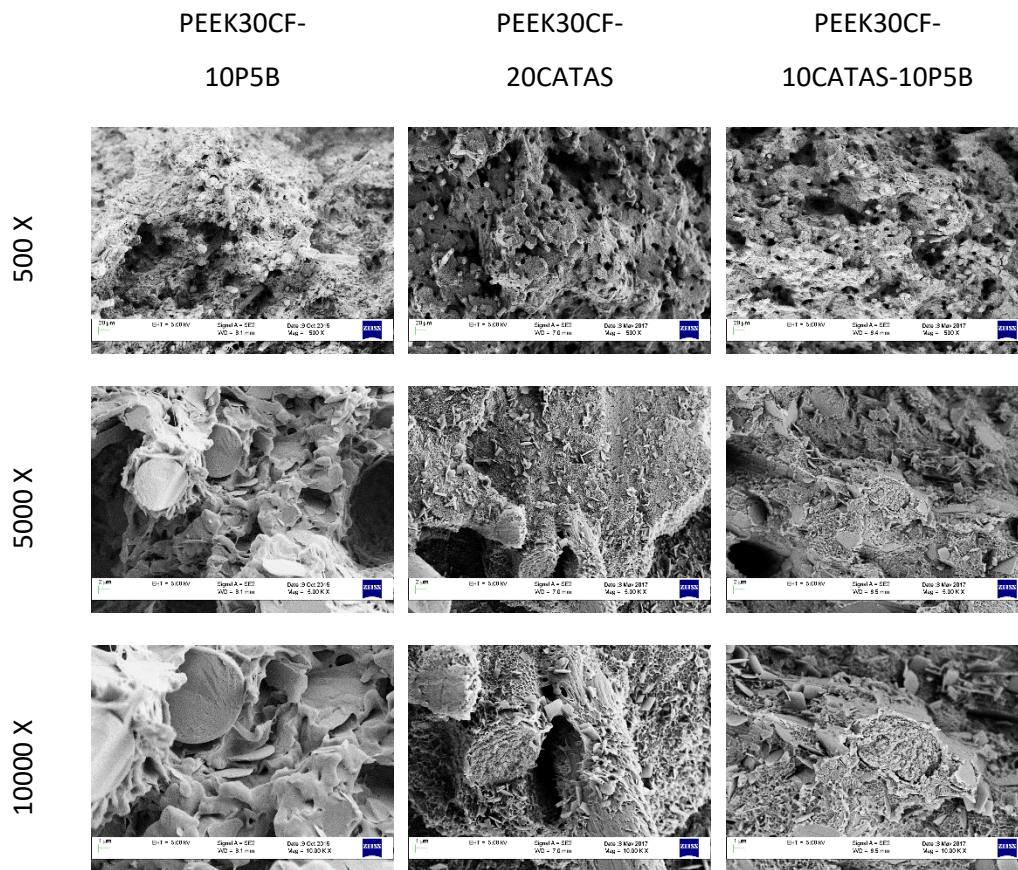


**Figure 8.8:** Micrographs of the fragile fracture surface on sample of composites with P5B and CATAS

**Figure 8.7** shows that the use of 30% wt. glass and carbon reinforcing fiber significantly increases the storage moduli of composite materials. It is seen that the complementary use of 10% and 20% wt. of terephthalate salts with 30% wt. of CF produces a further increase in the  $G'$  values in the whole temperature range. The values of  $G''$  remain substantially unchanged, although a slight increase is noted for the formulations with the highest quantities of reinforcements. The values of  $G'$  remain substantially unchanged, although a slight increase is noted for the formulations with the highest quantities of reinforcements. Variations in the displacements of the  $\tan \delta$  peak on the abscissa of temperatures are negligible, indicating that no variation occurred on the glass transition temperature of the composite materials, respect to the  $T_g \approx 167^\circ\text{C}$  of the matrix.

The morphology of the fractured surfaces for the composite materials (**Figure 8.8**) was observed with a SEM mod. Supra 25. For each material three micrographs at 500, 5000 and 10000 magnifications have been reported. Micrographs show fracture surfaces with homogeneous dispersion of nanometer-sized fillers. We observe an excellent adhesion between the matrix and the surface of the fibers in which the nanofillers participate in a cohesive manner. the lamellar morphology of both P5B and CATAS can be observed, the latter being slightly smaller in size.

Observed as a whole, the micrographs represent the appearance of fiber-reinforced and nanostructured composite materials with good interface compatibility, with good uniformity of reinforcement distribution and substantially effective.

### 8.3 Composites based on PBI / PEK

Considering the results in terms of improvement of mechanical properties and potential cost savings achievable with the use of treated reinforcements, it was decided to carry out another study with a dual objective of cost savings and improvement of performances. Currently, one of the best performing commercial product lines, based on thermoplastic matrix for extreme applications, is distributed by PBI Performance Products with in the name of Celazole. It is based on a polymer blend of PBI/PEEK and it is also supplied in grades containing reinforcing fiber. Given the high performances that make it suitable for exceptional applications and the consistent cost of the polymeric matrices used, this material is sold at high prices. An alternative material to Celazole is the Gazole produced by Gharda Chemicals. Gazole, based on a mixture of polyetherketone (PEK) and polybezimidazole, has a slightly lower cost than Celazole, but it is also less performing [Williams et al. (1986) Compositions Of Aromatic Polybenzimidazoles And Aromatic Polyimides Or Aromatic Polyetherimides, EPA 87301367.6; Musto et al., 1991; Goodwin and Simon, 1996; -].

The aim of the study is the realization of a nanostructured material with PBI/PEK with improved properties and reduced costs [Dawkins et al. 2013; Hopkins et al., 2013; <http://www.ghardaplastics.com>]. By reducing the gap between performance and increasing cost savings, this material could provide a convenient alternative to Celazole. After the preliminary thermal characterization with DSC and TGA, that allowed to establish the process parameters, the samples of PEK / PBI materials reported in **Table 8.6** were produced with melt compounding and injection moulding, similarly to the materials based on PEEK/PBI. The samples were subjected to DMTA tests in the temperature range from 40 to 250 °C, keeping the other test parameters unchanged compared to the tests carried out on the other produced materials.

**Table 8.6:** Formulations of samples produced based on PEK / PBI

MATRIX	FIBER REINFORCEMENT [%] wt.	NANOFILLER [%] wt.	SAMPLE NAME
PEK/PBI			PEK/PBI
PEK/PBI	30GF		PEK/PBI30GF
PEK/PBI	30CF		PEK/PBI30CF
PEK/PBI	30CF	10CATAS	PEK/PBI30CF-10CATAS
PEK/PBI	30CF	20CATAS	PEK/PBI30CF-20CATAS

The curves obtained by the DMTA tests are shown in the graphs in **Figure 8.9a** and **Figure 8.9b**.

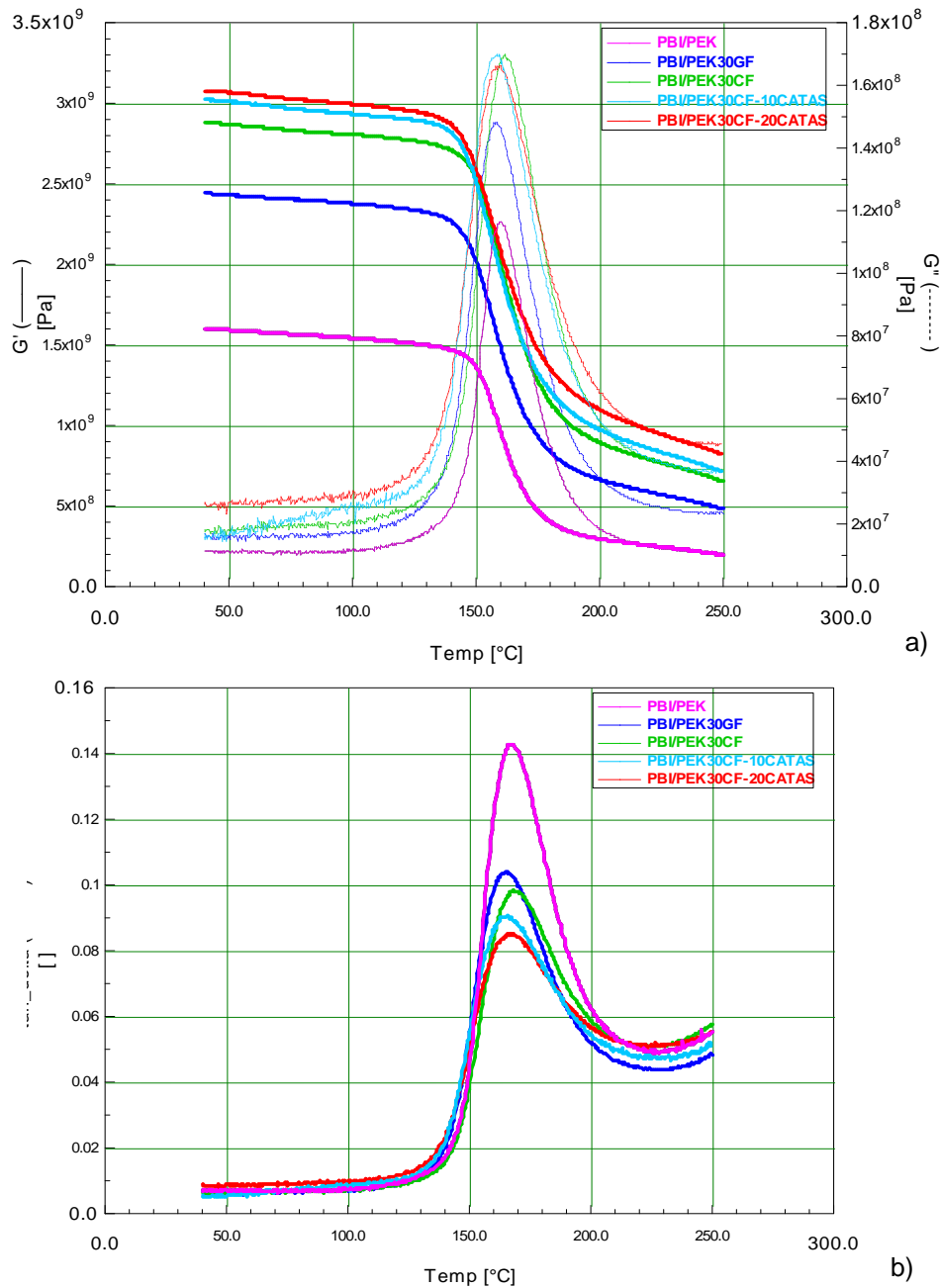


**Figure 8.9:** Results of DMTA tests for PEK/PBI materials:  $G'$  and  $G''$  (a) and  $\tan \delta$  (b)

**Figures 8.10** shows the values of the  $G'$  moduli at 100 °C and 200 °C for the matrix and the glass fiber reinforced composites, with 30% wt. of CF and nanostructured with 10, 20% of CATAS.

The values of  $G'$  are summarized in **Table 8.7** and the increase of the storage module at 100 °C and 200 °C of the composites was calculated with respect to the PEK / PBI matrix.

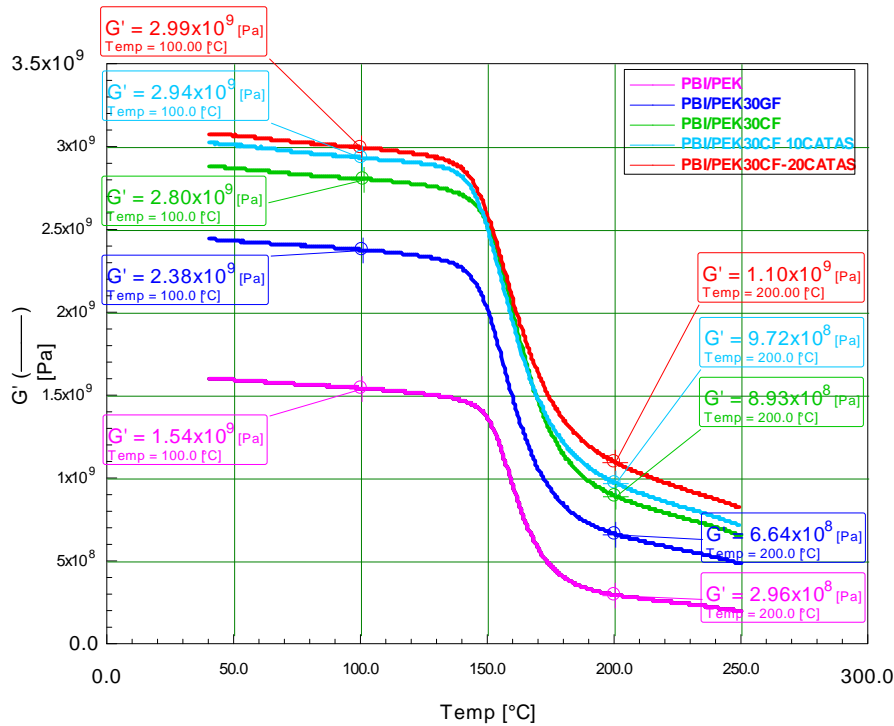


**Figure 8.10:** Graph of the DTMA curves with values of  $G'$  at 100 °C and 200 °C for PEK/PBI composites

**Table 8.7** shows that the use of carbon fiber as reinforcement significantly increases  $G'$  values, especially at higher temperatures. The effect of CATAS in the mixture does not produce significant increases in  $G'$  values, limiting itself to a percentage point of improvement. However, this result must be considered positive because, although only a slight increase in  $G'$  was obtained, 20% by weight of salts was added to replace an expensive matrix. This quantity of CATAS could make a savings on the costs of the matrix estimated at around 19%. This economic advantage, together with a slight improvement in performance, could offer new market segments to the Gazole currently being the prerogative of Celazole.

**Table 8.7:**  $G'$  values of DMTA at 100°C and at 200°C for CF and NS composite materials compared to the matrix

COMPOSITE			$G'$ [MPa] @100°C	$G'$ [MPa] @200°C	% $\Delta G'$ 100 vs PBI/PEK	% $\Delta G'$ 200 vs PBI/PEK
PEK/PBI			1.54E+09	2.96E+08		
PEK/PBI	30CF		2.80E+09	8.93E+08	+81.82%	+201.69%
PEK/PBI	30CF	10CATAS	2.94E+09	9.72E+08	+90.91%	+228.38%
PEK/PBI	30CF	20CATAS	2.99E+09	1.10E+09	+94.16%	+271.62%

## 8.4 References

- Dawkins, G., Gruender, M. Copeland, G.S. (2014) USOO8802789B2, POLYBENZIMIDAZOLE POLYETHERKETONEKETONE BLENDS AND MISCIBLE BLENDS US 2013/0331470.
- Goodwin, A. A. G. P. Simon (1996), *Polymer*, 37 (6) 991-995.
- Hopkins, J.B., Karin, J.R., Hudson, M., Copeland, G.S., Gruender, M. (2013) POROUS POLYBENZIMIDAZOLE RESIN AND METHOD OF MAKING SAME, App1. No.: 13/934,265.
- Jonas, A.M. Ivanov, D.A. *Macromolecules* 1998, 31, 5352-5362.
- Lee, H.S, Kim, W.N (1996) *Polymer*, 38(11) 2657.
- Musto, P., Wut, L., Karasz, F. E., MacKnight, W. J. *Polymer*, 1991, 32 (1), 3–11.
- Vasconcelos, G.C., Mazur, R.L., Ccchieri Botelho, E., Cerqueira Rezende, M., Leali Costa, M. (2010) *J. Aerosp. Technol. Manag.* [online]. 2010, vol.2, n.2, pp.155-162. ISSN 1984-9648. <http://dx.doi.org/10.5028/jatm.2010.02026310>.
- Williams, D.J., Leung, L., Karasz, F.E., Macknight, W., Jaffe, M. (1986) Compositions of Aromatic Polybenzimidazoles And Aromatic Polyimides Or Aromatic Polyetherimides, EPA 87301367.6.
- [www.ghardaplastics.com](http://www.ghardaplastics.com)

## CHAPTER 9: CONCLUSIONS

### 9.1 Results achieved

The purpose of this project was to study and characterize the high-performance polymers (HPPs) and to devise and produce, characterize and optimize, blends, fiber-reinforced composites, microcomposites, nanocomposites or hybrid formulations of the previous ones. The aims of the study can be identified in the production and characterization of innovative materials obtained with the use of HPPs opportunely blended, reinforced and filled in order to improve some properties for specific applications: main properties improved were thermal stability and mechanical properties at elevated temperatures, with the main aim of increasing stiffness, tensile strength or toughness, especially in severe conditions, such as very high temperature and corrosive environment.

Another main goal of the study was to address the cost problems: the reduction in the price of these materials allows access to composite materials based on high performance polymer matrices to a wide range of industrial sectors, that currently consider the HPPs not affordable.

A concomitant aim of this study was to put the basis and provide further information for the development and optimization of processing technologies for the production of this class of materials. The pursuit of these objectives allowed to reach another purpose, that was the acquisition of the knowledge that allow us to design and characterize hybrid materials: the combined effect of mixing HPP matrices, fiber reinforcement and nanostructured materials has allowed us to conceive, produce and define materials with various distinctive properties tailored to specific applications.

Up to date bibliographic give us useful information about the characteristics and the process of HPP matrices, the mixtures, the reinforcements, the nanofillers and the composites. The information acquired was followed by subsequent activity concerning the selection and finding of polymeric matrices belonging to different families, like Polyaryletherketones (PAEK) in particular PEEK and PEK, Polyetherimides (PEI), Polyamide-imide (PAI), Polyimides (PI), Thermoplastic Polyimides (TPI), Polybenzimidazole (PBI), Aromatic polyamides (PARA). The selection was done based on criteria like properties, costs, processability, versatility in applications, compatibility.

After defining the characterization and processing methods of the materials, samples of matrices, also in blends, and some glass fiber and carbon fiber reinforced composites were processed and tested, following a preliminary adaptation of the devices to the extreme characteristics of the treated materials.

The characterization performed with DSC, TGA, HDT, Impact test and Tensile test (both at  $T_{room}$  and at high temperature), DMTA and morphology tests provided important information, suggesting the next lines of investigation.

An important phase of the study concerned the nanostructured and fiber-reinforced composite materials based on PEEK. Optimized the process parameters, 8 nanoreinforcements were considered with which the PEEK-based composites were produced. The thermo mechanical characterization led to the exclusion of 3 fillers, while the others were selected to produce hybrid composites. At the same time, glass fiber and carbon fiber reinforced composites were produced and characterized with 4 different percentages, from 5% to 30% wt., to evaluate the most suitable formulation for the production of FR and NS composites. After that, the hybrid composites were formulated with different amounts of nanofillers and glass or carbon fiber. The samples produced for melt compounding and injection molding were characterized by tensile tests at  $T_{room}$  and at 200 °C. Proceeding with a feedback characterization and reformulation method, optimized composites were produced.

The main objective of the optimization was to increase the mechanical properties in terms of modulus and tensile strength, preserving reasonable deformation related to the toughness. The hybrid formulations with 15% wt. of glass fiber and 10% wt. of P5B and with 20% wt. of GF and 8% wt. of mica showed values of the elastic modulus, higher than doubled compared to the corresponding FR composites and, in any case, superior to the composites with the maximum amount of fiber of glass, to a greater extent at high temperatures. The tensile stress values also increased slightly, and above all the deformation at break values increased significantly. Viewed as a whole, these values represent materials with greater stiffness, increased strength and improved toughness. The hybrid formulations with 30% wt. of carbon fiber and 10% wt. of P5B and with 30% wt. of CF and 10% wt. of N8 showed values of the elastic modulus higher by 10-20% compared to the corresponding composites with 30% FR also at high temperatures. The tensile stress is slightly improved, as the breaking deformation appears to be significantly increased compared to the benchmark. At the end of this study phase, 4 fiber-reinforced and nanostructured materials were realized with improved characteristics compared to the products currently marketed. In addition, quantities of cheap nanofillers have been used to estimate savings of 10-30% on materials costs.

Another phase of the activity was devoted to the study of composites made with a new polymer mixture made with P84 polyimide and PEEK. The P84, with excellent thermomechanical properties, is usually processed with a little productive compression molding but in appropriate formulations with PEEK it is extrudable. They were produced and characterized by tensile test, with different proportions of PI/PEEK, to identify the most suitable blend for the production of composites. Composites were made using three different selected nanofiller and the blend made with 70% of PEEK and 30% of PI, resulted most suitable in previous tests. The characterizations on these nanostructured composites gave indications for the subsequent realization of the FR and NS material

formulations. The hybrid composites with 30% wt. glass fiber and 3 types of nanofillers were made together with two other materials, in which the amount of fiber and filler C130 was alternately halved. The thermal, morphological and thermo-mechanical characterizations have shown that the materials produced have significantly improved characteristics, compared to the reference matrices. In addition, important information has been obtained on how to design materials through variations in formulation. In this way, it was possible to obtain materials in which the tensile strength or the deformation or the stiffness were mainly improved.

The positive results obtained with the composite materials based on high temperature matrices studied up to now has suggested the further search for other suitable nanofillers to be used for this study. The usefulness of nanoreinforcements has a double advantage: both for the performance aspect and from an economic point of view, contributing to lower costs and expanding the market of HPPs composites. A nano-sized filler was synthesized in laboratories to be used for the first time as a nanoreinforcement in thermoplastic composites. The salts of terephthalic acid and in particular the calcium terephthalate trihydrate salts (CATS) have shown suitable characteristics to suggest its use as nanofillers after suitable treatment to make it anhydrous (CATAS). In addition, the raw materials for producing CATAS are low-cost and recycled.

The synthesized nanoreinforcements have been tested realizing 3 composites with 10%, 20% and 30% wt. of CATAS on a PEEK matrix. During mixing, it was noted that these nanofillers facilitate the melt compounding process. The DMTA characterization performed on samples showed significant improvements in increments of 60% to 115% of the storage module at 100 °C and 200 °C. The thermal study suggests that this type of nanofillers affects the PEEK phases with a slight nucleating effect, increasing the crystalline fraction. But above all, the CATAS have the effect of blocking a significant fraction of amorphous phase converting it into a more stable and performing rigid amorphous phase. The positive results suggested to try CATAS also in hybrid composites. Composites were made with 30% of CF and 10%, 20% and 25% wt. of CATAS. Thanks to the excellent processability of the salts, it was possible to add an additional 10% wt. of CATAS to the best formulation obtained in the first phase realized with 30% of CF and 10% of P5B. The samples of these materials subjected to DMTA tests showed increases from 20% to 50% of G' in the range between 100 °C and 200 °C and improvements also towards the previous best formulation PEEK30CF-10P5B. In addition, the replacement of the expensive matrix with reinforcements indicates an estimate of cost reduction from 25% for 30CF reinforced sample, to 35% for formulation with 30CF and 10P5B, up to 45% for the formulation PEEK30\_CF10\_P5B\_10CATAS.

A PEK/PBI blend (Gazole) is less expensive, but less efficient than a mechanically excellent but very expensive PBI/PEEK blend (Celazole). An attempt was made to make a PEK / PBI blend an



alternative to the PBI/PEEK mixture by reducing the performance gap of the two materials and increasing the cost savings of PEK/PBI. The economic advantage, together with a slight improvement in performance, could offer new market segments to the Gazole, currently being the prerogative of Celazole. Composites with 30% carbon fiber and 30CF and 10% wt. and 20% wt. of CATAS were produced and tested with DMTA. While the carbon fibers produced an increase of the 80% storage module at 100 °C and 200% at 200 °C, the effect of CATAS was moderate, with G' increments of no more than 10% compared to PEK / PBI-30CF. However, this result must be considered positive because, although only a slight increase in G' was obtained, 20% by weight of salts was added to replace an expensive matrix with an estimated cost savings of 18%.

Future developments of the present work are represented by the possibility of testing more focused properties, such as corrosion and fatigue resistance, that could be extended even to new composite formulations based on TPI/PEKK blend, PEI/PEEK, all containing the low cost and high performing synthesized terephthalate salts.